MIT-T-76-002 C. 2

MIT
SEA
GRANT
PROGRAM

CIRCULATING COPY
Sea Grant Depository

A HYBRID ELEMENT METHOD FOR CALCULATING THREE - DIMENSIONAL WATER WAVE SCATTERING

by

Dick K. P. Yue
H. S. Chen
and
Chiang C. Mei

Massachusetts Institute of Technology
Cambridge, Massachusetts 02139

Report No. MITSG 76-10
September 1, 1976

A HYBRID ELEMENT METHOD FOR CALCULATING THREE - DIMENSIONAL WATER WAVE SCATTERING

BY

DICK K. P. YUE

H. S. CHEN

AND

CHIANG C. MEI

Report No. MITSG 76-10
Index No. 76-310-Cbs

ABSTRACT

A HYBRID ELEMENT METHOD FOR CALCULATING
THREE-DIMENSIONAL SCATTERING OF WATER WAVES

by

DICK K. P. YUE, H. S. CHEN and C. C. MEI

Under the assumption of a harmonic, small-amplitude incident wave, an effective hybrid finite element method for calculating wave scattering by and resulting forces on a general three-dimensional body is presented.

The method is applied to four different geometries. Analytic or independently obtained solutions are available for two of the geometries and comparison indicates perfect agreement. No other solutions are known for the other two geometries.

All numerical results are checked using Optical Theorem, and convergence tests are performed. A user's manual for the computer program as well as suggested extensions to the program are also included.

While only the scattering problem is formulated and solved in the present work, extension to the solution of the mathematically similar radiation problem is quite straightforward.

The three-dimensional hybrid element method is a practical one for engineering applications in water wave problems, and offers a good alternate to the Green function method, especially for complex geometries.

ACKNOWLEDGEMENT

This is the final report of the work sponsored jointly by the Public Service Electric and Gas Company, Newark, New Jersey, as part of a study of a proposed offshore floating nuclear power facility, and by the National Oceanic and Atmospheric Administration as part of the M.I.T. Sea Grant Program.

The entire work was carried out at the Ralph M. Parsons Laboratory for Water Resources and Hydrodynamics of the Department of Civil Engineering at M.I.T. The material in this report is submitted by Mr. Yue in partial fulfillment of the requirements for the degree of Master of Science in Civil Engineering at M.I.T.

The authors are grateful to Ms. Louise Ketchen and Mary Mason for the excellent typing.

TABLE OF CONTENTS

	Page
TITLE PAGE	1
ABSTRACT	2
ACKNOWLEDGEMENT	3
TABLE OF CONTENTS	4
1. INTRODUCTION	7
1.1 Scope of the Present Study	10
1.2 Mathematical Statement of the Problem	12
1.3 Hybrid Finite Element Formulation--The Variational Principal	14
2. THE FINITE ELEMENT FORMULATION	18
2.1 The Volume Integral I_1	20
2.2 The Surface Integral I_2	26
2.3 Integrals on S, I_3 to I_6	28
2.3.1 Integral I_3	28
2.3.2 Integral I_4	30
2.3.3 Integral I_5	32
2.3.4 Integral I_6	33
2.4 Quadrature	35
2.5 Summary and the Total Global Matrix	37
3. NUMERICAL EXAMPLES	40
3.1 Vertical Circular Cylinder in Constant Water Depth	41
3.2 Circular Cylindrical Platform in Constant Water Depth	46
3.3 Rectangular Barge in Constant Depth	52
3.4 Elliptic Island with a Circular Base	85

Page

4. ERROR ESTIMATES AND CONVERGENCE TESTS 106

4.1 The Optical Theorem 106

4.2 Convergence of the Finite Element Approximation 107

4.3 Convergence of Series Terms in the Analytic Representation 114

5. COMPUTATIONAL ASPECTS AND THE PROGRAM USAGE 117

5.1 Program Implementation, Space and Time Requirements 117

5.2 The Hybrid Finite Element Program 119

5.2.1 Program Logic 119

5.2.1.1 MAIN 123
5.2.1.2 INPUT 123
5.2.1.3 MESHO, MESH1 123
5.2.1.4 EIGVAL 124
5.2.1.5 HANKEL 124
5.2.1.6 ASEMKV and ELKV 127
5.2.1.7 FMAP2 127
5.2.1.8 SURFAS 127
5.2.1.9 CROSSK, PLOAD, CLOAD, DIAGK 127
5.2.1.10 DENSE and COEFF 128
5.2.1.11 SOLV and BKSUBT 129
5.2.1.12 FORCE 129
5.2.1.13 OUTPUT 129

5.2.2 Input Requirements 129

5.2.3 Output Format 129

5.2.4 Illustrative Example: Program Listing, Sample Input and Output 131

5.2.4.1 Variable Name Table 131
5.2.4.2 Sample Input 134
5.2.4.3 Program Listing 134
5.2.4.4 Sample Output 180

6. CONCLUDING REMARKS 197

6.1 Suggested Improvements 197

6.2 Recommendations and Cost Estimates for the Atlantic Generating Station Problem 202

6.3 Conclusions 203

	Page
LIST OF REFERENCES	205
LIST OF FIGURES	207
LIST OF TABLES	212
LIST OF SYMBOLS	213
APPENDIX A: A PROOF OF THE OPTICAL THEOREM	218

1. INTRODUCTION

Along with the technological advances in the design and construction of large ships and off-shore structures, the need for an efficient and versatile method for calculating wave forces and other hydrodynamical effects to supplement laboratory testing is now widely recognized. The present work is also motivated by such needs in an imaginative project of ocean engineering, i.e., the Atlantic Generating Station project. To meet the increasing demand of electric power and to minimize environmental hazards, the Public Service Electric and Gas Company of New Jersey proposes to construct a nuclear power plant at a site three miles offshore from Atlantic City. Two nuclear power plants of 1150 MeW capacity will rest on two square platforms floating in a basin protected by two giant breakwaters. To ensure sufficient supply of cooling water at a low intake flow rate, two openings of 130 ft. width will be made in the breakwater system which is roughly 2000 ft. in diameter. For the proper design of mooring systems, prediction of possible basin and platform oscillation, and the wave forces, due to incoming sea is needed. This work deals with a modern numerical method which is potentially useful for the Atlantic Generating station as well as for other large ocean structures.

In reality, the waves in a severe storm are highly complicated, being large in amplitude and of a random nature. For theoretical work, it is often necessary to assume the incident wave amplitude to be small so that one can work with a linearized approximation. In this limited framework, useful general relationships among the hydrodynamical quantities can be deduced; see for example Haskind, 1957, Wehausen, 1971 and Newman, 1976.

For a few very specialized geometries, analytic solutions are also possible (for example, MacCamy and Fuchs, 1952). For general geometries, however, a largely numerical method is necessary, the semi-analytic Green function method being the most popular. By using a Green function of some sort, this method transforms the boundary value problem into an integral equation along a line for two-dimensional, or over a surface for three-dimensional problems, which usually includes the boundary of the solid structure. By dividing the interval into small segments and making piece-wise approximation, the integral equation is discretized to give an approximate set of algebraic equations. Solving the algebraic system, the unknown in the interval is found and the flow quantities in the entire field can be subsequently computed. This method is conceptually simple but the Green function or the kernel of the integral equation is singular, and numerical evaluation of its integral or derivative is laborious and complicated. The resulting algebraic equation has a fully populated coefficient matrix with very involved elements. Furthermore, the computation of flow quantities after the solution of the integral equation is found can also be quite time consuming. The method is consequently expensive, both computationally and in terms of the analytic preparation required. Nevertheless, this method has been successfully used by several authors; see for example Garrison, 1974. There are also situations where the Green functions are either too complicated or cannot be easily constructed. Alternative, more efficient methods are desirable.

We present here a more direct method involving finite elements. The general idea is to use discrete finite elements in the region near

complicated bodies and/or bottom surfaces, while some formal analytical representation is assumed in a region away from them. Similar ideas have been used long ago in conjunction with finite difference schemes where there is a singularity in the region of computation. It is based on a plausible argument that an analytical solution of reasonably elementary form which satisfies the differential equation and some of the boundary conditions, in particular the singularity condition, must provide a more efficient representation than a simple interpolation function which satisfies few or none of these conditions. Near solid surfaces of arbitrary geometry, analytic representation is often too cumbersome or impossible; it is here, however, that the power of finite elements can be most fully utilized.

In this hybrid approach, the boundary value problem is recast as a variational principle which incorporates the matching of the solutions in the finite element interior region and the analytic exterior region as natural boundary conditions so that all the unknown parameters associated with both regions can be solved simultaneously after discretization. This is the most important feature of the present hybrid method. Under this scheme, the finite element region can be greatly confined; the radiation condition is satisfied exactly; local and global matching are implicit, and no iteration is required. The total number of unknowns is greatly reduced, and the coefficient matrix involved is narrow-banded with quite simple components.

For two-dimensional problems, such as plane waves incident on an infinitely long cylinder, a body with rotational symmetry about the vertical

axis, or long waves in shallow water where the vertical dependence is omitted, this method has been applied with success by Chen and Mei, 1974, and Bai and Yeung, 1974, where computational experiments show that the hybrid element scheme is an attractive alternative to the integral equation method, especially for complex geometries.

For strictly three-dimensional bodies, the only numerical method that has been successful is the Green function method, and it is valuable to extend the hybrid element method to general three-dimensional problems to study its feasibility and efficiency. This is the task undertaken in the present study. Because of the significant increase in computation time and storage associated with an additional space dimension (Black, 1975 estimates a typical increase in computation time of the order 100 times for same body dimensions and wavelength), it is not clear *a priori* whether this method offers a viable alternative to the Green function method.

1.1 Scope of the Present Study

The linearized boundary value problem for general three-dimensional scattering of water waves is stated. By constructing an artificial surface to enclose all complex geometries, an equivalent variational statement, which states that a functional made up of certain integrals involving the unknown flow field is stationary, is given and proved. Based on this variational principle, and using a vertical circular cylindrical surface, a hybrid element method is formulated. The fluid region inside is discretized into a number of hexahedral (six-sided block) isoparametric quadratic finite elements, while a truncated eigenfunction series solution with

unknown coefficients is used in the exterior which is assumed to be of constant depth. Imposing the stationarity of the discretized functional, a system of linear algebraic equations is obtained, which includes as unknowns the finite element nodal parameters and the coefficients of the exterior analytic solution. This resultant system is solved by direct Gauss elimination.

For illustration, the three-dimensional wave scattering problem is solved numerically. We point out that the radiation problem, i.e. waves due to oscillating bodies, is mathematical so close to the scattering problem that the present method can be adapted with trivial modification. The following geometries are considered :

(1) a vertical circular cylinder in constant water depth,

(2) a circular cylindrical platform in water of constant depth,

(3) a square platform in constant depth, and

(4) an elliptical island with a circular toe.

Results for a range of wave periods and incidence angles for the cases are presented in Chapter 3. While all the four geometries involve one or more vertical planes of symmetry and therefore simpler methods of computation are available, we have taken no advantage of symmetry and each example is treated as a general three-dimensional problem. In particular, the first two geometries possess axisymmetry and can be solved in a two-dimensional manner, and analytic (MacCamy and Fuchs, 1952 for the vertical cylinder) and semi-analytic (Black, Mei and Bray, 1971 and Garrett, 1971 for the circular platform) solutions are available for comparison. To our knowledge, no other solution exists for the latter two examples.

The mathematical background—the boundary value problem and the variational principle—is given in the remainder of this chapter while Chapter 2 summarizes the hybrid element formulation. Convergence tests and error estimates are presented in Chapter 4, computational aspects and program usage are discussed in Chapter 5 where sample computer listings are also included. Conclusions and suggestions for improving and extending the program are given in the last chapter.

1.2 Mathematical Statement of the Problem

The general three-dimensional scattering of water waves in an ocean is formulated under the following assumptions:

(a) incompressible, inviscid, irrotational flow;

(b) small wave amplitude;

(c) simple harmonic incident waves;

(d) impermeable, perfectly reflective solid boundaries.

If we define the velocity potential as the real part of $\Phi = \phi\, e^{-i\omega t}$ where ω is the angular frequency of the oscillations, then ϕ must satisfy (see Fig. 1.1):

$$\nabla^2\phi = 0 \qquad \text{in } V \tag{1.2.1}$$

$$\frac{\partial\phi}{\partial z} - \frac{\omega^2}{g}\,\phi = 0 \qquad \text{on } z = 0 \text{ (in F)} \tag{1.2.2}$$

$$\frac{\partial\phi}{\partial n} = 0 \qquad \text{on all solid boundaries (in B)} \tag{1.2.3}$$

The scattered wave defined by $\phi_s = \phi - \phi_I$ where ϕ_I is the incident wave, must satisfy the radiation boundary condition:

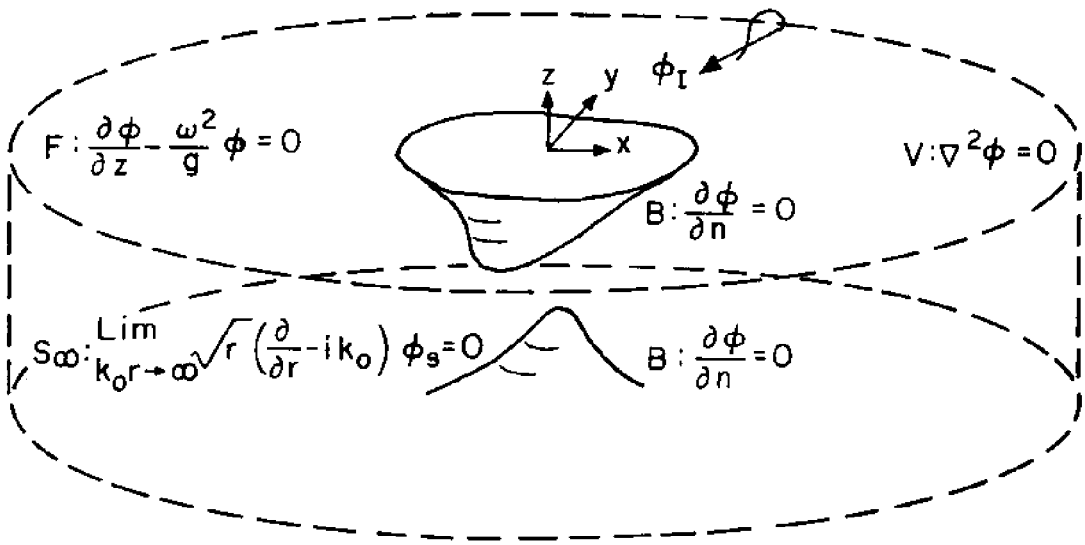

Figure 1.1 The boundary value problem

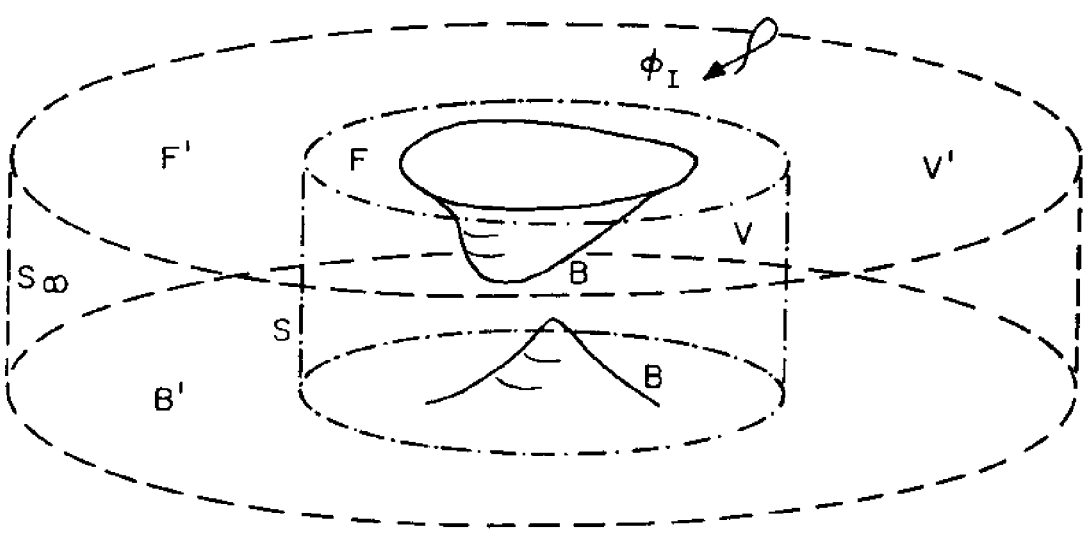

Figure 1.2 Introduction of the artificial circular cylindrical boundary, S

$$\lim_{k_o r \to \infty} \sqrt{r}\,\left(\frac{\partial}{\partial r} - ik_o\right)\phi_s = 0 \qquad \text{on } S_\infty \tag{1.2.4}$$

where k_o is the wave number associated with ω. The solid boundary B includes all floating or submerged bodies and the sea bottom.

1.3 Hybrid Finite Element Formulation - the Variational Principle

Assuming that all body and depth irregularities are reasonably confined, say, within a radius r_s, we introduce an artificial vertical circular cylindrical surface S of that radius so that all solid bodies and depth variations are just enclosed (see Fig. 1.2).

We now show the equivalence of the boundary value problem and the stationarity of the following functional (Chen and Mei, 1974):

$$J(\phi) = \int_V \frac{1}{2}(\nabla\phi)^2\, dV - \int_F \frac{\omega^2}{2g}\phi^2\, dF + \int_S \left[\left(\frac{\phi_s'}{2} - \phi_s\right)\frac{\partial\phi'}{\partial r} - \frac{\phi_s'}{2}\frac{\partial\phi_I}{\partial r}\right] dS \tag{1.3.1}$$

For clarity, we use the ( )' notation to denote quantities outside of S while the non-primed variables denote now only quantities associated with the fluid region inside of S. The first integral is hence a volume integral over the finite element fluid volume, V; while the integrals over F and S are surface integrals, the former only over the free surface in the interior of S. The total wave potential outside of S, ϕ' and the scattered potential $\phi_s' = \phi' - \phi_I$ are assumed to satisfy Eqts. (1.2.1) - (1.2.3) and Eqt. (1.2.4) respectively. Clearly, if ϕ also satisfies Eqs. (1.2.1) - (1.2.3) in V, and if ϕ and ϕ' are matched on S such that

$$\phi = \phi' \tag{1.3.2}$$

on S

$$\frac{\partial\phi}{\partial r} = \frac{\partial\phi'}{\partial r} \tag{1.3.3}$$

then ϕ and ϕ' form the complete solution in V and V'.

By assuming constant depth in V', it is easily shown that the scattered potential ϕ_s' can be represented by a double series of eigenfunctions:

$$\phi_s' = \sum_{n=0}^{\infty} (\alpha_{on} \cos n\theta + \beta_{on} \sin n\theta) \cosh k_o (z + h) H_n^{(1)} (k_o r)$$

$$+ \sum_{m=1}^{\infty} \sum_{n=0}^{\infty} (\alpha_{mn} \cos n\theta + \beta_{mn} \sin n\theta) \cos \kappa_m (z + h) K_n (\kappa_m r) \tag{1.3.4}$$

where h is the constant depth in V', and k_o, κ_m, m = 1, 2, 3, ... are respectively the positive real roots of the equivalent dispersion relations

$$k_o \tanh k_o h = \frac{\omega^2}{g}$$

$$\kappa_m \tan \kappa_m h = -\frac{\omega^2}{g} \qquad m = 1, 2, 3, \ldots \tag{1.3.5}$$

The proof of equivalence goes as follows. Taking the first variation, we have

$$\delta J(\phi) = \int_V (\nabla\phi \cdot \nabla\delta\phi) dV - \int_F \frac{\omega^2}{g} \phi\delta\phi \, dF$$

$$+ \int_S \left[\left(\frac{\delta\phi_s'}{2} - \delta\phi_s\right) \frac{\partial\phi'}{\partial r} - \left(\frac{\phi_s'}{2} - \phi_s\right) \frac{\partial\delta\phi'}{\partial r} - \frac{\delta\phi_s'}{2} \frac{\partial\phi_I}{\partial r} \right] dS$$

where use is made of the fact that ϕ_I is prescribed (i.e., $\delta\phi_I = 0$). Now by Green's theorem:

$$\int_V (\nabla\phi\cdot\nabla\delta\phi)\,dV = -\int_V \nabla^2\phi\delta\phi\ dF + \int_B \frac{\partial\phi}{\partial n}\,\delta\phi\ dB + \int_F \frac{\partial\phi}{\partial z}\,\delta\phi\ dF + \int_S \frac{\partial\phi}{\partial r}\,\delta\phi\ dS$$

where $\vec{n}$ is the unit normal pointing outward from the fluid, so

$$\delta J(\phi) = -\int_V \nabla^2\phi\delta\phi\ dV + \int_F \left(\frac{\partial\phi}{\partial z} - \frac{\omega^2}{g}\,\phi\right)\delta\phi\ dF + \int_B \frac{\partial\phi}{\partial n}\,\delta\phi\ dB$$

$$+ \int_S \left[\left(\frac{\partial\phi}{\partial r} - \frac{\partial\phi'}{\partial r}\right)\delta\phi - (\phi - \phi')\,\frac{\partial\delta\phi'}{\partial r}\right]dS$$

$$+ \frac{1}{2}\int_S \left[\delta\phi'\,\frac{\partial}{\partial r}\,(\phi' - \phi_I) - (\phi' - \phi_I)\,\frac{\partial\delta\phi'}{\partial r}\right]dS$$

The last integral

$$\frac{1}{2}\int_S \left[\delta\phi'\,\frac{\partial}{\partial r}\,(\phi' - \phi_I) - (\phi' - \phi_I)\,\frac{\partial\delta\phi'}{\partial r}\right]dS$$

$$= \frac{1}{2}\int_S \left[\delta\phi_s'\,\frac{\partial\phi_s'}{\partial r} - \phi_s'\,\frac{\partial\delta\phi_s'}{\partial r}\right]dS$$

$$= \frac{1}{2}\int_{V'} (\phi_s'\ \nabla^2\delta\phi_s' - \delta\phi_s'\ \nabla^2\ \phi_s')\,dV'$$

$$- \frac{1}{2}\int_{S_\infty \cup F' \cup B'} \left(\delta\phi_s'\,\frac{\partial\phi_s'}{\partial n} - \phi_s'\,\frac{\partial\delta\phi_s'}{\partial n}\right) dS \qquad = 0$$

vanishes by virtue of Eqs. (1.2.1) - (1.2.4), whence

$$\delta J(\phi) = -\int_V \nabla^2\phi\ \delta\phi\ dV + \int_F (\frac{\partial\phi}{\partial z} - \frac{\omega^2}{g}\phi)\delta\phi\ dF + \int_B \frac{\partial\phi}{\partial n}\delta\phi\ dB$$

$$+ \int_S [\ (\frac{\partial\phi}{\partial r} - \frac{\partial\phi'}{\partial r})\delta\phi - (\phi - \phi')\frac{\partial\delta\phi'}{\partial r}\ ]dS = 0$$

on account of Eqs. (1.2.1) - (1.2.3) and the matching conditions (1.3.2), (1.3.3) on S. Thus $J(\phi)$ is stationary if and only if ϕ is a solution to the boundary value problem in V, ϕ' a solution to the boundary value problem in V', and the coefficients of ϕ_s' in Eqt. (1.3.4) are such that ϕ, ϕ' are matched on S according to Eqts. (1.3.2) and (1.3.3).

It should be noted that only ϕ_I must be prescribed and all other matching and boundary conditions are satisfied as natural boundary conditions.

Before we conclude this chapter, a few comments are due. First, it should be noted that while we have chosen a circular cylindrical surface for S for simplicity of evaluating the integrals over it, S can in practice take on quite general (say elliptical, spherical etc.) shapes. Secondly, later investigation (see Sections 4.3) indicates that it is almost always more efficient to choose S as small as possible at the cost of having to use more series terms in the analytic expression for the solution in V'. Of course, S must still enclose all floating or submerged bodies and bottom changes, and for numerical accuracy, S must allow finite element aspect ratio not to deviate significantly from unity.

Thirdly, the analytic expression in V' (Eqt. (1.3.4)) may in general be chosen in a number of other ways, say, using a Green function representation. The latter choice, however, would lead to an integral equation on S, and hence possesses much of the undesirability of the direct integral equation approach.

2. THE FINITE ELEMENT FORMULATION

We rewrite the functional (1.3.1) as

$$
\begin{aligned}
J(\phi) = & \int_V \frac{1}{2} (\nabla\phi)^2 \, dV && I_1 \\
& - \int_F \frac{\omega^2}{2g} \phi^2 \, dF && I_2 \\
& + \int_S \frac{1}{2} \phi_s' \frac{\partial}{\partial r} \phi_s' \, dS && I_3 \\
& - \int_S \phi \frac{\partial}{\partial r} \phi_s' \, dS && I_4 \\
& + \int_S \phi_I \frac{\partial}{\partial r} \phi_s' \, dS && I_5 \\
& - \int_S \phi \frac{\partial}{\partial r} \phi_I \, dS && I_6
\end{aligned}
\tag{2.0}
$$

Here the incident wave ϕ_I can also be expressed as partial waves

$$\phi_I = - \frac{iga_o}{\omega} e^{ik_o r \cos(\theta - \theta_I)} \frac{\cosh k_o(z + h)}{\cosh k_o h} \tag{2.1.a}$$

$$= - \frac{iga_o}{\omega} \frac{\cosh k_o(z + h)}{\cosh k_o h} \sum_{n=0}^{\infty} \varepsilon_n i^n J_n(k_o r) \cos n(\theta - \theta_I) \tag{2.1.b}$$

where a_o and θ_I are respectively the amplitude and incidence angle of the incident wave, and the Jacobi symbol

$$
\begin{aligned}
\varepsilon_n &= 1 && n = 0 \\
&= 2 && n = 1, 2, 3, \ldots
\end{aligned}
$$

is introduced. The scattered wave in the outer region V' is as before

$$\phi_s' = \sum_{n=0}^{\infty} [\alpha_{on} \cos n\theta + \beta_{on} \sin n\theta] \cosh k_o(z + h) H_n^{(1)}(k_o r)$$
$$+ \sum_{m=1}^{\infty} \sum_{n=0}^{\infty} (\alpha_{mn} \cos n\theta + \beta_{mn} \sin n\theta) \cos \kappa_m(z + h) K_n(\kappa_m r) \quad (1.2.4)$$

where k_o, κ_m, $m = 1, 2, \ldots$ are defined as in Eq. (1.2.5). For simplicity we define

$$k_m = i\,\kappa_m \qquad m = 1, 2, 3, \ldots \qquad (2.2)$$

and k_m are now the roots of

$$k_m \tanh k_m h - \frac{\omega^2}{g} = 0 \qquad m = 0, 1, 2, 3, \ldots$$

which are real for $m = 0$ and pure imaginary for $m = 1, 2, 3, \ldots$. Note that for $m = 1, 2, 3, \ldots$

$$\cosh k_m(z + h) = \cos \kappa_m(z + h)$$
$$H_n^{(1)}(k_m r) = K_n(\kappa_m r)\, \frac{2}{\pi}\, e^{-\frac{\pi}{2} i(n+1)}$$

and

$$H_n^{(1)\prime}(k_m r) = -i\, K_n'(\kappa_m r)\, \frac{2}{\pi}\, e^{-\frac{\pi}{2} i(n+1)}$$

We can now rewrite, by redefining α_{mn} and β_{mn},

$$\phi_s' = \sum_{m=0}^{\infty} \sum_{n=0}^{\infty} (\alpha_{mn} \cos n\theta + \beta_{mn} \sin n\theta) \cosh k_m(z + h) H_n^{(1)}(k_m r) \qquad (2.3)$$

The evaluation of each of the integrals (denoted as I_1, I_2, ... I_6) are presented in the following sections.

2.1 The Volume Integral I_1

$$I_1 = \int_V \frac{1}{2} (\nabla\phi)^2 \, dV$$

If we subdivide the domain V into M_V finite elements and choose N_V nodal points x_i in V, $i = 1, 2, \ldots, N_V$, such that the potential in each element can be approximated as a linear function of the potential values on nodes within or on that element, using superscript $(\ )^e$ to denote quantities associated with element e, we have, for an element with M^e nodes

$$\phi^e \simeq \sum_{i=1}^{M^e} N_i^e \, \phi_i^e \tag{2.1.1.a}$$

or if we let

$$\{N^e\}^T = \{N_1^e, N_2^e, \ldots, N_{M^e}^e\} \qquad 1 \times M^e$$

and

$$\{\phi^e\}^T = \{\phi_1^e, \phi_2^e, \ldots, \phi_{M^e}^e\} \qquad 1 \times M^e$$

then

$$\phi^e \simeq \{N^e\}^T \{\phi^e\} \tag{2.1.1.b}$$

Here the interpolation functions N_i^e are in general functions of coordinates, whether global or local to the element e.

For properly chosen elements and associated interpolations, and for sufficiently large M_V, we can write

$$I_1 \simeq \sum_{\substack{e=1 \\ e\varepsilon V}}^{M_V} \int_{V^e} \frac{1}{2} (\nabla\phi^e)^2 \, dV^e$$

$$= \sum_{\substack{e=1 \\ e\varepsilon V}}^{M_V} \int_{V^e} \frac{1}{2} (\nabla\{N^e\}^T\{\phi^e\})^2 \, dV^e$$

$$= \sum_{\substack{e=1 \\ e\varepsilon V}}^{M_V} \frac{1}{2} \{\phi^e\}^T \, [\int_{V^e} \nabla\{N^e\} \, \nabla\{N^e\}^T \, dV^e]\{\phi^e\}$$

$$= \sum_{\substack{e=1 \\ e\varepsilon V}}^{M_V} \frac{1}{2} \{\phi^e\}^T \, [K_V^e] \, \{\phi^e\}$$

$$= \frac{1}{2} \{\phi\}^T \, [K_V] \, \{\phi\} \qquad (2.1.2)$$

where

$$[K_V^e] \equiv [\int_{V^e} \nabla\{N^e\} \, \nabla\{N^e\}^T \, dV^e] \qquad M^e \times M^e$$

and

$$K_{V\,ij}^e = \int_{V^e} (\frac{\partial N_i^e}{\partial x}\frac{\partial N_j^e}{\partial x} + \frac{\partial N_i^e}{\partial y}\frac{\partial N_j^e}{\partial y} + \frac{\partial N_i^e}{\partial z}\frac{\partial N_j^e}{\partial z}) \, dx^e \, dy^e \, dz^e$$

$$i, j = 1 \text{ to } M^e \qquad (2.1.3)$$

and in the last equality of Eq. (2.1.2) an assemblage is implicit where

$$\{\phi\}^T = \{\phi_1, \phi_2, \ldots, \phi_{N_V}\}$$

is the union of all the $\{\phi^e\}$'s which in general are not mutually exclusive.

Clearly each $[K_V^e]$ is symmetric and real (N_i^e are real), and hence the globally assembled result $[K_V]$ is also real and symmetric. Furthermore, with shrewd node-numbering, $[K_V]$ can usually be made banded.

In this study, we have chosen isoparametric hexahedral elements of the "Serendipity" family containing 20 exterior nodes and quadratic interpolation functions, N_i, i = 1 to 20 (Zienkiewicz et al, 1969)(see Fig. 2.1):

$$N_i = \frac{1}{8}(1 + \xi\xi_i)(1 + \eta\eta_i)(1 + \zeta\zeta_i)(\xi\xi_i + \eta\eta_i + \zeta\zeta_i - 2) \qquad i = 1 \text{ to } 8$$

$$\xi_i,\ \eta_i,\ \zeta_i = \pm 1 \text{ (corner nodes)}$$

$$\left.\begin{aligned} N_i &= \frac{1}{4}(1 - \xi^2)(1 + \eta\eta_i)(1 + \zeta\zeta_i) \qquad i = 9 \text{ to } 12 \\ &\qquad \xi_i = 0;\ \eta_i,\ \zeta_i = \pm 1 \\ N_i &= \frac{1}{4}(1 + \xi\xi_i)(1 - \eta^2)(1 + \zeta\zeta_i) \qquad i = 13 \text{ to } 16 \\ &\qquad \eta_i = 0;\ \xi_i,\ \zeta_i = \pm 1 \\ N_i &= \frac{1}{4}(1 + \xi\xi_i)(1 + \eta\eta_i)(1 - \zeta^2) \qquad i = 17 \text{ to } 20 \\ &\qquad \zeta_i = 0;\ \xi_i,\ \eta_i = \pm 1 \end{aligned}\right\} \text{midside nodes} \tag{2.1.4}$$

where ξ, η, ζ form the local coordinates and ξ_i, η_i, ζ_i = 0, ±1 are the nodal coordinate values.

By choosing the same functions N_i to map a local point from the ξ, η, ζ space into the global x, y, z space via the nodal coordinates, we get

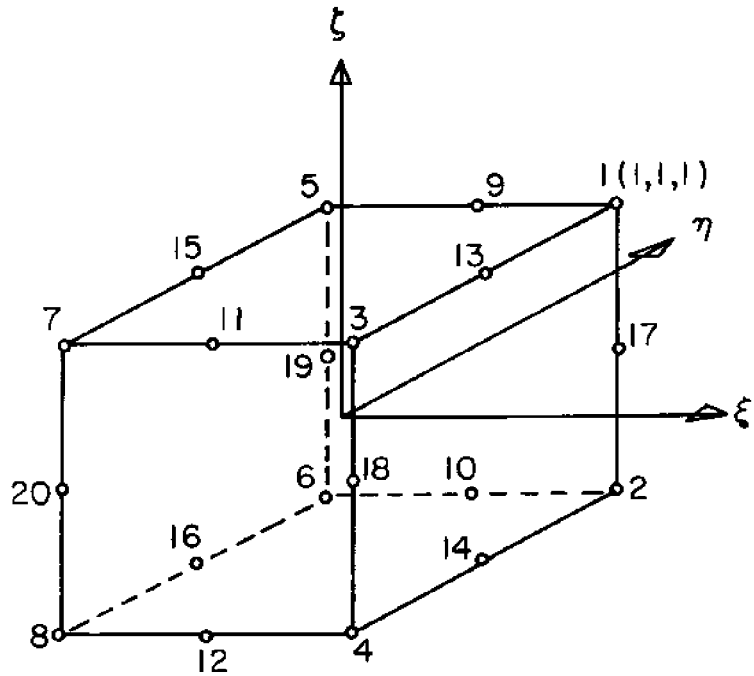

Figure 2.1 The 20-node hexahedral element with exterior nodes only (in local coordinates)

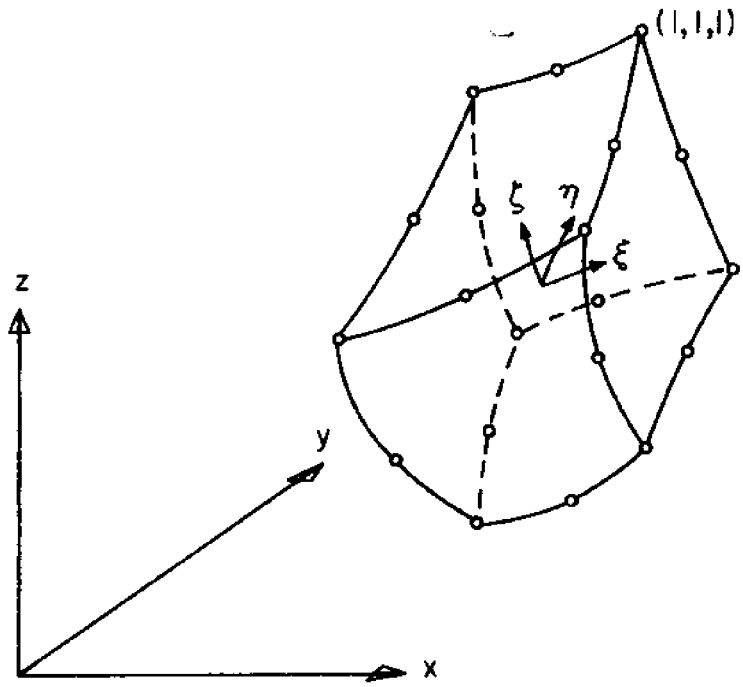

Figure 2.2 The daughter arbitrarily oriented, quadratic-sided hexahedral element in global coordinates after isoparametric mapping

$$\begin{Bmatrix} x^e \\ y^e \\ z^e \end{Bmatrix} = [X^e]\{N^e\} \tag{2.1.5.a}$$

where

$$[X^e] = \begin{bmatrix} x_1 & x_2 & \cdots & x_{20} \\ y_1 & y_2 & \cdots & y_{20} \\ z_1 & z_2 & \cdots & z_{20} \end{bmatrix} \tag{2.1.5.b}$$

is the 3 x 20 matrix of the global coordinates of the nodes and

$$\{N^e\}^T = [N_1\ (\xi, \eta, \zeta), \ldots, N_{20}(\xi, \eta, \zeta)] \tag{2.1.5.c}$$

Arbitrarily shaped and oriented hexahedral daughter elements with quadratic sides can be adopted in region V (see Fig. 2.2). Note that aside from aspect ratio considerations for good numerical convergence, the sides of the daughter element need not be of equal length nor the "midside" nodes be at mid-distance, under this isoparametric mapping.

The choice of the element is made for several reasons. The block shape allows for convenience of element arrangement and of node numbering. The element is quadratic so that a much smaller number of them would be required to achieve the same accuracy; furthermore, isoparametric mapping results in much better approximation of boundary surfaces, for example, for quadratic surfaces, the representation is exact.

Returning to Eq. (2.1.3), we note that since Eq. (2.1.4) cannot be readily inverted, the integration must be performed in local coordinates.

$$K^e_{V\ ij} = \int_{V^e} \left(\frac{\partial N^e_i}{\partial x}\frac{\partial N^e_j}{\partial x} + \frac{\partial N^e_i}{\partial y}\frac{\partial N^e_j}{\partial y} + \frac{\partial N^e_i}{\partial z}\frac{\partial N^e_j}{\partial z}\right) dx^e\, dy^e\, dz^e \tag{2.1.6}$$

$$i, j = 1 \text{ to } 20$$

writing

$$\int_{V^e} dx^e\, dy^e\, dz^e = \int_{-1}^{1}\int_{-1}^{1}\int_{-1}^{1} |J|\, d\xi\, d\eta\, d\zeta$$

and

$$\begin{Bmatrix} \frac{\partial}{\partial x} \\ \frac{\partial}{\partial y} \\ \frac{\partial}{\partial z} \end{Bmatrix} = [J]^{-1} \begin{Bmatrix} \frac{\partial}{\partial \xi} \\ \frac{\partial}{\partial \eta} \\ \frac{\partial}{\partial \zeta} \end{Bmatrix}$$

where $|J|$ is the determinant and $[J]^{-1}$ the inverse of the Jacobian matrix

$$[J] = \begin{Bmatrix} \frac{\partial}{\partial \xi} \\ \frac{\partial}{\partial \eta} \\ \frac{\partial}{\partial \zeta} \end{Bmatrix} [x,\ y,\ z] = \begin{bmatrix} \frac{\partial x}{\partial \xi} & \frac{\partial y}{\partial \eta} & \frac{\partial z}{\partial \zeta} \\ \frac{\partial x}{\partial \xi} & \frac{\partial y}{\partial \eta} & \frac{\partial z}{\partial \zeta} \\ \frac{\partial x}{\partial \xi} & \frac{\partial y}{\partial \eta} & \frac{\partial z}{\partial \zeta} \end{bmatrix}$$

Substituting from Eq. (2.1.5)

$$[J] = \begin{Bmatrix} \frac{\partial}{\partial \xi} \\ \frac{\partial}{\partial \eta} \\ \frac{\partial}{\partial \zeta} \end{Bmatrix} \{N^e\}^T [X^e]^T$$

which can be evaluated in terms of ξ, η, ζ and $[X^e]$ since N_i is explicit in ξ, η, ζ as given in Eq. (2.1.4). Since the integrand in Eq. (2.1.6) is in general a function of the nodal coordinates of the element, numerical quadrature is necessary in the integration.

2.2 The Surface Integral I_2

$$I_2 = \frac{1}{2} \int_F \left(-\frac{\omega^2}{g} \phi^2\right) dF$$

Substituting from Eq. (2.1.1.b), we obtain

$$I_2 \cong \frac{1}{2} \sum_{e \varepsilon F} \left(-\frac{\omega^2}{g}\right) \int_{F^e} (\{\bar{N}^e\}^T \{\bar{\phi}^e\})^2 \, dF^e$$

$$= \frac{1}{2} \sum_{e \varepsilon F} \{\bar{\phi}^e\}^T \left[\left(-\frac{\omega^2}{g}\right) \int_{F^e} \{\bar{N}^e\}\{\bar{N}^e\}^T \, dF^e\right] \{\bar{\phi}^e\}$$

$$= \frac{1}{2} \sum_{e \varepsilon F} \{\bar{\phi}^e\}^T [K_F^e] \{\bar{\phi}^e\}$$

$$= \frac{1}{2} \{\phi\}^T [K_F] \{\phi\} \qquad (2.2.1)$$

where $\{\bar{N}^e\}$, $\{\bar{\phi}^e\}$ are the subvectors of $\{N^e\}$, $\{\phi^e\}$ containing entries corresponding only to the nodes on the free surface, i.e., $\phi_i^e \varepsilon F^e$.

For simplicity, we require elements on F to have exactly one face on F, and $\{\bar{N}^e\}$, $\{\bar{\phi}^e\}$ are 8×1 so that

$$[K_F^e] \equiv \left(-\frac{\omega^2}{g}\right) \left[\int_{F^e} \{\bar{N}^e\}\{\bar{N}^e\}^T \, dF^e\right] \qquad 8 \times 8$$

and

$$K_{F\,ij}^e = -\frac{\omega^2}{g} \int_{F^e} N_i^e N_j^e \, dF^e \qquad i, j = 1 \text{ to } 8 \qquad (2.2.2)$$

Again assemblage is implied in the last equality of Eq. (2.2.1) where only $\phi_i \in F$ are involved. Note also that as in I_1, $[K_F^e]$ and $[K_F]$ are real and symmetric, and since $\{\bar{\phi}^e\} \subset \{\phi^e\}$, $[K_F]$ always has a bandwidth less than or equal to that of $[K_V]$.

To evaluate I_2 and in particular $K_{F\ ij}^e$, we perform the integration in local coordinates

$$K_{F\ ij}^e = -\frac{\omega^2}{g} \int_{-1}^{1} \int_{-1}^{1} (N_i^e N_j^e \ |J_F|)_{\zeta=1} \, d\xi \, d\eta \tag{2.2.3}$$

where the Jacobian is given by

$$|J_F|^2 = [(\frac{\partial x}{\partial \xi})^2 + (\frac{\partial y}{\partial \xi})^2][(\frac{\partial x}{\partial \eta})^2 + (\frac{\partial y}{\partial \eta})^2] - [\frac{\partial x}{\partial \xi}\frac{\partial x}{\partial \eta} + \frac{\partial y}{\partial \xi}\frac{\partial y}{\partial \eta}]^2 \tag{2.2.4}$$

which is readily evaluated in terms of local coordinates and $[X^e]$ by using Eqs. (2.1.5).

The resulting integral is again evaluated by quadrature.

2.3 Integrals on S, I_3 to I_6

For computation the series (2.1.b) and (2.3) are truncated as follows:

$$\phi_I \cong -\frac{iga_o}{\omega}\frac{\cosh k_o(z+h)}{\cosh k_o h}\sum_{n=0}^{N_o} \varepsilon_n\, i^n\, J_n(k_o r)\cos n(\theta-\theta_I) \qquad (2.3.1)$$

and

$$\phi'_s \cong \sum_{m=0}^{M}\sum_{n=0}^{N_m}(\alpha_{mn}\cos n\theta + \beta_{mn}\sin n\theta)\cosh k_m(z+h)\, H_n^{(1)}(k_m r) \qquad (2.3.2)$$

where N_i, $i = 0, 1, \ldots, M$, and M are chosen depending on wave period and geometry.

2.3.1 Integral I_3

$$I_3 = \int_S \frac{1}{2}\phi'_s \frac{\partial}{\partial r}\phi'_s\, dS$$

$$\cong \frac{1}{2}\int_{-h}^{0} dz \int_0^{2\pi} d\theta\, r_S$$

$$\left(\sum_{m=0}^{M}\sum_{n=0}^{N_m}(\alpha_{mn}\cos n\theta + \beta_{mn}\sin n\theta)\cosh k_m(z+h) H_n^{(1)}(k_m r_S)\right)$$

$$\left(\sum_{m=0}^{M}\sum_{n=0}^{N_m}(\alpha_{mn}\cos n\theta + \beta_{mn}\sin n\theta)\cosh k_m(z+h) H_n^{(1)\prime}(k_m r_S) k_m\right)$$

$$= \frac{r_S}{2}\sum_{\ell=0}^{M}\sum_{m=0}^{M}\sum_{n=0}^{N_m}\frac{2\pi k_m}{\varepsilon_n}(\alpha_{\ell n}\alpha_{mn} + \beta_{\ell n}\beta_{mn}) H_n^{(1)}(k_\ell r_S) H_n^{(1)\prime}(k_m r_S)$$

$$\int_{-h}^{0} \cosh k_\ell(z + h)\cosh k_m(z + h)\, dz$$

$$= \frac{r_S}{2} \sum_{m=0}^{M} \sum_{n=0}^{N_m} \frac{2\pi k_m}{\epsilon_n} (\alpha_{mn}^2 + \beta_{mn}^2) H_n^{(1)}(k_m r_S) H_n^{(1)\prime}(k_m r_S) \left(\frac{\sinh 2k_m h}{4k_m} + \frac{h}{2}\right)$$

If we define a coefficient vector

$$\{\mu\}^T = \{\alpha_{00}, \alpha_{01}, \beta_{01}, \alpha_{02}, \beta_{02}, \ldots\ldots, \alpha_{0N_0}, \beta_{0N_0},$$
$$\alpha_{10}, \alpha_{11}, \beta_{11}, \alpha_{12}, \beta_{12}, \ldots\ldots, \alpha_{1N_1}, \beta_{1N_1},$$
$$\vdots$$
$$\alpha_{M0}, \alpha_{M1}, \beta_{M1}, \alpha_{M2}, \beta_{M2}, \ldots\ldots, \alpha_{MN_M}, \beta_{MN_M}\}^T$$
$$1 \times N_T \text{ (say)} \qquad (2.3.1.1)$$

noting that all the terms associated with β_{i0}, $i = 0$ to M are zero and so β_{i0} are excluded, then we can write

$$I_3 \cong \frac{1}{2} \{\mu\}^T [K_D]\{\mu\} \qquad (2.3.1.2)$$

where $[K_D]$ $N_T \times N_T$ is diagonal and

$$K_{D_i} = \frac{\pi r_S}{2\epsilon_n} H_n^{(1)}(k_m r_S) H_n^{(1)\prime}(k_m r_S)\ (\sinh 2k_m h + 2k_m h) \qquad i = 1 \text{ to } N_T$$

where the i-th element of $\{\mu\}$ is α_{mn} or β_{mn}. Clearly by our notation in Eq. (2.3), K_{D_ℓ} are complex for $\ell \leq 2N_0 - 1$, and real otherwise.

2.3.2 Integral I_4

$$I_4 = -\int_S \phi \frac{\partial}{\partial r} \phi'_s \, dS$$

$$\cong -\sum_{e\varepsilon S} \int_{S^e} \{\hat{N}^e\}^T \{\hat{\phi}^e\} \sum_{m=0}^{M} \sum_{n=0}^{N_m} (\alpha_{mn} \cos n\theta + \beta_{mn} \sin n\theta) \cosh k_m(z + h)$$

$$H_n^{(1)\prime}(k_m r_S) k_m \, dS^e$$

where we have substituted from Eqs. (2.1.1.b) and (2.3.2) and $\{\hat{N}^e\}$, $\{\hat{\phi}^e\}$ are subvectors of $\{N^e\}$, $\{\phi^e\}$ where only entries corresponding to $\phi_i^e \varepsilon S$ are included.

Again in this formulation, we require, for simplicity, elements on S to have exactly 1 face on S and $\{\hat{N}^e\}$, $\{\hat{\phi}^e\}$ are vectors of dimension 8. We now write, using the definition (2.3.1.1)

$$I_4 \simeq \sum_{e\varepsilon S} \{\mu\}^T [K_C^e]^T \{\hat{\phi}^e\}$$

here $[K_C^e]$ is defined as the $8 \times N_T$ matrix with

$$K_{C\ ij}^e = -\int_{S^e} \hat{N}_i^e \cosh k_m(z + h) H_n^{(1)\prime}(k_m r_S) k_m \begin{pmatrix} \cos n\theta \\ \sin n\theta \end{pmatrix} dS^e$$

where the j-th element of $\{\mu\}$ is $\begin{pmatrix} \alpha_{mn} \\ \beta_{mn} \end{pmatrix}$, and a choice of cos $n\theta$ or sin $n\theta$ is indicated depending on j, since $\{\mu\}$ is defined to include both α's and β's.

To perform the integration in local coordinates, we write

$$K_{C\ ij}^{e} = -\int_{-1}^{1}\int_{-1}^{1} (\hat{N}_i^e \cosh k_m(z+h) H_n^{(1)\prime}(k_m r_S)\ k_m \begin{pmatrix} \cos n(\cos^{-1}(\frac{x}{r_S})) \\ \sin n(\sin^{-1}(\frac{y}{r_S})) \end{pmatrix} |J_S|)_{\eta=1}\ d\xi\ d\zeta$$

where

$$|J_S|^2 = [(\frac{\partial x}{\partial \xi})^2 + (\frac{\partial y}{\partial \xi})^2 + (\frac{\partial z}{\partial \xi})^2][(\frac{\partial x}{\partial \zeta})^2 + (\frac{\partial y}{\partial \zeta})^2 + (\frac{\partial z}{\partial \zeta})^2]$$

$$- [\frac{\partial x}{\partial \xi}\frac{\partial x}{\partial \zeta} + \frac{\partial y}{\partial \xi}\frac{\partial y}{\partial \zeta} + \frac{\partial z}{\partial \xi}\frac{\partial z}{\partial \zeta}]^2 \qquad (2.3.2.0)$$

Substituting for x, y, z from Eq. (2.1.5), the integral can be evaluated directly by numerical integration.

The element matrices are then assembled to give

$$I_4 \cong \{\mu\}^T[K_C]^T\{\phi\}$$

$$= \frac{1}{2}\{\mu\}^T[K_C]^T\{\phi\} + \frac{1}{2}\{\phi\}^T[K_C]\{\mu\} \qquad (2.3.2.1)$$

where again only $\phi_i \in S$ are involved, and the latter manipulation is necessary to give rise to a symmetric global matrix, as will be shown later. For a total of N_S nodes on S, the global assembled matrix $[K_C]$ is $N_S \times N_T$. It is easily observed that $[K_C]$ is in general full and complex.

2.3.3 Integral I_5

$$I_5 = \int_S \phi_I \frac{\partial}{\partial r} \phi_s' \, dS$$

$$\cong \int_{-h}^{0} dz \int_0^{2\pi} r_S \, d\theta \left(-\frac{iga_o}{\omega}\right) \frac{\cosh k_o(z+h)}{\cosh k_o h} \left(\sum_{n=0}^{N_o} \varepsilon_n \, i^n J_n(k_o r_S) \cos n(\theta - \theta_I)\right)$$

$$\left(\sum_{m=0}^{M} \sum_{n=0}^{N_m} (\alpha_{mn} \cos n\theta + \beta_{mn} \sin n\theta) \cosh k_m(z+h) H_n^{(1)\prime}(k_m r_S) k_m\right)$$

$$= \left(-\frac{iga_o}{\omega}\right) r_S \int_{-h}^{0} dz \int_0^{2\pi} d\theta \, \frac{\cosh k_o(z+h)}{\cosh k_o h} \left(\sum_{n=0}^{N_o} \varepsilon_n \, i^n J_n(k_o r_S)(\cos n\theta \cos n\theta_I\right.$$

$$\left. + \sin n\theta \sin n\theta_I\right) \cdot$$

$$\cdot \left(\sum_{m=0}^{M} \sum_{n=0}^{N_m} (\alpha_{mn} \cos n\theta + \beta_{mn} \sin n\theta) \cosh k_m(z+h) H_n^{(1)\prime}(k_m r_S) k_m\right)$$

$$= \left(-\frac{iga_o}{\omega}\right) r_S \int_0^{2\pi} \left(\sum_{n=0}^{N_o} \varepsilon_n \, i^n J_n(k_o r_S)(\cos n\theta \cos n\theta_I + \sin n\theta \sin n\theta_I)\right) \cdot$$

$$\cdot \left(\sum_{n=0}^{N_o} (\alpha_{on} \cos n\theta + \beta_{on} \sin n\theta) \cosh k_o(z+h) H_n^{(1)\prime}(k_o r_S)\right) \cdot$$

$$\cdot \frac{(\sinh 2k_o h + 2k_o h)}{4 \cosh k_o h}$$

$$= \left(-\frac{iga_o}{\omega}\right) \quad r_S \sum_{n=0}^{N_o} (\alpha_{on} \cos n\theta_I + \beta_{on} \sin n\theta_I) i^n \, J_n(k_o r_S) H_n^{(1)\prime}(k_o r_S) \pi \cdot$$

$$\cdot \frac{(\sinh 2k_o h + 2k_o h)}{2 \cosh k_o h}$$

$$= \left(-\frac{iga_o}{\omega}\right)(\pi\ r_S) \sum_{n=0}^{N_o} (\alpha_{on} \cos n\theta_I + \beta_{on} \sin n\theta_I) \cdot$$

$$\cdot \frac{i^n\ J_n(k_o r_S) H_n^{(1)\prime}(k_o r_S)}{2 \cosh k_o h} (\sinh 2k_o h + 2k_o h)$$

where the orthogonality properties in z and θ are invoked. Now we write

$$I_5 \simeq - \{Q_C\}^T \{\mu\} \ ; \tag{2.3.3.1}$$

here $\{Q_C\}$ is defined as the $(2N_o - 1)$ by 1 vector with

$$Q_{C_i} = \left(-\frac{iga_o}{\omega}\right)(-\pi\ r_S)\left(i^n\ J_n(k_o r_S) H_n'(k_o r_S)\ \frac{\sinh 2k_o h + 2k_o h}{2 \cosh k_o h}\right) \cdot$$

$$\cdot \begin{pmatrix} \cos n\theta_I \\ \sin n\theta_I \end{pmatrix} \tag{2.3.3.2}$$

where the i-th element of $\{\mu\}$ is $\begin{pmatrix} \alpha_{on} \\ \beta_{on} \end{pmatrix}$.

2.3.4 Integral I_6

$$I_6 = - \int_S \phi \frac{\partial}{\partial r} \phi_I$$

Substituting ϕ_I from Eq. (2.1.a),

$$I_6 \cong - \sum_{e \in S} \int_{S^e} \{\hat{N}_e\}^T \{\hat{\phi}_e\} \left(-\frac{iga_o}{\omega}\right) ik_o \cos(\theta - \theta_I) e^{ik_o r_S \cos(\theta - \theta_I)} \cdot$$

$$\cdot \frac{\cosh k_o(z + h)}{\cosh k_o h}\ dS^e$$

$$= - \sum_{e \varepsilon S} \{Q_P^e\}^T \{\hat{\phi}_e\} \tag{2.3.4.1}$$

where we have defined the 8×1 vector $\{Q_P^e\}$ so that

$$Q_{P_i}^e = \int_{S^e} \hat{N}_i^e \left(- \frac{iga_o}{\omega}\right) ik_o \cos(\theta - \theta_I) e^{ik_o r_S \cos(\theta - \theta_I)} \cdot$$

$$\cdot \frac{\cosh k_o(z + h)}{\cosh k_o h} \, dS^e$$

$$= \frac{\left(- \frac{iga_o}{\omega}\right) ik_o}{\cosh k_o h} \int_{-1}^{1} \int_{-1}^{1} \left(\hat{N}_i^e \left(\frac{x}{r_S} \cos \theta_I + \frac{y}{r_S} \sin \theta_I\right)\right) \cdot$$

$$\cdot e^{ik_o(x \cos \theta_I + y \sin \theta_I)} \cosh k_o(z + h) \, |J_S|)_{\eta=1} \, d\xi \, d\zeta \tag{2.3.4.2}$$

which after expressing x, y, z in terms of local coordinates can be integrated numerically. Assembling $\{Q_P^e\}$'s for all $e \varepsilon S$, we obtain

$$I_6 \cong - \{Q_P\}^T \{\phi\} \tag{2.3.4.3}$$

where now $\{Q_P\}$ is an $N_S \times 1$ complex vector.

2.4 Quadrature

Three different Gauss-Legendre quadrature formulas (Kopal, 1955; Abramowitz and Stegun, 1964) are used in the evaluation of the integrals I_1, I_2, I_4 and I_6:

(1) for I_1 a 21 point formula is used for the cubic volume:

$$\frac{1}{8\ell^3}\int_{-\ell}^{\ell}\int_{-\ell}^{\ell}\int_{-\ell}^{\ell} f(\xi, \eta, \zeta)d\xi\, d\eta\, d\zeta$$

$$= \frac{1}{360}\,[-\,496\, f_m + 128\,\Sigma\, f_r + 8\,\Sigma\, f_f + 5\,\Sigma\, f_v] + O(\ell^6) \qquad (2.4.1)$$

where $f_m = f(0, 0, 0)$

$\Sigma\, f_r$ = sum of values of f at the 6 points midway from the center to the 6 faces.

$\Sigma\, f_f$ = sum of values of f at the 6 centers of the faces.

$\Sigma\, f_v$ = sum of values of f at the 8 vertices.

(2) for I_2 and I_6, the evaluation over the square surface is approximated at 9 integration points:

$$\int_{-1}^{1}\int_{-1}^{1} f(\xi, \eta)d\xi\, d\eta = \sum_{i=1}^{3}\sum_{j=1}^{3} w_i w_j\, f(\xi_i, \eta_j) \qquad (2.4.2)$$

where

i	ξ_i, η_i	w_i
2	0	.8888889
1,3	± 0.7745967	.5555556

(3) for I_4, we note the presence of rapidly varying functions sin $n\theta$ and cos $n\theta$ in the integrand and adopted a more accurate 16 point formula for the square surface area:

$$\int_{-1}^{1}\int_{-1}^{1} f(\xi,\eta)d\xi\, d\eta = \sum_{i=1}^{4}\sum_{j=1}^{4} w_i w_j\, f(\xi_i,\ \eta_i) \tag{2.4.3}$$

where

i	ξ_i, η_i	w_i
1,4	±.3478548	.7745967
2,3	±.6521452	.3399810

2.5 Summary and the Total Global Matrix

Summarizing and treating $\{\mu\}$ as unknown also, the functional (2.0) becomes

$$J(\{\phi\},\{\mu\}) = \frac{1}{2}\{\phi\}^T[K_V]\{\phi\} \quad (1)$$

$$+ \frac{1}{2}\{\phi\}^T[K_F]\{\phi\} \quad (2)$$

$$+ \frac{1}{2}\{\mu\}^T[K_D]\{\mu\} \quad (3)$$

$$+ \frac{1}{2}\{\mu\}^T[K_C]^T\{\phi\} + \frac{1}{2}\{\phi\}^T[K_C]\{\mu\} \quad (4)$$

$$- \{Q_C\}^T\{\mu\} \quad (5)$$

$$- \{Q_P\}^T\{\phi\} \quad (6) \qquad (2.5.1)$$

For J to be stationary, we require

$$\frac{\partial J}{\partial \phi_i} = 0 \qquad i = 1, \ldots, N_V$$

and

$$\frac{\partial J}{\partial \mu_i} = 0 \qquad i = 1, \ldots, N_T \qquad (2.5.2.a,b)$$

which gives

$$[K_V]\{\phi\} + [K_F]\{\phi\} + [K_C]\{\mu\} = \{Q_p\} \qquad (2.5.3.a)$$

and

$$[K_D]\{\mu\} + [K_C]^T\{\phi\} = \{Q_C\} \qquad (2.5.3.b)$$

If we define

$$\{\psi\}^T = [\{\phi\}^T, \{\mu\}^T] \qquad 1 \times (N_V + N_T) \qquad (2.5.4.a)$$

and assign the last positions of $\{\phi\}$ to all ϕ_i for nodes on S, i.e.

$$\{\psi\}^T = [\{\phi_i | \phi_i \notin S\}^T, \{\phi_i | \phi_i \varepsilon S\}^T, \{\mu\}^T] \qquad (2.5.4.b)$$

then Eqs. (2.4.3.a,b) combine to give a system of linear equations

$$[K]\{\psi\} = \{Q\}$$

where

$$\{Q\}^T = [\{Q_P\}^T, \{Q_C\}^T] \qquad 1 \times (N_V + N_T) \qquad (2.5.5)$$

and the total global matrix [K], $(N_V + N_T) \times (N_V + N_T)$ has the following structure:

$$[K] = \begin{array}{c} \\ N_V \\ \\ N_T \end{array} \begin{array}{c} \begin{array}{ccc} \longleftarrow N_V \longrightarrow & & \longleftarrow N_T \longrightarrow \end{array} \\ \left[\begin{array}{ccc|c} & & 0 & \\ & [K_V] + [K_F] & & 0 \\ 0 & & & \\ \hline & & & [K_C] \\ \hline 0 & & [K_C]^T & \begin{matrix} 0 & [K_D] & 0 \end{matrix} \end{array}\right] \\ \begin{array}{ccc} & & \longleftarrow N_S \longrightarrow \end{array} \end{array} \begin{array}{c} \\ \\ \\ N_S \\ \\ \\ \end{array} \qquad (2.5.6)$$

We note that $[K_V] + [K_F]$ is real symmetric and banded and $[K_D]$ is diagonal and complex while $[K_C]$ is full and complex; they are positioned as shown in (2.5.6). [K] is consequently complex and symmetric which is partly a result of the rearrangement in Eq. (2.3.2.1).

Having obtained [K], $\{\psi\}$ can then be solved by inversion, or formally

$$\{\psi\} = [K]^{-1}\{Q\} \qquad (2.5.7)$$

and the nodal potentials in V as well as the coefficients of the expansion in V' are solved. For efficiency the total global matrix is condensed to eliminate the unknowns $\{\mu\}$, which can be recovered by substitution after $\{\phi\}$ is solved.

From Eq. (2.5.3.b)

$$\{\mu\} = [K_D]^{-1} (\{Q_C\} - [K_C]^T\{\phi\}) \tag{2.5.8}$$

which when substituted into Eq. (2.5.3.a) gives

$$([K_V] + [K_F] - [K_C]^T[K_D]^{-1}[K_C]) \{\phi\} = \{Q_P\} - [K_C] [K_D]^{-1}\{Q_C\}$$

or

$$[K'] \{\phi\} = \{Q'\} \tag{2.5.9.a,b}$$

where

$$[K'] \equiv [K_V] + [K_F] - [K_C]^T[K_D]^{-1}[K_C]$$

and

$$\{Q'\} \equiv \{Q_P\} - [K_C] [K_D]^{-1}\{Q_C\}$$

Clearly, $[K']$ is still symmetric and banded, and complex, and only the symmetric half band of $[K']$ is stored.

A direct method (Gauss elimination) is used for solution.

3. NUMERICAL EXAMPLES

Three-dimensional diffraction by four different geometries are treated and presented in the following sections. For the first case, the analytic solution is known, while for the second, accurate numerical results are available by other techniques. They are therefore useful for testing the present method. The last two examples have no other known solutions, and are chosen to illustrate the versatility and efficiency of our method, while for simplicity of grid generation, they are still chosen to have relatively elementary geometries.

All the finite element grid systems are generated by computer with automatically minimized bandwidths.

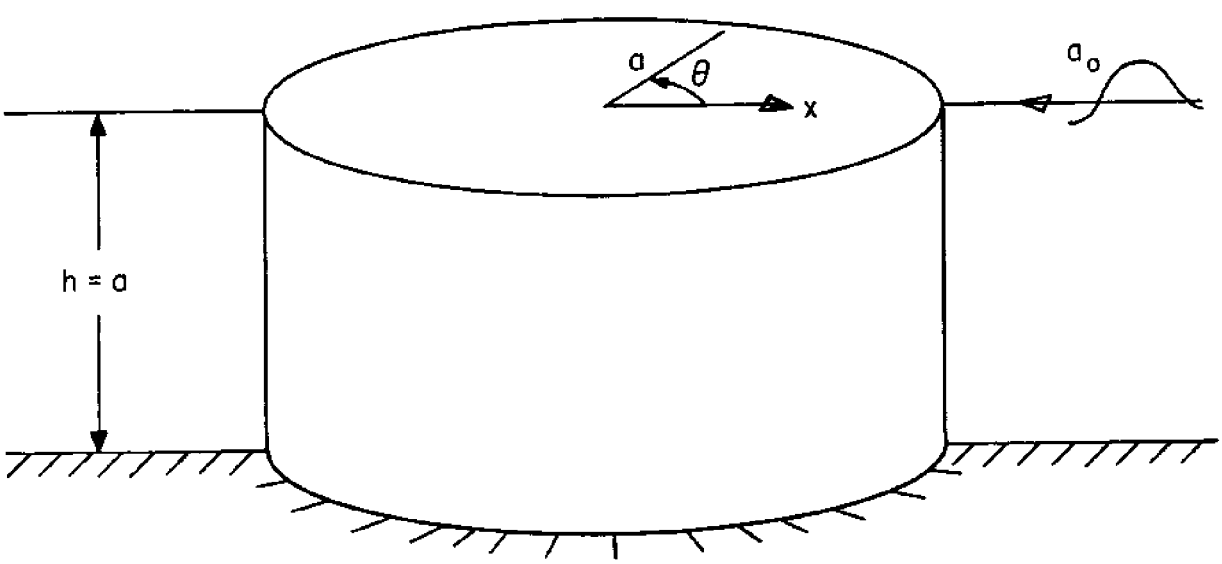

Figure 3.1 Wave incident on a bottom-seated circular cylinder of radius a ($\theta_I = \pi$; h = a)

3.1 Vertical Circular Cylinder in Constant Water Depth (Fig. 3.1)

The cylinder has radius a and is centered along the z-axis. The water depth is everywhere constant h. For the case of h = a, we use a finite element grid consisting of 36 elements—two layers of 18 elements each stacked vertically forming a ring surrounding the cylinder. (See Fig. 3.2). There are a total of 342 nodes, and the average element dimension, L_e, is about .48a. The incidence angle is taken as $\theta_I = \pi$.

In the analytical theory for this two-dimensional geometry, only the coefficients corresponding to the first eigenvalue k_o are involved and all other coefficients vanish. For generality and for an indication of the accuracy, however, 5 eigenvalues are chosen ($M = 4$; $N_o = 12$; $N_1 = N_2 = N_3 = N_4 = 10$), which corresponds to a total of 99 terms in the exterior analytic representation(Eq.(2.3.2)).The following quantities are presented:

(1) coefficients of the series solution in the far field: α_{mn}, β_{mn};

(2) normalized free surface elevation on the cylinder (r = a): η/a_o where $\eta(a,\theta) = \frac{i\omega}{g}\phi(a,\theta,0)$; and,

(3) horizontal force coefficient.

We define dimensionless force and moment coefficients by

$$\left.\begin{aligned} C_{F_i} &= \frac{F_i}{\rho g \pi\, a H a_o} \\ &\text{and} \\ C_{M_i} &= \frac{M_i}{\rho g \pi\, a^2 H a_o} \end{aligned}\right\} \quad i = x,\ y,\ z \qquad (3.1.1.a,b)$$

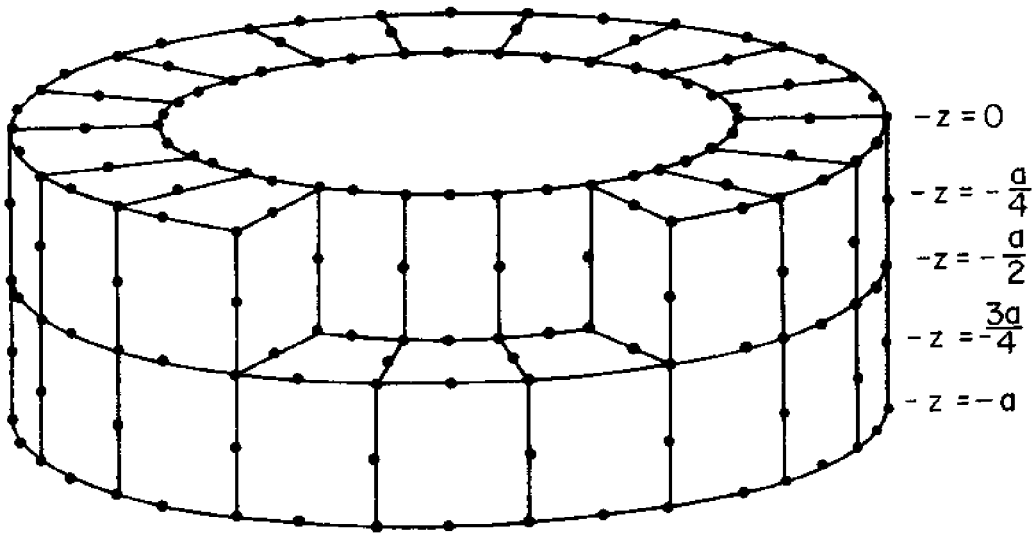

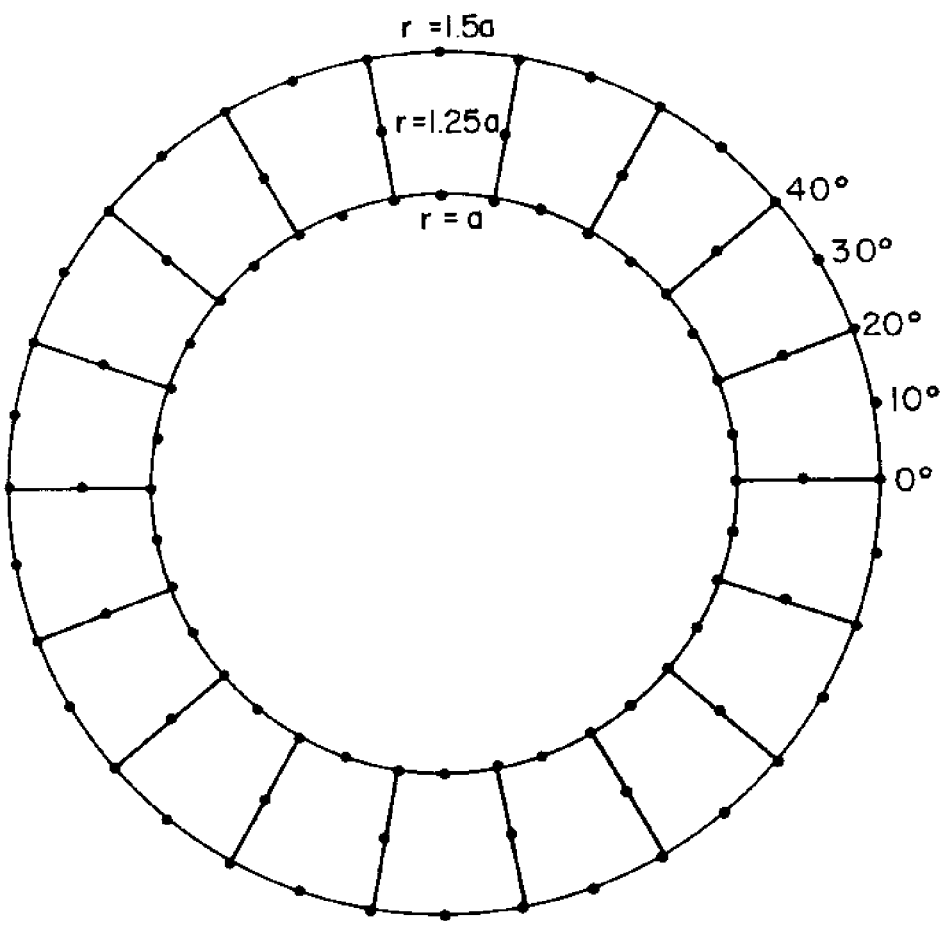

Figure 3.2 Finite Element Structure for a Uniform Cylinder

36 elements, 342 nodal points.

where H, a are the typical draft and horizontal dimension of the body respectively. F_i refers to the force component in the i direction, and M_i the moment component about the i-axis, i.e.

$$\vec{F} = \mathrm{Re}[\ \{F_i\}^T\ e^{-i\omega t}]\ ,\quad \vec{M} = \mathrm{Re}[\ \{M_i\}^T\ e^{-i\omega t}]$$

For example, in this case, we have

$$C_{F_x} = \frac{F_x}{\rho g \pi\ a h a_o} = -\frac{1}{\pi h} \int_{-h}^{0} \int_{0}^{2\pi} \frac{\phi}{\left(-\frac{i g a_o}{\omega}\right)} \cos\theta\ d\theta\ dz \tag{3.1.2}$$

which is evaluated by numerical integration of the solution $\{\phi\}$.

Comparisons are made to known analytic results (see, for example, MacCamy and Fuchs, 1952):

$$\begin{pmatrix} \alpha_{mn} \\ \beta_{mn} \end{pmatrix} = \begin{cases} -\varepsilon_n\ i^n\ \dfrac{J_n'(k_o a)}{H_n^{(1)'}(k_o a)}\ \dfrac{1}{\cosh k_o h} \begin{pmatrix} \cos n\theta_I \\ \sin n\theta_I \end{pmatrix} & \text{for } m = 0 \\ 0 & \text{for } m \neq 0 \end{cases} \tag{3.1.3}$$

$$\frac{\eta}{a_o} = \sum_{n=0}^{\infty} \varepsilon_n\ i^n \cos n(\theta - \theta_I)\ \left[J_n(k_o r) - \frac{J_n'(k_o a)}{H_n^{(1)'}(k_o a)} H_n^{(1)}(k_o r)\right] \tag{3.1.4}$$

and

$$C_{F_x} = \frac{4 \cos\theta_I}{\pi k_o^2\ a h} \frac{\tanh k_o h}{H_1^{(1)'}(k_o a)} \tag{3.1.5}$$

$k_o a$	C_{F_x} MAGNITUDE	C_{F_x} PHASE	η/a_o at $r = a$, $\theta = 0$ MAGNITUDE	$\theta = 0$ PHASE	$\theta = \pi/2$ MAGNITUDE	$\theta = \pi/2$ PHASE	$\theta = \pi$ MAGNITUDE	$\theta = \pi$ PHASE	
0.5	.92684	1.75052	1.43159	- .89376	.97834	- .14149	.99513	.99919	ANALYTIC
	.92675	1.75073	1.43215	- .89349	.97863	- .14110	.99597	.99965	FEM
1	1.04461	1.92866	1.70707	-1.20729	1.17128	- .26486	.88819	1.97993	ANALYTIC
	1.04429	1.92903	1.70758	-1.20698	1.17041	- .26522	.88891	1.98056	FEM
2	.54066	1.45696	1.85852	-2.15222	1.29659	- .05608	.73185	-2.51741	ANALYTIC
	.54009	1.45568	1.86347	-2.15381	1.29066	- .05960	.73499	-2.52060	FEM
4	.19979	- .29682	1.94666	2.18331	1.32091	- .04645	.54326	.87932	ANALYTIC
	.19841	- .34190	1.95468	2.13330	1.24850	- .12744	.54794	.72607	FEM
6	.10873	-2.22042	1.97158	.20828	1.33563	- .04263	.43974	-3.11790	ANALYTIC
	.10805	-2.46338	1.86278	- .05721	1.03539	- .54210	.99513	.99965	FEM

Table 3.1 Comparison Between Analytic and Finite Element Results for Scattering off a Uniform Cylinder ($\theta_I = \pi$): Horizontal Force Coefficient C_{F_x} and Free Surface Elevation η/a_o at $r = a$.

n	$\lvert\alpha_{on}\rvert$ COMPUTED	$\lvert\alpha_{on}\rvert$ THEORETICAL	$\lvert\beta_{on}\rvert$ COMPUTED	$\lvert H_n^{(1)}(k_o r_S)\rvert$	$\lvert\alpha_{1n}\rvert$ COMPUTED	$\lvert\beta_{1n}\rvert$ COMPUTED	$K_n(\kappa_1 r_S)$	$\lvert\alpha_{2n}\rvert$ COMPUTED	$\lvert\beta_{2n}\rvert$ COMPUTED	$K_n(\kappa_2 r_S)$	
0	3.1786×10^{-1}	3.1806×10^{-1}	0.	6.3893×10^{-1}	4.3667×10^{-3}	0.	7.7690×10^{-3}	9.2842×10^{-1}	0.	3.9503×10^{-5}	.
1	4.5437×10^{-1}	4.5399×10^{-1}	2.6227×10^{-5}	6.9375×10^{-1}	7.5561×10^{-3}	4.7437×10^{-4}	8.6241×10^{-3}	1.7222×10	3.3863×10^{-2}	4.1588×10^{-5}	.
2	1.0765×10^{-1}	1.0775×10^{-1}	2.5023×10^{-5}	9.6064×10^{-1}	8.1164×10^{-4}	5.5296×10^{-4}	1.1757×10^{-2}	1.5015×10^{-1}	2.1417×10^{-2}	4.8505×10^{-5}	.
3	4.5773×10^{-3}	4.6072×10^{-3}	2.6910×10^{-6}	2.1613	1.6645×10^{-3}	3.7254×10^{-4}	1.9498×10^{-2}	5.1925×10^{-1}	2.9639×10^{-2}	6.2586×10^{-5}	.
4	9.2719×10^{-5}	9.8327×10^{-5}	4.1044×10^{-7}	7.3619	5.6594×10^{-4}	1.4088×10^{-4}	3.8805×10^{-2}	1.7695×10^{-1}	1.3230×10^{-2}	8.9144×10^{-5}	.
5	6.3953×10^{-7}	1.2543×10^{-6}	3.8556×10^{-8}	3.7190×10	5.1419×10^{-5}	2.1634×10^{-5}	9.1276×10^{-2}	2.3676×10^{-2}	7.7892×10^{-3}	1.3976×10^{-4}	.
6	9.9653×10^{-9}	1.0609×10^{-8}	5.7707×10^{-9}	2.4057×10^{2}	1.0952×10^{-5}	3.2649×10^{-6}	2.4985×10^{-1}	1.7037×10^{-3}	6.2347×10^{-3}	2.40397×10^{-4}	.
7	7.2035×10^{-10}	6.3852×10^{-11}	1.2038×10^{-9}	1.8874×10^{3}	1.5324×10^{-6}	4.8261×10^{-7}	7.8449×10^{-1}	6.8944×10^{-4}	2.5935×10^{-3}	4.5196×10^{-4}	.
8	4.6155×10^{-11}	2.8748×10^{-13}	1.0010×10^{-10}	1.7375×10^{4}	1.9536×10^{-7}	1.1768×10^{-7}	2.7892	6.7291×10^{-4}	5.6510×10^{-4}	9.2516×10^{-4}	.
.	.	.	.	.	.	.	.	.	.	.	
.	.	.	.	.	.	.	.	.	.	.	
.	.	.	.	.	.	.	.	.	.	.	

Table 3.2 Comparison between analytic and finite element results for scattering off a uniform cylinder ($\theta_I = \pi$): coefficients α_{mn}, β_{mn} of the exterior solution, $k_o a = 1$.

(Note: theoretical $\alpha_{mn} = 0$ for $m \neq 0$ and $\beta_{mn} = 0$ for all m, n)

For $\theta_I = \pi$, the comparison for a range of wavelengths $k_o a$ for C_{F_x} and $\frac{\eta}{a_o}$ are presented in Table 3.1. It is evident that the results are quite satisfactory(<1%) for up to $k_o a \sim 4$. This implies a maximum $(k_o L_e)_{max}$ of about 1.9, ($\lambda_{min} \sim 3.3\ L_e$). In Table 3.2, a sample of the coefficients calculated for the case $k_o a = 1$ is listed for comparison. Note that their contribution to ϕ_s' decreases rapidly (though the magnitude of the coefficients themselves are not necessarily small) due to the magnitude of the Bessel functions.

See also Section 4.2 for summary of present and other results.

3.2 Circular Cylindrical Platform in Constant Water Depth

We consider a fixed dock in the form of a circular cylinder with its axis vertical. The radius of the cylinder is designated by a and the draft by H. The water depth h is constant. Specifically we have chosen $H = .5a$ and $h = .75a$ (see Fig. 3.3).

The finite element grid system now has a total of 56 elements (two rings of 16 elements each stacked vertically outside the dock and 24 under it) and 435 nodes (see Fig. 3.4). Note in particular the use of the hexahedral elements in the center core, and the choice of greater node density near sharp edges.The average element dimension for this example is $L_e \sim .36a$. Again, 5 eigenvalues and a total of 99 terms ($M = 4$; $N_o = 12$, $N_1 = N_2 = N_3 = N_4 = 10$) are used in the outer series solution (Eq. (2.3.2)), and we choose $\phi_I = \pi$. The vertical and horizontal force coefficients are now respectively

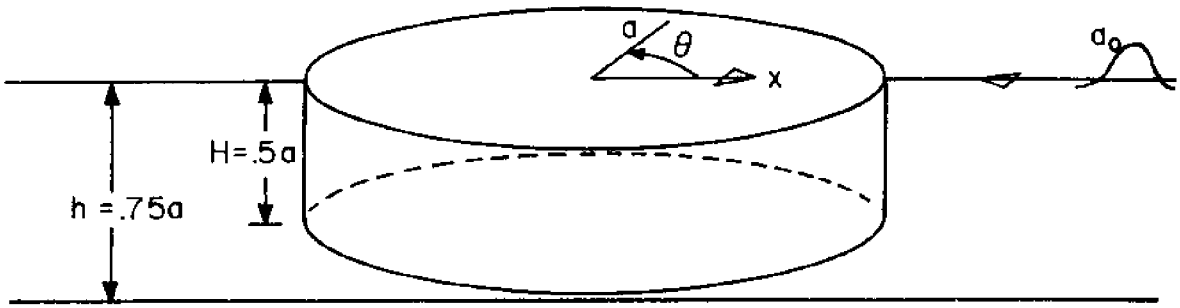

Figure 3.3 Wave incident on a floating cylindrical dock of radius a ($\theta_I = \pi$; h = .75 a)

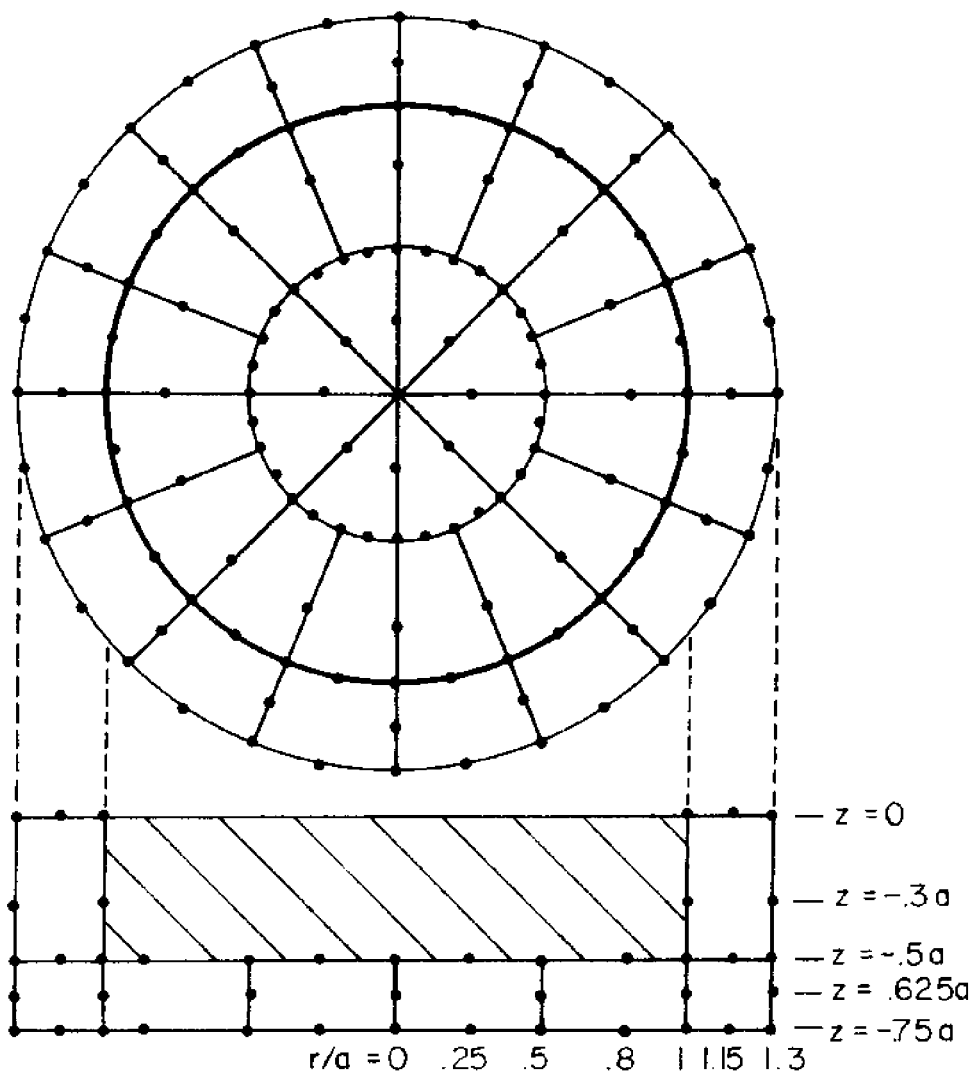

Figure 3.4 Finite element structure for a floating dock: 56 elements, 435 nodal points

$$C_{F_z} = \frac{F_z}{\rho g \pi a H a_o} = \frac{1}{\pi H} \int_0^a \int_0^{2\pi} \left(\frac{\phi}{-\frac{i g a_o}{\omega}} \right) d\theta \, dr \tag{3.2.1}$$

and

$$C_{F_x} = \frac{F_x}{\rho g \pi a H a_o} = \frac{1}{\pi H} \int_{-H}^{0} \int_0^{2\pi} \left(\frac{\phi}{-\frac{i g a_o}{\omega}} \right) \cos\theta \, d\theta \, dz \tag{3.2.2}$$

A table of these coefficients for a range of $k_o a$ and their plot in comparison to those obtained by Garrett, 1971, is presented in Table 3.3 and Fig. 3.5.a,b. The results are clearly satisfactory and discrepancies are imperceptible on the graphs for the entire range we considered. A complete list of nodal potential and series coefficient solutions for $k_o a = 1$ is also given as a part of the sample computer output in Section 5.2.4.4.

$k_o a$	C_{F_x} MAGNITUDE	C_{F_x} PHASE	C_{F_z} MAGNITUDE	C_{F_z} PHASE
.5	.75528	1.66158	1.58020	- .17740
1	1.06098	1.76166	1.10559	- .52303
2	.75928	1.37349	.48747	-1.39937
4	.35205	- .37081	.10316	-3.36901
6	.21295	-2.40384	.03283	-5.40133

Table 3.3 Computed horizontal and vertical force coefficients for a semi-immersed circular cylinder ($\frac{h}{a} = .75$, $\frac{H}{a} = .5$)

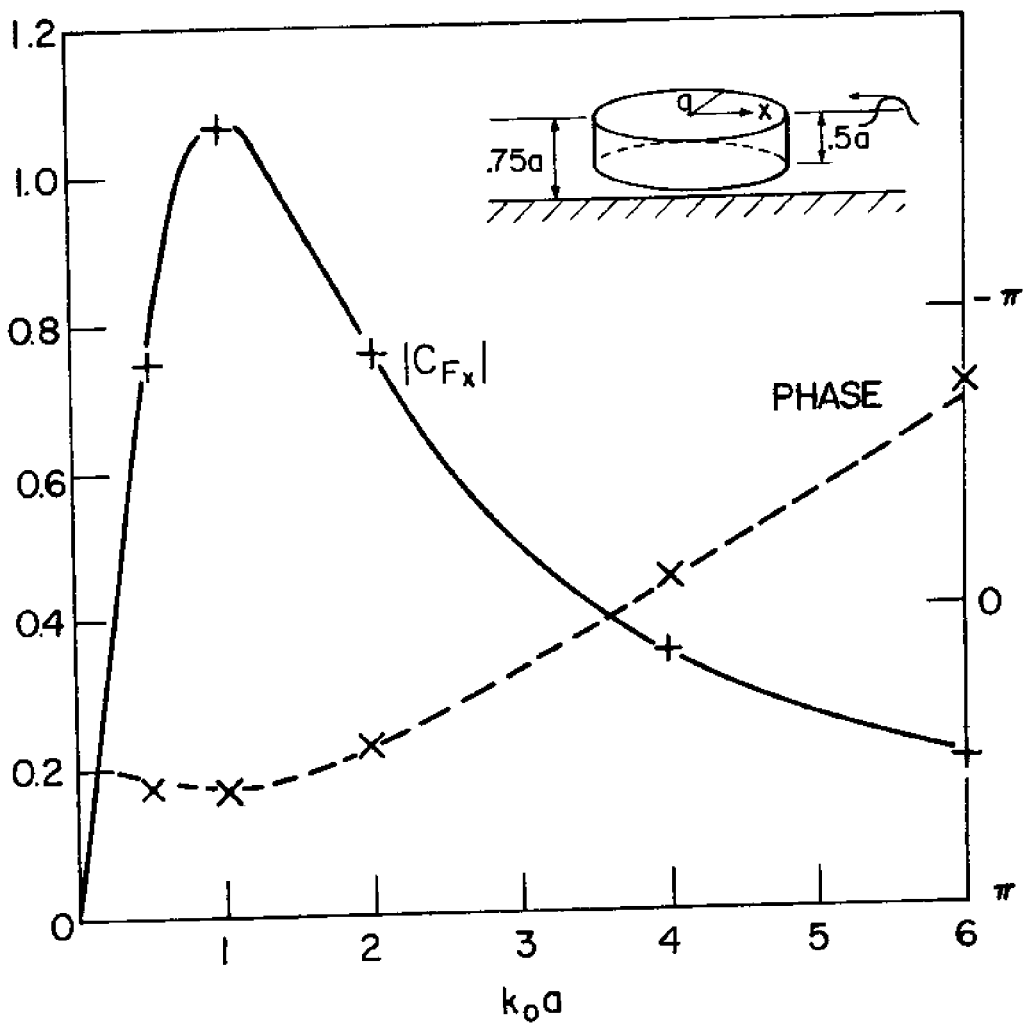

Figure 3.5 (a) Horizontal force coefficient for a semi-immersed cylinder ($\frac{h}{a}$ = .75; $\frac{H}{a}$ = .5: $\theta_I = \pi$).

+, amplitude; X, phase: finite element solution

____, amplitude; ---- phase: Garrett, 1971 results

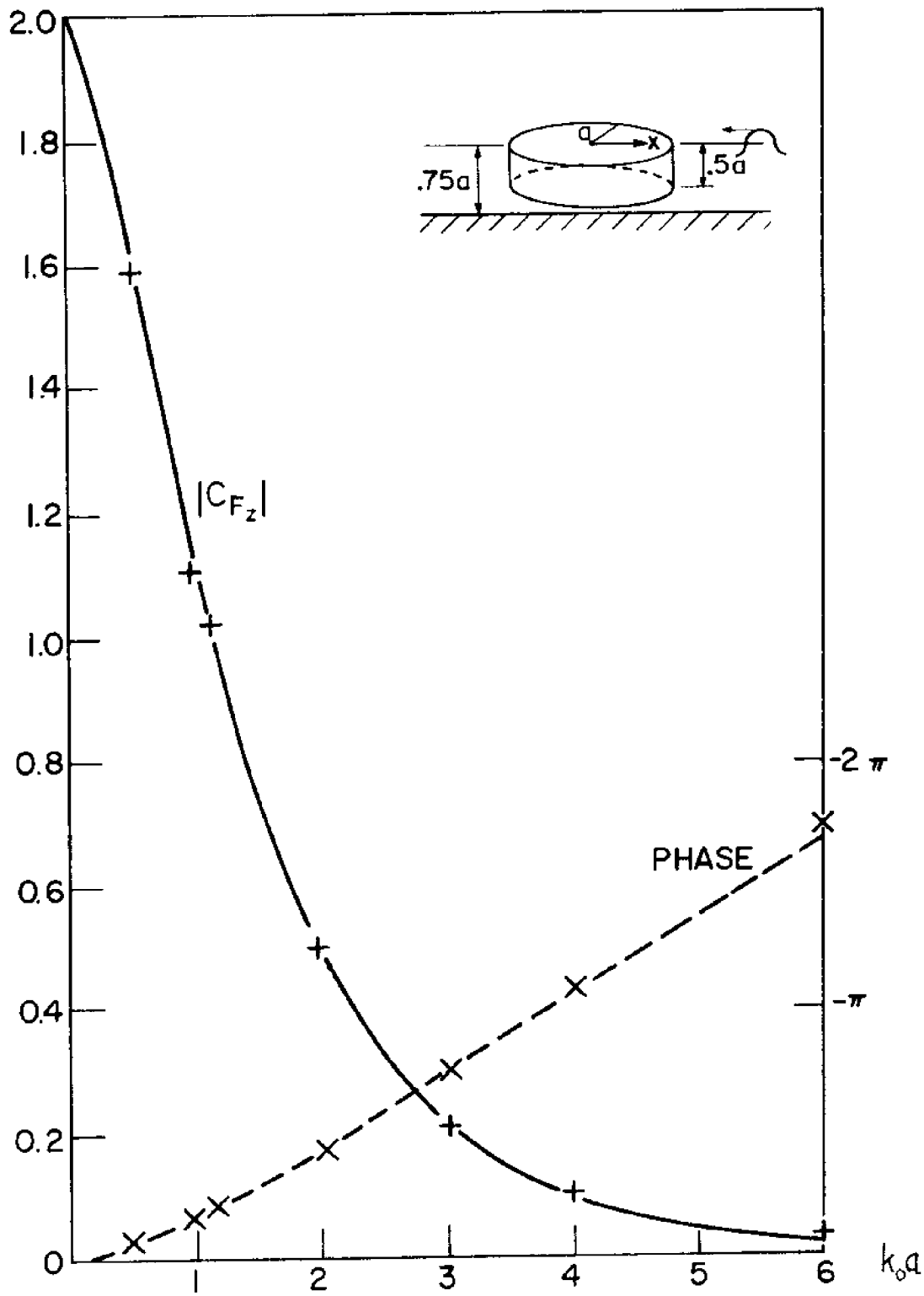

Figure 3.5 (b) Vertical force coefficient for a semi-immersed cylinder (See description in Figure 3.5 (a))

3.3 Rectangular Barge in Constant Depth

We now consider diffraction by a fixed semi-immersed (draft H) rectangular box in constant water depth h. Unlike the previous two examples, this problem must be treated as a fully three-dimensional one. We choose a special case of a square barge, length 2a, H = .5a and h = a, and consider two different incidence angles $\theta_I = \pi$ and $5\pi/4$.

The finite element grid employed is similar to the one we use for the circular dock and has 56 elements and 435 nodes. The previous choice of the number of series terms is still kept.

The force and moment coefficients for both angles of incidence over a range of wave number $k_o a$ are plotted in Figs. 3.6.a,b,c and Figs. 3.7.a,b,c. In general, for a given grid, the finite element approximation becomes more accurate as the wavelength relative to it increases ($k_o a$ decreases). On account of the comparisons in the last section for a cylindrical dock where a similar grid system is used, we expect the present results to be reasonably reliable at least for $k_o a$ up to ~ 6, and certainly far beyond the regions of peak values around $k_o a = 1$.

In Figs. 3.8.a,b,c,d and Figs. 3.9.a,b,c,d, the run-up, η/a_o, on the sides of this square barge for $k_o a = 1,2,3,4$ and both incidence angles are presented. Note that this local value becomes quite highly varying as the wavelength decreases to about the body length ($k_o a = 4$), and the interpolation between the nodal values in those instances are somewhat unreliable. Furthermore, due to the finite element smoothing, both the value of $|\eta/a_o|$ (which is proportional to the potential) and its derivative are finite at the sharp edges, while according to two-dimensional potential flow around

a 90° wedge, the gradient of the potential exhibits a $r^{-1/3}$ type singularity. This local discrepency can in principle be corrected (see Chen and Mei, 1974) by constructing special analytic elements similar to S around all sharp edges and corners. Such a procedure is however, unnecessary if one is only interested in averaged (global) results such as forces and moments, or in local values in the major region not close to singularities. This is evidenced by comparisons for the circular dock where a bottom sharp edge is also present.

For a measure of the angular intensity of scattered wave energy, we define the differential scattering cross-section $|A(\theta)|^2$, where $A(\theta)$ is the angular variation of the far-field scattered wave, i.e.

$$\phi_s \sim \frac{-iga_o}{\omega} \sqrt{\frac{2}{\pi}}\, e^{-i\pi/4} \cosh k_o(z+h) \frac{e^{ik_o r}}{\sqrt{k_o r}} A(\theta) \qquad (k_o r \gg 1) \tag{3.3.1}$$

and if we substitute in this asymptotic form of ϕ_s into Eq. (1.3.4), we have

$$A(\theta) = \sum_{n=0}^{\infty} (-i)^n \left(\alpha_{on} \cos n\theta + \beta_{on} \sin n\theta\right) \Big/ \left(- \frac{iga_o}{\omega} \right) \tag{3.3.2}$$

The differential scattering cross-section, $|A(\theta)|^2$, as a function of θ for $k_o a = 1,2,3,4$ and the two incidence angles are given in Figs. 3.10.a,b,c,d and Figs. 3.11.a,b,c,d; and in polar coordinates in Figs. 3.12.a,b,c,d.(i), d.(ii) and in Figs. 3.13.a,b,c,d for a better physical picture.

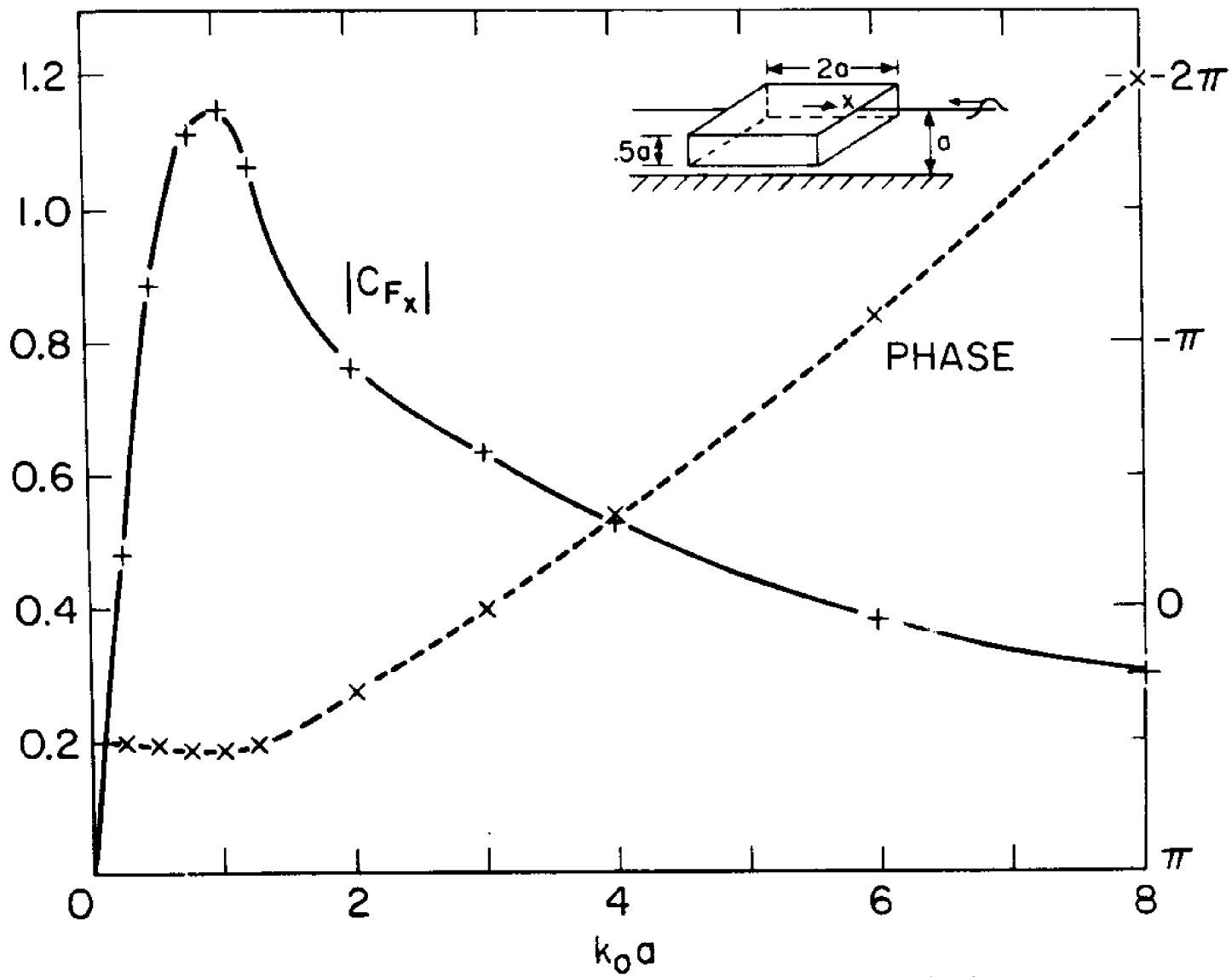

Figure 3.6(a) Forces on a square dock: ——— + ——— , magnitude; -- x --, phase. Normal incidence: $\theta_I = \pi$. a. Horizontal Force Coefficient

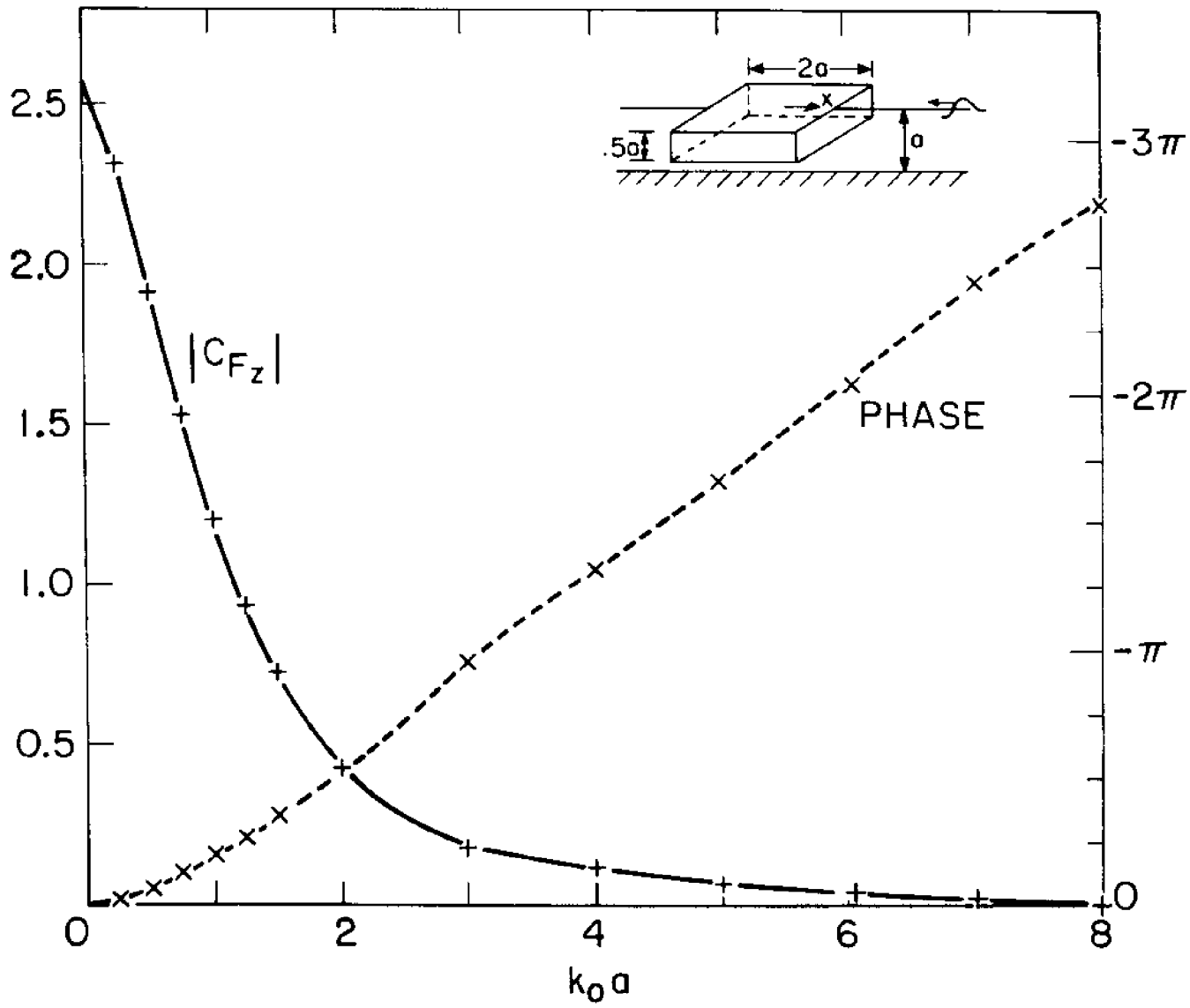

Figure 3.6(b) Forces on a square dock: —— + —— , magnitude; -- x -- , phase. Normal incidence: $\theta_I = \pi$. b. Vertical Force Coefficient

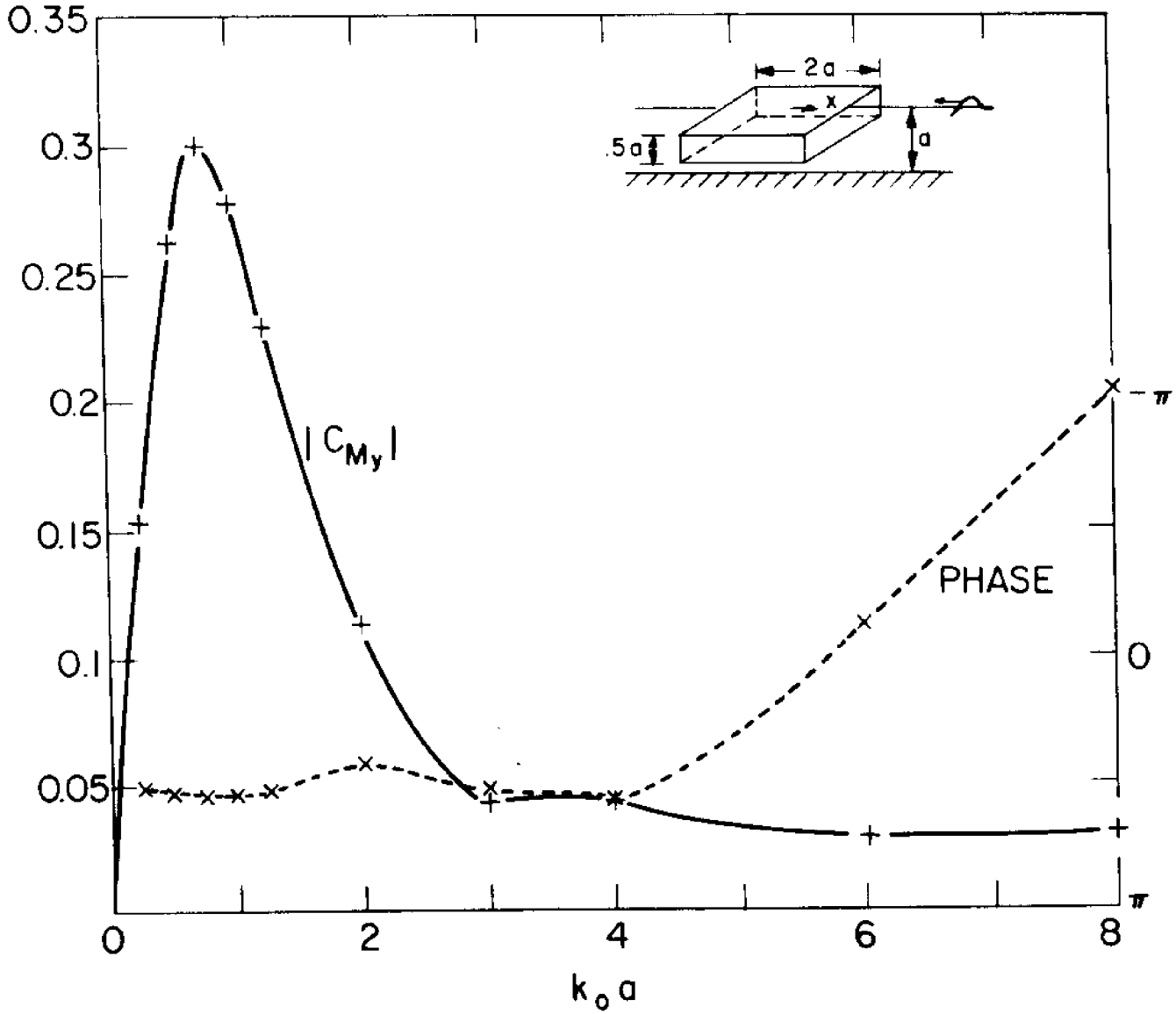

Figure 3.6(c) Forces on a square dock: —— + ——, magnitude; -- x --, phase. Normal incidence: $\theta_I = \pi$. c. Moment Coefficient About y-axis

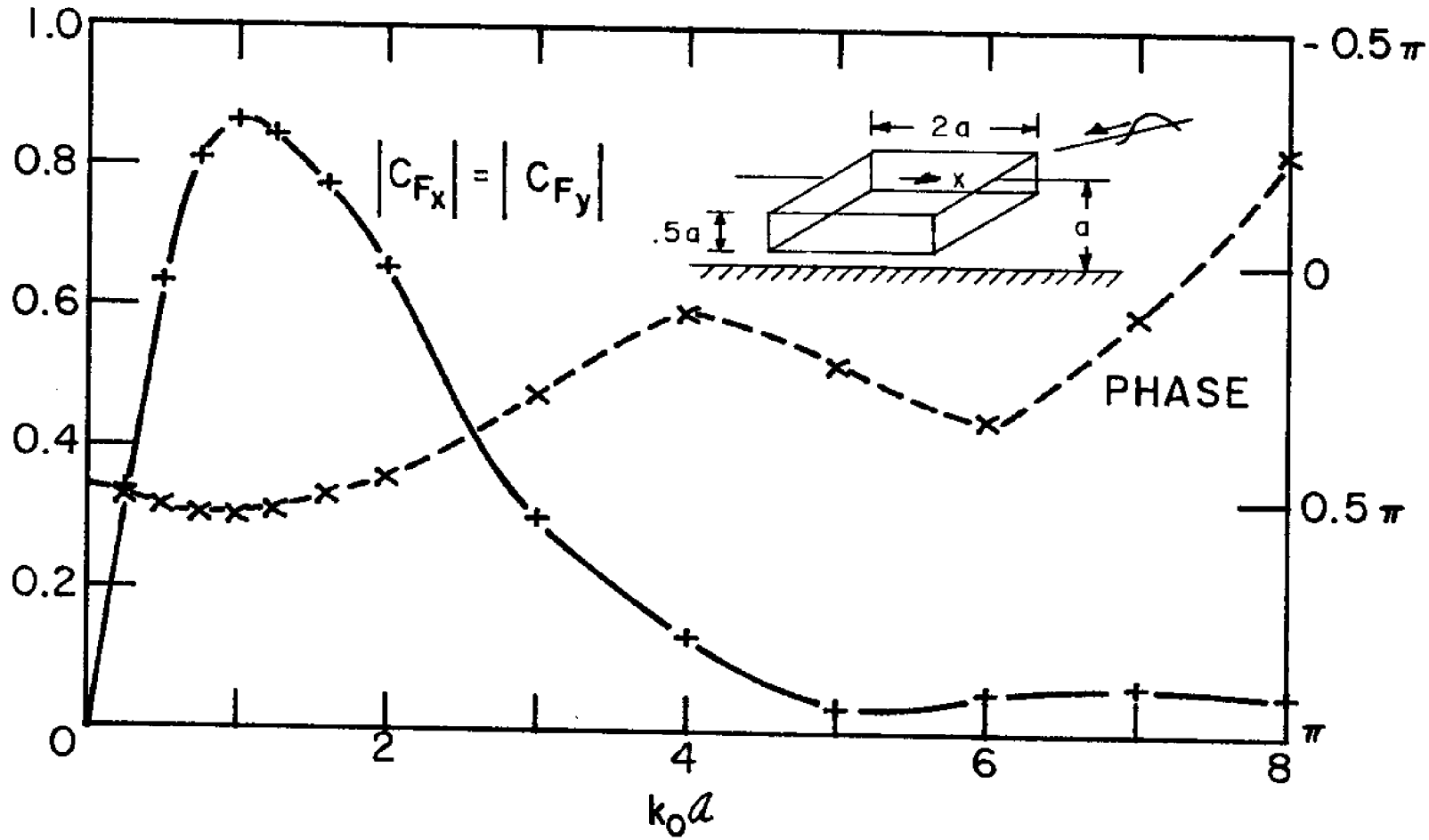

Figure 3.7(a) Forces on a Square Dock: ——— + ———, magnitude
-- x --, phase. Oblique Incidence: $\theta_I = 5\pi/4$.
a. Horizontal Force Coefficient

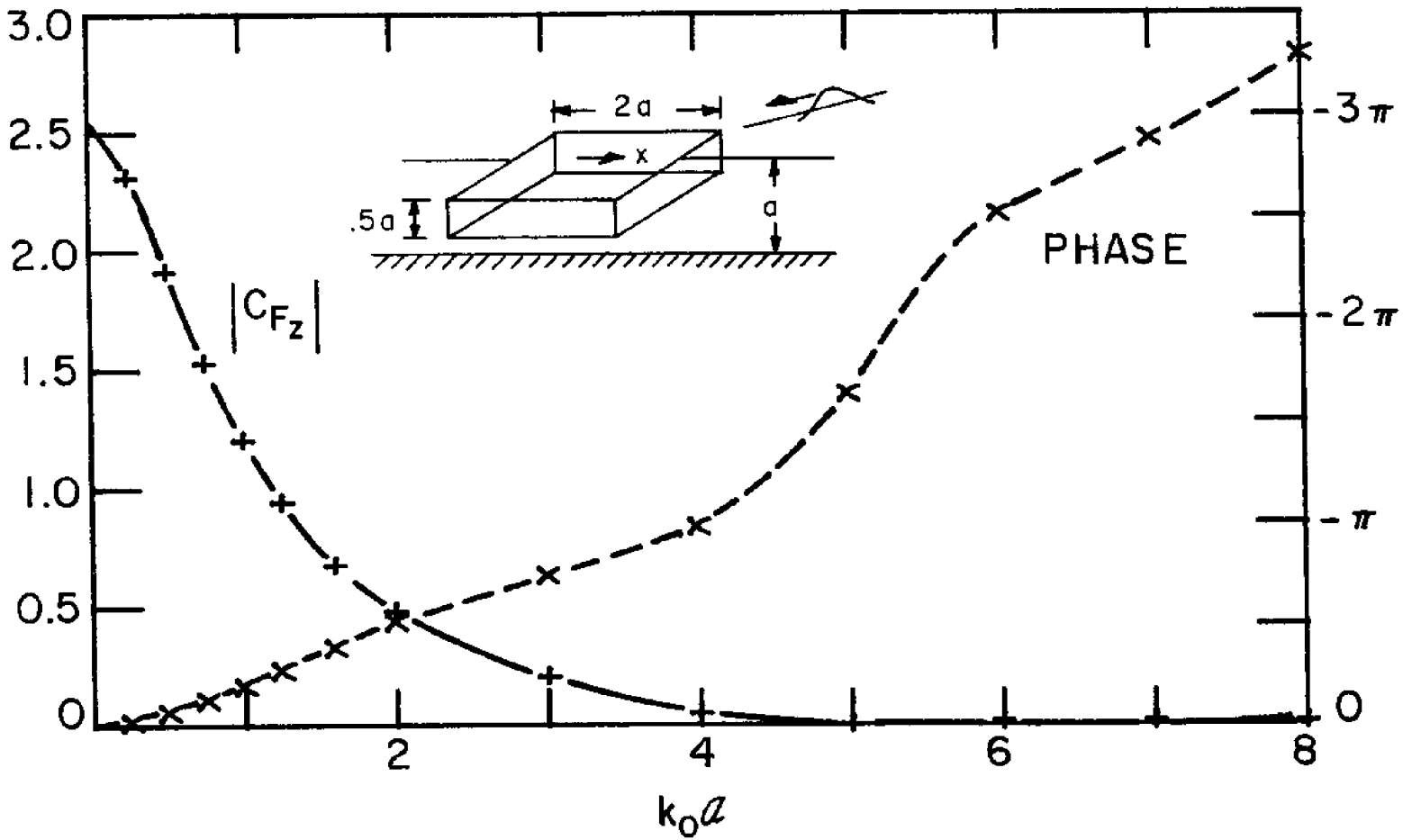

Figure 3.7(b) Forces on a Square Dock: ——— + ———, magnitude
-- x --, phase. Oblique Incidence: $\theta_I = 5\pi/4$.
b. Vertical Force Coefficient

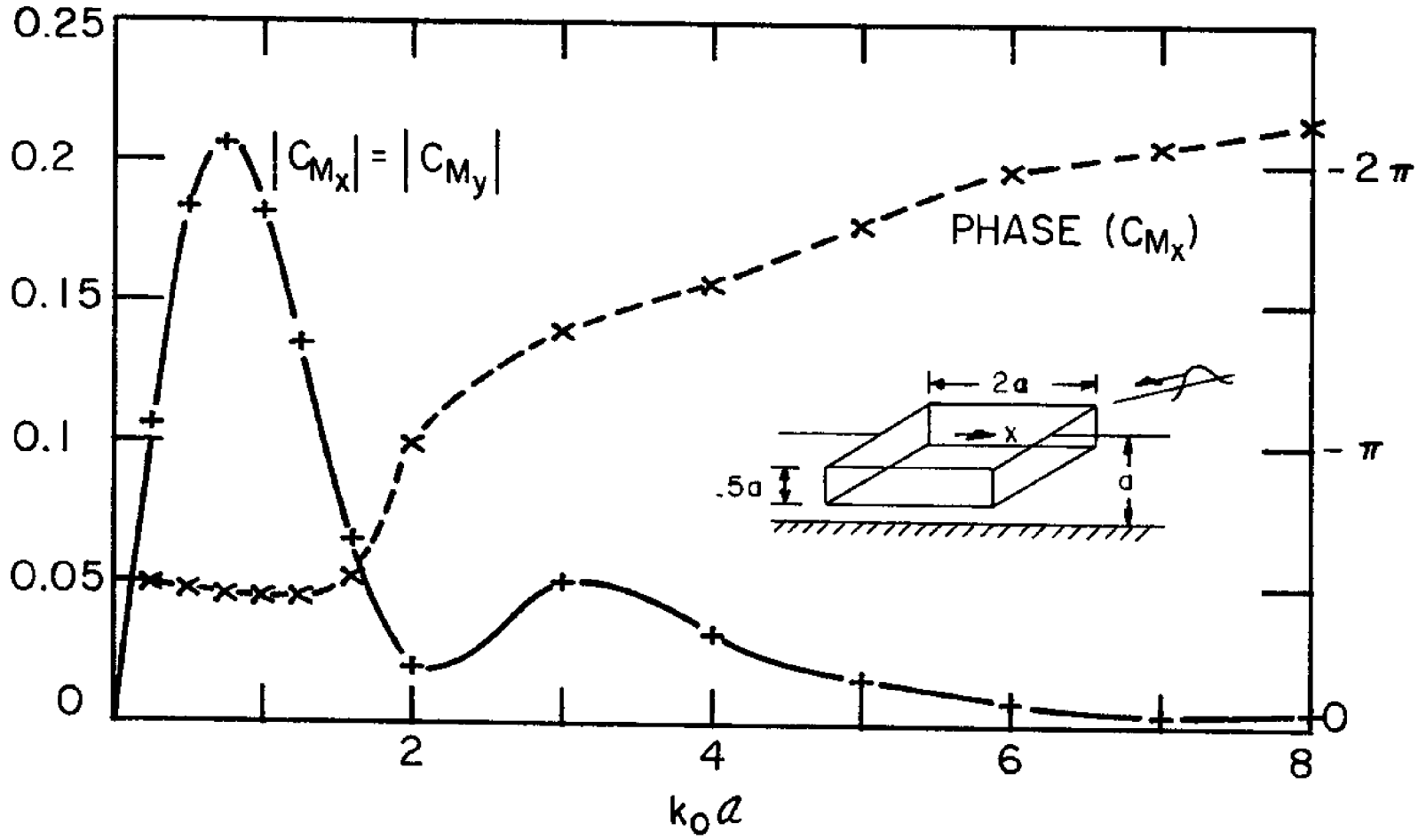

Figure 3.7(c) Forces on a Square Dock: ——— + ——— , magnitude
-- x --, phase. Oblique Incidence: $\theta_I = 5\pi/4$.
c. Moment Coefficient About Horizontal Axis

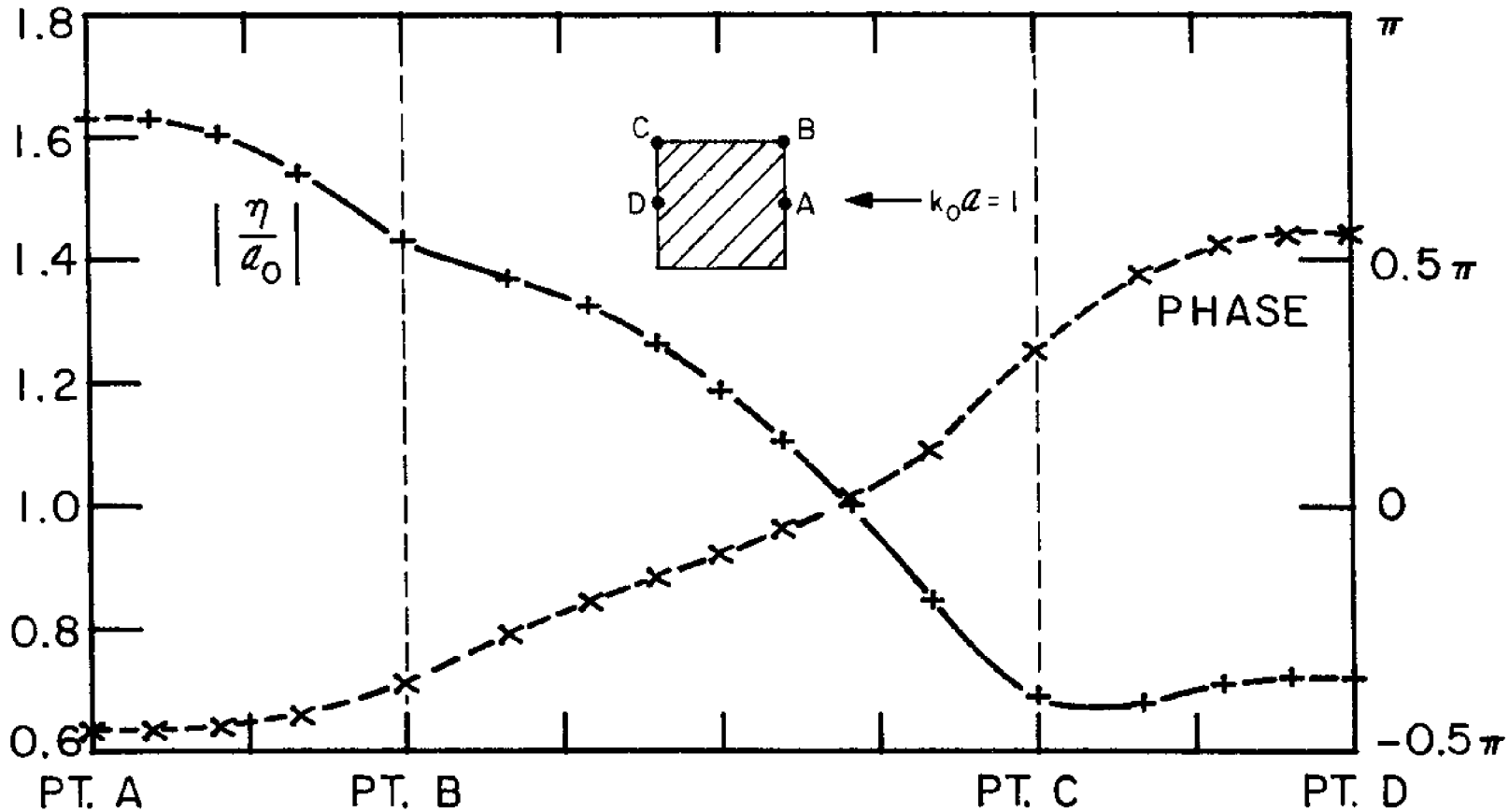

Figure 3.8(a) Run-up η/a_o, on the Sides of a Square Barge: (+) ——— : (nodal)magnitude; (x) ---- : (nodal) phase. Normal incidence: $\theta_I = \pi$.

a. $k_o a = 1$

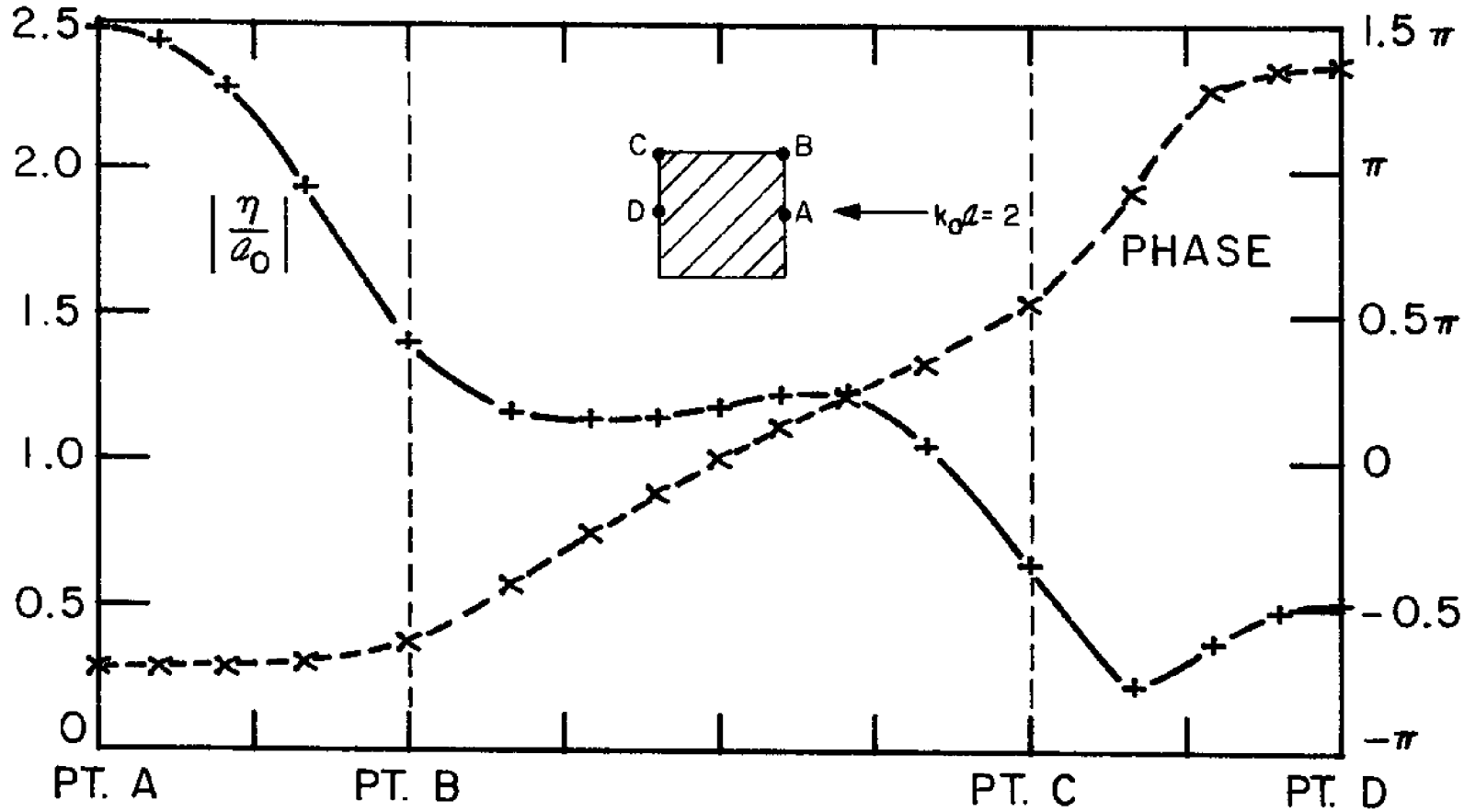

Figure 3.8(b) Run-up η/a_o, on the Sides of a Square Barge: (+) ——— : (nodal) magnitude; (x) ---- : (nodal) phase. Normal incidence: $\theta_I = \pi$.

b. $k_o a = 2$

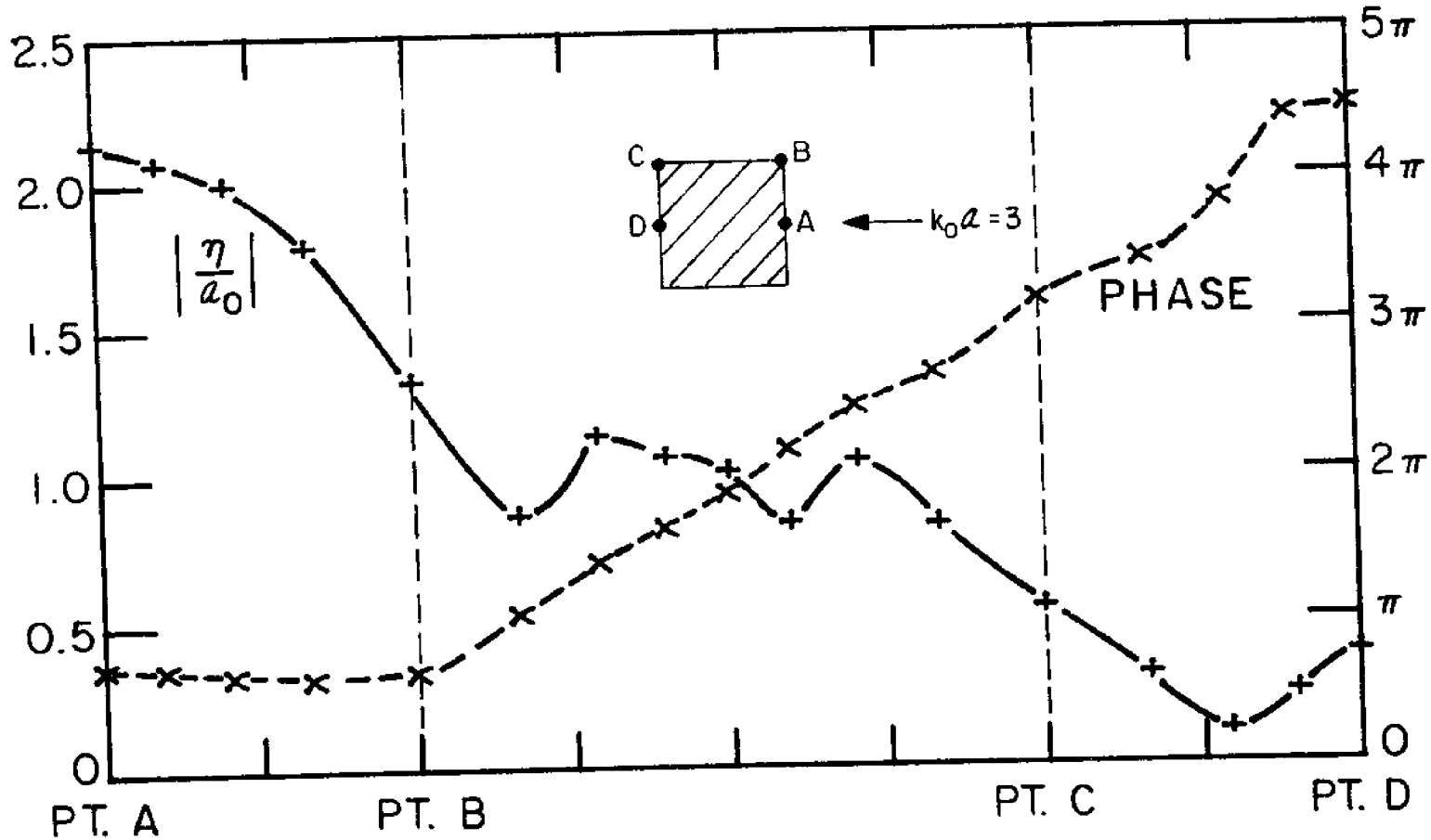

Figure 3.8(c) Run-up η/a_o, on the Sides of a Square Barge: (+) ——— : (nodal) magnitude; (x) ---- : (nodal) phase. Normal incidence: $\theta_I = \pi$.

c. $k_o a = 2$

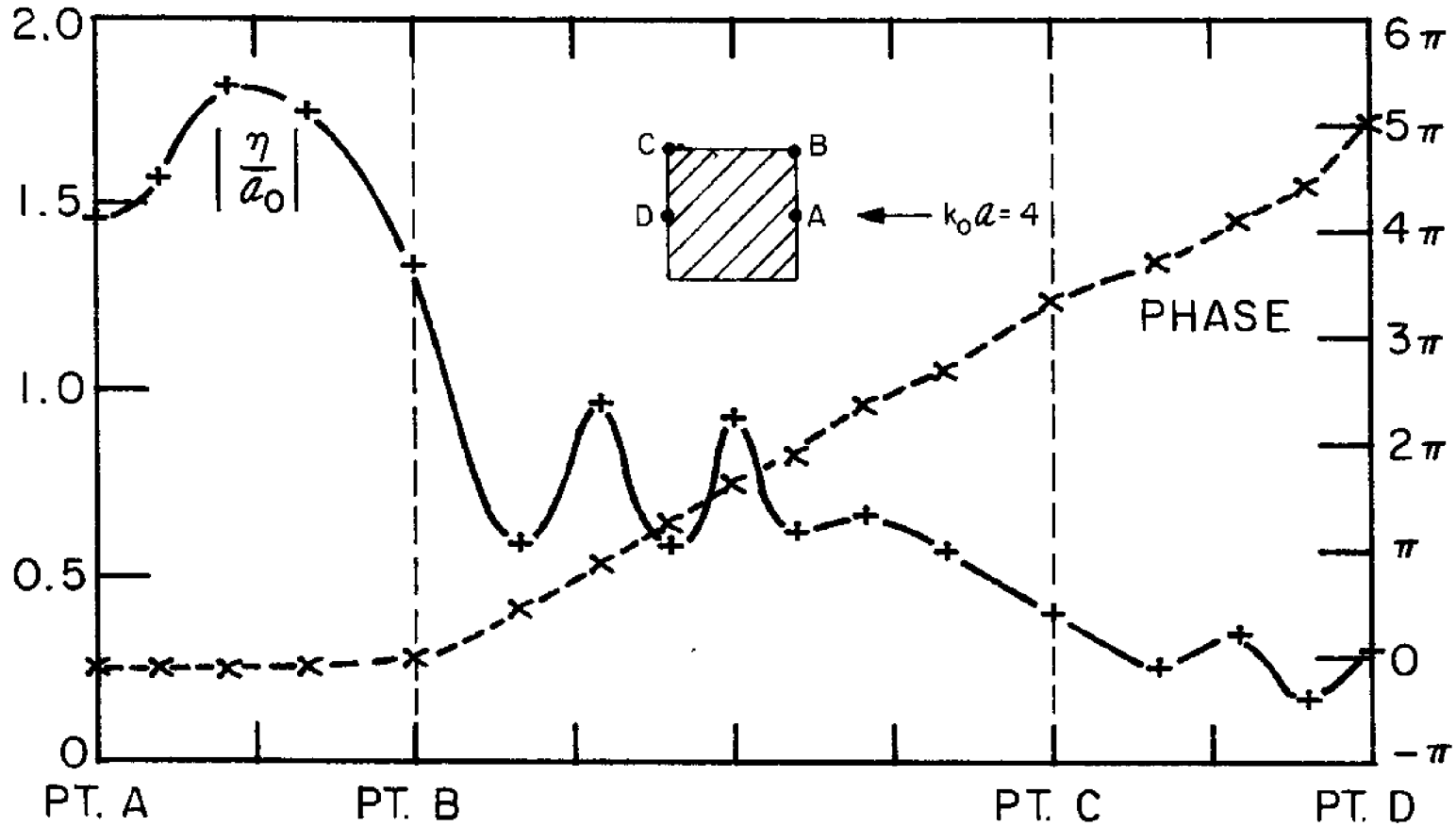

Figure 3.8(d) Run-up η/a_o, on the Sides of a Square Barge:
(+) ——— : (nodal) magnitude; (x) ---- : (nodal) phase.
Normal incidence: $\theta_I = \pi$.

d. $k_o a = 4$

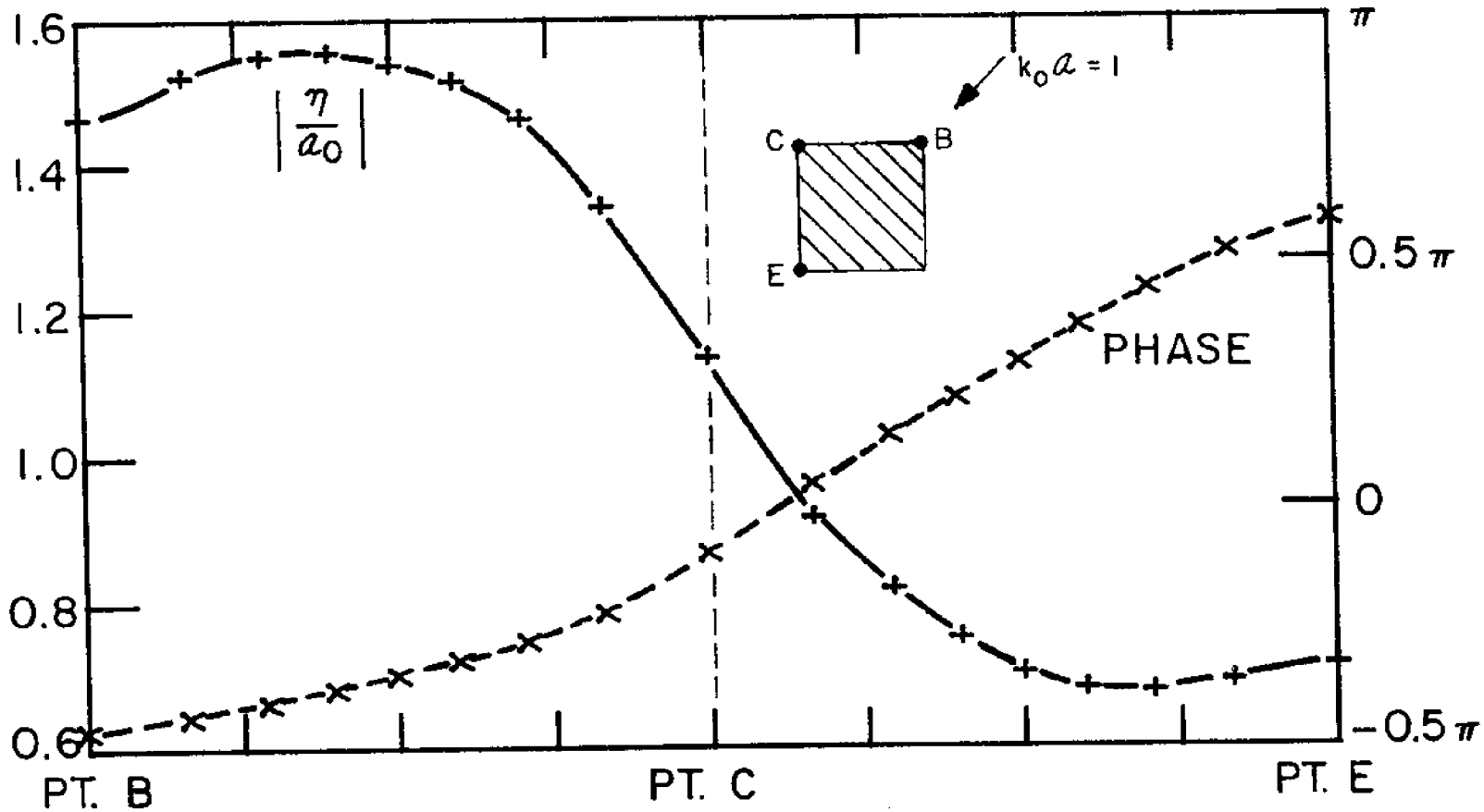

Figure 3.9(a) Run-up, η/a_o, on the Sides of a Square Barge:
(+) ——— : (nodal) magnitude; (x) ---- : (nodal) phase.
Oblique Incidence: $\theta_I = 5\pi/4$.
a. $k_o a = 1$

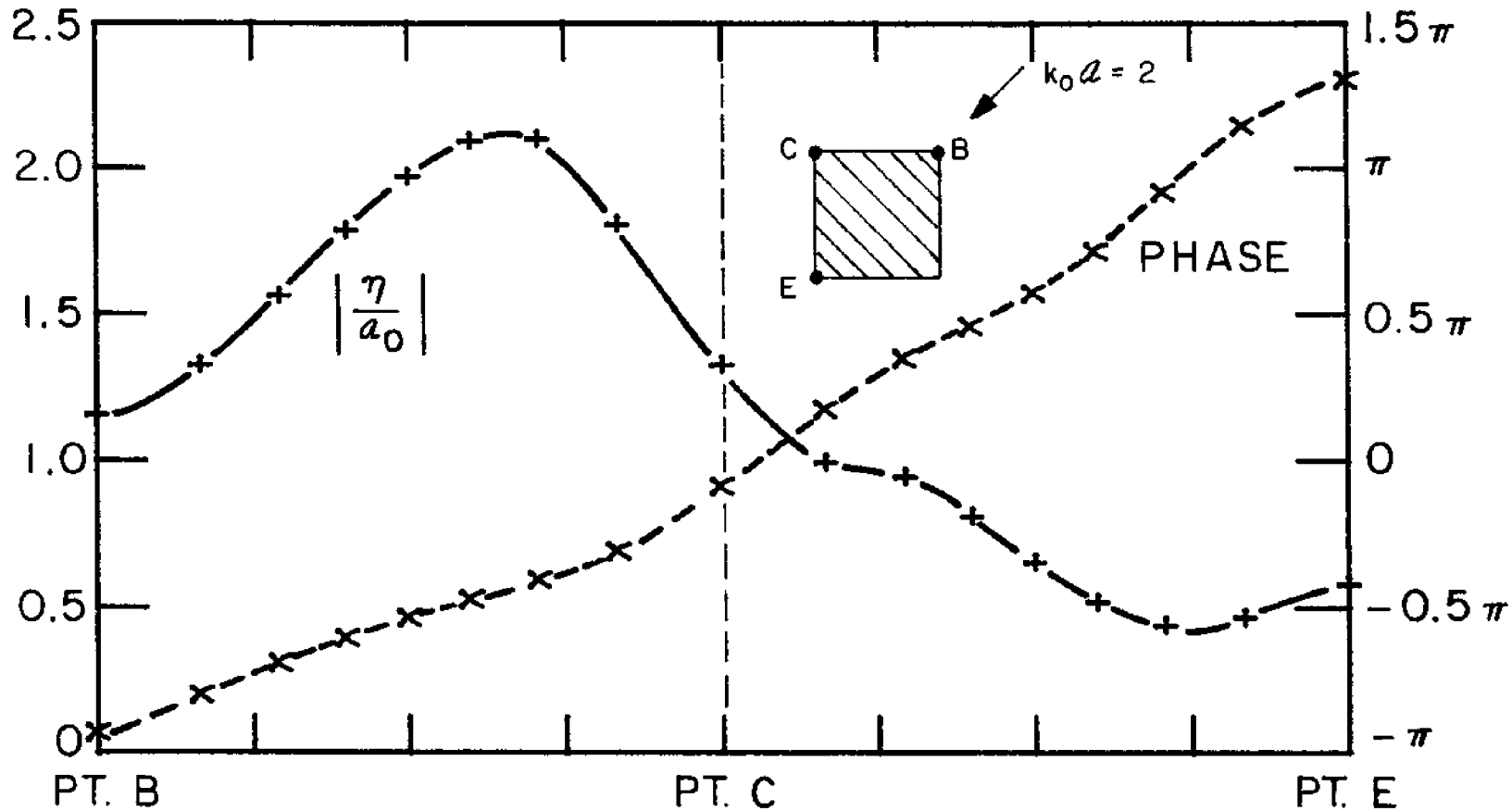

Figure 3.9(b) Run-up, η/a_o, on the Sides of a Square Barge:
(+) ——— : (nodal)magnitude; (x) ---- : (nodal) phase.
Oblique Incidence $\theta_I = 5\pi/4$.
b. $k_o a = 2$

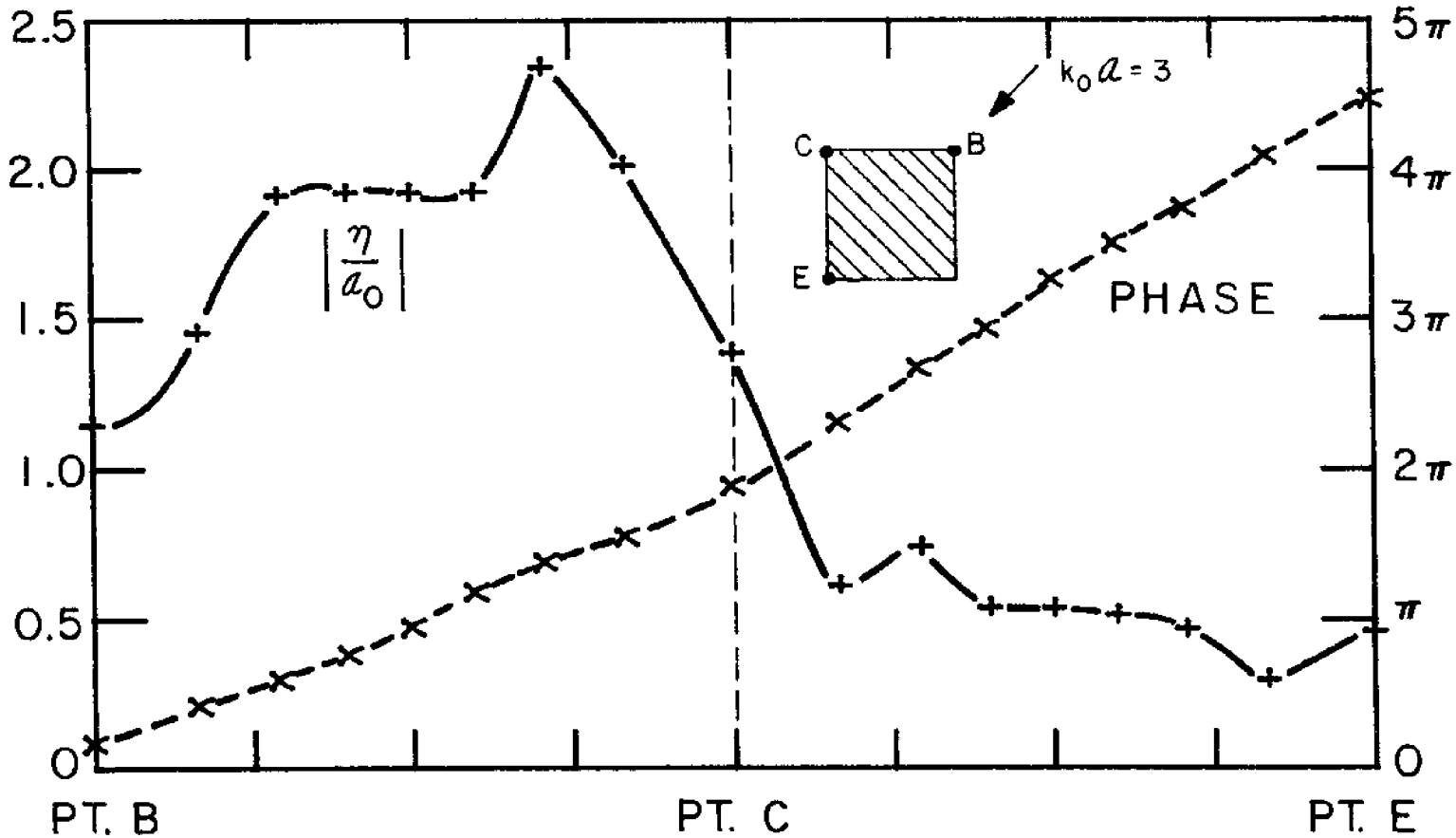

Figure 3.9(c) Run-up, η/a_o, on the Sides of a Square Barge:
(+) ——— : (nodal) magnitude; (x) ---- : (nodal) phase.
Oblique Incidence: $\theta_I = 5\pi/4$.
c. $k_o a = 3$

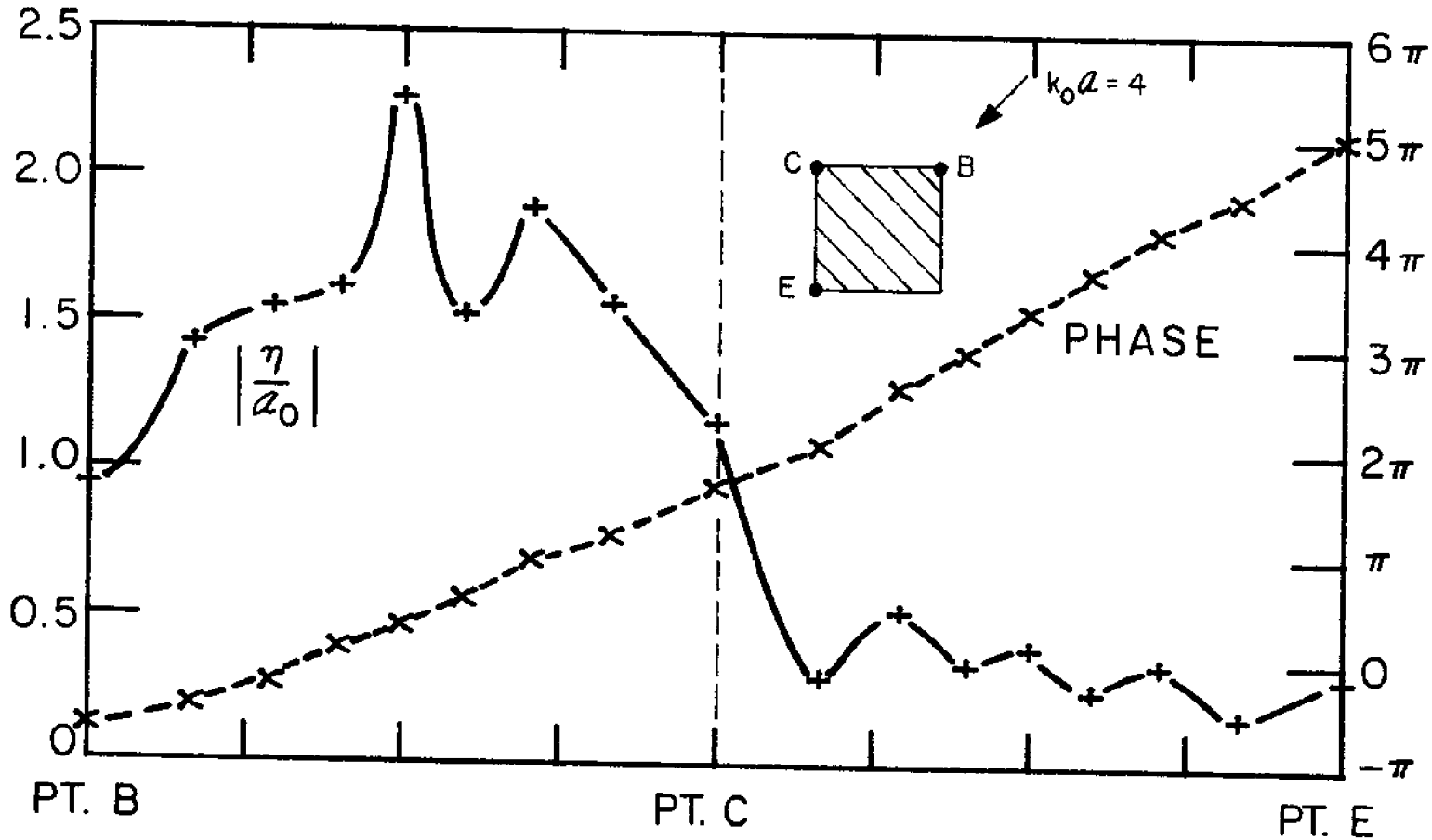

Figure 3.9(d) Run-up, η/a_o, on the Sides of a Square Barge:
(+) ——— : (nodal) magnitude; (x) ---- : (nodal) phase.
Oblique Incidence: $\theta_I = 5\pi/4$.
d. $k_o a = 4$

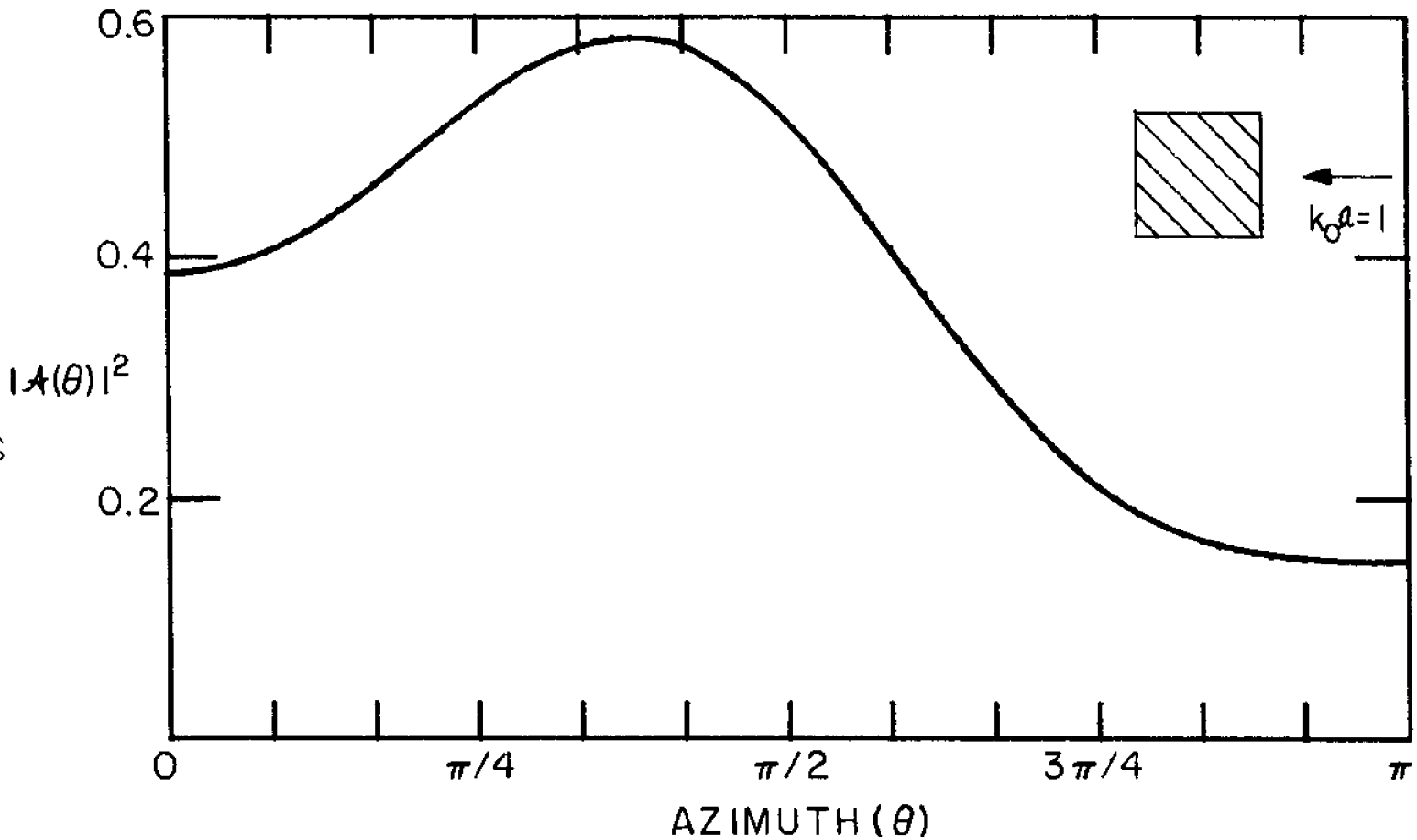

Figure 3.10(a) Differential Scattering Cross-section, $|A(\theta)|^2$, for a Square Barge. Normal Incidence: $\theta_I = \pi$.

a. $k_o a = 1$

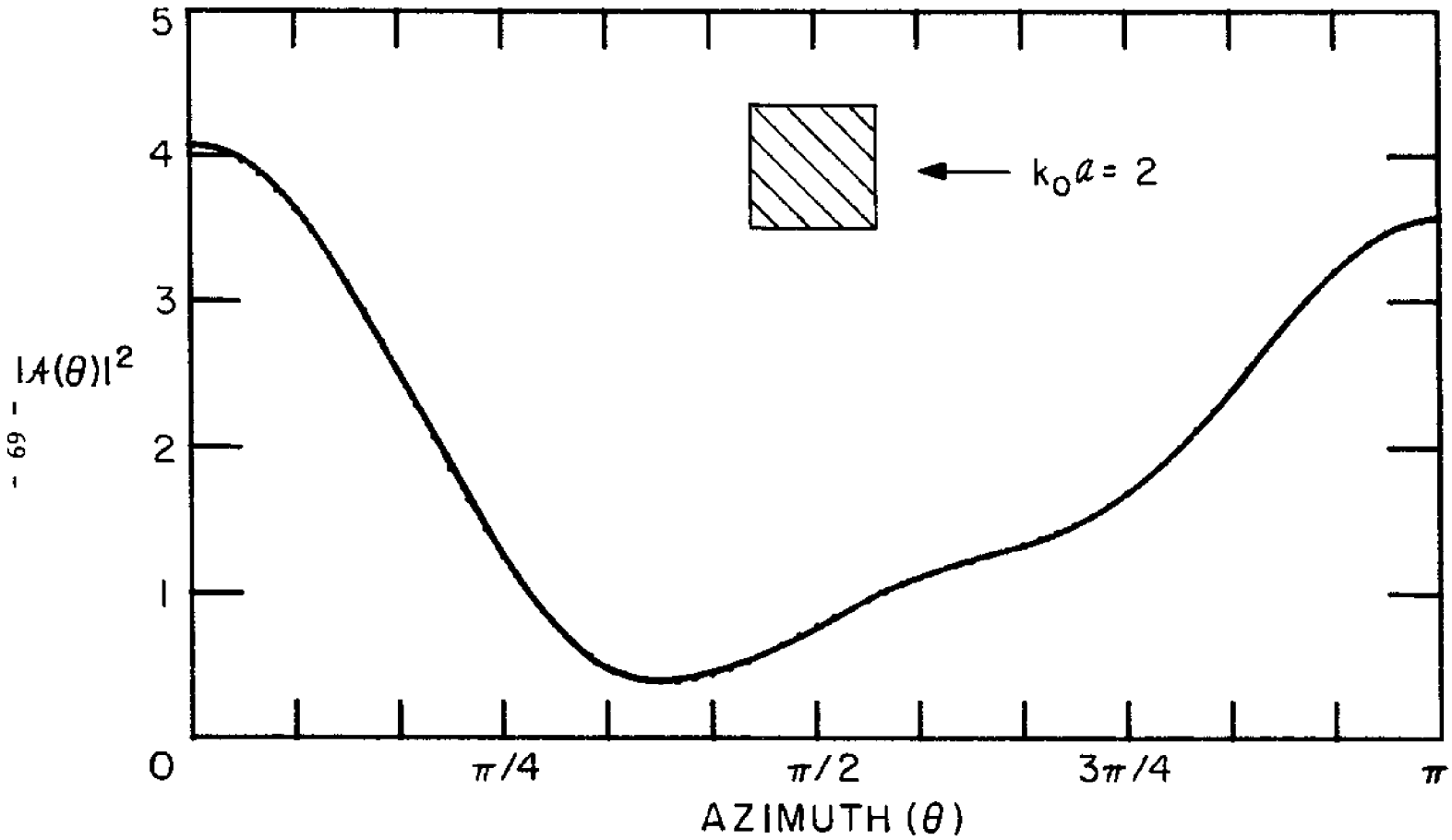

Figure 3.10(b) Differential Scattering Cross-section, $|A(\theta)|^2$, for a Square Barge. Normal Incidence: $\theta_I = \pi$.

b. $k_o a = 2$

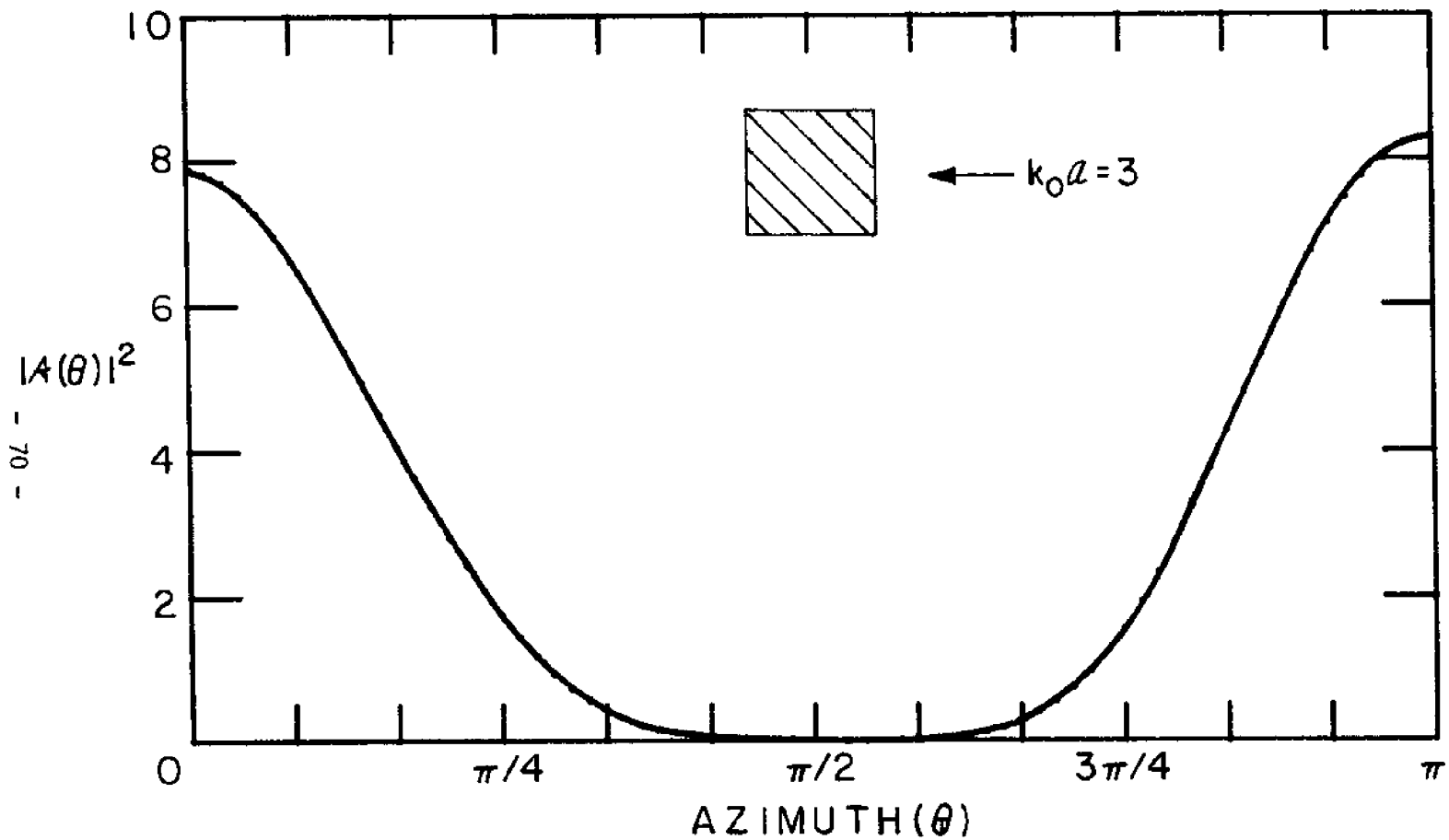

Figure 3.10(c) Differential Scattering Cross-section, $|A(\theta)|^2$, for a Square Barge. Normal Incidence: $\theta_I = \pi$.

c. $k_o a = 3$

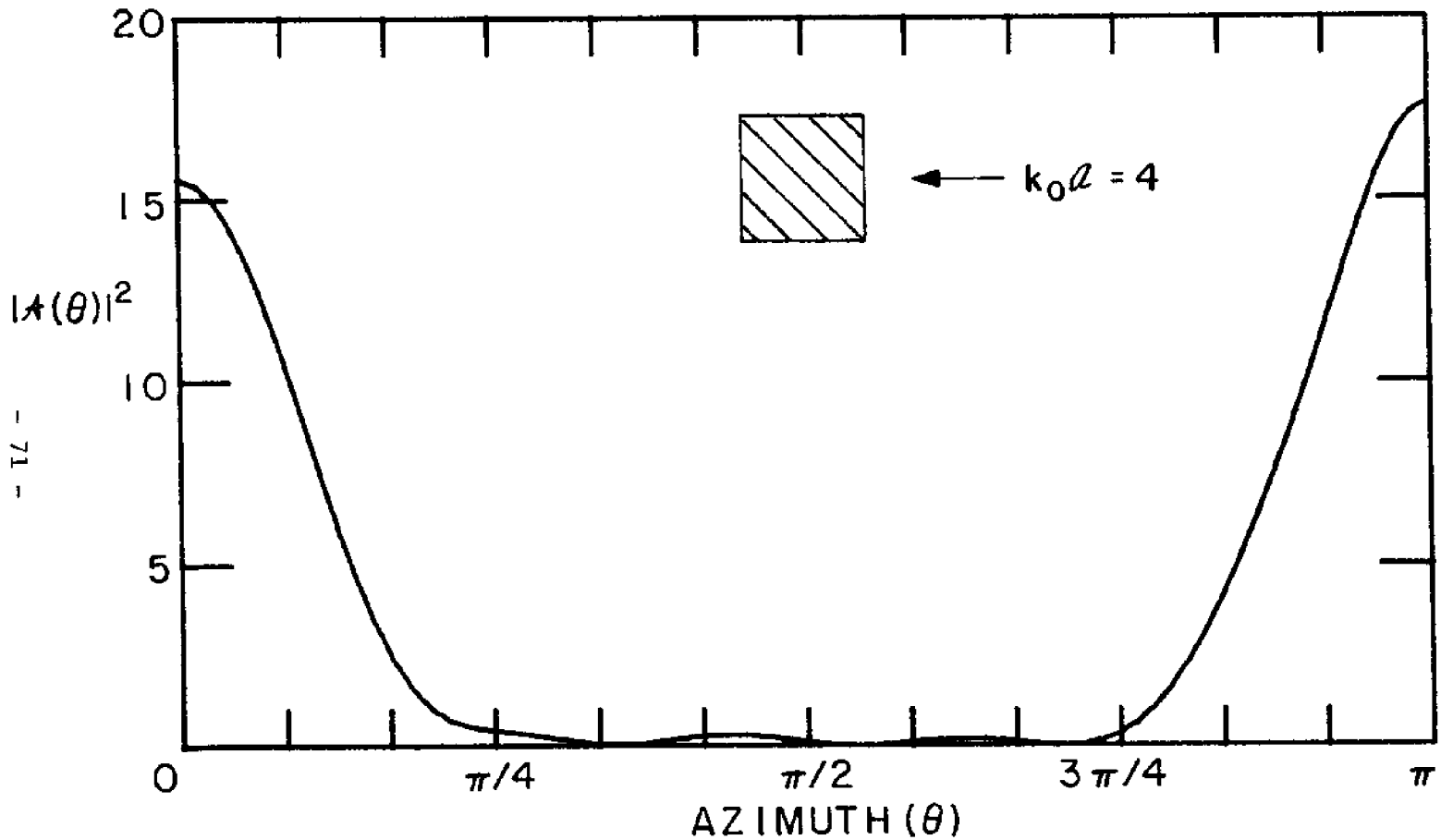

Figure 3.10(d) Differential Scattering Cross-section, $|A(\theta)|^2$, for a Square Barge. Normal Incidence: $\theta_I = \pi$.

d. $k_o a = 4$

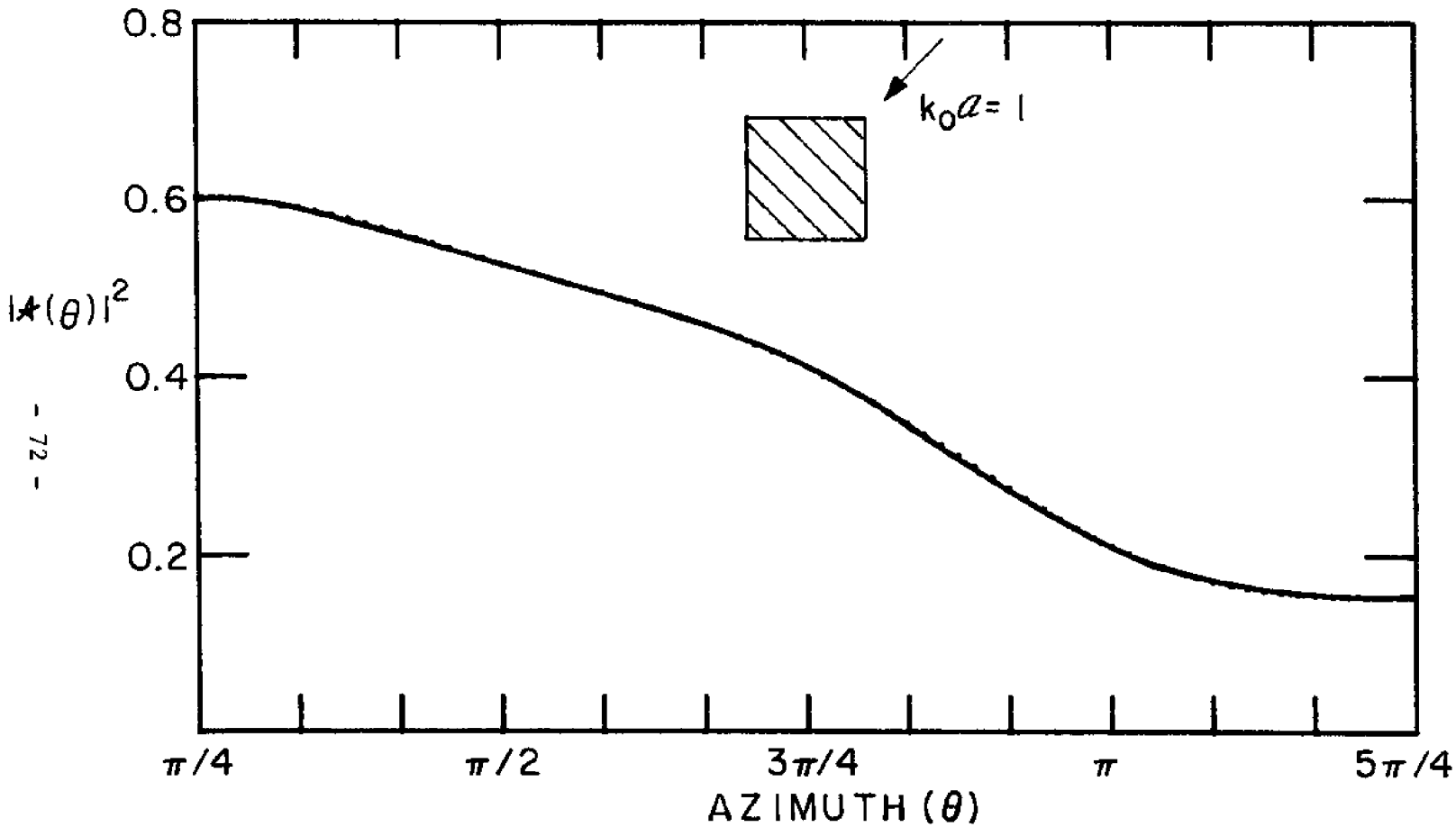

Figure 3.11(a) Differential Scattering Cross-section, $|A(\theta)|^2$, for a Square Barge. Oblique Incidence: $\theta_I = 5\pi/4$.

a. $k_o a = 1$

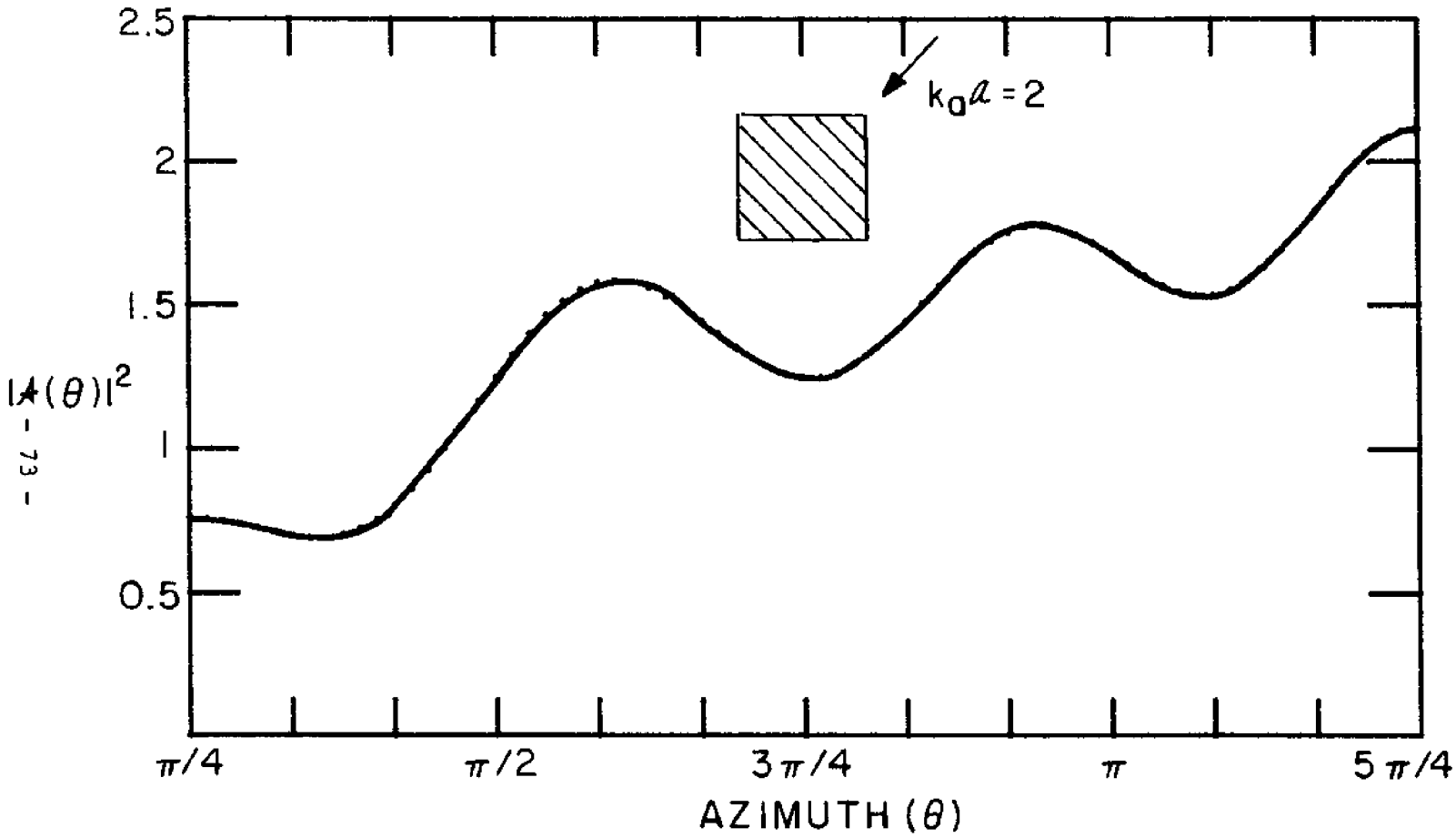

Figure 3.11(b) Differential Scattering Cross-section, $|A(\theta)|^2$, for a Square Barge. Oblique Incidence: $\theta_I = 5\pi/4$.

b. $k_o a = 2$

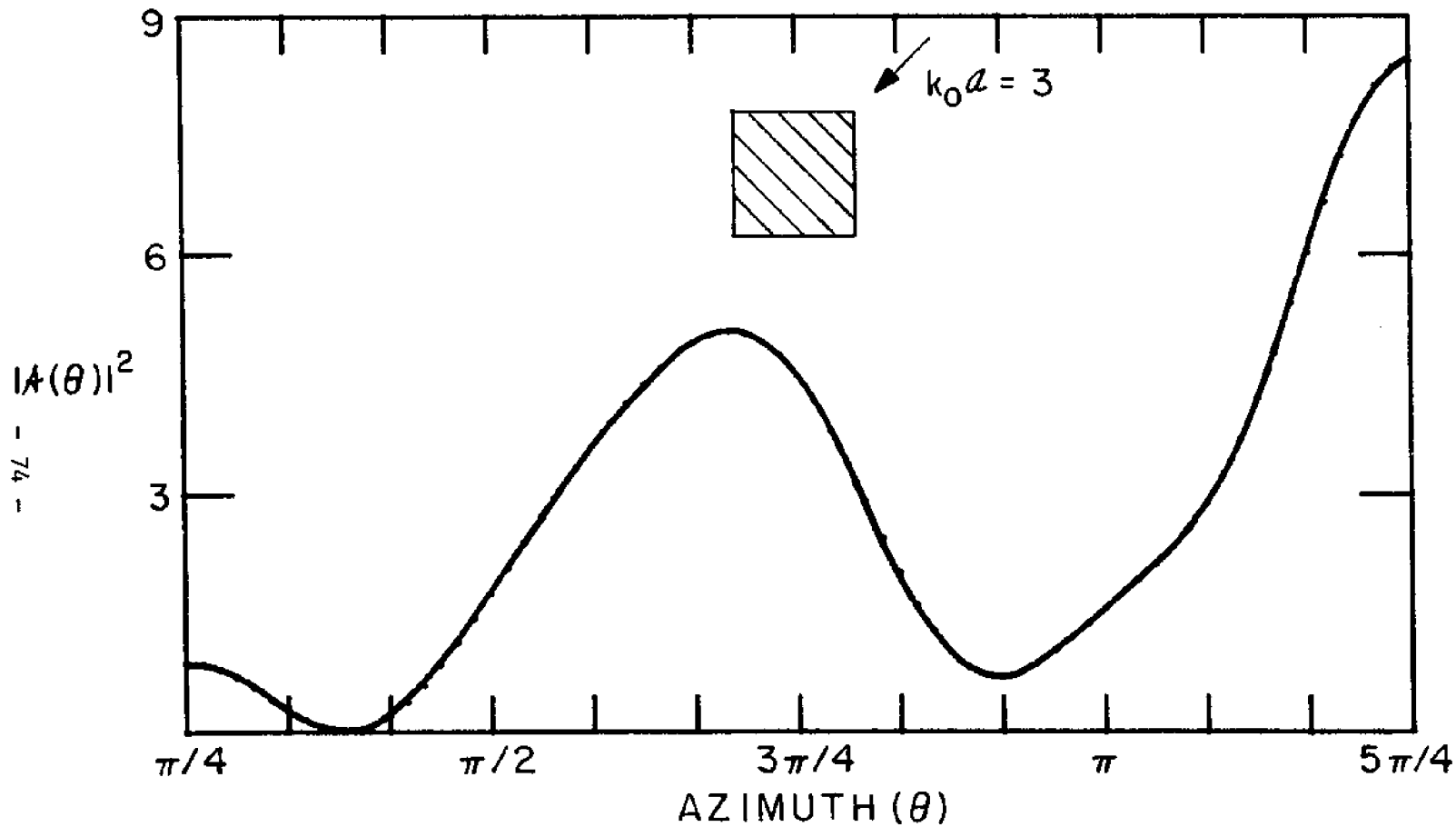

Figure 3.11(c) Differential Scattering Cross-section, $|A(\theta)|^2$, for a Square Barge. Oblique Incidence: $\theta_I = 5\pi/4$.

c. $k_o a = 3$

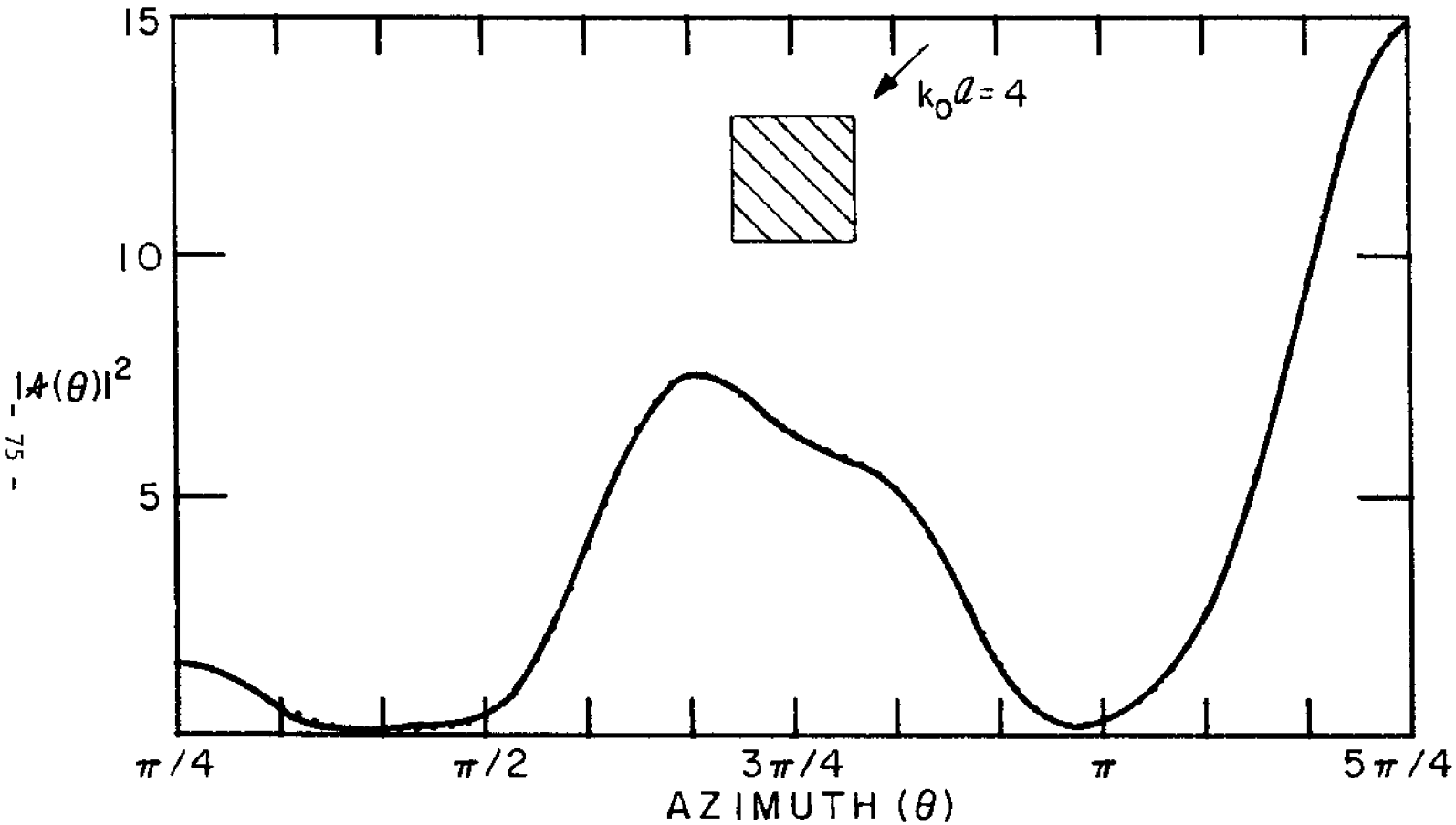

Figure 3.11(d) Differential Scattering Cross-section, $|A(\theta)|^2$, for a Square Barge. Oblique Incidence: $\theta_I = 5\pi/4$.

d. $k_o a = 4$

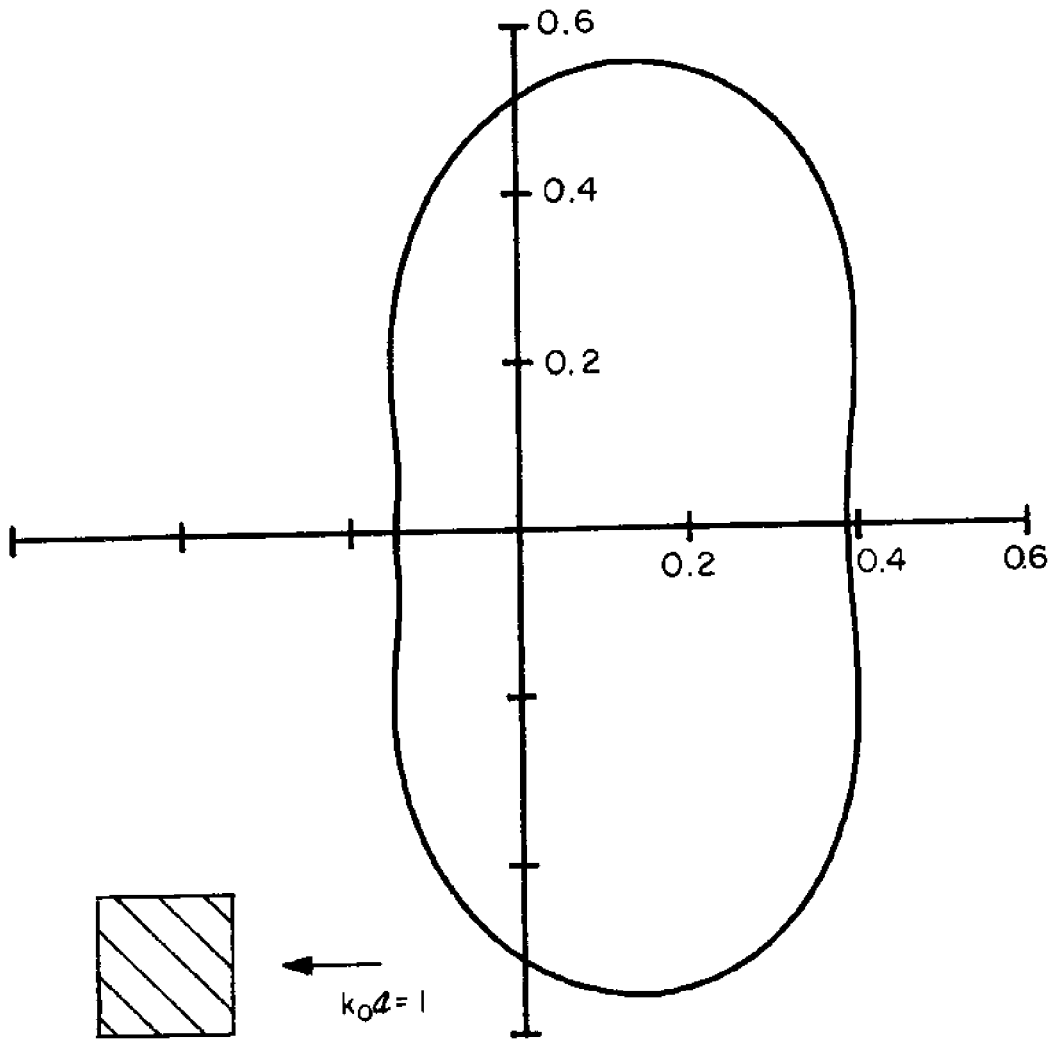

Figure 3.12(a) Polar Plot of Differential Scattering Cross-section, $|A(\theta)^2|$, for a Square Barge. Normal Incidence: $\theta_I = \pi$.

a. $k_o a = 1$

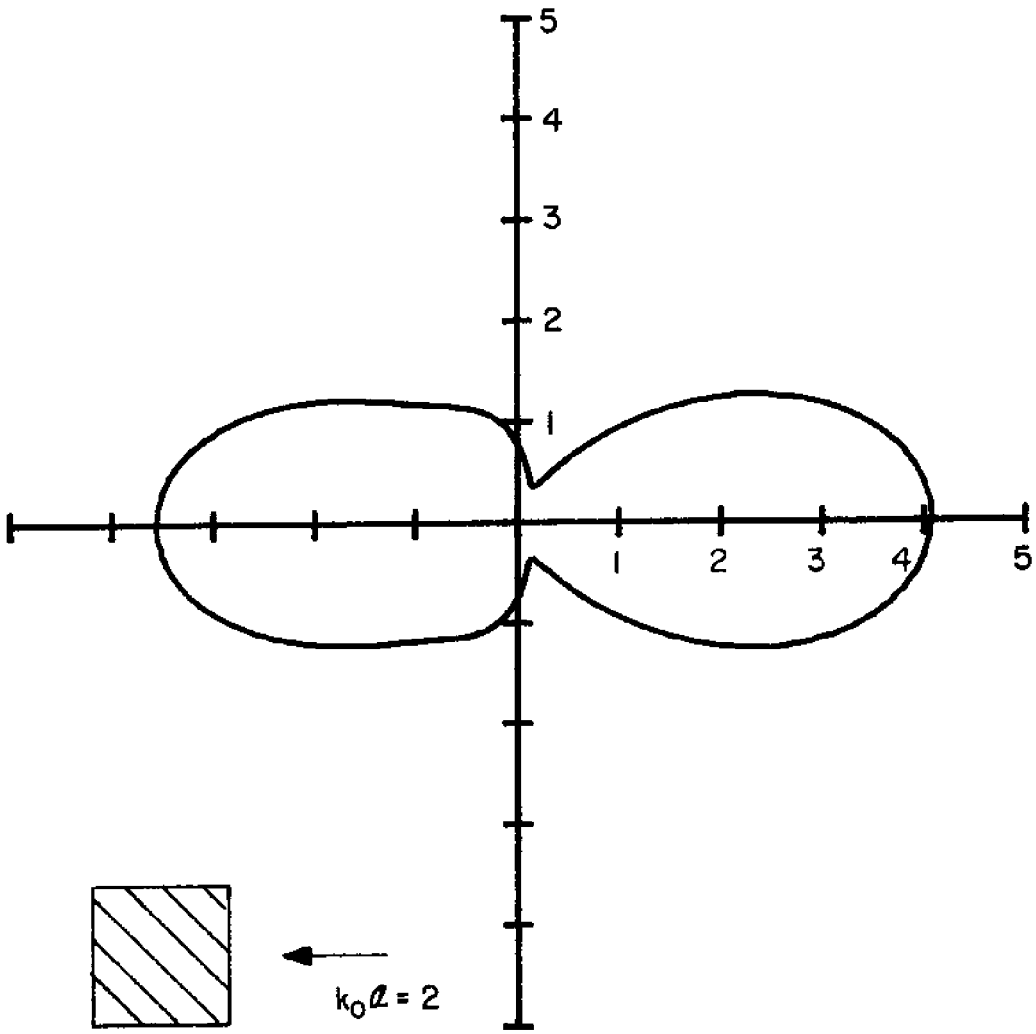

Figure 3.12(b) Polar Plot of Differential Scattering Cross-section, $|A(\theta)^2|$, for a Square Barge. Normal Incidence: $\theta_I = \pi$.

b. $k_o a = 2$

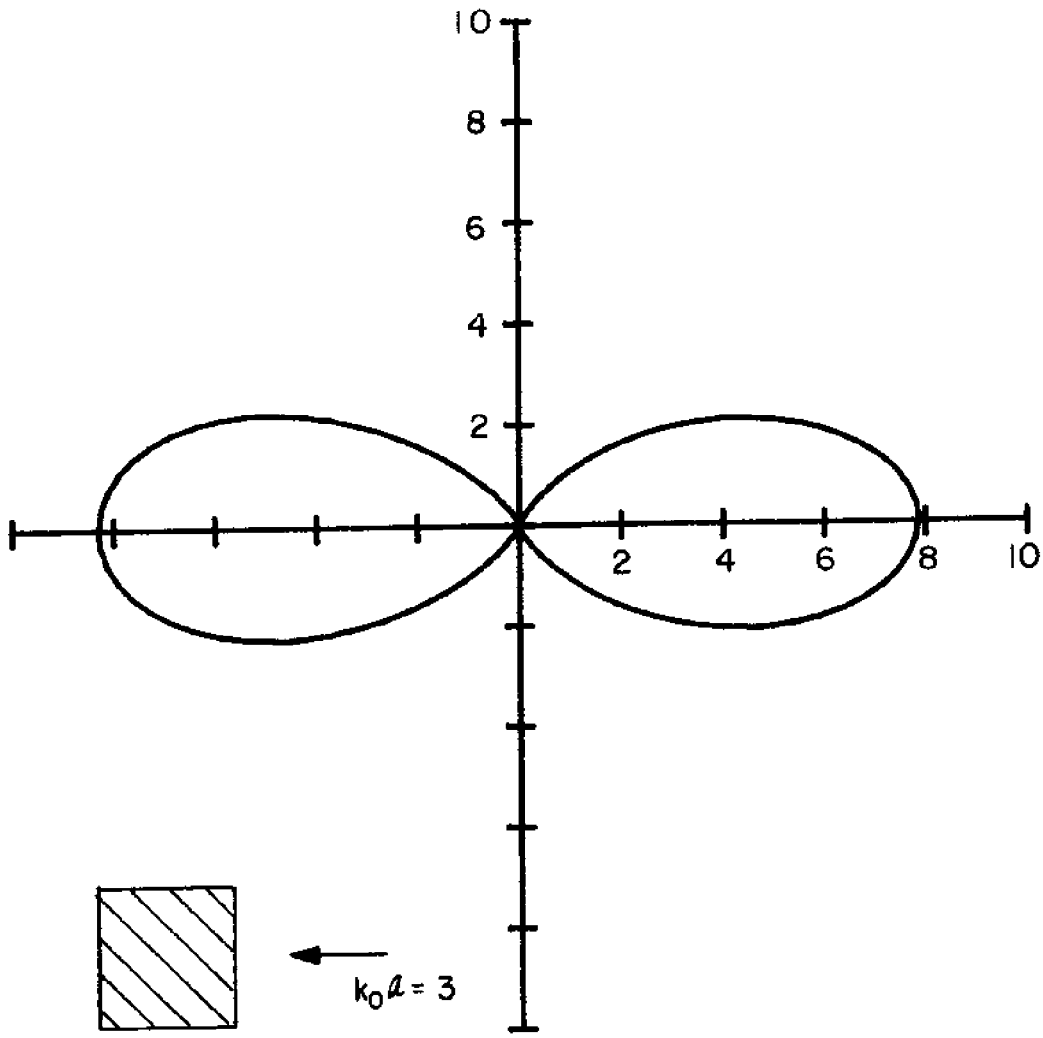

Figure 3.12(c) Polar Plot of Differential Scattering Cross-section, $|A(\theta)^2|$, for a Square Barge. Normal Incidence: $\theta_I = \pi$.

c. $k_o a = 3$

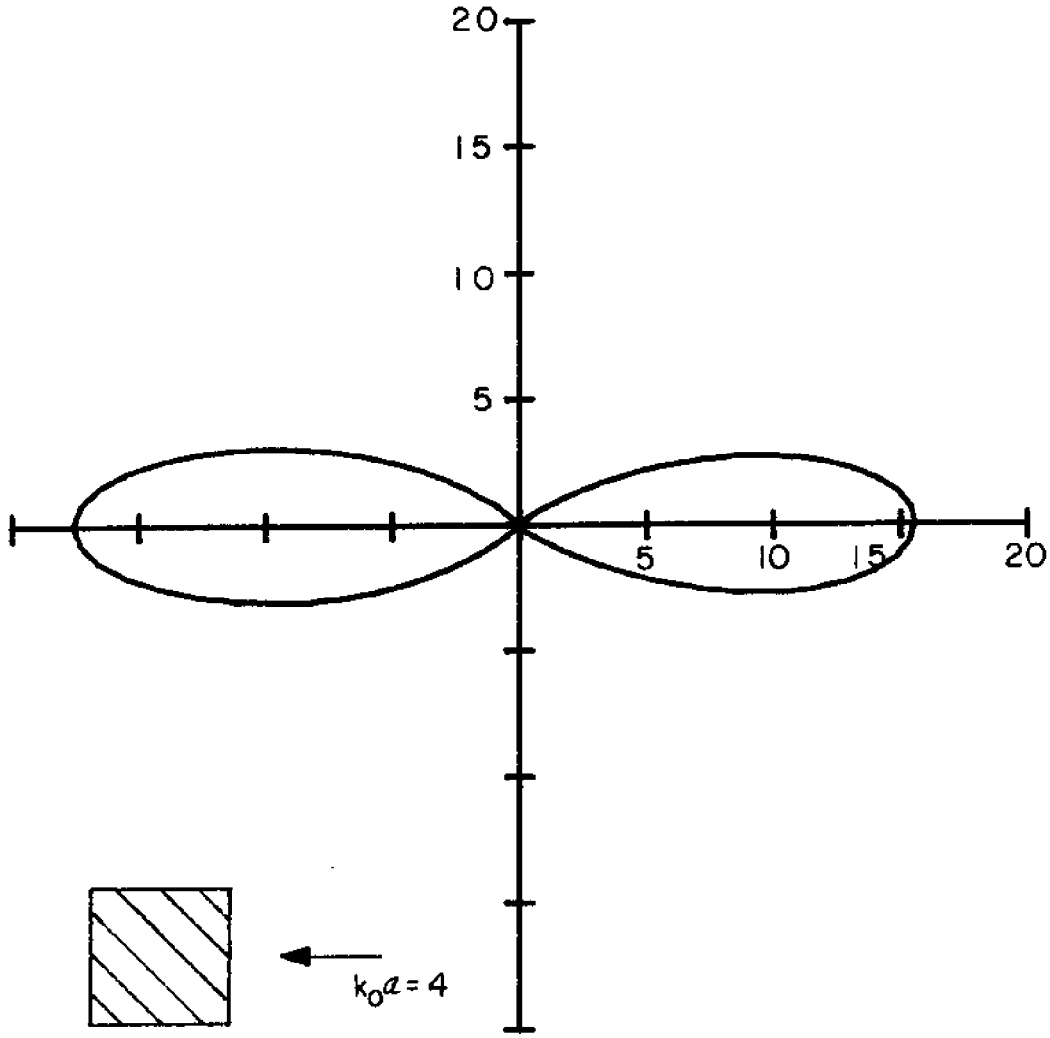

Figure 3.12(d).(i) Polar Plot of Differential Scattering Cross-section, $|A(\theta)^2|$, for a Square Barge. Normal Incidence: $\theta_I = \pi$.

d.i $k_o a = 4$

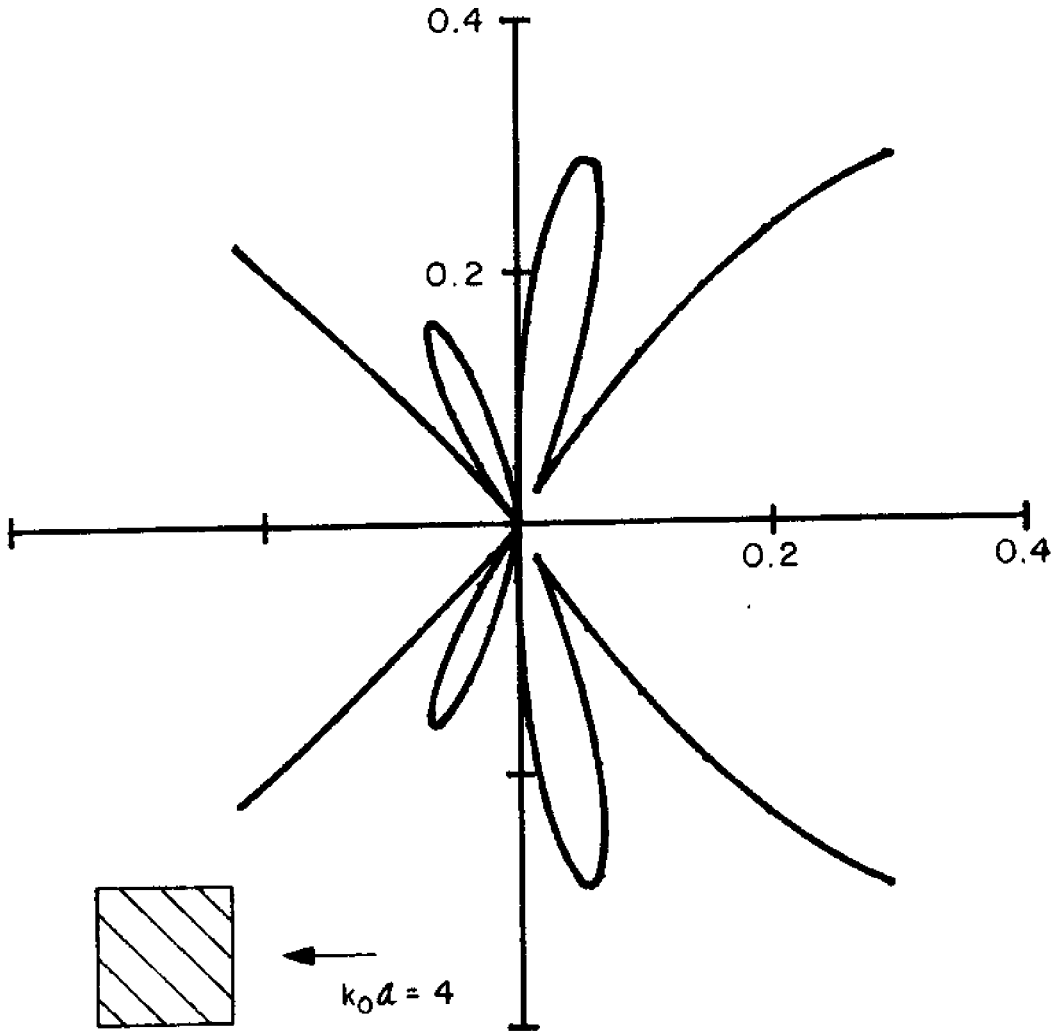

Figure 3.12(d).(ii) Polar Plot of Differential Scattering Cross-section, $|A(\theta)^2|$, for a Square Barge. Normal Incidence: $\theta_I = \pi$.

d.ii $k_o a = 4$

Details for $\frac{\pi}{4} < \theta < \frac{3\pi}{4}$ and $\frac{5\pi}{4} < \theta < \frac{7\pi}{4}$.

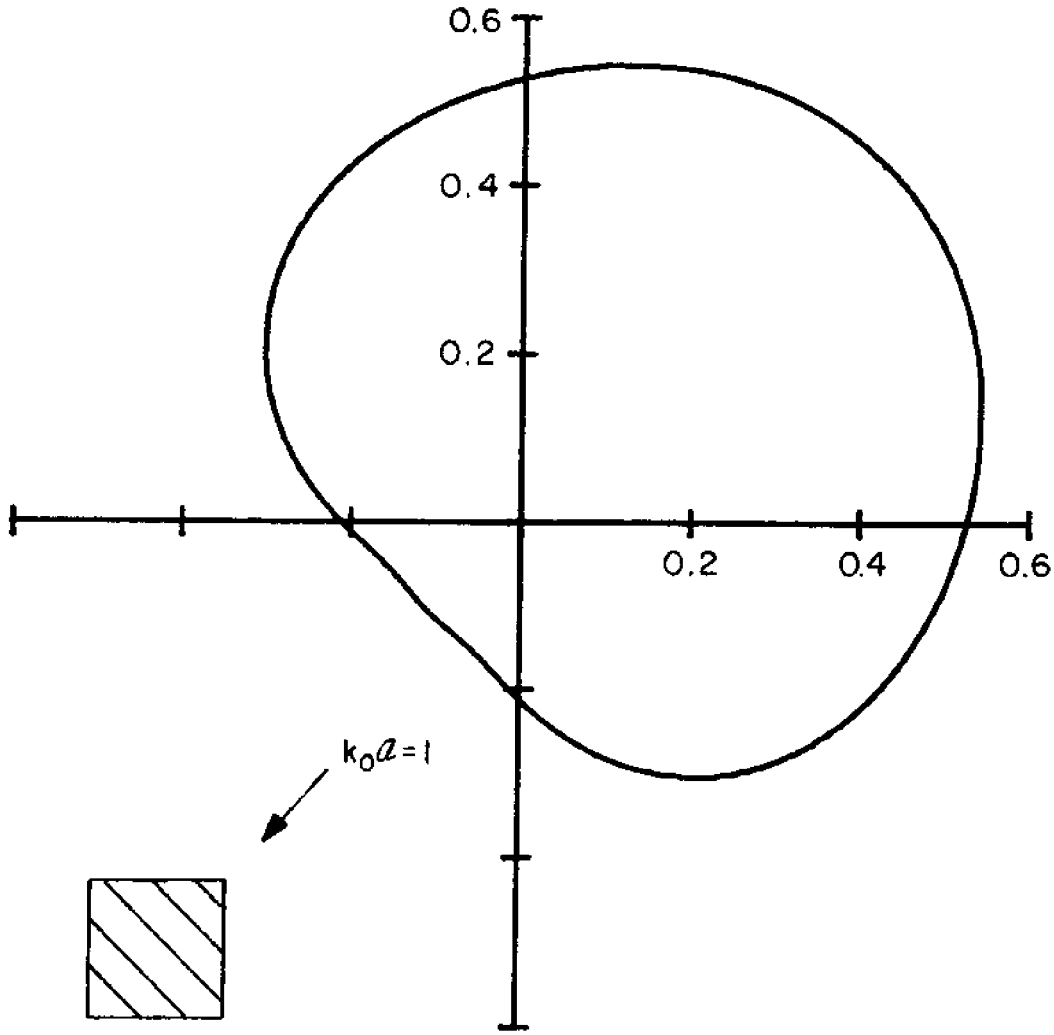

Figure 3.13(a) Polar Plot of Differential Scattering Cross-section, $|A(\theta)|^2$, for a Square Barge. Oblique Incidence: $\theta_I = 5\pi/4$.

a. $k_o a = 1$

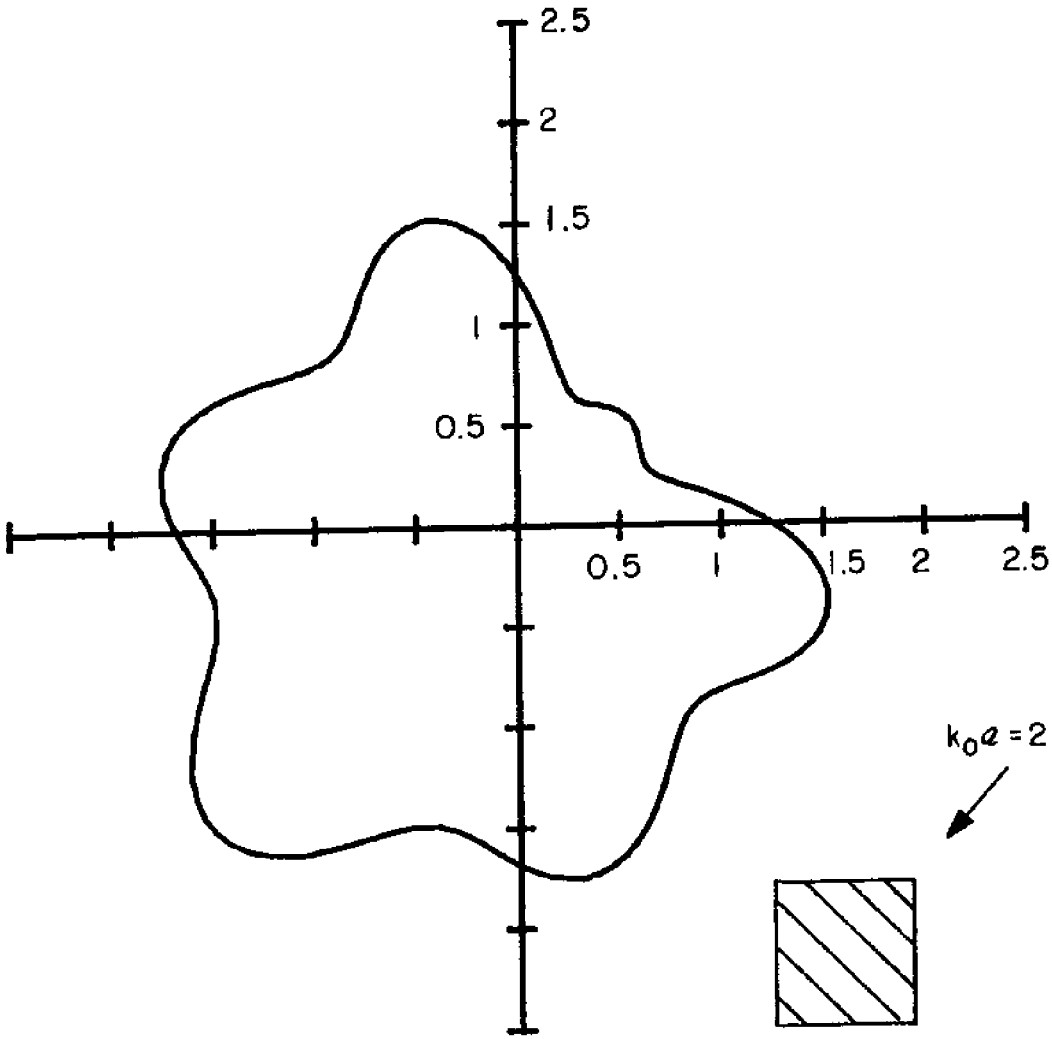

Figure 3.13(b) Polar Plot of Differential Scattering Cross-section, $|A(\theta)|^2$, for a Square Barge. Oblique Incidence: $\theta_I = 5\pi/4$.

b. $k_0a = 2$

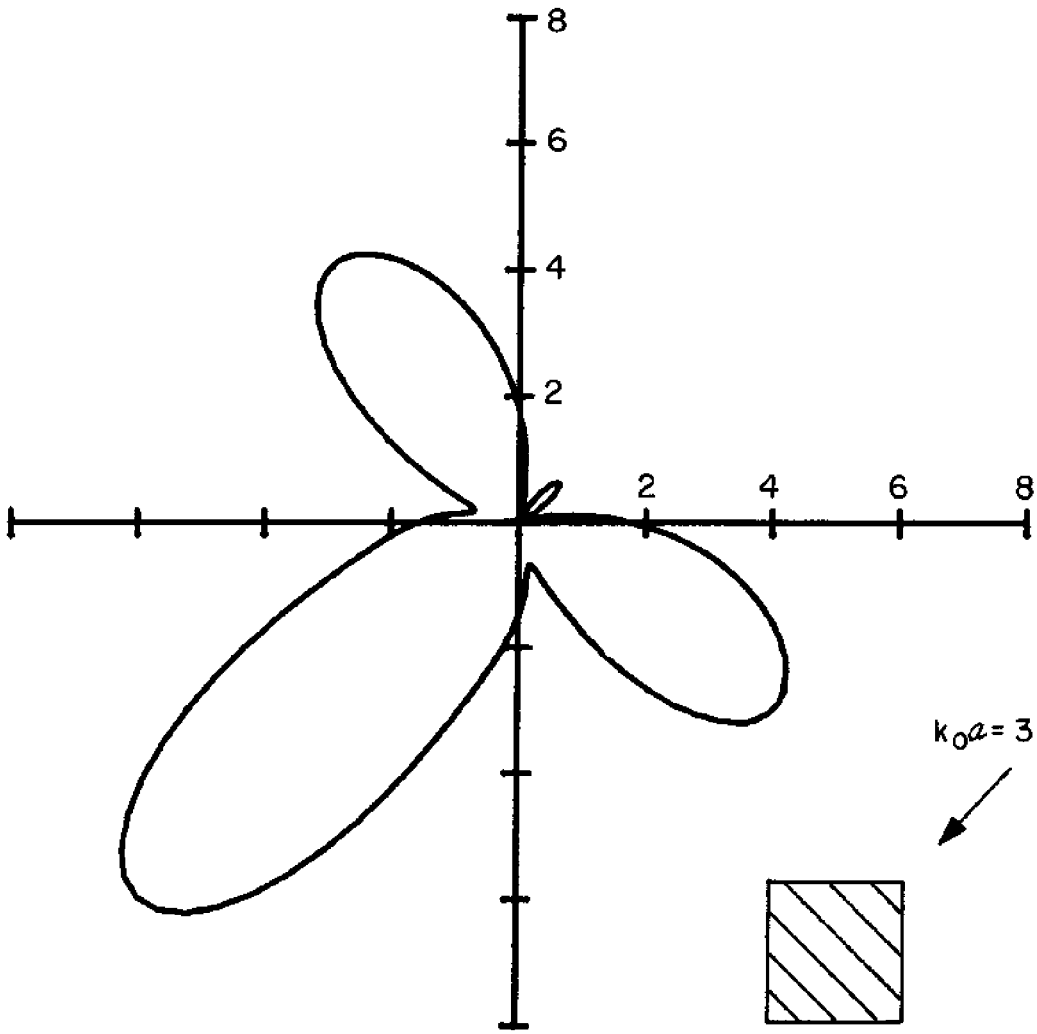

Figure 3.13(c) Polar Plot of Differential Scattering Cross-section, $|A(\theta)|^2$, for a Square Barge. Oblique Incidence: $\theta_I = 5\pi/4$.

c. $k_0a = 3$

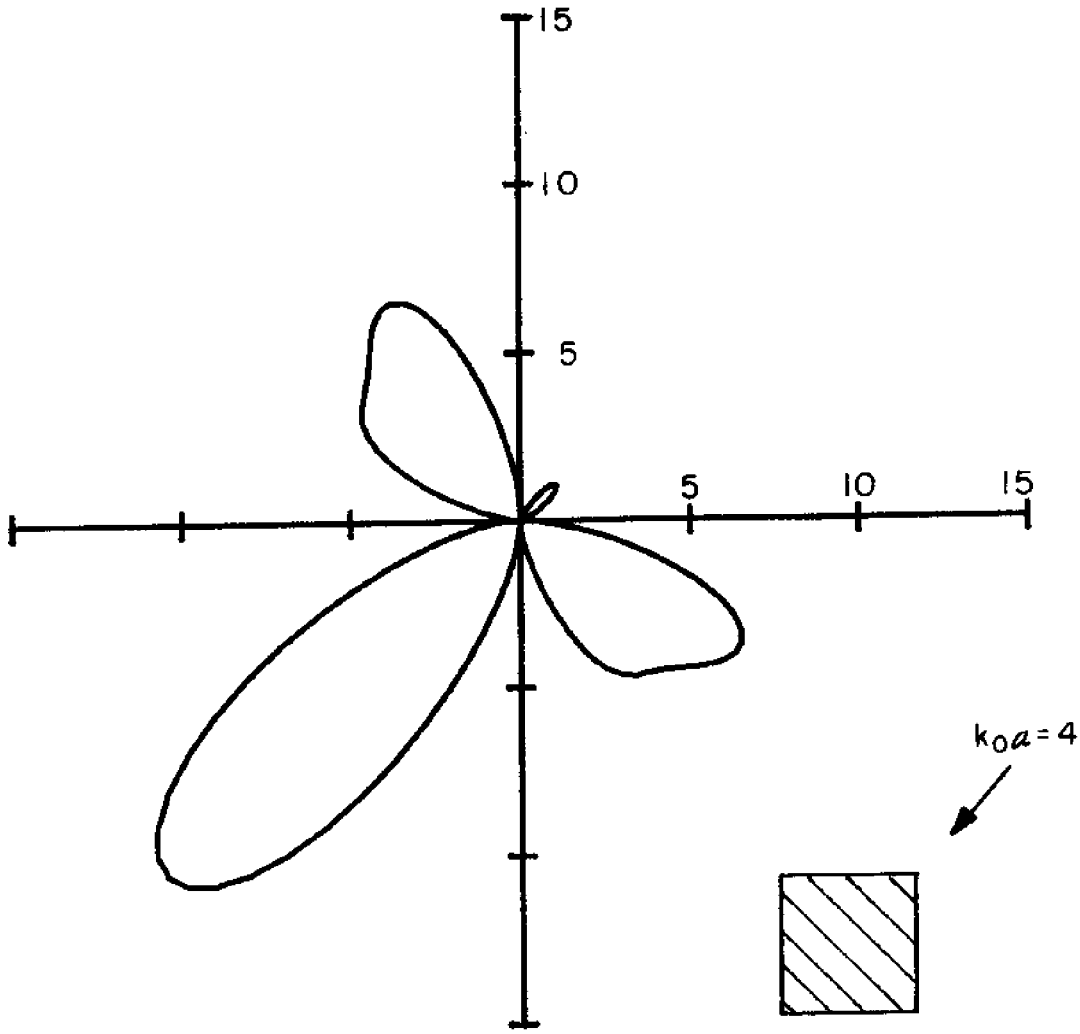

Figure 3.13(d) Polar Plot of Differential Scattering Cross-section, $|A(\theta)|^2$, for a Square Barge. Oblique Incidence: $\theta_I = 5\pi/4$.

d. $k_o a = 4$

3.4 Elliptic Island with a Circular Base

The scattering of a plane wave by an island has been of theoretical and practical interest in recent years. Longuet-Higgins, 1967 showed the existence of trapped waves around circular islands, while Vastano and Reid, 1966, 1967, Lautenbacher, 1970, Smith and Sprinks, 1975 and Jonssen, Skovgaard, Kjaer (1975) studied the tsunami run-up on various islands of somewhat specialized geometries. All existing treatments require either an assumption allowing linear shallow water (long wave) theory which ignores vertical variations, or that the ocean bottom is slowly varying (mild slope theory). It is of interest to point out that owing to both bottom refraction and possible resonance of the trapped modes, the maximum run-up on an island can often be very large.

In this last example, we consider the diffraction by an island that extends from the free surface in the form of a vertical elliptic cylinder up to a depth H, then slopes out "conically" to form a circular toe on an ocean bottom of constant depth h. The geometry and finite element grid (36 elements—two rings of 18 each, and 342 nodes) are shown in Fig. 3.14. For an upper elliptic cylinder of major and minor axes A, B and length (submergence) H, (i.e. from z = 0 to - H), the lower "conical" portion is generated by the parameters λ and θ:

$$x = [\lambda A + (1 - \lambda)R] \cos\theta$$

$$y = [\lambda B + (1 - \lambda)R] \sin\theta \qquad (3.4.1.a,b,c)$$

and

$$z + h = \lambda(h - H)$$

where R is the radius of the circular toe at the sea bottom ($z = -h$). Cut planes normal to the z-axis ($-h < z < -H$) yield elliptic cut sections given by

$$\frac{x^2}{[\lambda(A-R) + R]^2} + \frac{y^2}{[\lambda(B-R) + R]^2} = 1 \tag{3.4.2}$$

with eccentricity, e, varying from $\sqrt{1-(\frac{B}{A})^2}$ to 0 as λ varies from 1 ($z = -H$) to 0 ($z = -h$):

$$e(\lambda) = \frac{\lambda\ (A-B)}{\lambda A + (1-\lambda)R} \tag{3.4.3}$$

As a particular example, we choose $A = a$, $B = .5a$, $H = .5a$, $h = a$ and $R = 1.5a$ (as in Fig. 3.14). The "conical" beach now varies from a width of a with a 1 on 2 slope at $\theta = \pi/2, 3\pi/2$ to a 1 on 1 beach of width 0.5a at $\theta = 0,\pi$. Three incident wave-numbers ($k_o a = 1,2,3$) at two angles of incidence ($\theta_I = \pi$ and $3\pi/2$) are considered.

The run-up, η/a_o, on the island ($z = 0$, $x = A\cos\theta$, $y = B\sin\theta$) are plotted versus azimuth (θ) in Figs. 3.15.a,b,c and Figs. 3.16.a,b,c. Due to the rather short and steep beach, the run-up does not exceed 2 for $\theta_I = \pi$ or ~ 2.5 for $\theta_I = 3\pi/2$.

Again, plots of $|A(\theta)|^2$ as a function of θ are given in Figs. 3.17.a,b,c and Figs. 3.18.a,b,c, and in polar coordinates in Figs. 3.19.a,b,c and Figs. 3.20,a,b,c.

Unfortunately, our present geometry does not resemble sufficiently any of those studied by other investigators to justify quantitative comparisons.

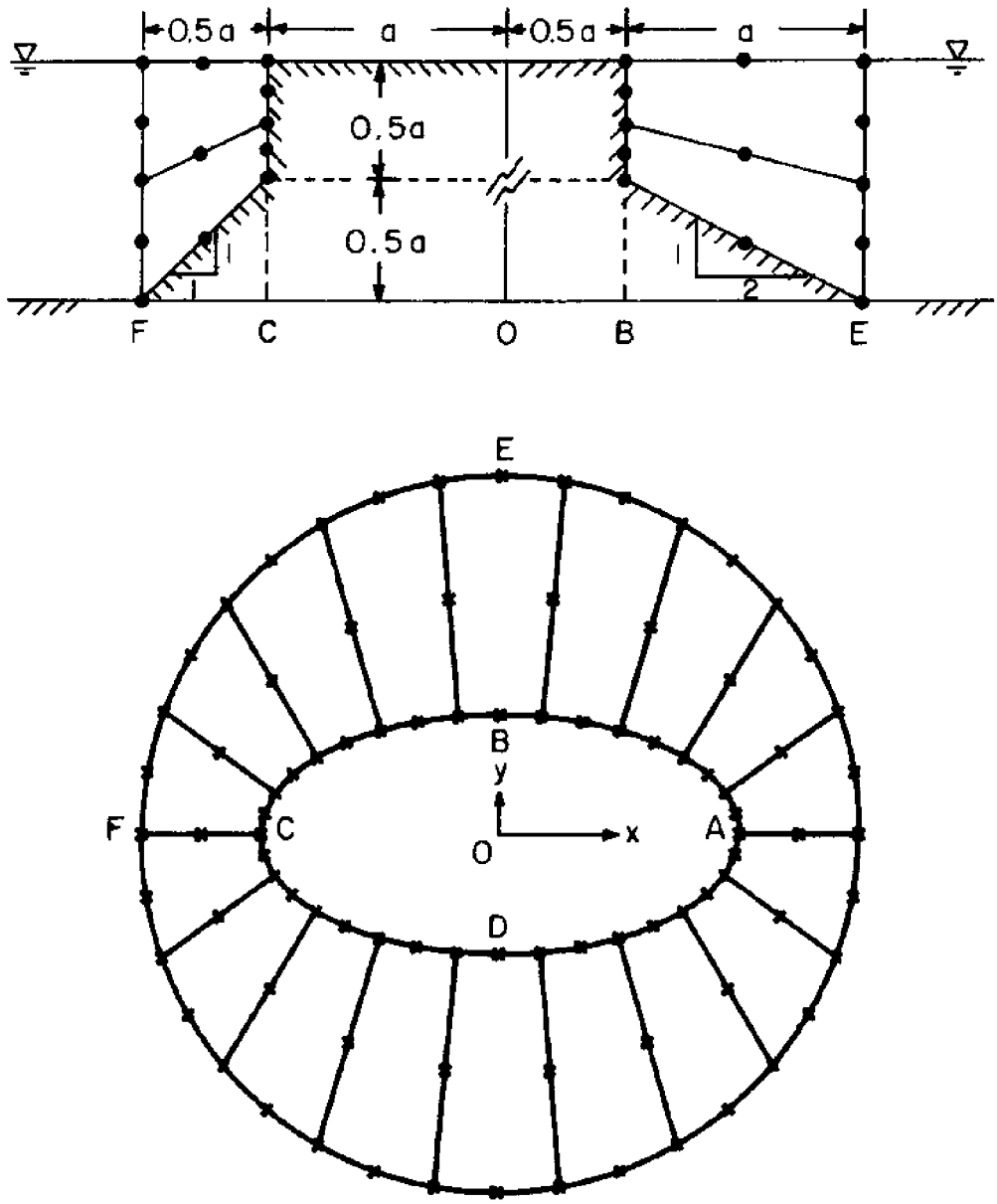

Figure 3.14 Geometry and Finite-element Structure for an Elliptical Island with a Circular Base. (Major and Minor axes: A = a, B = .5a; "draft" of elliptic cylinder: H = .5a, radius of circular toe: R = 1.5a; water depth: h = a.

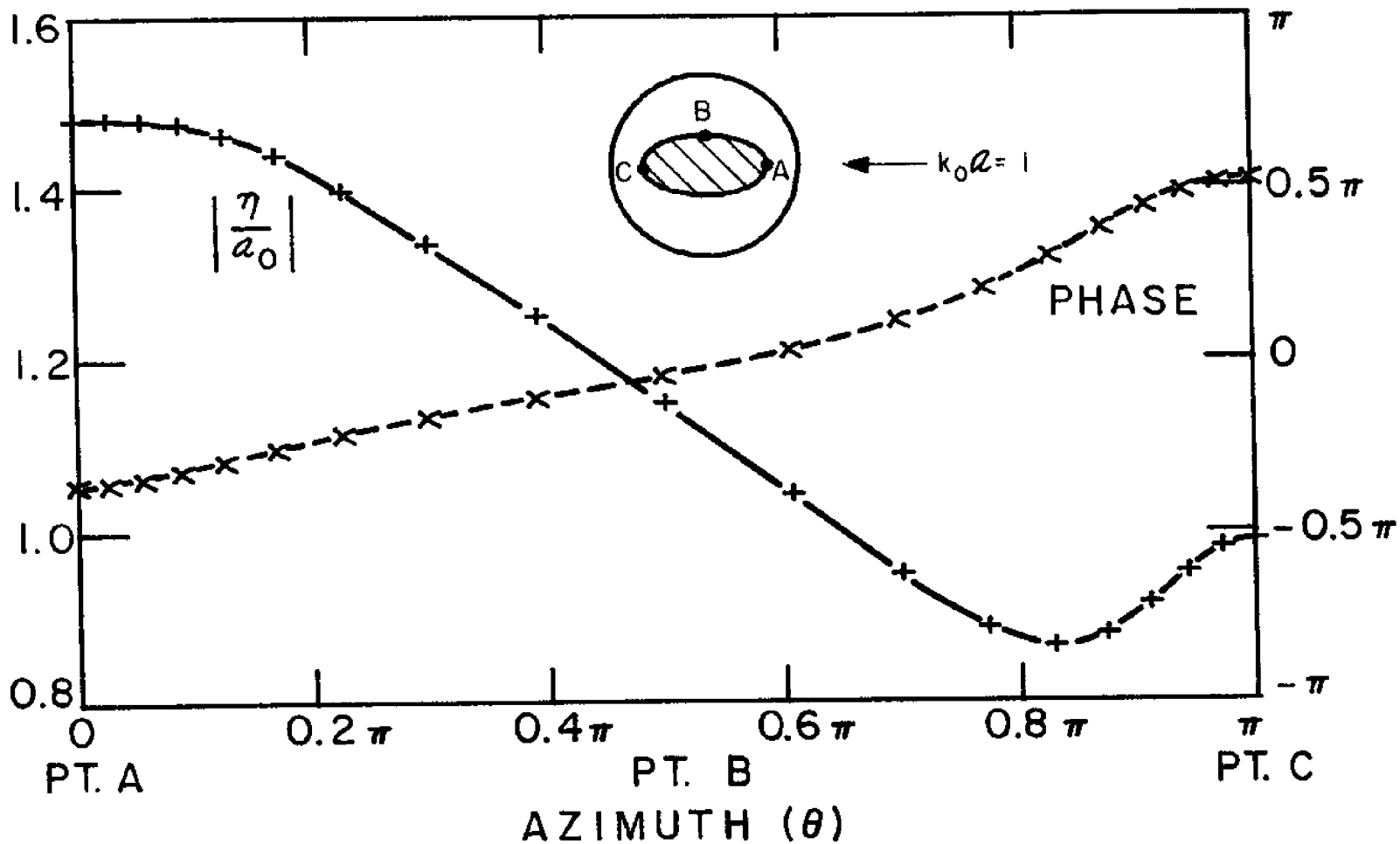

Figure 3.15 Run-up, η/a_o, on an Elliptic Island with a Circular Base: (+) ——— : (nodal) magnitude; (x) ----: (nodal) phase. Wave Incident from $x \sim +\infty$. ($\theta_I = \pi$). a. $k_o a = 1$.

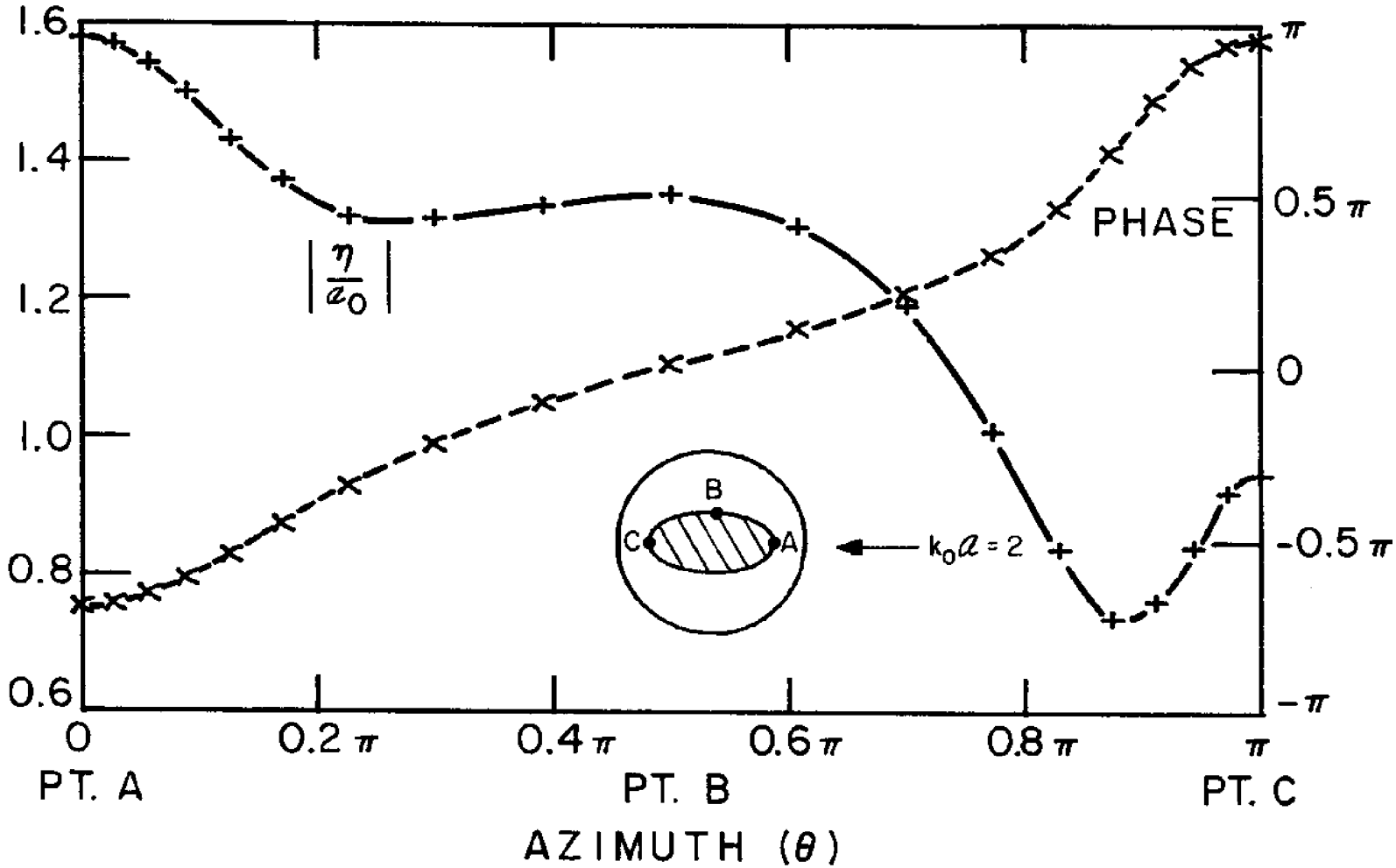

Figure 3.15(b) Run-up, η/a_o, on an Elliptic Island with a Circular Base: (+) ——— : (nodal) magnitude; (x) ---- : (nodal) phase. Wave Incident from $x \sim +\infty$. ($\theta_I = \pi$).

b. $k_o a = 2$

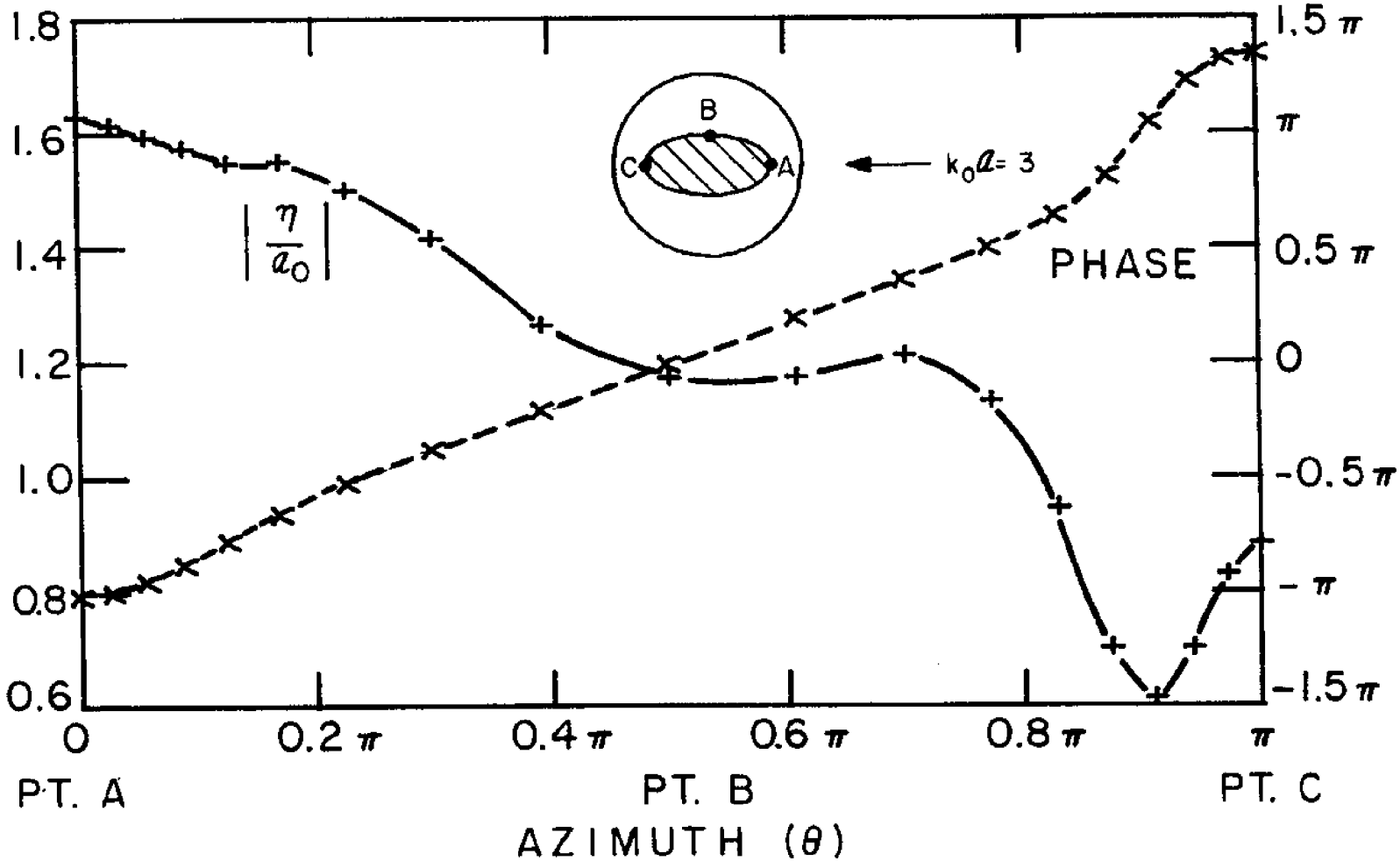

Figure 3.15(c) Run-up, η/a_o, on an Elliptic Island with a Circular Base: (+) ——— : (nodal) magnitude; (x) ---- : (nodal) phase. Wave Incident from $x \sim +\infty$. ($\theta_I = \pi$).

c. $k_o a = 3$

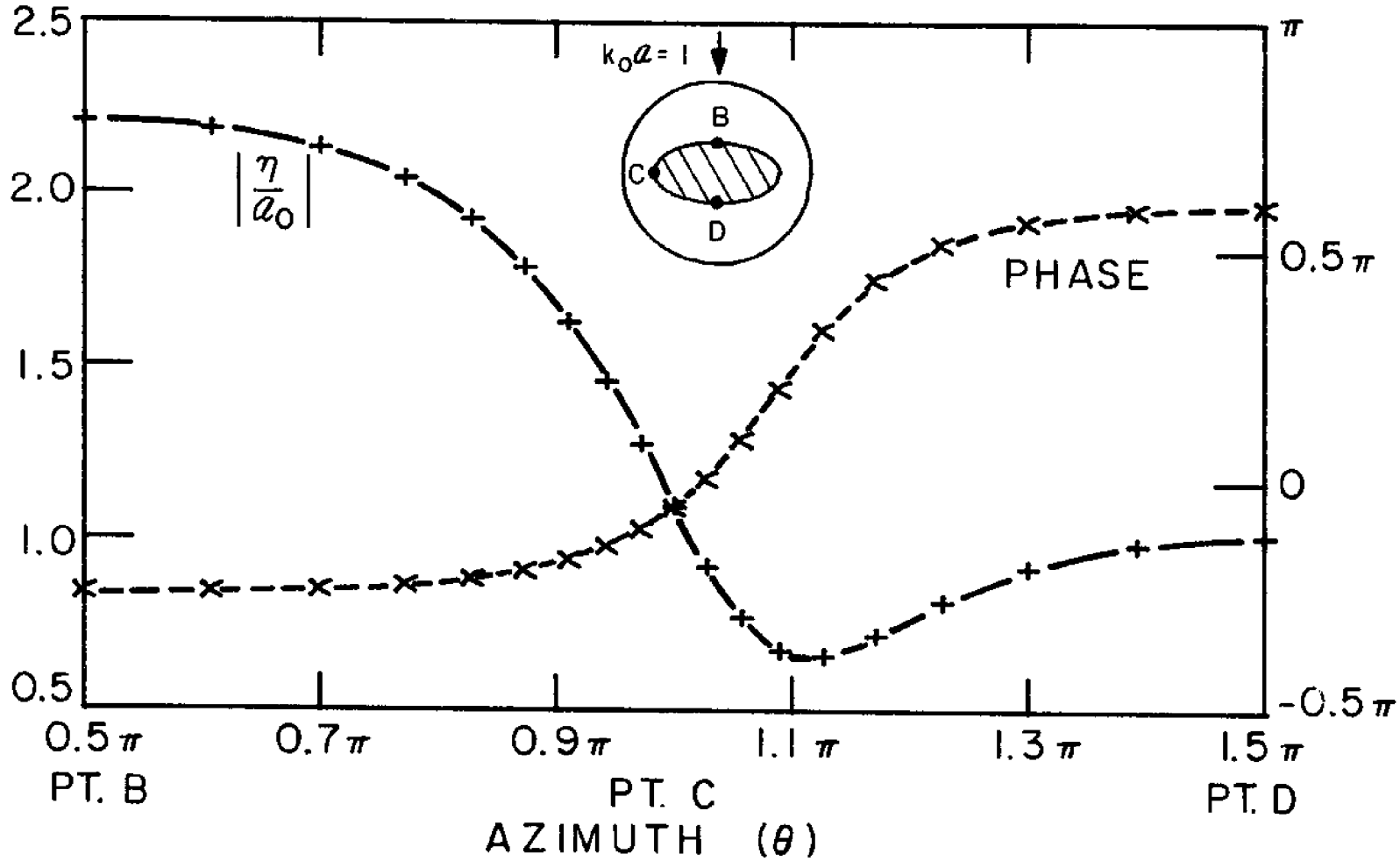

Figure 3.16(a) Run-up, η/a_o, on an Elliptic Island with a Circular Base: (+) —— : (nodal) magnitude; (x) ---- : (nodal) phase. Wave Incident from $y \sim +\infty$. ($\theta_I = 3\pi/2$).

a. $k_o a = 1$

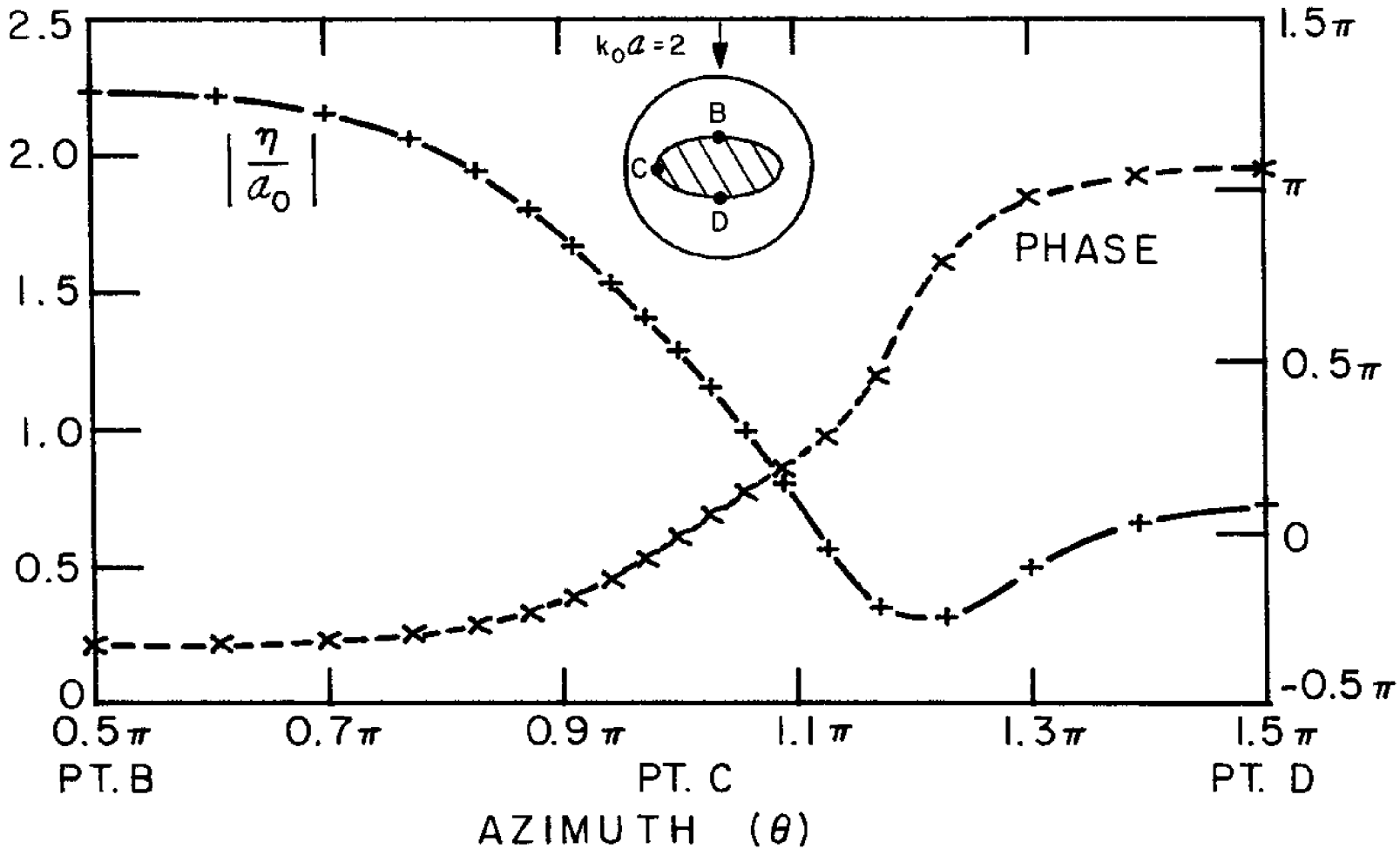

Figure 3.16(b) Run-up, η/a_o, on an Elliptic Island with a Circular Base: (+) ——— : (nodal) magnitude; (x) ---- : (nodal) phase. Wave Incident from $y \sim +\infty$. ($\theta_I = 3\pi/2$).

b. $k_o a = 2$

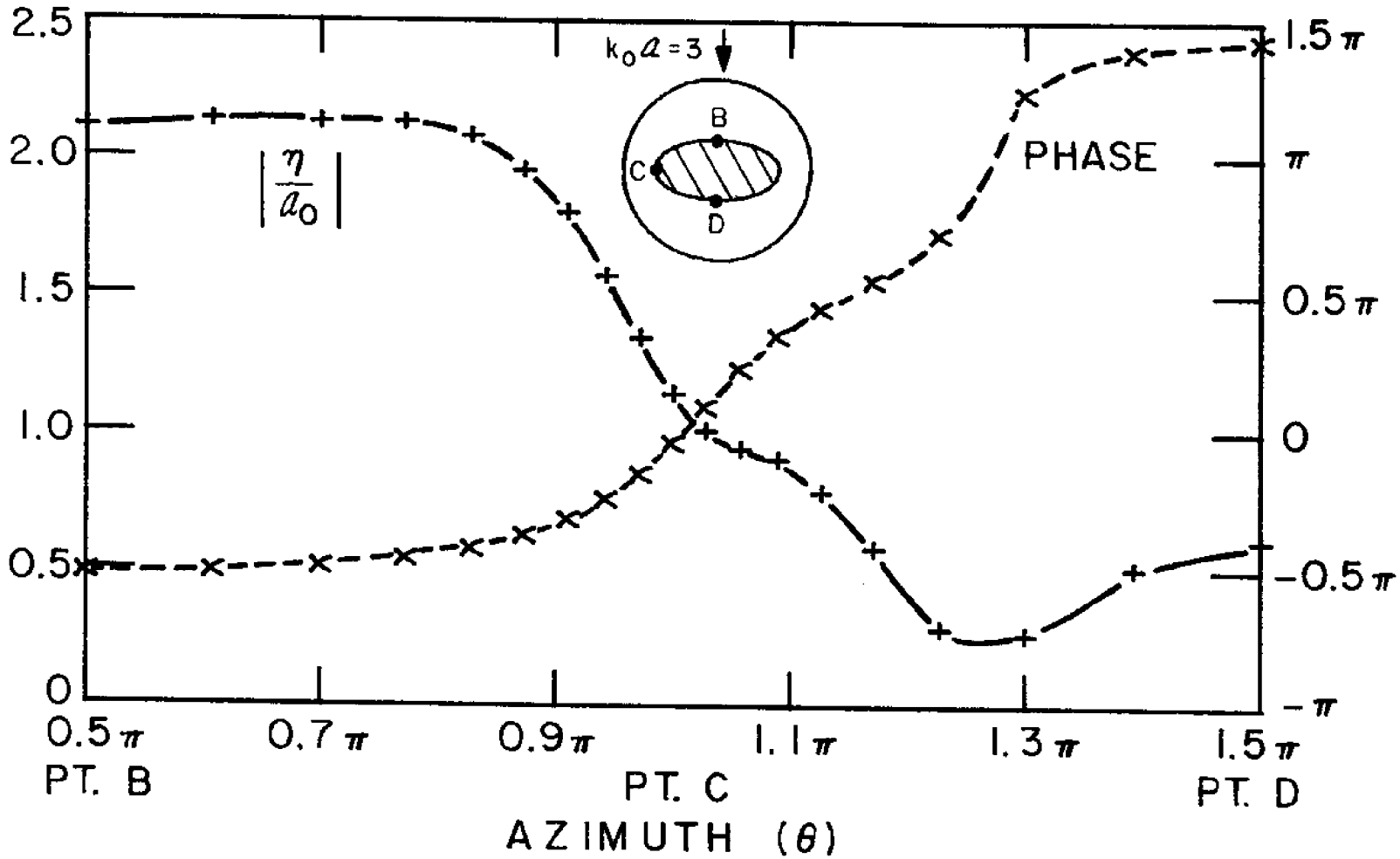

Figure 3.16(c) Run-up, η/a_o, on an Elliptic Island with a Circular Base: (+) ——— : (nodal) magnitude; (x) ---- : (nodal) phase. Wave Incident from $y \sim +\infty$. ($\theta_I = 3\pi/2$).

c. $k_o a = 3$

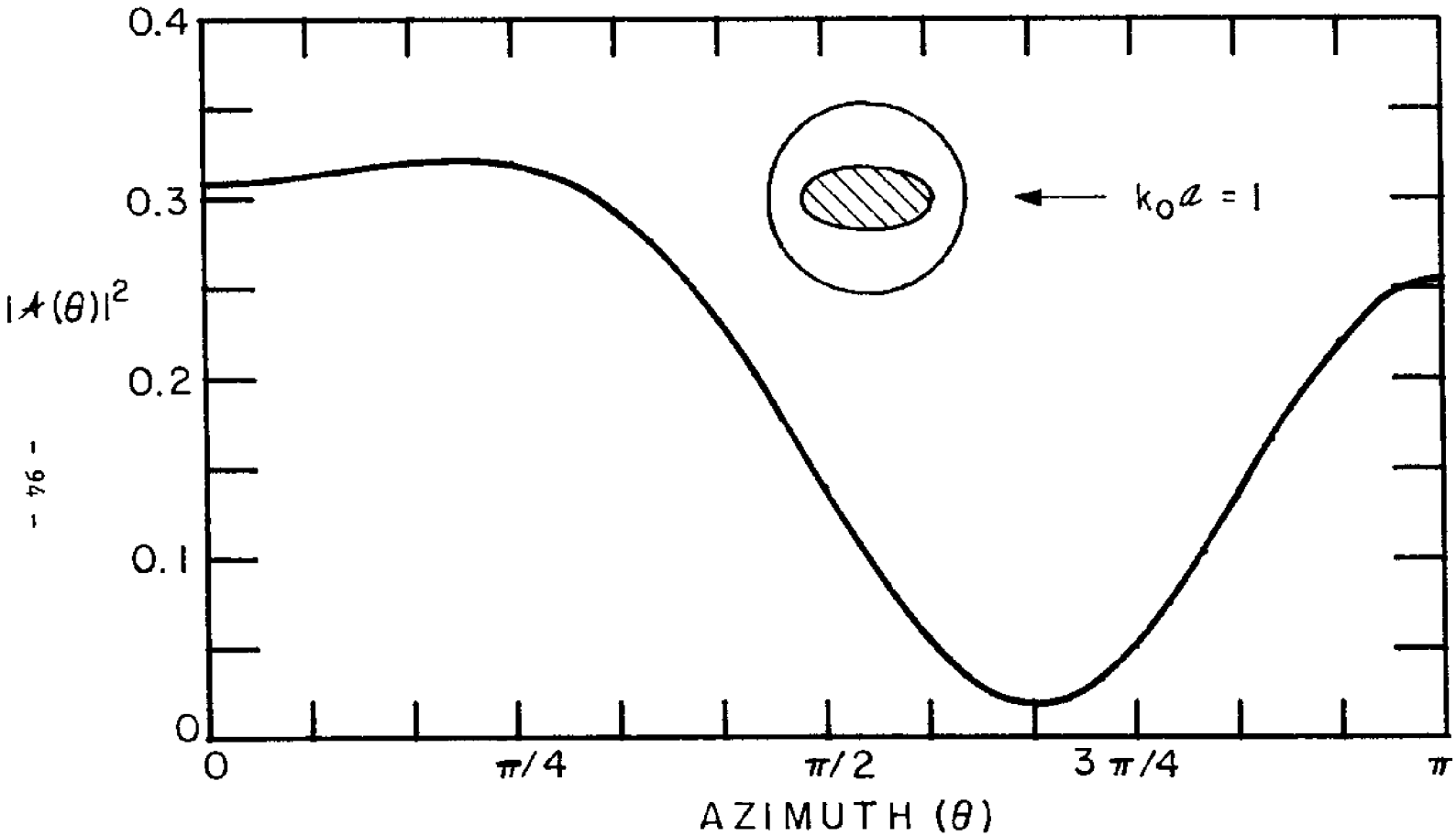

Figure 3.17 Differential Scattering Cross-section, $|A(\theta)|^2$, for an Elliptic Island with a circular Base. Wave Incident from $x \sim +\infty$. ($\theta_I = \pi$).

a. $k_o a = 1$

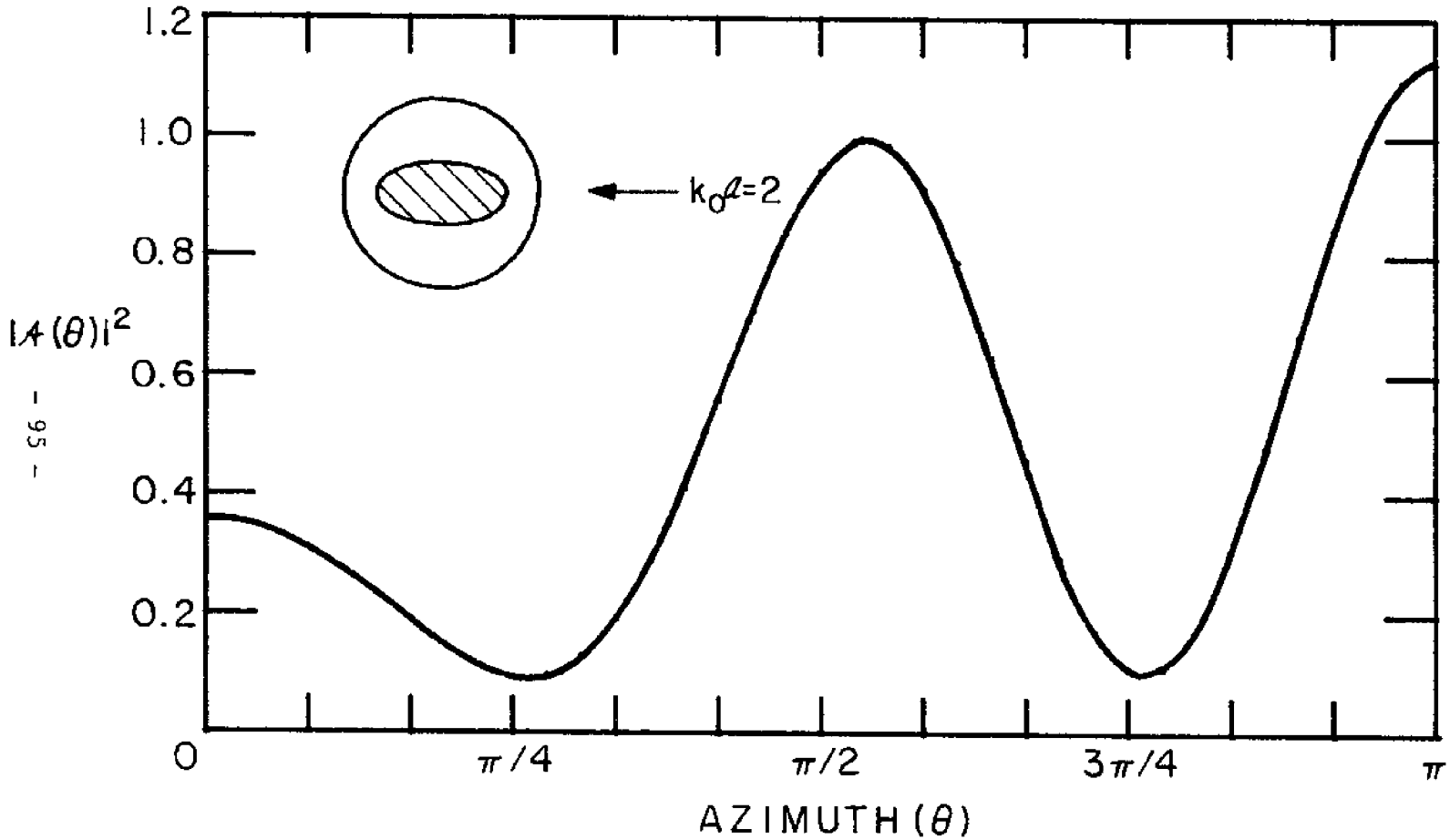

Figure 3.17(b) Differential Scattering Cross-section, $|A(\theta)|^2$, for an Elliptic Island with a circular Base. Wave Incident from $x \sim +\infty$. ($\theta_I = \pi$).

b. $k_0 a = 2$

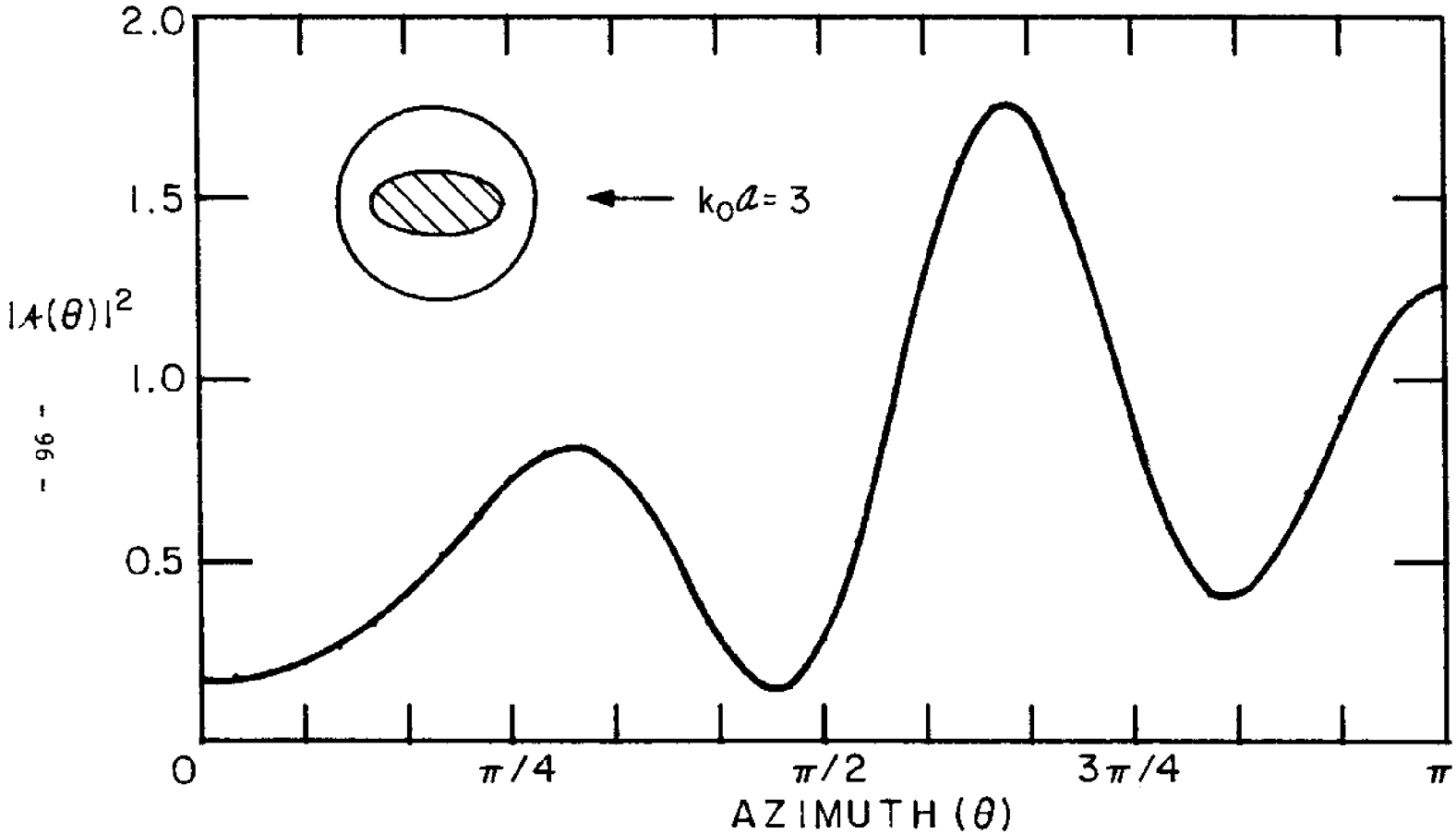

Figure 3.17(c) Differential Scattering Cross-section, $|A(\theta)|^2$, for an Elliptic Island with a circular Base. Wave Incident from $x \sim +\infty$. ($\theta_I = \pi$).

c. $k_o a = 3$

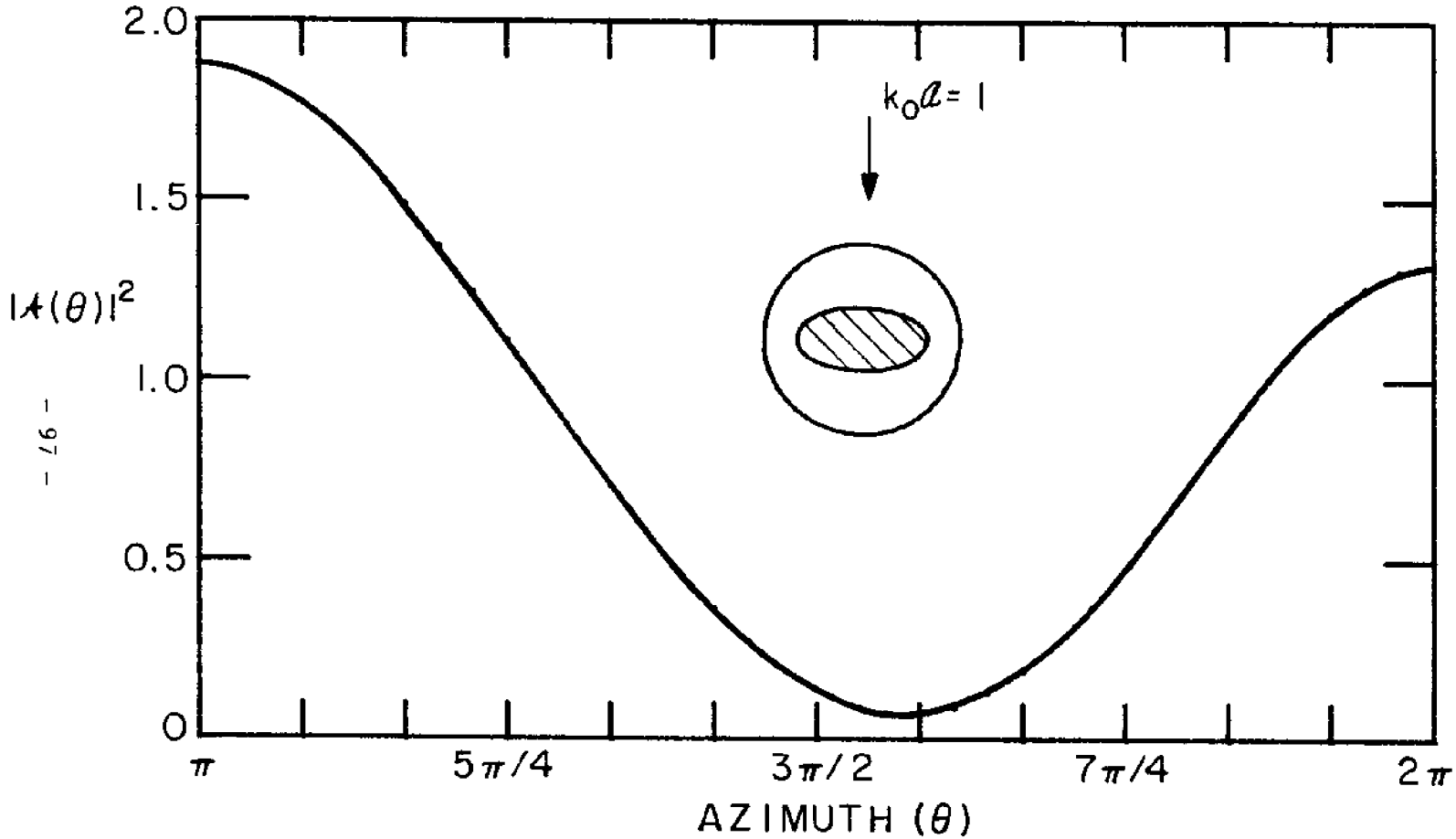

Figure 3.18(a) Differential Scattering Cross-section, $|A(\theta)|^2$, for an Elliptic Island with a Circular Base. Wave Incident from $y \sim +\infty$. ($\theta_I = 3\pi/2$).

a. $k_0 a = 1$

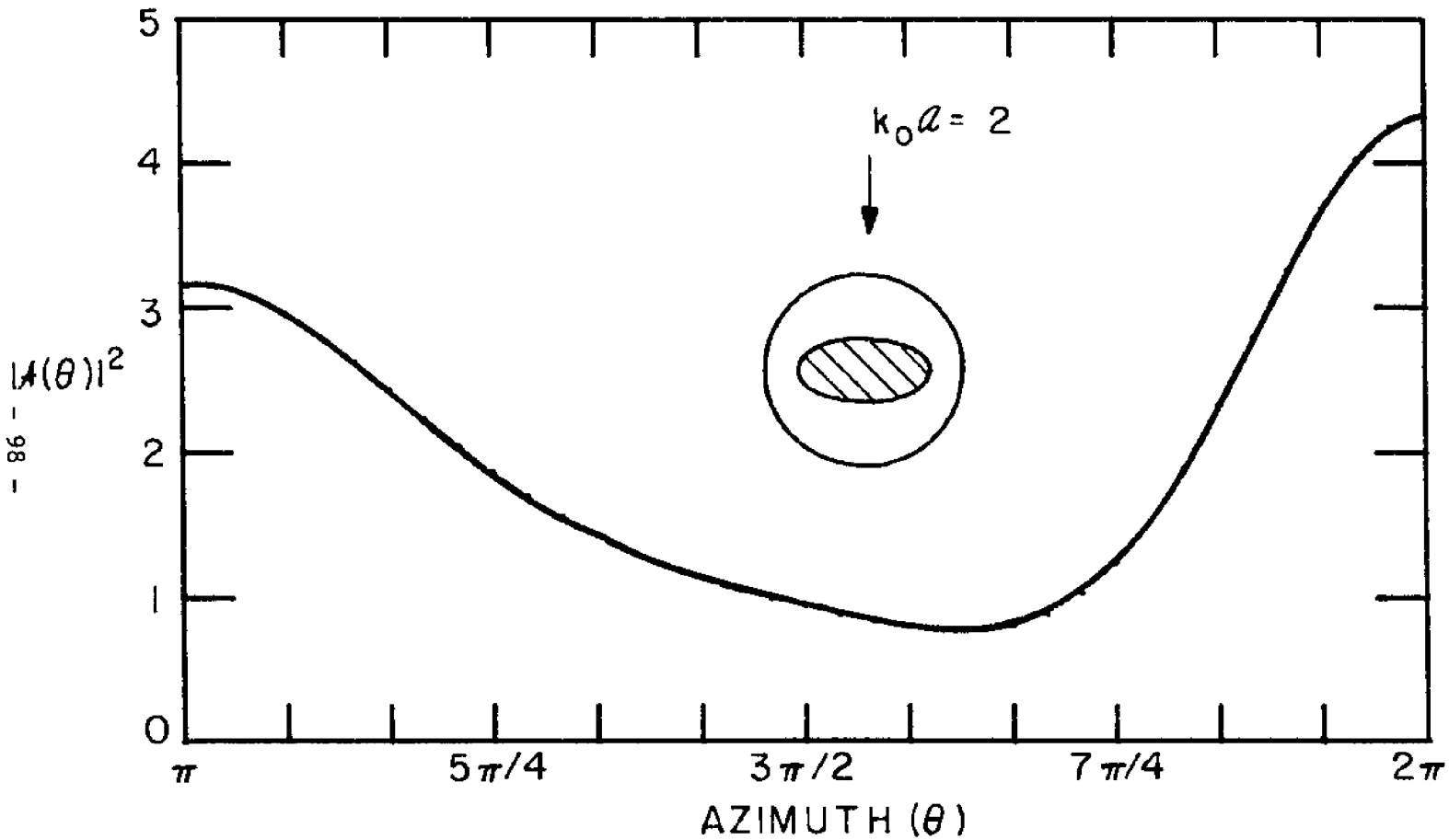

Figure 3.18(b) Differential Scattering Cross-section, $|A(\theta)|^2$, for an Elliptic Island with a Circular Base. Wave Incident from $y \sim +\infty$. ($\theta_I = 3\pi/2$).

b. $k_0 a = 2$

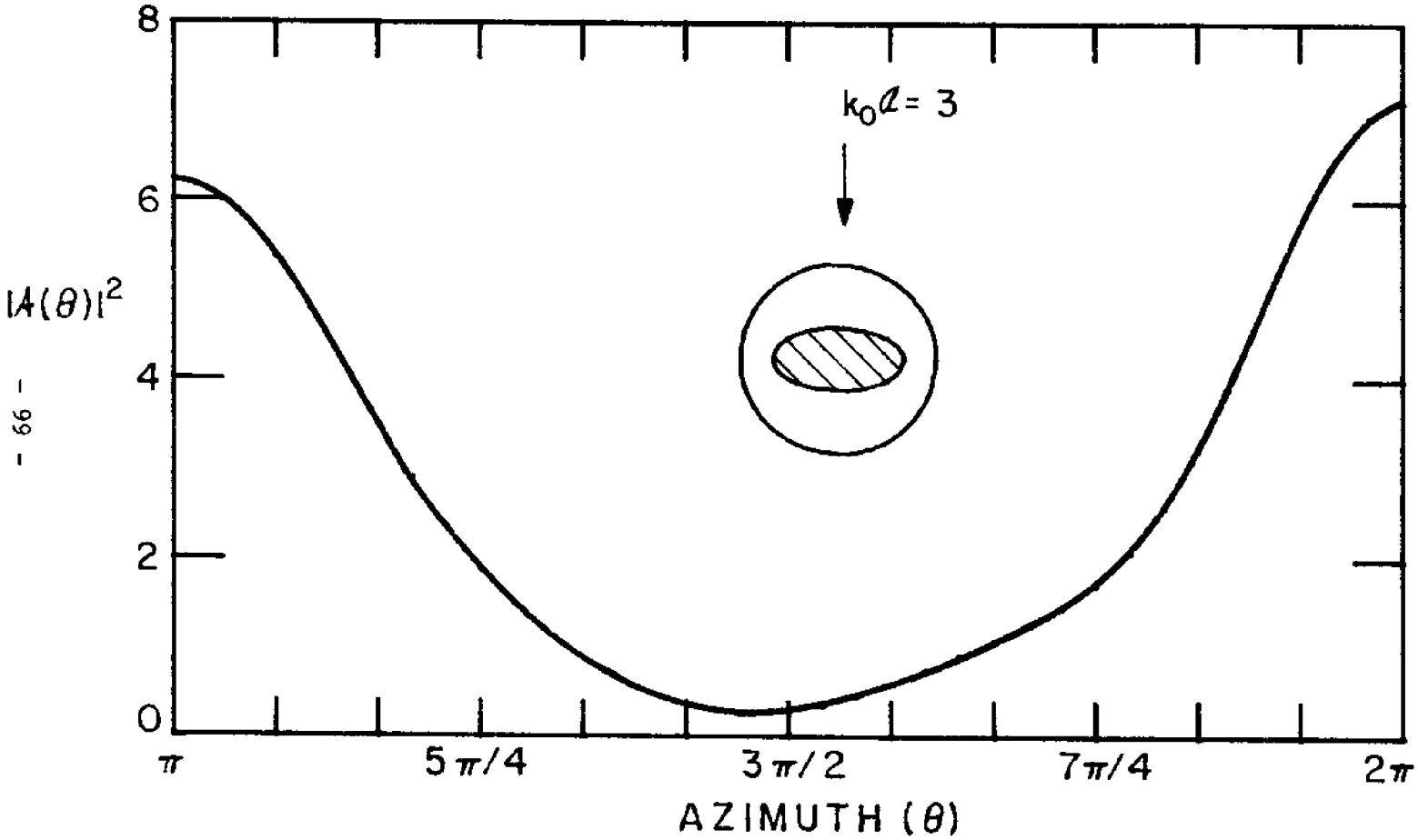

Figure 3.18(c) Differential Scattering Cross-section, $|A(\theta)|^2$, for an Elliptic Island with a Circular Base. Wave Incident from $y \sim +\infty$. ($\theta_I = 3\pi/2$).

c. $k_o a = 3$

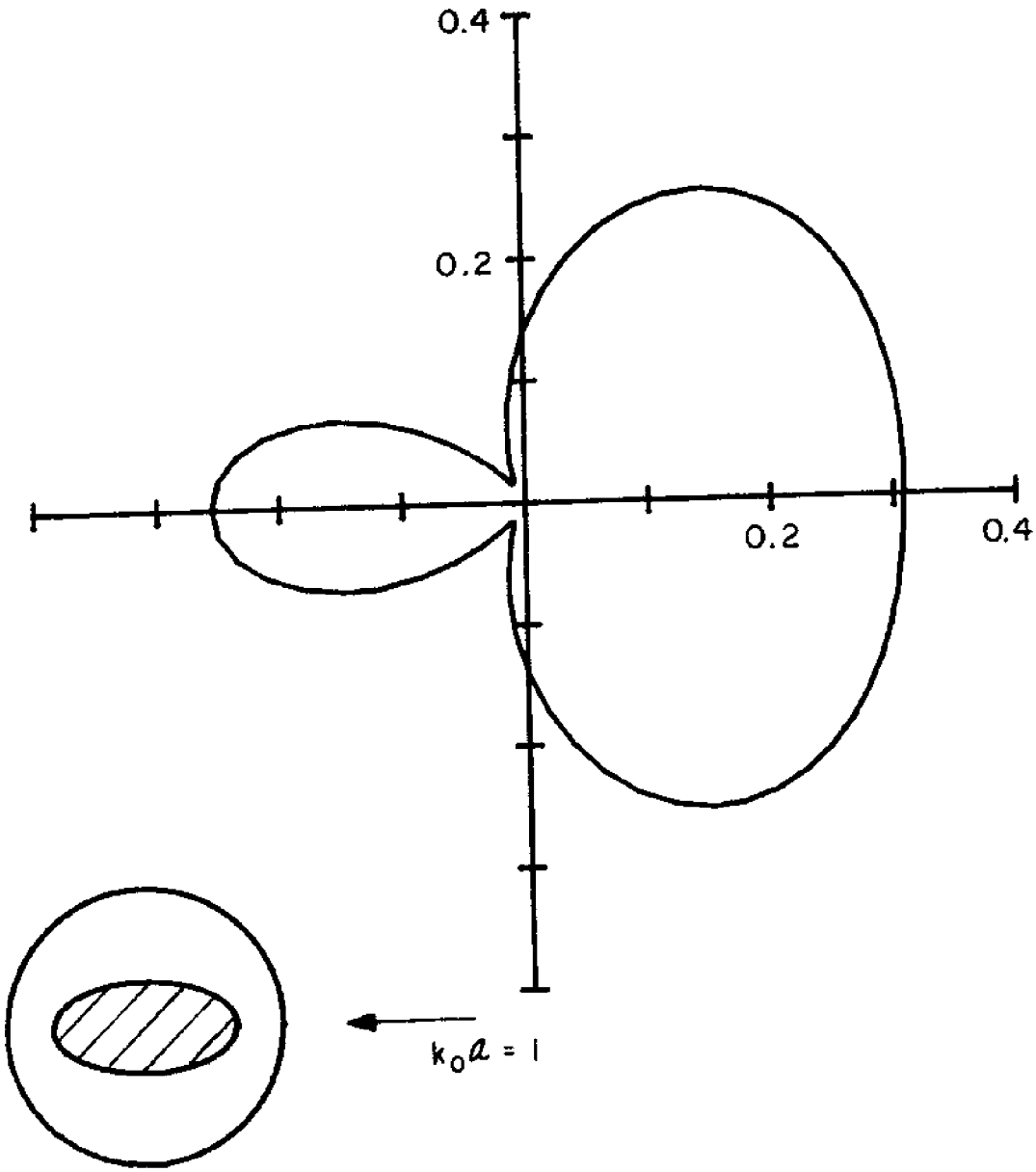

Figure 3.19(a) Polar Plot of Differential Scattering Cross-section, $|A(\theta)|^2$, for an Elliptic Island with a Circular Base. Wave Incident from $x \sim +\infty$. $(\theta_1 = \pi)$.

a. $k_0 a = 1$

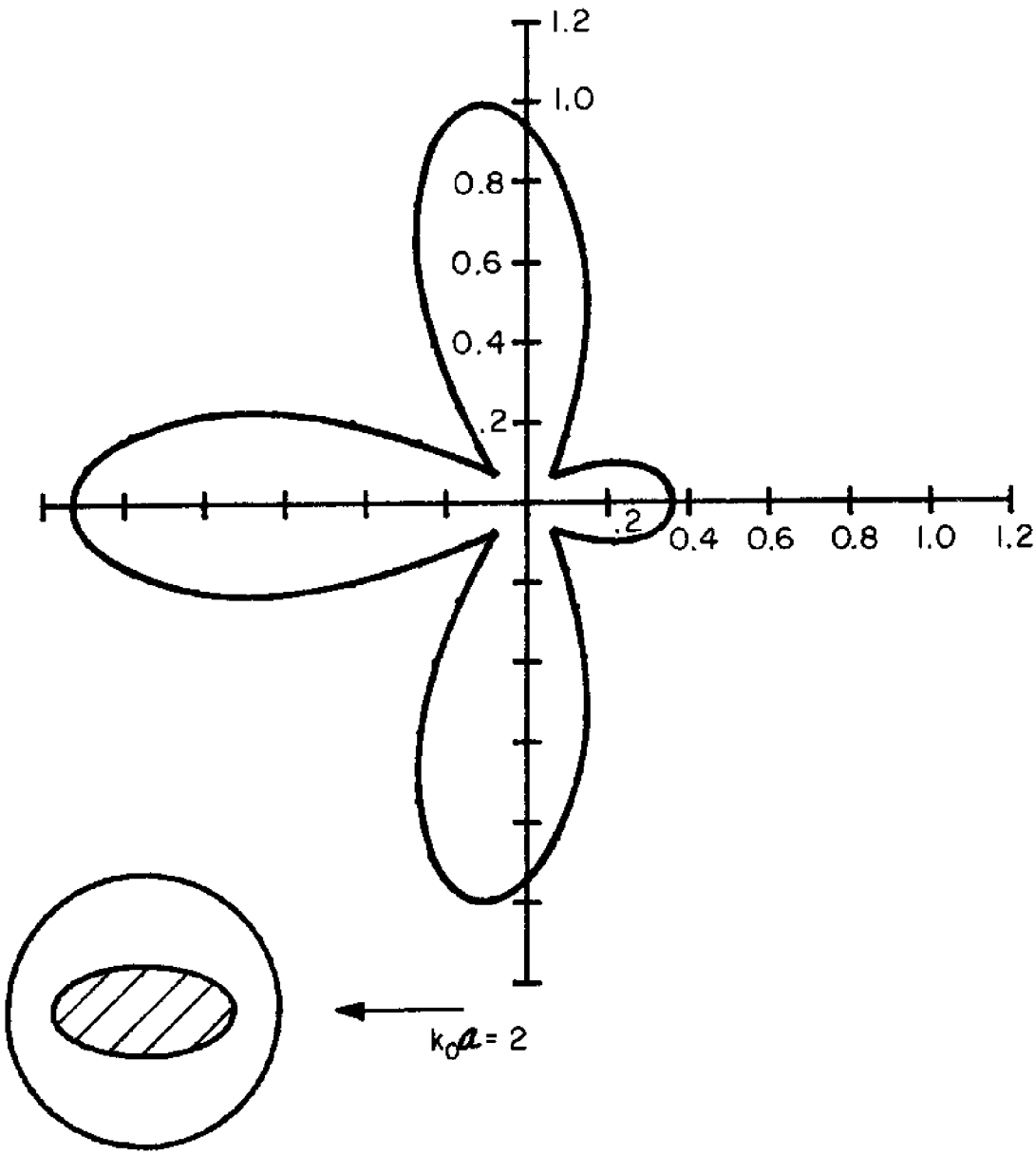

Figure 3.19(b) Polar Plot of Differential Scattering Cross-section, $|A(\theta)|^2$, for an Elliptic Island with a Circular Base. Wave Incident from $x \sim +\infty$. $(\theta_I = \pi)$.

b. $k_o a = 2$

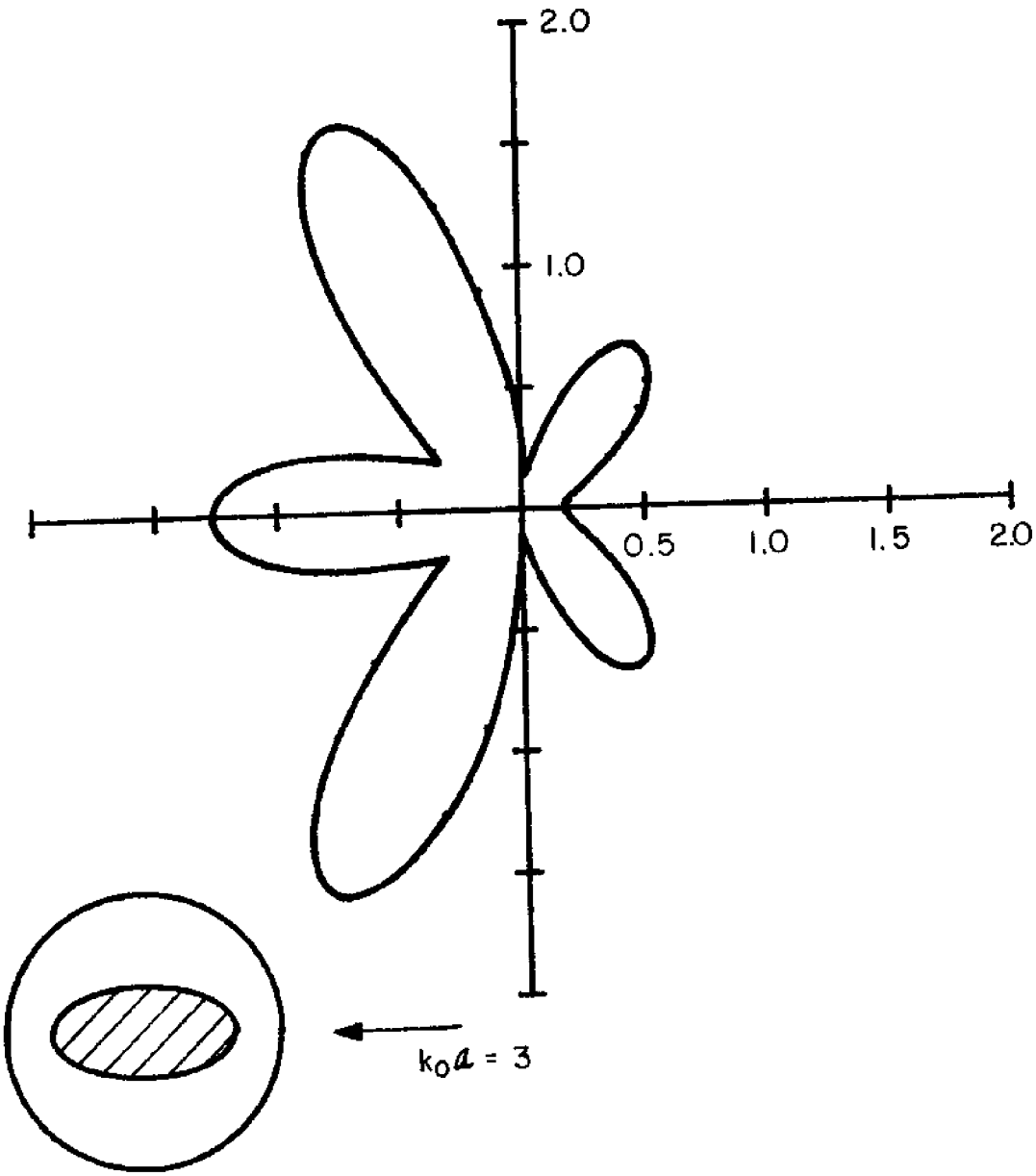

Figure 3.19(c) Polar Plot of Differential Scattering Cross-section, $|A(\theta)|^2$, for an Elliptic Island with a Circular Base. Wave Incident from $x \sim +\infty$. $(\theta_I = \pi)$.

c. $k_0 a = 3$

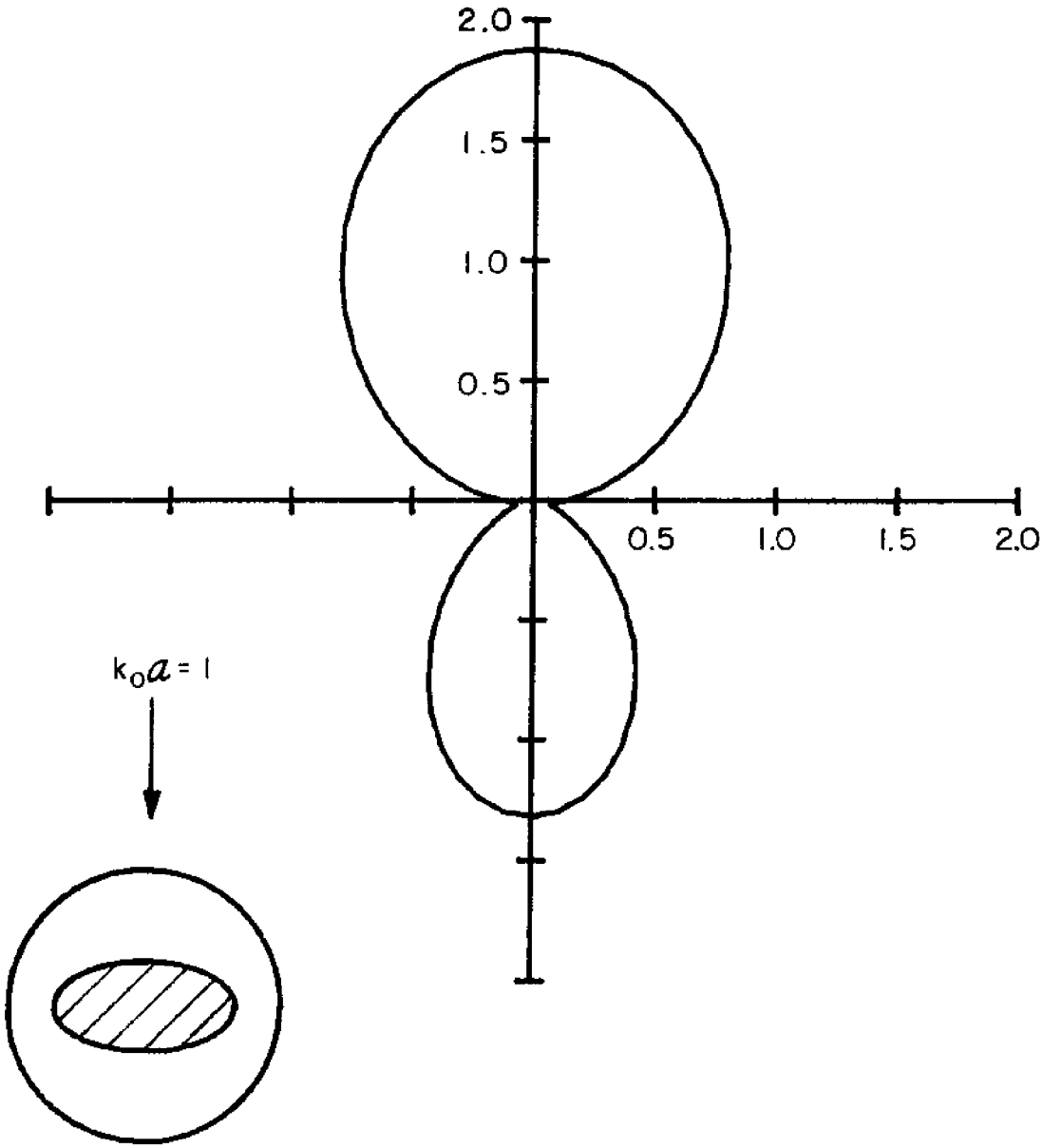

Figure 3.20(a) Polar Plot of Differential Scattering Cross-section, $|A(\theta)|^2$, for an Elliptic Island with a Circular Base. Wave Incident from $y \sim +\infty$. ($\theta_I = 3\pi/2$).

a. $k_o a = 1$

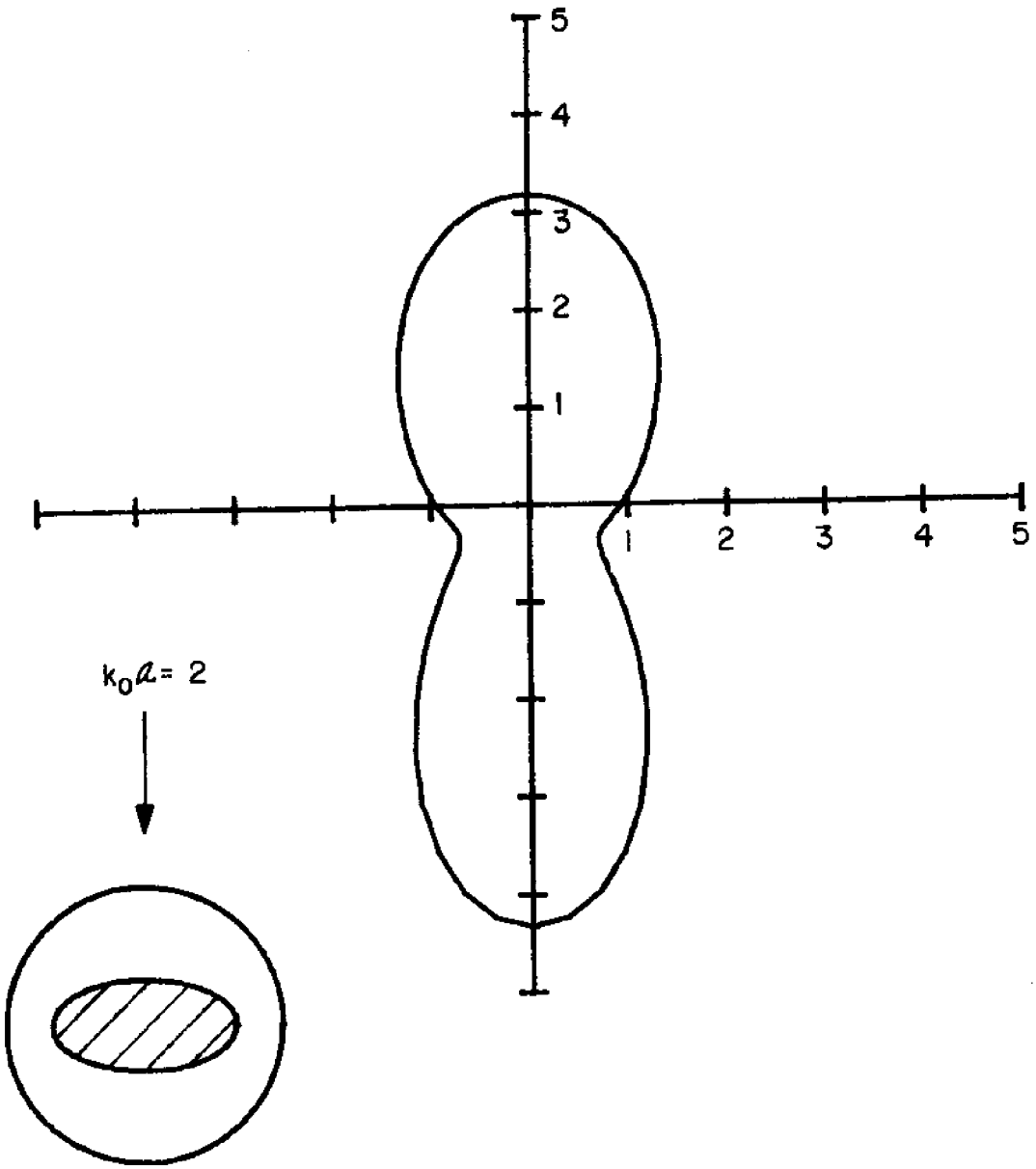

Figure 3.20(b) Polar Plot of Differential Scattering Cross-section, $|A(\theta)|^2$, for an Elliptic Island with a Circular Base. Wave Incident from $y \sim +\infty$. $(\theta_I = 3\pi/2)$.

b. $k_c a = 2$

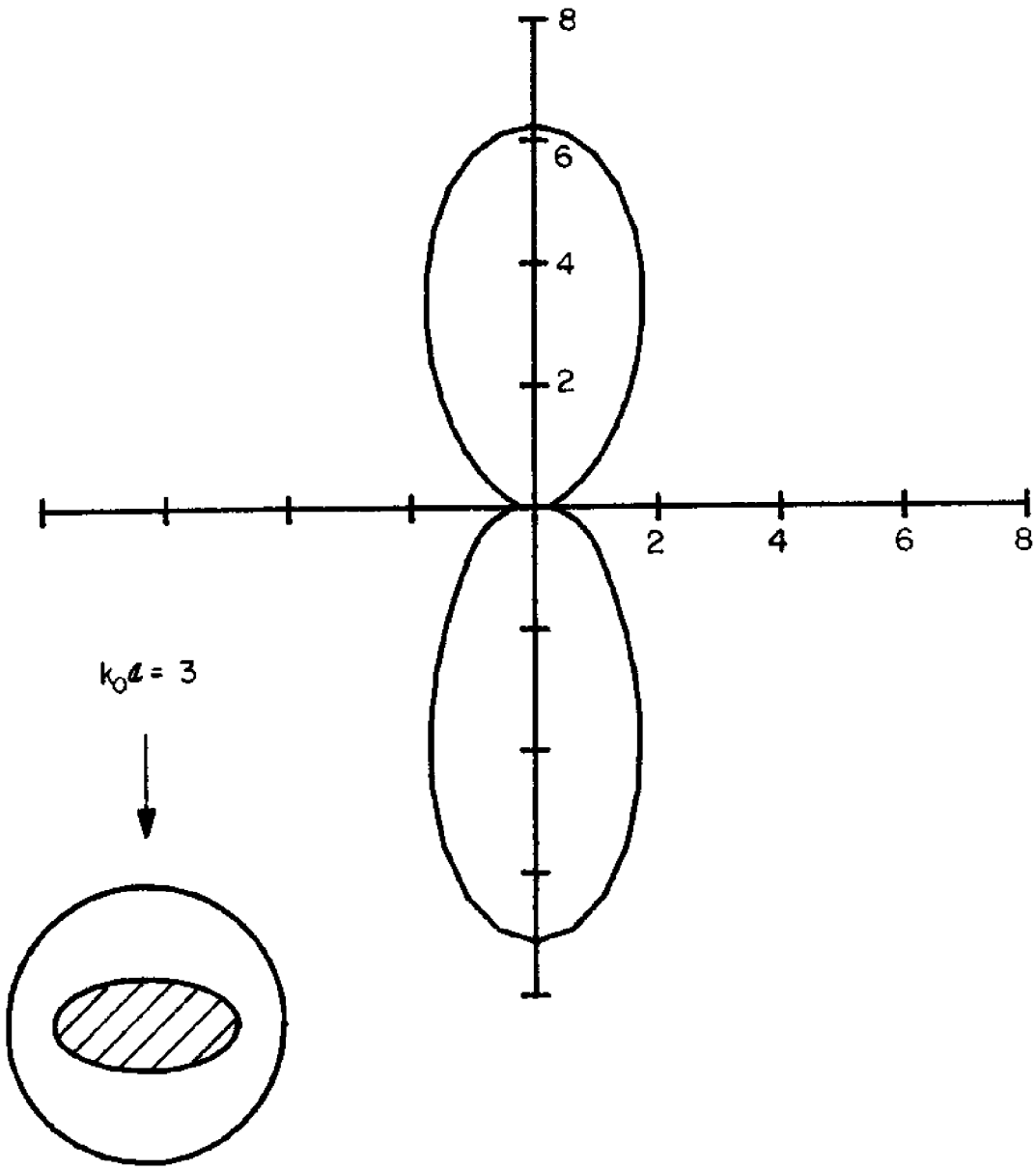

Figure 3.20(c) Polar Plot of Differential Scattering Cross-section, $|A(\theta)|^2$, for an Elliptic Island with a Circular Base. Wave Incident from $y \sim +\infty$. $(\theta_I = 3\pi/2)$.

c. $k_o a = 3$

4. ERROR ESTIMATES AND CONVERGENCE TESTS

4.1 The Optical Theorem

While a number of general relationships governing the scattering and radiation of ocean structures (Haskind, 1957; Wehausen, 1971; Newman, 1976) are available, there is just one relationship that relates the far-field scattered wave only. It is a statement of global conservation of wave energy and is well known in quantum physics as the Optical Theorem. For scattering of a plane wave by a two-dimensional body, it is the familiar

$$|R|^2 + |T|^2 = 1 \tag{4.1.1}$$

where R and T are respectively the reflection and transmission coefficients. For three-dimensional scattering, it can be stated as

$$\frac{1}{2\pi} \int_0^{2\pi} |A(\theta)|^2 \, d\theta = \frac{-1}{\cosh k_o h} \, \mathrm{Re}[A(\theta_I)] \tag{4.1.2}$$

where h is the constant depth at infinity and $A(\theta)$ is the angular variation of the far-field scattered wave, as given in Eqs. (3.3.1) and (3.3.2).

The integral on the left-hand-side is proportional to what is commonly known as the total scattering cross-section in physics, while the expression on the right of the equality is a measure of the wave energy in the forward direction, i.e. the direction of the incident wave. There are several slightly different proofs of Eq. (4.1.2) all based on Green's theorem, a rather direct one using the method of stationary phase is given in Appendix A.

We define a normalized error measure based on this theorem:

$$E_{OPT} = \left| \frac{\text{L.H.S.} - \text{R.H.S.}}{\text{L.H.S.}} \right| \tag{4.1.3}$$

where L.H.S. and R.H.S. refer to the left and right-hand side respectively of Eq. (4.1.2).

For all our numerical examples, E_{OPT} ranged from $\sim 10^{-6}$ to $\sim 10^{-2}$ depending on wave-number, finite element grid fineness and number of series terms used in the analytic expression in the exterior. As an example, in Fig. 4.1, we plot E_{OPT} over a range of $k_o a$ for the particular case of the square dock in Section 3.3 under obliquely incident waves ($\theta_I = 5\pi/4$). While E_{OPT} is useful as a global error estimate, its expression involves only the propagating modes directly, and it is possible for one to make some small error in an evanescent mode without causing an equal discrepancy in E_{OPT}. Hence, it is also necessary and useful to study some local quantities such as integrated forces on a body or a local pressure to estimate the actual error.

4.2 Convergence of the Finite Element Approximation

Once a geometry is given, an appropriate choice of finite element grid size and number of series terms must be made. In general, elements should

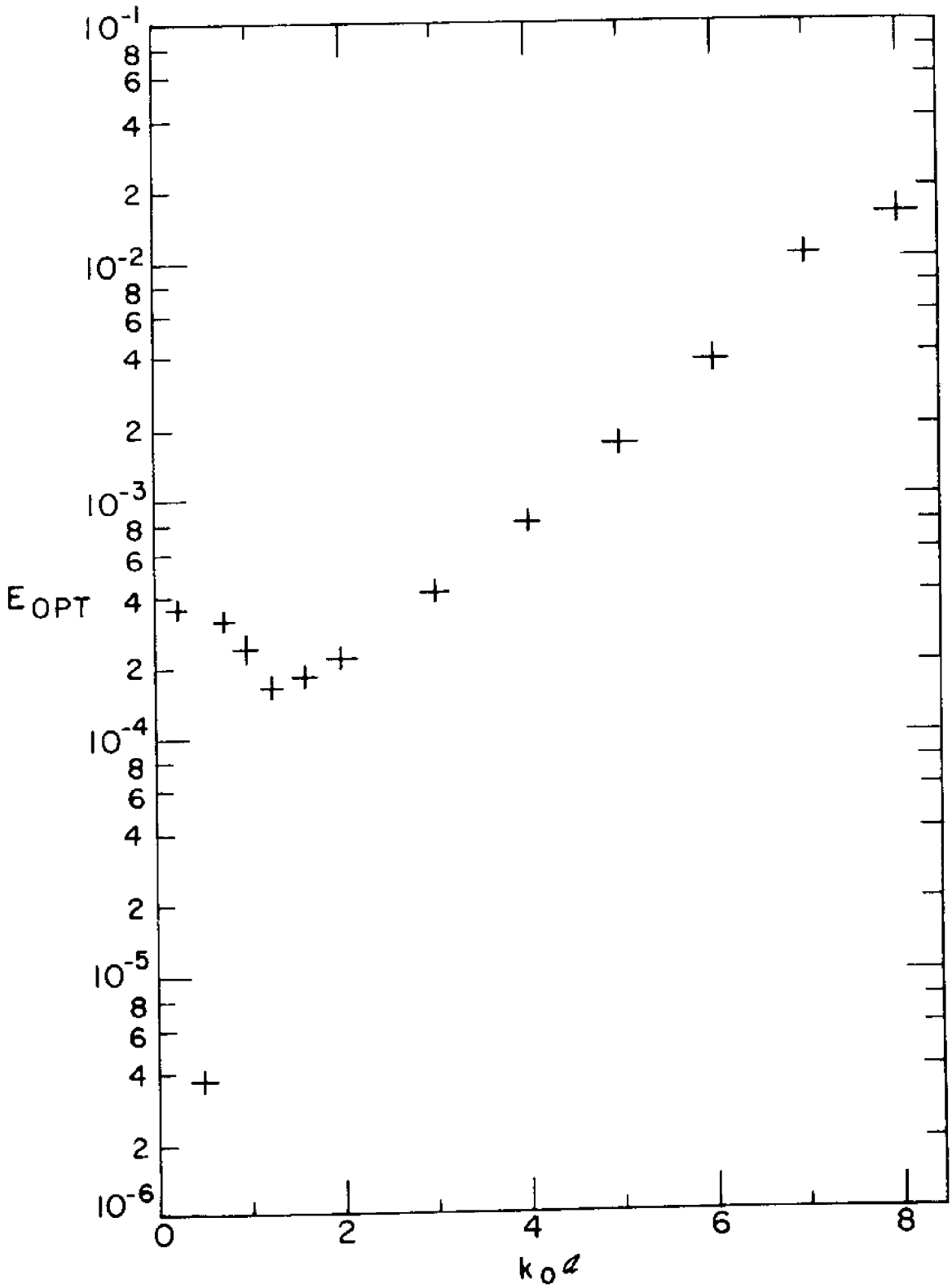

Figure 4.1 Relative Error in Optical Theorem for the Square Dock under Obliquely Incident Waves ($\theta_I = 5\pi/4$).

be chosen with aspect ratio of order unity for optimal accuracy and convergence. The local grid size should be selected according to the length scale of flow variation which in turn is dependent on the length of the incident wave, local body dimensions and depth. To establish some useful criteria on the maximum element size allowed, we take the special case of the uniform vertical cylinder in Section 3.1 (radius a, depth a), where exact analytic solution is available for comparison. Convergence tests are performed, first by fixing the grid system (36 elements - 2 x 18, 342 nodes as shown in Fig. 3.2: average element dimension $\sim$.48a) and varying the incident wave-number, and then by using a range of grid structures for a fixed wave-number ($k_o a = 1$). Five vertical eigenvalues (M=4) and a total of 99 series terms ($N_o = 12$, $N_1 = N_2 = N_3 = N_4 = 10$) are used for all the test cases.

Figure 4.2 presents a plot of $E_{|F|}$ for a range of wave number where we define

$$E_{|F|} = \frac{|F_x|_{analytic} - |F_x|_{FEM}}{|F_x|_{analytic}}$$

For a local measure, we define $E_{|\eta|_\theta}$ by

$$E_{|\eta|_\theta} = \left| \frac{|\eta|_{analytic} - |\eta|_{FEM}}{|\eta|_{analytic}} \right| \quad \text{at } (r = a, \theta)$$

A plot of $E_{|\eta|_\theta}$, for $\theta = 0$, $\pi/2$ and π, versus $k_o a$ is given in Fig. 4.3.

The error in the integrated quantity $E_{|F|}$ is less than 1% for $k_o a$ up to $\sim$6, while the same requirement for a local quantity $E_{|\eta|_\theta}$ would be satisfied only for $k_o a \gtrsim 4$. This implies a maximum average element

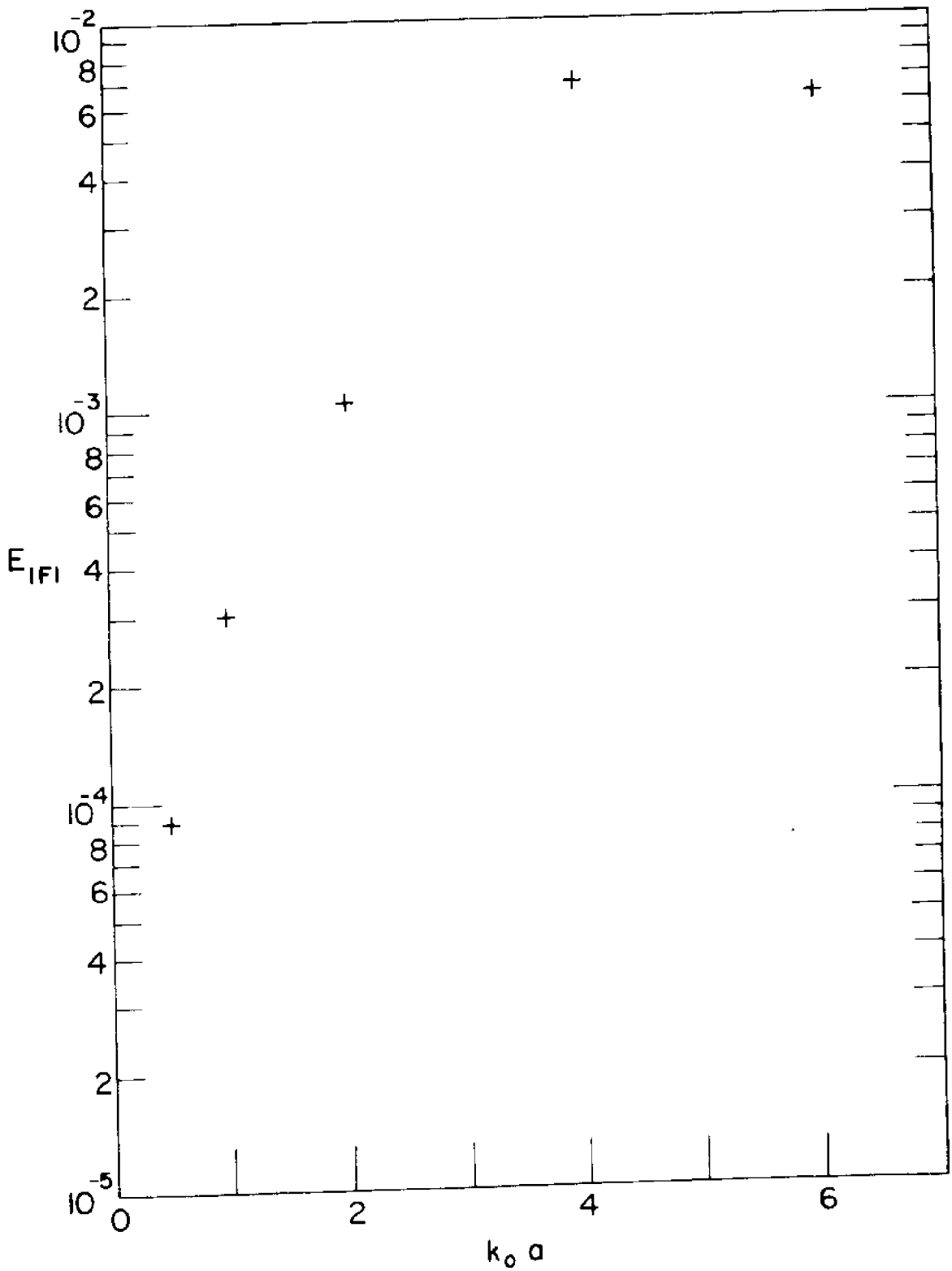

Figure 4.2 Relative Error in the Magnitude of the Horizontal Force on a Uniform Cylinder.

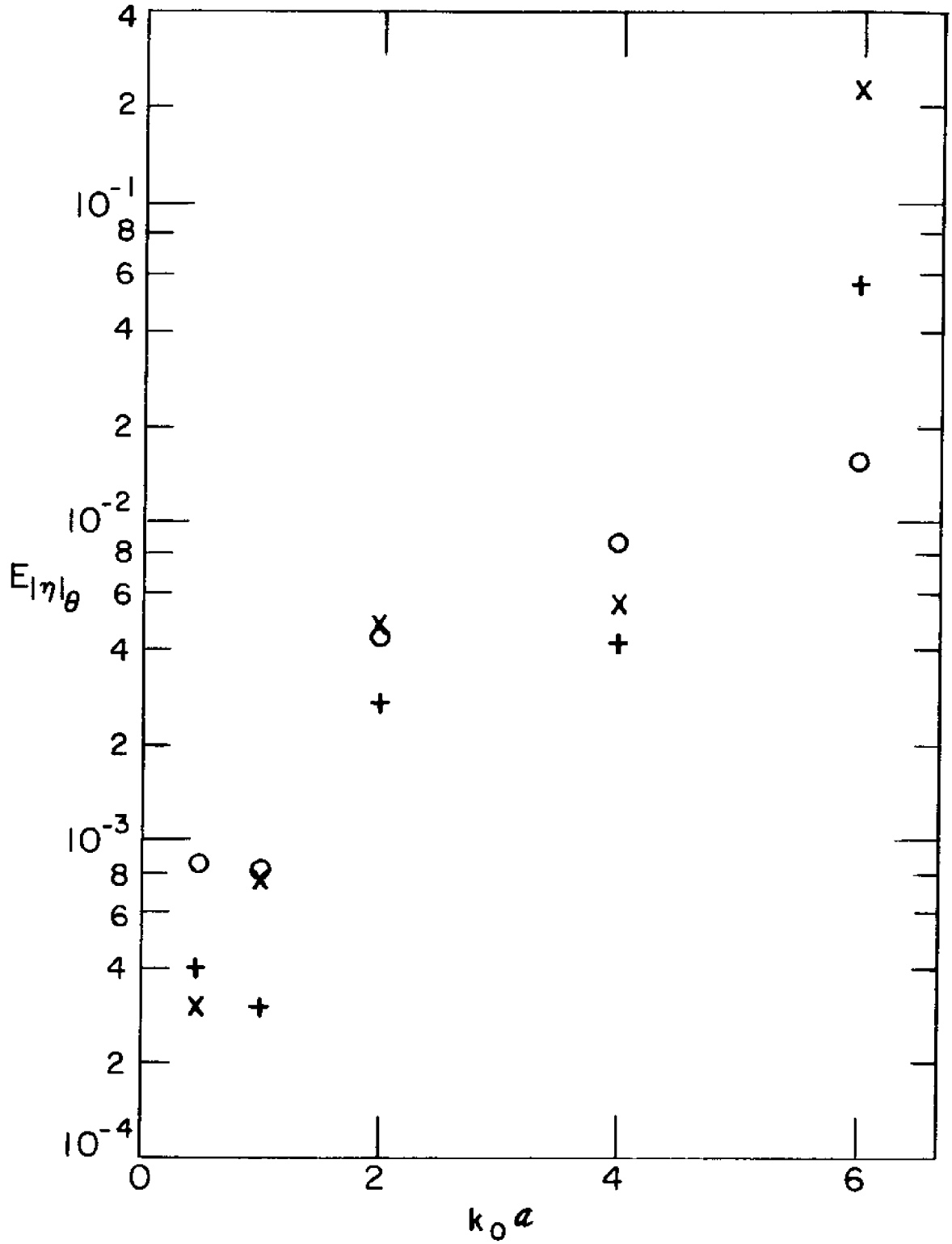

Figure 4.3 Relative Error in the Magnitude of the Run-up on a Uniform Cylinder at: + : $\theta = 0$; X: $\theta = \pi/2$; o: $\theta = \pi$. ($\theta_I = \pi$).

dimension $L_{e_{max}}$: $k_o L_{e_{max}} \sim 2.9$ ($\lambda_{min} \sim 2.2\ L_e$) for an integrated quantity such as forces and $k_o L_{e_{max}} \sim 1.9$ ($\lambda_{min} \sim 3.3\ L_e$) for a local quantity such as pressure or wave height.

In Table 4.1, we tabulate the results for a given $k_o a = 1$ for several different grid systems (note that p x q means a finite element structure of p vertical layers of elements and q radial elements per layer). Here we define relative error in the total scattering cross-section by

$$E_S = \frac{\left| \left(\int_o^{2\pi} |A(\theta)|^2\, d\theta \right)_{analytic} - \left(\int_o^{2\pi} |A(\theta)|^2\, d\theta \right)_{FEM} \right|}{\left(\int_o^{\pi} |A(\theta)|^2\, d\theta \right)_{analytic}}$$

The results are quite satisfactory even when the number of radial elements are reduced by about half (2 x 10), but a few percent error is introduced when only 1 layer of elements is used (1 x 18). This is somewhat surprising since the average element dimension in the radial direction is about .8a for (2 x 10) grid which is not much smaller than a vertical dimension of a for the (1 x 18) grid. The implication is that the vertical length scale of the velocity is smaller or at best equal to the horizontal scale for this case ($k_o a = 1$) even though for the present geometry, only the first vertical mode is present $\phi(x, y, z) = \phi(x, y, 0)\ \frac{\cosh k_o(z + h)}{\cosh k_o h}$. The importance of using a sufficient number of elements in the vertical dimension should not be overlooked for a general problem.

FINITE ELEMENT GRID	C_{F_x}	E_{F}	$\lvert\eta/a_o\rvert$ at $r = a$: $\theta = 0$	$E_{\lvert\eta\rvert_o}$	$\theta = \frac{\pi}{2}$	$E_{\lvert\eta\rvert_{\pi/2}}$	$\theta = \pi$	$E_{\lvert\eta\rvert_\pi}$	F_{OPT}	$\frac{1}{2\pi}\int_0^{2\pi}\lvert A(\theta)\rvert^2 d\theta$	E_S
EXACT	1.04461	0	1.70707	0	1.10627	0	.888192	0	0	.210027	0
2 x 18 (342 nodes)	1.04429	3.063×10^{-4}	1.70758	2.988×10^{-4}	1.10659	2.893×10^{-4}	.888906	8.039×10^{-4}	3.809×10^{-6}	.210056	1.381×10^{-4}
2 x 14 (266 nodes)	1.04430	2.968×10^{-4}	1.70727	1.172×10^{-4}	1.10622	4.520×10^{-5}	.889032	9.457×10^{-4}	4.762×10^{-5}	.210008	9.046×10^{-5}
2 x 10 (190 nodes)	1.04421	3.829×10^{-4}	1.70644	3.691×10^{-4}	1.10528	8.949×10^{-4}	.889266	1.209×10^{-3}	8.433×10^{-5}	.209878	7.094×10^{-4}
1 x 18 (216 nodes)	.96800	7.334×10^{-2}	1.66004	2.755×10^{-2}	1.04343	5.680×10^{-2}	.694663	2.179×10^{-1}	6.806×10^{-5}	.198346	5.562×10^{-2}

Table 4.1

Comparison of results for diffraction by a uniform cylinder, $k_o a = 1$, $\theta_I = \pi$, using a variety of finite element grid structures: p x q —— p rings, stacked vertically of q finite elements each.

4.3 Convergence of Series Terms in the Analytic Representation

For numerical computations, it is necessary to truncate the doubly infinite series in Eq. (1.3.4) to the finite sum in Eq. (2.3.2). Unlike many other "hybrid" finite element methods, the present formulation reduces matching conditions to natural boundary conditions and an arbitrary number of vertical eigenfunctions (M) as well as the angular eigenfunctions (N_m) for each vertical mode is permitted. The number of such terms that is required for a given accuracy depends on the incident wavelength, the body and bottom geometry and depth, and more particularly on the size of the artificial boundary S and the finite element grid structure inside S. To provide some guidelines on the number of series terms that is necessary for a given problem, we solve the particular example of the square barge in Section 3.3 (length 2a, draft .5a, depth a) under a normally incident ($\theta_I = \pi$) wave of unit wavenumber ($k_o a = 1$) for several sets of series terms. We start from the original choice ($M = 4$, $N_o = 12$, $N_1 = N_2 = N_3 = N_4 = 10$, total 99 terms) and reduce, first M, keeping N_i fixed, then reduce N_i keeping M fixed. The results of a set of such convergence tests are presented in Table 4.2. Note that

$$\Delta(\ ) \equiv \left| \frac{(\ )_o - (\ )_p}{(\ )_o} \right|$$

and

$$\delta(\ ) \equiv |(\ )_o - (\ )_p|$$

where $(\ )_o$ refers to a quantity computed with the original choice of number of series terms and $(\ )_p$ refers to that computed with the present set.

# OF COEFF. (N_1)	$\lvert C_{F_x} \rvert$	Δ	$\lvert C_{F_z} \rvert$	Δ	$\lvert C_{M_y} \rvert$	Δ	$E_{OPT} \times 10^{-4}$	$\delta \times 10^{-4}$	$\frac{1}{2\pi}\int_0^{2\pi} \lvert A(\theta) \rvert^2 d\theta$	Δ	$\lvert \eta(a,0,0) \rvert / a_o$	Δ	$\lvert \eta(-a,0,0) \rvert / a_o$	Δ
12, 10, 10, 10, 10 (total 99 terms)	1.15098	0	1.20502	0	.278105	0	1.32281	0	.159509	0	1.63129	0	.719368	0
10, 8, 8, 8, 8 (total 79 terms)	1.15100	1.738×10^{-5}	1.20503	8.299×10^{-6}	.278104	3.596×10^{-6}	1.37924	.05643	.159508	6.269×10^{-6}	1.63139	6.130×10^{-5}	.719416	6.673×10^{-5}
6, 5, 5, 5, 5 (total 47 terms)	1.15120	1.911×10^{-4}	1.20504	1.660×10^{-5}	.278102	3.344×10^{-4}	1.54800	.22519	.159561	3.260×10^{-4}	1.63153	1.471×10^{-4}	.719203	2.294×10^{-4}
4, 3, 3, 3, 3 (total 27 terms)	1.15219	1.051×10^{-3}	1.20509	5.809×10^{-5}	.277975	4.674×10^{-4}	23.0409	21.718	.159499	6.269×10^{-5}	1.63201	4.414×10^{-4}	.716928	3.392×10^{-3}
12, 10, 10, 10 (total 80 terms)	1.15100	1.738×10^{-5}	1.20524	1.826×10^{-4}	.278622	1.859×10^{-3}	1.34848	.02567	.159438	4.451×10^{-4}	1.63412	1.735×10^{-3}	.721197	2.543×10^{-3}
12, 10, 10 (total 61 terms)	1.15105	6.082×10^{-5}	1.20527	2.075×10^{-4}	.278569	1.668×10^{-3}	1.32958	.00677	.159449	3.762×10^{-4}	1.63377	1.520×10^{-3}	.720736	1.902×10^{-3}
12, 10 (total 42 terms)	1.15116	1.564×10^{-4}	1.20515	1.079×10^{-4}	.278443	1.223×10^{-3}	1.78560	.03721	.159458	3.197×10^{-4}	1.63400	1.661×10^{-3}	.720836	2.041×10^{-3}
4, 3 (total 12 terms)	1.15240	1.233×10^{-3}	1.20516	1.162×10^{-4}	.278335	8.270×10^{-4}	23.1520	21.829	.159425	5.266×10^{-4}	1.63479	2.146×10^{-3}	.718747	8.633×10^{-4}

Table 4.2
Comparison of results for diffraction by a square barge, $k_o a = 1$, $\theta_I = \pi$, using a range of numbers of coefficient terms.

While the present results are not unrelated to the incident wave, the particular geometry and element grid, they do indicate that the original set using 99 series terms is extremely conservative with error in both local and integrated quantities less than $\sim 10^{-5}$. It is quite amazing to note for example that the solution converged to within much less than 1% even when only a total of 12 terms ($M = 1$, $N_o = 4$, $N_1 = 3$) are used.

This confirms the earlier observation that it is almost always numerically advantageous to use a smaller S, and hence reduce the number of finite element nodes, even at the cost of having to include more unknowns in the exterior series representation, since the total number of series terms required is much smaller than the semi-bandwidth of the finite element grid for most problems.

It should be noted that a complete study of convergence of the series terms would require a systematic set of tests similar to the one performed, for a range of incident wave lengths, depths and body dimensions (or geometry), as well as the size of S and of the finite elements. While such extensive tests are beyond the scope of this work, this and especially the last section on convergence of the finite elements should already provide the basic guidelines to the choice of number of series terms, and the element size to use for a given problem.

5. COMPUTATIONAL ASPECTS AND THE PROGRAM USAGE

5.1 Program Implementation, Space and Time Requirements

The program is implemented on an IBM 370/168 computer running in an OS/MVT environment at the M.I.T. Information Processing Center (IPC). The program is written in IBM FORTRAN G1 language (extensive testing also done using a WATFIV compiler). Three routines (BJS, BYS, BKS) to calculate Bessel and related functions are called from the IBM SL-MATH library and an assembly language program to set consecutive array elements to zero, ERASE (not WATFIV compatible) supported and provided for unrestricted use by M.I.T. (IPC) is also called.

The FORTRAN program (including comment statements) is 1308 cards long and requires about 78 K (1 K = 1024 storage locations (bytes) of 8 bits each) object code.

The total primary core storage requirements (object code and arrays) and the CPU processing time required for each of the examples in Chapter 3 and 4 are summarized in Table 5.1. Single precision accuracy (4 bytes, equivalent to approximately 7.2 decimal digits accuracy) is adopted throughout, and no secondary storage is used. The timing, which includes mesh generation, but not input/output operations or program compilation, is calculated from operating system cost summaries and not from direct timing routines. It is hence only an approximate estimate, and in light of the findings in Chapter 4, likely to be on the conservative side since an extravagent number of coefficients and conservative finite element grids are always used.

Example	Number Of Nodal Unknowns	Total # of Coefficient Unknowns	Semi-bandwidth	Core Storage Required (K) (approximate)	CPU Processing Minutes Per Wavenumber (estimated)
Uniform Cylinder:					
2 x 18 grid	342	99	217	800	2.6
2 x 14 grid	266	99	173	554	1.4
2 x 10 grid	190	99	129	362	0.7
1 x 18 grid	216	99	139	412	0.8
Semi-immersed Cylinder	435	99	195	874	2.8
Square Dock	435	99	195	878	2.8
	435	80	195	859	2.7
	435	61	195	840	2.5
	435	42	195	821	2.4
	435	27	195	826	2.2
	435	12	195	791	2.1
Elliptic Island	342	99	217	800	2.6

Table 5.1 Summary of Computational Requirements

5.2 The Hybrid Finite Element Program

5.2.1 Program Logic

The total program consists of a main program and 19 subroutines. The program is general with regard to geometry, choice of grids or coefficients, or incident wave period or angle, with the exception of the following routines:

(1) MAIN, the main program which must be slightly modified to reflect correct array sizes;

(2) INPUT, the input program which must be changed for any changes in geometry or grid structure;

(3) FORCE, this routine to calculate force and moment coefficients is dependent on the particular body geometry; and

(4) MESHO, MESH1. While these mesh generation routines are quite general, they are particularly suitable for cylindrical geometries as in the examples treated. Minor modifications for other geometries are very advisable.

The overall program logic is best illustrated in Fig. 5.1 by the flow of control among the subprograms.

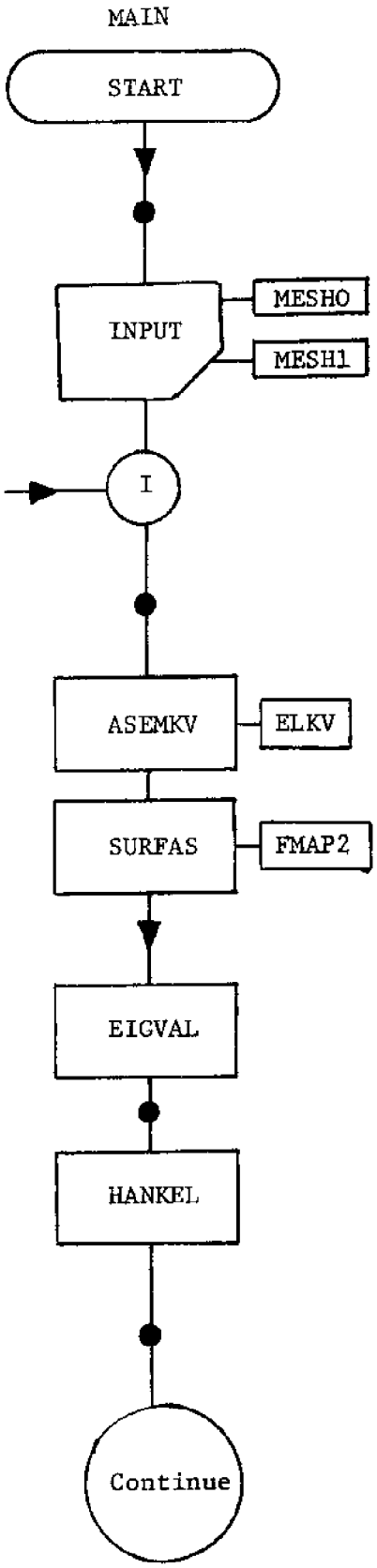

initialize constants and I/O device numbers

set up and print geometrical and grid data

loop over each frequency point

input and print physical data

assemble $[K_V]$ corresponding to the volume integral

assemble into $[K_V]$ the matrix $[K_F]$ resulting from the integral over the free surface

calculate all required eigenvalues k_m

output summary of eigenvalues etc.

calculate all required normalized Hankel and related functions

output summary of Hankel functions, normalization factors, etc.

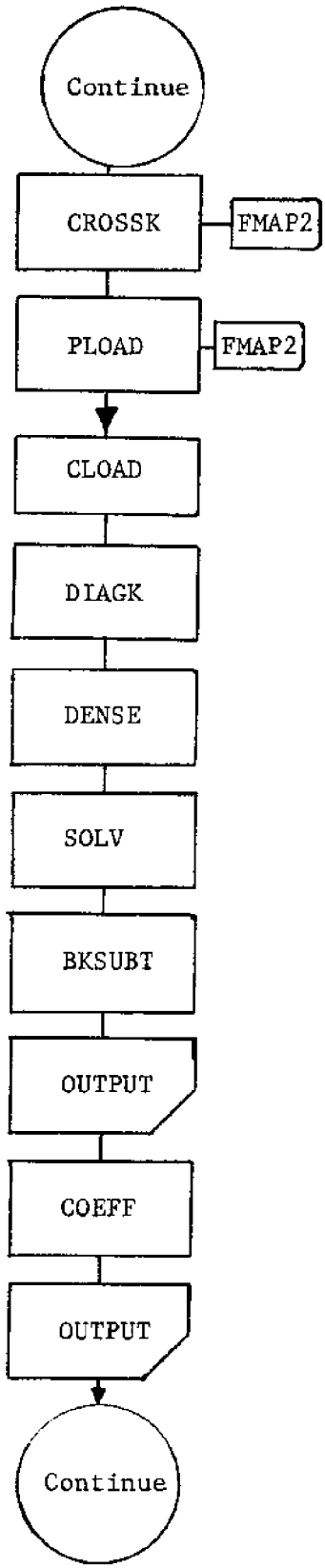

assemble matrices / vectors due to artificial boundary S

static condensation to eliminate coefficient unknowns $\{\mu\}$

Gauss elimination to reduce equation matrix to upper triangular form

back substitution for solution $\{\phi\}$

print dimensionless nodal potential solution

substitute to recover $\{\mu\}$

unnormalize and output all dimensionless coefficient solutions

calculate and output optical theorem results

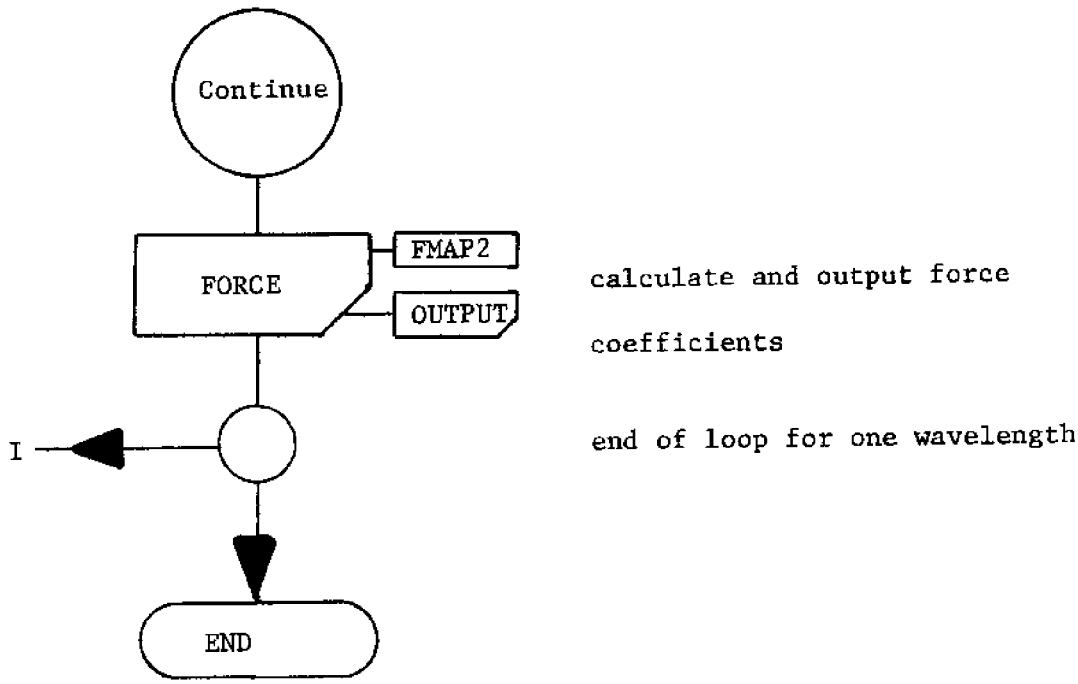

Figure 5.1 Flow chart for the program

The following is a description of each of the programs used:

5.2.1.1 MAIN

This main program is responsible for the transfer of control indicated in Fig. 5.1. It also initiates universal constants, input/output device numbers and performs basic conversions, input and output, and error calculation (Optical Theorem).

5.2.1.2 INPUT

This subroutine sets up and prints all geometric and grid data. *It must be rewritten for any change in geometry.* For all the examples studied , no data is input and the grids are generated via calls to mesh generation programs: MESHO and MESH1.

5.2.1.3 MESHO, MESH1

These routines generate vertical cylindrical rings of 20-node hexahedral elements: the node coordinates and the element node connectivities. The number of vertical, angular and radial layers of elements and the positions of the nodal points, as well as the initial values for node and element numbering can be arbitrarily specified. Node numbering is radially, from top to bottom and sprials out. By using a suitable set of calling parameters, the resulting bandwidth of the system can be minimized. This is achieved in all the examples treated.

The element node connectivities are set-up in the order assumed

in all the other subprograms.

For grid geometries that can be described in cylindrical coordinates by constant coordinate surfaces, MESH0 and MESH1 can be used directly to generate the complete grid system. When the geometry deviates only slightly from the former shapes, only those particular regions need to be input (see Fig. 5.2). For a problem where grid systems of other analytic (such as rectangular, elliptic, etc.) shapes are more efficient, MESH0, MESH1 must be modified. The general program structure, however, is still valid and required changes can be quite minor.

5.2.1.4 EIGVAL

This routine obtains the specified number of eigenvalues k_m of Eq. (2.3) by using fixed-point iteration.

5.2.1.5 HANKEL

The required functions $J_n(k_o r_S)$, $H_n^{(1)}(k_o r_S)$, $K_n(k_m r_S)$, $H_n^{(1)'}(k_o r_S)$ and $K_n'(k_m r_S)$ are calculated and normalized in the following manner:

$$(H_n^{(1)}(x))_{\text{normalized}} = \frac{H_n^{(1)}(x)}{P(n,x)}$$

where

$$P(n,x) = \begin{cases} (x^2 - n^2)^{-1/4} & \text{for } x^2 - n^2 > \sqrt{x} \\ x^{-1/3} & \text{for } |x^2 - n^2| \leq \sqrt{x} \\ (n^2 - x^2)^{-1/4} \exp[-(n^2 - x^2)^{1/2} + n \cosh^{-1}(\frac{n}{x})] & \\ & \text{for } n^2 - x^2 > \sqrt{x} \end{cases}$$

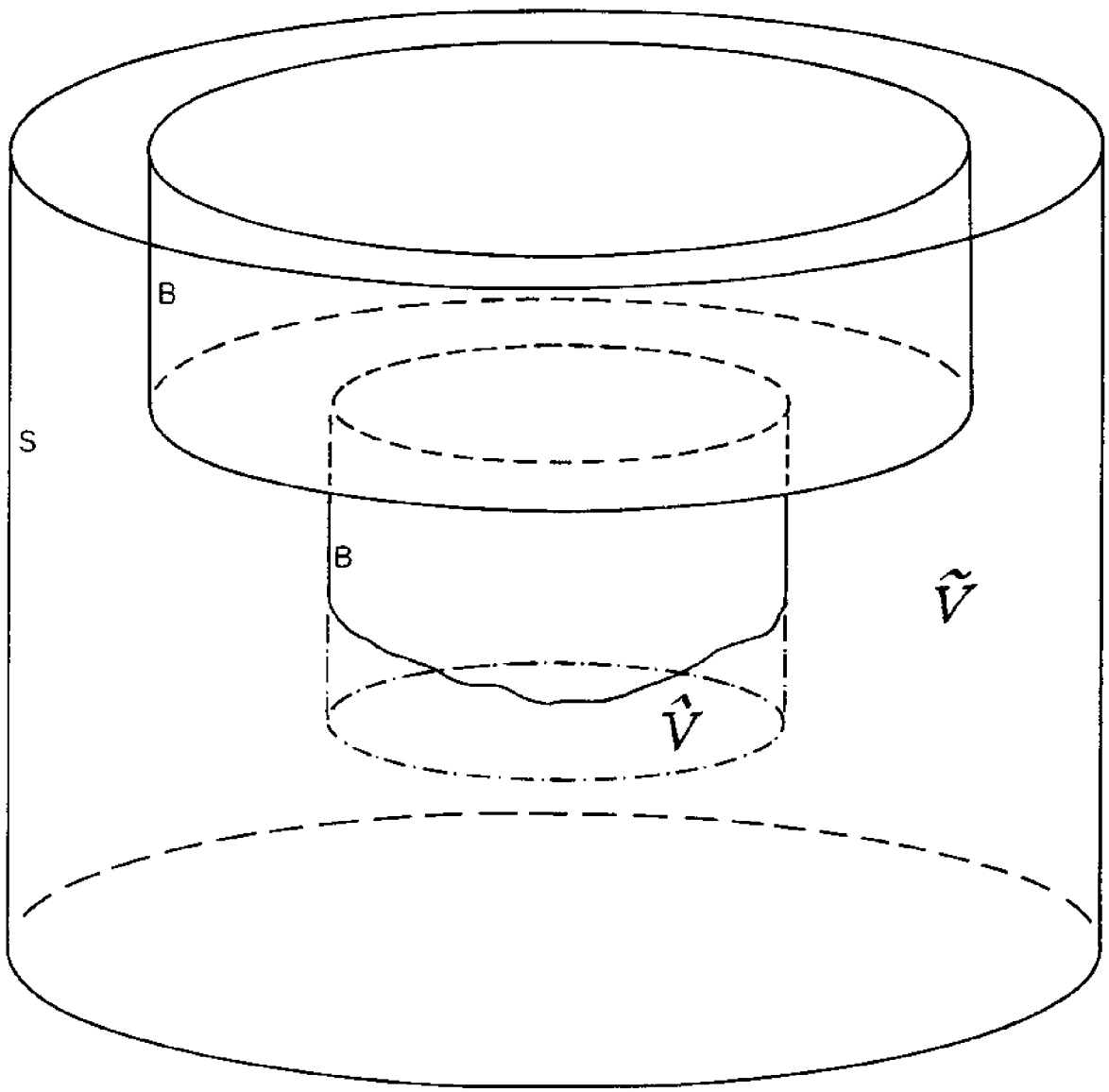

Figure 5.2 An example using both automatic generation (in region $\tilde{V}$) and direct input (in region $\hat{V}$) to set up finite element grids

and

$$(K_n(x))_{normalized} = \frac{K_n(x)}{Q(n,x)}$$

where

$$Q(n,x) = (n^2 + x^2)^{-1/4} \, e^{-\sqrt{n^2 + x^2}} \left(\frac{n + \sqrt{n^2 + x^2}}{x}\right)^n$$

It follows from recursive formulae that

$$(H_n^{(1)'}(x))_{normalized} = \frac{H_{n-1}^{(1)}(x) - \frac{n}{x} H_n^{(1)}(x)}{P(n,x)}$$

and

$$(K_n'(x))_{normalized} = \frac{-K_{n-1}^{(1)}(x) - \frac{n}{x} K_n^{(1)}(x)}{Q(n,x)}$$

$J_n(k_o r_S)$ occurs only in the right-hand side vector and is not normalized.

The above normalization is clearly not unique but is adequate to make the special functions involved to be of order unity for the entire range of m and n. These normalized values are used throughout the programs. Although the final system of linear equations is well conditioned, this normalization may be important especially when round-off accumulation may be significant.

5.2.1.6 ASEMKV and ELKV

ASEMKV assembles the global matrix $[K_V]$ from the element matrices $[K_V^e]$ which are calculated in ELKV using numerical integration. The mathematical procedure is as described in Section 2.1, which involves the isoparametric mapping (2.1.5).

5.2.1.7 FMAP2

This mapping routine is called by four other programs SURFAS, CROSSK, PLOAD and FORCE. It performs the numerical isoparametric mapping from one face of the parent element in local coordinates onto a face of the daughter element on the free surface F or the cylindrical surface S in global x,y,z coordinates. The Jacobian and/or the corresponding global coordinate values are returned as required for numerical quadrature (see Eqs. (2.1.5), (2.2.4), (2.3.2.0)).

5.2.1.8 SURFAS

The matrix $[K_F]$ due to the integral over the free surface, I_2, is assembled directly into $[K_V]$ from each element on the free surface. Numerical integration is performed in local coordinates and mapped into global coordinate space (see Section 2.2).

5.2.1.9 CROSSK, PLOAD, CLOAD, DIAGK

These four routines construct respectively $[K_C]$, $\{Q_P\}$, $\{Q_C\}$, $[K_D]$, which are the vectors and matrices resulting from integrals on the

artificial boundary S (I_3-I_6). CROSSK and PLOAD require quadrature and mapping, while $\{Q_C\}$ and $[K_D]$ are evaluated directly. The procedures follow quite directly from Section 2.3.

The load vectors $\{Q_P\}$, $\{Q_C\}$ are nondimensionalized by the factor $(-\frac{iga_o}{\omega})$, i.e.,

$$(\{Q_P\})_{\text{dimensionless}} = \frac{\{Q_P\}}{(-\frac{iga_o}{\omega})}$$

and

$$(\{Q_C\})_{\text{dimensionless}} = \frac{\{Q_C\}}{(-\frac{iga_o}{\omega})}$$

The resulting nodal potential and series coefficient solutions are hence also dimensionless:

$$(\{\phi\})_{\text{dimensionless}} = \frac{\{\phi\}}{(-\frac{iga_o}{\omega})}$$

and

$$(\{\mu\})_{\text{dimensionless}} = \frac{\{\mu\}}{(-\frac{iga_o}{\omega})}$$

5.2.1.10 DENSE and COEFF

For computational efficiency in Gauss elimination, DENSE performs static condensation to eliminate the unknowns $\{\mu\}$ (see Eq. (2.5.9.a)). No matrix inversion is required here as $[K_D]$ is diagonal. Subroutine COEFF recovers $\{\mu\}$ by substitution (Eq. (2.5.8)) of the solution $\{\phi\}$.

5.2.1.11 SOLV and BKSUBT

We have used two general routines to perform Gauss elimination and back-substitution respectively for a system of linear algebraic complex equations. The coefficient matrix of the equations is symmetric and banded, and is therefore stored in a symmetric packed form.

No pivoting (partial or complete) is performed (or is necessary).

5.2.1.12 FORCE

This program calculates force and moment coefficients (Eqs. (3.1.1.a,b) from $\{\phi\}$. Numerical integration is performed using Eq. (2.4.2).

5.2.1.13 OUTPUT

This routine outputs the real and imaginary parts and the magnitude and phase of each entry of a complex vector.

5.2.2 Input Requirements

In addition to the geometric input and the finite element grid as described in Section 5.2.1.2, we must prescribe physical data regarding the incident wave, the number of eigenvalues and of the coefficient unknowns for each frequency point to be solved. These are described here. We remark that if the boundary geometry is complicated so that additional input cards are needed, they must preceed those described in the present section. The following input is required:

CARD NO.	DESCRIPTION OF INPUT	FORMAT
1	NCASE: a right-justified integer giving the number of frequency points to be analyzed in the current run	I5
2	NWK, THETAI, WAVET NWK = right-justified integer representing no. of eigenvalues k_0, k_1, ... k_{NWK-1} to be used for first frequency point THETAI = floating-point number for the wave incident angle in radians WAVET = floating-point no. for the normalized wave period: WAVET = $T/\sqrt{\frac{a}{g}}$ where T is the wave period	I5, 2F15.7
3	N_0, N_1, ..., N_{NWK-1} (if NWK > 20, continue on as many cards as necessary) right-justified integer indicating number of coefficient terms chosen for eigenvalues k_0, k_1, ..., k_{NWK-1}, e.g., if $N_0 = 3$, then cos 0θ, cos θ, sin θ, cos 2θ, sin 2θ, are included.	20I4

Repeat cards 2 and 3 (or more cards) for as many points as indiciated in card 1.

5.2.3 Output Format

The INPUT program prints a summary of geometry and physical data:

a) far-field depth, radius of cylindrical surface S and other geometrical data,

b) total number of nodes and elements,

c) elements on S, on F, on B, etc.,

d) a node-coordinate table,

e) an element-connectivity table,

f) information on semi-bandwidth of resulting matrix.

For each frequency, the following results are printed:

a) wave period and angle of incidence,

b) table of the eigenvalues and the number of coefficients chosen for each,

c) table of Bessel functions required,

d) table of normalized (modified) Hankel functions and their derivative and the normalization factors P and Q,

e) complete list of all dimensionless nodal potentials solutions $(\{\phi\})_{\text{dimensionless}}$,

f) complete list of unnormalized dimensionless coefficient solutions,

g) optical theorem results,

h) force coefficients.

5.2.4 Illustrative Example: Program Listing, Sample Input and Output

The program listing together with sample input and output are presented here for the case of the semi-immersed cylinder using five eigenvalues as described in Section 3.2.

5.2.4.1 Variable name table

The following is a list of variable names used in the main program, these names are preserved as far as possible in the subroutines. The

radius of the cylinder a and the incident amplitude a_o are used as normalization factors throughout. They are assumed to be unity and do not appear in the programs.

Program Variables	Explanation/Notation in Text	Type
Variables in common:		
NELE	total number of elements/ M_V	INTEGER*4
NNOD	total number of nodes/ N_V	"
NS	number of elements on F	"
NB	number of elements on S	"
NODR	number of nodes on S/N_S	"
NEQT	number of equations in final condensed system, equals NNOD	"
NBAND	semi-bandwidth of final condensed system	"
NMAX	$N_o + 1$	"
NTOTL	$\sum_{i=0}^{M} (N_i + 1)$	"
NTOTL2	total number of coefficients used/ N_T	"
NWK	number of eigenvalues chosen in $\phi_s'/M + 1$	"
NMAX2	number of coefficient terms for M = 0/NMAX*2 - 1	"
NFX	number of elements on circumference of cylinder of radius a	"

NFZ	number of elements on bottom of cylinder of radius a	INTERGER*4
IREAD	card input device number	"
IWRITE	printer output device number	"
THETAI	wave incidence angle/θ_I	REAL*4
WAVET	normalized wave period/$\frac{T}{\sqrt{a/g}}$	"
R	radius of S/r_S	"
H	asymptotic depth/h	"
HH	depth of immersion/H	"

Important variables not in common:

NCASE	number of frequency points to solve	INTECER*4
PAI	π	REAL*4
OPR	right hand side of Optical Theorem	"
OPL	left hand side of Optical Theorem	"
CJ	$-i$	COMPLEX*8

Arrays:

NCON (3, NELE)	matrix of element node connectivities	INTEGER*4
NELES (NS)	vector of numbers of elements on F	"
NELEB (NB)	vector of numbers of elements on S	"
NCOF (NWK)	vector of number of coefficients chosen for each eigenvalue/$(N_i + 1)$	"
NELEFX (NFX)	vector of numbers of elements on cylinder circumference	"
NELEFZ (NFZ)	vector of number of elements on cylinder base	"
WK (NWK)	vector of eigenvalues k_m	REAL*4
WKH (NWK)	vector of $k_m h$ values	"

WKR (NWK)	vector of $k_m r_S$ values	REAL*4
XJ (NMAX)	vector of $J_n(k_o r_S)$ values	"
SN (NMAX)	workspace required by routine CROSSK	"
CS (NMAX)	workspace required by routine CROSSK	"
WORK (NMAX)	workspace required by routine HANKEL	"
XYZ (3, NNOD)	matrix of node coordinates	"
FNORM (NWK, NMAX)	matrix of normalization factors for Hankel functions, etc./P(n,x), Q(n,x)	"
SYSK (NEQT, NBAND)	$[K_V]$	COMPLEX*8
SYSQ (NEQT)	$\{Q_P\}$	"
SYSKC (NODR, NTOTL2)	$[K_C]$	"
SYSKD (NTOTL2)	$[K_D]$ (diagonal)	"
SYSQM (NTOTL2)	$\{Q_C\}$	"
XH (NWK, NMAX)	matrix of $(H_n^{(1)}(k_o r_S))_{normalized}$ and $(K_n(\kappa_m r_S))_{normalized}$ values	"
DH (NWK, NMAX)	matrix of $((H_n^{(1)'}(k_o r_S))_{normalized}$ and $(K_n'(\kappa_m r_S))_{normalized}$ values	"

5.2.4.2 Sample Input

For one wavelength solved, only three cards are used:

```
CARD COLUMN  12345678901234567890123456789012345678901234567890...
Card 1:          1
     2:          5       7.8839178      3.1415926
     3:       12   10  10  10  10
```

5.2.4.3 Program listing

```
C
C     MAIN PROGRAM - MAIN
C
      COMPLEX*8 CJ
      COMPLEX*8 SYSK(435,195),SYSQ(435),SYSKC(128,99),SYSKD(99),
     *          SYSQM(99),XH(5,12),DH(5,12),ELKC(8,5,23)
      REAL*4 WK(5),WKH(5),WKR(5),XJ(12),SN(12),CS(12),WORK(12),
     *       XYZ(3,435),FNORM(5,12)
      INTEGER*4 NCON(20,56),NELES(16),NELEB(32),NCUF(5),
     *          NELEFX(16),NELEFZ(24)
      COMMON NELE,NNOD,NS,NB,NODR,NEQT,NBAND,NMAX,NTOTL,NTOTL2,NWK,
     *       THETAI,WAVET,R,H,NMAX2,NFX,NFZ,HH
      COMMON /IO/IREAD,IWRITE
C
C     SET I/O DEVICE NUMBERS
C     PRINTER IS ASSUMED FOR IWRITE
      IREAD=5
      IWRITE=6
      PAI=3.1415926
C
C     SET UP GRID SYSTEM
      CALL INPUT( XYZ,NCON,NELES,NELEB,NELEFX,NELEFZ)
      READ(IREAD,907) NCASE
C
C     BEGINNING OF LOOP OVER FREQUENCY POINTS TO STUDY
      DO 1000 ICASE=1,NCASE
      WRITE(IWRITE,901) ICASE
  901 FORMAT('1',15('*')/' *** CASE ',I2,' ***'/1X,15('*')//)
C
C     I/O FOR PHYSICAL DATA
      READ(IREAD,907) NWK,THETAI,WAVET
  907 FORMAT(I5,2F15.7)
      WRITE(IWRITE,902) WAVET,THETAI
  902 FORMAT(/' DIMENSIONLESS WAVE PERIOD, T/SQRT(A/G)=',F15.7/
     *       ' INCIDENCE ANGLE=',F15.7,' RADIANS'/)
C
```

```
C     ASSEMBLE 'VOLUME' MATRIX SYSK                                     MAIN0037
      CALL ASEMKV( XYZ,NCON,SYSK)                                       MAIN0038
C     ASSEMBLE 'FREE SURFACE' MATRIX INTO SYSK                          MAIN0039
      CALL SURFAS( NELES,NCON,XYZ,SYSK )                                MAIN0040
C                                                                       MAIN0041
      READ(IREAD,908) (NCOF(I),I=1,NWK)                                 MAIN0042
  908 FORMAT(20I4)                                                      MAIN0043
      NMAX=NCOF(1)                                                      MAIN0044
      NMAX2=2*NMAX-1                                                    MAIN0045
      NTOTL=0                                                           MAIN0046
      DO 8 I=1,NWK                                                      MAIN0047
    8 NTOTL=NTOTL+NCOF(I)                                               MAIN0048
      NTOTL2=2*NTOTL-NWK                                                MAIN0049
      ARG=4.*H*PAI*PAI/(WAVET*WAVET)                                    MAIN0050
C                                                                       MAIN0051
C     FIND REQUIRED EIGENVALUES                                         MAIN0052
      CALL EIGVAL( NWK,ARG,WKH )                                        MAIN0053
      DO 12 I=1,NWK                                                     MAIN0054
      WK(I) = WKH(I)/H                                                  MAIN0055
   12 WKR(I)=WK(I)*R                                                    MAIN0056
C                                                                       MAIN0057
C     OUTPUT SUMMARY OF EIGENVALUES                                     MAIN0058
      WRITE(IWRITE,903)                                                 MAIN0059
  903 FORMAT(//1X,'EIGENVALUE NO.',4X,'NO. OF COEFFS.',13X,'K',16X,     MAIN0060
     *'K*H',14X,'K*R'//1X,40('-*-')/)                                   MAIN0061
      WRITE(IWRITE,904) (I,NCOF(I),WK(I),WKH(I),WKR(I),I=1,NWK)         MAIN0062
  904 FORMAT(10X,I2,11X,I2,10X,3E17.6)                                  MAIN0063
C                                                                       MAIN0064
C     CALCULATE ALL REQUIRED NORMALIZED HANKEL & RELATED FUNCTIONS      MAIN0065
      CALL HANKEL(NCOF,WKR,XJ,XH,DH,NMAX,NWK,WORK,FNORM)                MAIN0066
C                                                                       MAIN0067
C     OUTPUT SUMMARY OF HANKEL FUNCTIONS ETC.                           MAIN0068
      WRITE(IWRITE,905)                                                 MAIN0069
  905 FORMAT(//'  ARG.  ORDER',54X,'NORMALIZED',18X,'NORMALIZED'/       MAIN0070
     *        '   M       N',8X,'J(KR)',21X,'FNORM',20X,'H(KR)',22X,    MAIN0071
     *        'H''(KR)'//1X,40('-*-')/60X,'REAL PT.',7X,'IMAG. PT.',    MAIN0072
```

```
     *         8X,'REAL PT.',7X,'IMAG. PT.')                                MAIN0073
      DO 15 M=1,NWK                                                        MAIN0074
      WRITE(IWRITE,910)                                                    MAIN0075
  910 FORMAT(/)                                                            MAIN0076
      M1=M-1                                                               MAIN0077
      NN=NCOF(M)                                                           MAIN0078
      DO 15 N=1,NN                                                         MAIN0079
      N1=N-1                                                               MAIN0080
      IF(M.GT.1) GO TO 14                                                  MAIN0081
      WRITE(IWRITE,906) M1,N1,XJ(N),FNORM(M,N),XH(M,N),DH(M,N)             MAIN0082
      GO TO 15                                                             MAIN0083
   14 WRITE(IWRITE,909) M1,N1,FNORM(M,N),XH(M,N),DH(M,N)                   MAIN0084
   15 CONTINUE                                                             MAIN0085
  906 FORMAT(I4,I7,2X,E15.6,10X,E15.6,2X,2E15.6,2X,2E15.6)                 MAIN0086
  909 FORMAT(I4,I7,27X,E15.6,2X,2E15.6,2X,2E15.6)                          MAIN0087
C                                                                          MAIN0088
C     ASSEMBLE REMAINING MATRICES & VECTORS DUE TO ARTIFICIAL BOUNDARY     MAIN0089
      CALL CROSSK( NELEB,NCON,XYZ,SYSKC,NCOF,WK,DH,ELKC,CS,SN)             MAIN0090
      CALL PLOAD( NELEB,NCON,XYZ,SYSQ,WK,WKH )                             MAIN0091
      CALL CLOAD(SYSQM,XJ,DH,WKH)                                          MAIN0092
      CALL DIAGK( SYSKD,XH,DH,WKH,NCOF )                                   MAIN0093
C                                                                          MAIN0094
C     STATIC CONDENSATION                                                  MAIN0095
      CALL DENSF( SYSK,SYSQ,SYSKC,SYSKD,SYSQM,NNOD,NBAND,NODR,NTOTL2)      MAIN0096
C                                                                          MAIN0097
C     PERFORM GAUSS ELIMINATION & BACK-SUBSTITUTION FOR SOLUTION           MAIN0098
      CALL SOLV(SYSK,SYSQ,NEQT,NBAND)                                      MAIN0099
      CALL BKSUBT(SYSK,SYSQ,NEQT,NBAND)                                    MAIN0100
C                                                                          MAIN0101
C     OUTPUT NODAL SOLUTION                                                MAIN0102
      WRITE(IWRITE,20)                                                     MAIN0103
   20 FORMAT(/// 24('*')/ '**** SYSTEM SOLUTION ***'/24('*')///            MAIN0104
     *' NODAL POINT')                                                      MAIN0105
      CALL OUTPUT(SYSQ,NEQT)                                               MAIN0106
C                                                                          MAIN0107
C     PERFORM SUBSTITUTION TO RECOVER COEFFICIENT SOLUTION                 MAIN0108
```

```
      CALL COEFF( SYSQ,SYSKC,SYSKD,SYSQM,NNOD,NODR,NTOTL2)
C
C     UNNORMALIZE & OUTPUT COEFFICIENT SOLUTION
      WRITE(IWRITE,23)
   23 FORMAT(///' COEFF. IN THE EXPANSION FOR THE FAR-FIELD'/)
      CJ=(0.,-1.)
      I=1
      DO 30 M=1,NWK
      J=1
      WRITE(IWRITE,24) M
   24 FORMAT(/' EIGENVALUE ',I3)
      SYSQM(J)=SYSQM(I)/FNORM(M,1)
      IF(M.EQ.1) OPL=2.*CABS(SYSQM(J))**2
      IF(M.EQ.1) OPR=REAL(SYSQM(J))
      I=I+1
      J=J+1
      NN=NCOF(M)
      IF(NN.LT.2) GO TO 30
      DO 40 N=2,NN
      SYSQM(J)=SYSQM(I)/FNORM(M,N)
      SYSQM(J+1)=SYSQM(I+1)/FNORM(M,N)
      IF(M.EQ.1) OPL=OPL+CABS(SYSQM(J))**2+CABS(SYSQM(J+1))**2
      IF(M.EQ.1) OPR=OPR+REAL((SYSQM(J)*COS(THETAI*(N-1))+
     *   SYSQM(J+1)*SIN(THETAI*(N-1)))*CJ**MOD(N-1,4))
      J=J+2
   40 I=I+2
      CALL OUTPUT(SYSQM,2*NN-1)
   30 CONTINUE
      OPL=OPL/2.
      OPR=-OPR/COSH(WKH(1))
      WRITE(IWRITE,911) OPL,OPR
  911 FORMAT(///1X,23('*')/' *** OPTICAL THEOREM ***',10X,'L.H.S.=',
     *   E15.7/1X,23('*'),10X,'R.H.S.=',E15.7)
C
C     CALCULATE & OUTPUT FORCE COEFFICIENTS
      CALL FORCE(SYSQ,NELEFX,NELEFZ,XYZ,NCON)
```

```
 1000 CONTINUE                                                          MAIN0145
C     END OF LOOP OVER FREQUENCY POINTS                                 MAIN0146
C                                                                       MAIN0147
      STOP                                                              MAIN0148
      END                                                               MAIN0149
```

```
      SUBROUTINE ASEMKV( XYZ,NCON,SYSK)                                 ASKV0001
C                                                                       ASKV0002
C     THIS SUBROUTINE ASSEMBLES THE 'VOLUME' MATRIX SYSK                ASKV0003
C     SYSK IS STORED IN SYMMETRIC PACKED FORM                           ASKV0004
C                                                                       ASKV0005
      COMPLEX SYSK                                                      ASKV0006
      INTEGER*4 NCON,NR                                                 ASKV0007
      COMMON NELE,NNOD,NS,NB,NODR,NEQT,NBAND,NMAX,NTOTL,NTOTL2,NWK,     ASKV0008
     *       THETAI,WAVET,R,H,NMAX2                                     ASKV0009
      DIMENSION XYZ(3,NNOD),NCON(20,NELE),SYSK(NEQT,NBAND)              ASKV0010
      DIMENSION NR(20),ELK(20,20),P(20,3)                               ASKV0011
C                                                                       ASKV0012
C     INITIATE ENTIRE SYSK TO ZERO                                      ASKV0013
C     ERASE IS A MIT IPC SUPPLIED FORTLIB ASSEMBLE LANGUAGE ROUTINE     ASKV0014
C     TO SET CONSECUTIVE ARRAY ELEMENTS TO ZERO                         ASKV0015
      CALL ERASE(SYSK,2*NEQT*NBAND)                                     ASKV0016
C                                                                       ASKV0017
C     LOOP OVER ALL ELEMENTS                                            ASKV0018
      DO 25 L=1,NELE                                                    ASKV0019
      DO 14 J=1,20                                                      ASKV0020
   14 NR(J)= NCON(J,L)                                                  ASKV0021
      DO 16 M=1,20                                                      ASKV0022
      DO 16 N=1,3                                                       ASKV0023
   16 P(M,N)=XYZ(N,NR(M))                                               ASKV0024
C                                                                       ASKV0025
C     ELKV RETURNS ELEMENT MATRIX ELK                                   ASKV0026
      CALL ELKV(P,ELK )                                                 ASKV0027
C                                                                       ASKV0028
C     ASSEMBLAGE                                                        ASKV0029
      DO 20 I=1,20                                                      ASKV0030
      DO 18 J=I,20                                                      ASKV0031
      IF( NR(J)-NR(I) .GE. 0 ) GO TO 17                                 ASKV0032
      LR=NR(I)-NR(J)+1                                                  ASKV0033
      SYSK(NR(J),LR)=SYSK(NR(J),LR)+ELK(I,J)                            ASKV0034
      GO TO 18                                                          ASKV0035
   17 LS=NR(J)-NR(I)+1                                                  ASKV0036
```

```
      SYSK(NR(I),LS)=SYSK(NR(I),LS)+ELK(I,J)                            ASKV0037
   18 CONTINUE                                                          ASKV0038
   20 CONTINUE                                                          ASKV0039
   25 CONTINUE                                                          ASKV0040
      RETURN                                                            ASKV0041
      END                                                               ASKV0042
```

```
      SUBROUTINE BKSUBT(CA,CB,NEQT,NBAND)                               BKBT0001
C                                                                       BKBT0002
C     BACK-SUBSTITUTION FOR SOLN. CX GIVEN (CA)*(CX)=CB                 BKBT0003
C     CA IS A SYMMETRIC PACKED UPPER TRIANGULAR MATRIX                  BKBT0004
C     SOLUTION IS RETAINED IN CB                                        BKBT0005
C                                                                       BKBT0006
      IMPLICIT COMPLEX(C)                                               BKBT0007
      DIMENSION CA(1),CB(1)                                             BKBT0008
      JB=NBAND-1                                                        BKBT0009
      DO 100 I=1,NEQT                                                   BKBT0010
      C=1./CA(I)                                                        BKBT0011
      CB(I)=CB(I)*C                                                     BKBT0012
      IF(I.EQ.NEQT) GO TO 100                                           BKBT0013
      IB=MIN0(JB,NEQT-I)                                                BKBT0014
      DO 200 II=1,IB                                                    BKBT0015
      INDEX=II*NEQT+I                                                   BKBT0016
      CA(INDEX)=CA(INDEX)*C                                             BKBT0017
  200 CONTINUE                                                          BKBT0018
  100 CONTINUE                                                          BKBT0019
      I1=NEQT-1                                                         BKBT0020
      DO 300 I=1,I1                                                     BKBT0021
      J=NEQT-I                                                          BKBT0022
      IB=MIN0(JB,I)                                                     BKBT0023
      DO 400 II=1,IB                                                    BKBT0024
      CB(J)=CB(J)-CA(J+II*NEQT)*CB(II+J)                                BKBT0025
  400 CONTINUE                                                          BKBT0026
  300 CONTINUE                                                          BKBT0027
      RETURN                                                            BKBT0028
      END                                                               BKBT0029
```

```
      SUBROUTINE CLOAD( SYSQM,XJ,DH,WKH )                               CLOD0001
C                                                                       CLOD0002
C     THIS SUBROUTINE CALCULATES THE LOAD VECTOR SYSQM DUE TO COEFFS.   CLOD0003
C                                                                       CLOD0004
      COMPLEX CI,SYSQM,DH,TM                                            CLOD0005
      COMMON NELE,NNOD,NS,NB,NODR,NEQT,NBAND,NMAX,NTOTL,NTOTL2,NWK,     CLOD0006
     *       THETAI,WAVET,R,H,NMAX2                                     CLOD0007
      DIMENSION SYSQM(NTOTL2),XJ(NMAX),DH(NWK,NMAX),WKH(NWK)            CLOD0008
      CALL ERASE(SYSQM,2*NTOTL2)                                        CLOD0009
      CI=(0.0,1.0)                                                      CLOD0010
      PRKH=-3.1415926  *R*WKH(1)                                        CLOD0011
      WKH2 = 2.*WKH(1)                                                  CLOD0012
      CZ=(1.+SINH(WKH2)/WKH2)/COSH(WKH(1))                              CLOD0013
      PC=PRKH*CZ                                                        CLOD0014
      SYSQM(1)= PC*XJ(1)*DH(1,1)                                        CLOD0015
      DO 14 I=2,NMAX2,2                                                 CLOD0016
      N2=I/2+1                                                          CLOD0017
      TM=PC*(CI**MOD(N2-1,4))*XJ(N2)*DH(1,N2)                           CLOD0018
      THETAN=THETAI*FLOAT(N2-1)                                         CLOD0019
      SYSQM( I   ) = TM*COS(THETAN)                                     CLOD0020
   14 SYSQM( I+1) = TM*SIN(THETAN)                                      CLOD0021
      RETURN                                                            CLOD0022
      END                                                               CLOD0023
```

```
      SUBROUTINE COEFF( SYSQ,SYSKC,SYSKD,SYSQM,NNOD,NODR,NTOTL2)
C
C     THIS SUBROUTINE SOLVES FOR COEFF. UNKNOWNS BY DIRECT SUBSTITUTION
C     RESULT IS STORED IN SYSQM
C
      COMPLEX SYSQ,SYSKC,SYSKD,SYSQM
      DIMENSION SYSQ(NNOD),SYSKC(NODR,NTOTL2),SYSKD(NTOTL2),
     *          SYSQM(NTOTL2)
      NN=NNOD-NODR
      DO 24 I=1,NTOTL2
      DO 14 J=1,NODR
      JJ= NN+J
      SYSQM(I) = SYSQM(I)-SYSQ(JJ)*SYSKC(J,I)
   14 CONTINUE
      SYSQM(I)=SYSQM(I)/SYSKD(I)
   24 CONTINUE
      RETURN
      END
```

```
      SUBROUTINE CROSSK( NELEB,NCON,XYZ,SYSKC,NCOF,WK,DH,EKC,CS,SN)
C
C     THIS SUBROUTINE ASSEMBLES FULL MATRIX SYSKC CONTAINING CROSS TERMS
C
      INTEGER*4 NELEB,NCON,NCOF,NR
      REAL*4 PS(4),WS(4),A(1)
      COMPLEX EKC,TM,DH,XH,SYSKC
      COMMON NELE,NNOD,NS,NB,NODR,NEQT,NBAND,NMAX,NTOTL,NTOTL2,NWK,
     *       THETAI,WAVET,R,H,NMAX2,NFX,NFZ,HH
      DIMENSION NCON(20,NELE),XYZ(3,NNOD),NELEB(NB),SYSKC(NODR,NTOTL2),
     *          NCOF(NWK),WK(NWK),DH(NWK,NMAX ),
     *          EKC(8,NWK,NMAX2),CS(NMAX ),SN(NMAX)
      DIMENSION NR(8),P(8,3),Q(8),DQ(2,8),INOD(8)
C
C     QUADRATURE DATA
      DATA INOD/1,8,7,12,19,20,13,9/
      DATA PS/.8611363 ,.3399810 ,-.3399810 ,-.8611363 /
      DATA WS/.3478548 ,.6521451 ,.6521451 ,.3478548 /
C
      CALL ERASE(SYSKC,2*NODR*NTOTL2)
      NNOR=NNOD-NODR
C
C     LOOP OVER ALL ELEMENTS ON ARTIFICIAL BOUNDARY
      DO 40 L=1,NB
      K= NELEB(L)
      CALL ERASE(EKC,16*NWK*NMAX2)
      DO 10 I=1,8
      NR(I)=NCON(INOD(I),K)
      DO 10 J=1,3
   10 P(I,J)=XYZ(J,NR(I))
C
C     QUADRATURE LOOP 1
      DO 20 IS=1,4
      S=PS(IS)
C
C     CALL FMAP2 FOR GLOBAL ANGLE THETA OF INTEGRATION POINT
```

```
      CALL FMAP2( S,T,P,Q,DQ,XX,YY,ZZ,THETA,3)                          CRSK0037
      DO 12 N=1,NMAX                                                    CRSK0038
      CS(N)=COS(THETA*(N-1))                                            CRSK0039
   12 SN(N)=SIN(THETA*(N-1))                                            CRSK0040
C                                                                       CRSK0041
C     QUADRATURE LOOP 2                                                 CRSK0042
      DO 20 IT=1,4                                                      CRSK0043
      T=PS(IT)                                                          CRSK0044
C                                                                       CRSK0045
C     FMAP2 RETURNS JACOBIAN CJ AND GLOBAL COORDINATES XX,YY,ZZ         CRSK0046
      CALL FMAP2( S,T,P,Q,DQ,XX,YY,ZZ,CJ,1 )                            CRSK0047
      CJW=CJ*WS(IS)*WS(IT)                                              CRSK0048
      DO 18 J=1,8                                                       CRSK0049
      DO 19 M=1,NWK                                                     CRSK0050
      CHS=COS(WK(M)*(ZZ+H))                                             CRSK0051
      IF(M.EQ.1) CHS=COSH(WK(1)*(ZZ+H))                                 CRSK0052
      CA=WK(M)*CHS*CJW*Q(J)                                             CRSK0053
      EKC(J,M,1)=EKC(J,M,1)+CA*DH(M,1)*CS(1)                            CRSK0054
      IF(NCOF(M).LT.2) GO TO 19                                         CRSK0055
      NN=NCOF(M)                                                        CRSK0056
      DO 50 N=2,NN                                                      CRSK0057
      TM=CA*DH(M,N)                                                     CRSK0058
      N2=2*(N-1)                                                        CRSK0059
      EKC(J,M,N2  ) = EKC(J,M,N2  ) + TM*CS(N)                          CRSK0060
      EKC(J,M,N2+1) = EKC(J,M,N2+1) + TM*SN(N)                          CRSK0061
   50 CONTINUE                                                          CRSK0062
   19 CONTINUE                                                          CRSK0063
   18 CONTINUE                                                          CRSK0064
   20 CONTINUE                                                          CRSK0065
C                                                                       CRSK0066
C     ASSEMBLAGE                                                        CRSK0067
      DO 30 I=1,8                                                       CRSK0068
      IND=0                                                             CRSK0069
      DO 30 M=1,NWK                                                     CRSK0070
      NN=2*NCOF(M)-1                                                    CRSK0071
      DO 30 N=1,NN                                                      CRSK0072
```

```
      IND=IND+1                                                         CRSK0073
      SYSKC(NR(I)-NNDR ,IND)= SYSKC( NR(I)-NNDR ,IND) - EKC(I,M,N)      CRSK0074
   30 CONTINUE                                                          CRSK0075
   40 CONTINUE                                                          CRSK0076
      RETURN                                                            CRSK0077
      END                                                               CRSK0078
```

```
      SUBROUTINE DENSE(SYSK,SYSQ,SYSKC,SYSKD,SYSQM,NNOD,NBAND,NODR,
     *                 NTOTL2)
C
C     THIS SUBROUTINE ELIMINATES COEFF. TERMS SYSKC,SYSKD,SYSQM INTO
C     SYSK,SYSQ BY CONDENSATION
C
      COMPLEX SYSK,SYSQ,SYSKC,SYSKD,SYSQM
      DIMENSION SYSK(NNOD,NBAND),SYSQ(NNOD),SYSKC(NODR,NTOTL2),
     *          SYSKD(NTOTL2),SYSQM(NTOTL2)
C
C     MERGE LOADING TERM FROM SYSQM TO SYSQ
      NN= NNOD-NODR
      DO 14 I=1,NODR
      II=NN+I
      DO 14 J=1,NTOTL2
      SYSQ(II) =SYSQ(II) - SYSQM(J)*SYSKC(I,J)/SYSKD(J)
   14 CONTINUE
C
C     MERGE TERMS FROM SYSKC,SYSKD INTO SYSK
C
      DO 28 K=1,NODR
      KK= NN+K
      DO 26 J=1,NODR
      KJ=J-K+1
      IF(KJ .LT. 1) GO TO 26
      DO 24 I=1,NTOTL2
      SYSK(KK,KJ)= SYSK(KK,KJ)-SYSKC(K,I)*SYSKC(J,I)/SYSKD(I)
   24 CONTINUE
   26 CONTINUE
   28 CONTINUE
      RETURN
      END
```

```
      SUBROUTINE DIAGK( SYSKD,XH,DH,WKH,NCOF )                          DIGK0001
C                                                                       DIGK0002
C     THIS SUBROUTINE CALCULATES THE DIAGONAL MATRIX SYSKD              DIGK0003
C                                                                       DIGK0004
      INTEGER*4 NCOF                                                    DIGK0005
      COMPLEX SYSKD,XH,DH,CZ,TM                                         DIGK0006
      COMMON NELE,NNOD,NS,NB,NODR,NEQT,NBAND,NMAX,NTOTL,NTOTL2,NWK,     DIGK0007
     *       THETAI,WAVET,R,H,NMAX2                                     DIGK0008
      DIMENSION SYSKD(NTOTL2),XH(NWK,NMAX),DH(NWK,NMAX),WKH(NWK),       DIGK0009
     *          NCOF(NWK)                                               DIGK0010
C                                                                       DIGK0011
C     PR=PAI*R/4                                                        DIGK0012
      PR=0.78539816 *R                                                  DIGK0013
      INDX=0                                                            DIGK0014
      DO 20 M=1,NWK                                                     DIGK0015
      WKH2=2.*WKH(M)                                                    DIGK0016
      CZ=WKH2+SIN(WKH2)                                                 DIGK0017
      IF(M.EQ.1) CZ=WKH2+SINH(WKH2)                                     DIGK0018
      NN=NCOF(M)                                                        DIGK0019
      DO 15 N=1,NN                                                      DIGK0020
      TM=PR*XH(M,N)*DH(M,N)*CZ                                          DIGK0021
      IF( N .NE. 1 ) GO TO 12                                           DIGK0022
      INDX=INDX+1                                                       DIGK0023
      SYSKD(INDX)=2.*TM                                                 DIGK0024
      GO TO 15                                                          DIGK0025
   12 INDX=INDX+1                                                       DIGK0026
      SYSKD(INDX)=TM                                                    DIGK0027
      INDX=INDX+1                                                       DIGK0028
      SYSKD(INDX)=TM                                                    DIGK0029
   15 CONTINUE                                                          DIGK0030
   20 CONTINUE                                                          DIGK0031
      RETURN                                                            DIGK0032
      END                                                               DIGK0033
```

```
      SUBROUTINE EIGVAL(N,C,X)                                          EIGV0001
C                                                                       EIGV0002
C     N  IS  NO.  OF SOLNS.  WANTED                                     EIGV0003
C     SOLVES THE EQT. X*TANH(X)=C BY FIX-POINT ITERATION                EIGV0004
C     SOLNS.  RETURNED  IN A  VECTOR X N-LONG                           EIGV0005
C                                                                       EIGV0006
      DIMENSION X(N)                                                    EIGV0007
      TOLR=1.E-5                                                        EIGV0008
C                                                                       EIGV0009
C     INITIAL GUESS X=C                                                 EIGV0010
      XJ=C                                                              EIGV0011
C                                                                       EIGV0012
C     LOOP TO CALCULATE REAL ROOT                                       EIGV0013
   10 XI=XJ                                                             EIGV0014
      XJ=C/TANH(XI)                                                     EIGV0015
      IF( ABS(XI-XJ) .GT. TOLR) GO TO 10                                EIGV0016
      X(1)=XJ                                                           EIGV0017
      IF( N .LE. 1 ) RETURN                                             EIGV0018
      PAI=3.1415926                                                     EIGV0019
C                                                                       EIGV0020
C     LOOP OVER IMAGINERY ROOTS REQUIRED                                EIGV0021
      DO  100  I=2,N                                                    EIGV0022
C                                                                       EIGV0023
C     INITIAL GUESS: MULTIPLES OF PAI                                   EIGV0024
      XJ=(I-1)*PAI                                                      EIGV0025
      DX=XJ                                                             EIGV0026
C                                                                       EIGV0027
C     LOOP TO CALCULATE PURE IMAGINERY ROOTS                            EIGV0028
   20 XI=XJ                                                             EIGV0029
      XJ=ATAN(-C/XI)+DX                                                 EIGV0030
      IF(ABS(XI-XJ).GT.TOLR)  GO TO 20                                  EIGV0031
      X(I)=XJ                                                           EIGV0032
  100 CONTINUE                                                          EIGV0033
      RETURN                                                            EIGV0034
      END                                                               EIGV0035
```

```
      SUBROUTINE ELKV(P,ELK)                                            ELKV0001
C                                                                       ELKV0002
C     THIS SUBROUTINE CALCULATES ELEMENT MATRIX ELK BY QUADRATURE       ELKV0003
C                                                                       ELKV0004
      REAL*4 PV(21,3),WV(21)                                            ELKV0005
      DIMENSION A(3,20),B(3,20),AJ(3,3),BJ(3,3),P(20,3),ELK(20,20)      ELKV0006
C                                                                       ELKV0007
C     NUMERICAL INTEGRATION DATA                                        ELKV0008
      DATA PV/0.,.5,0.,0.,-.5,0.,0.,1.,-1.,0.,0.,0.,0.,1.,-1.,-1.,1.,1., ELKV0009
     * -1.,-1.,1.,0.,0.,.5,0.,0.,-.5,0.,0.,0.,1.,-1.,0.,0.,1.,1.,-1.,   ELKV0010
     * -1.,1.,1.,-1.,-1.,0.,0.,0.,.5,0.,0.,-.5,0.,0.,0.,0.,1.,-1.,1.,1., ELKV0011
     * 1.,1.,-1.,-1.,-1.,-1./                                           ELKV0012
      DATA WV/-11.02222 ,6*2.844444 ,6*.1777778 ,8*.1111111 /           ELKV0013
C                                                                       ELKV0014
      CALL ERASE(ELK,400)                                               ELKV0015
C                                                                       ELKV0016
C     BEGINNING OF INTEGRATION LOOP                                     ELKV0017
      DO 50 I=1,21                                                      ELKV0018
      X= PV(I,1)                                                        ELKV0019
      Y= PV(I,2)                                                        ELKV0020
      Z= PV(I,3)                                                        ELKV0021
      XP=1.+X                                                           ELKV0022
      YP=1.+Y                                                           ELKV0023
      ZP=1.+Z                                                           ELKV0024
      XN=1.-X                                                           ELKV0025
      YN=1.-Y                                                           ELKV0026
      ZN=1.-Z                                                           ELKV0027
      XPYP= XP*YP                                                       ELKV0028
      XPZP= XP*ZP                                                       ELKV0029
      YPZP= YP*ZP                                                       ELKV0030
      XPYN= XP*YN                                                       ELKV0031
      XPZN= XP*ZN                                                       ELKV0032
      XNYN= XN*YN                                                       ELKV0033
      XNZN= XN*ZN                                                       ELKV0034
      YNZN= YN*ZN                                                       ELKV0035
      XNYP= XN*YP                                                       ELKV0036
```

```
      XNZP= XN*ZP                                                       ELKV0037
      YNZP= YN*ZP                                                       ELKV0038
      YPZN= YP*ZN                                                       ELKV0039
C                                                                       ELKV0040
C     A IS THE MATRIX OF DERIVATIVES OF THE INTERPOLATION FUNCTIONS     ELKV0041
C     W.R.T. 3 LOCAL COORDINATES                                        ELKV0042
      A(1,1)= YPZP * (2.*X+Y-ZN)/8.                                     ELKV0043
      A(2,1)= XPZP * (X+2.*Y-ZN)/8.                                     ELKV0044
      A(3,1)= XPYP * (X-YN+2.*Z)/8.                                     ELKV0045
      A(1,2)=-X*YPZP/2.                                                 ELKV0046
      A(2,2)=XN*XPZP/4.                                                 ELKV0047
      A(3,2)=XN*XPYP/4.                                                 ELKV0048
      A(1,3)= YPZP*(2.*X-Y+ZN)/8.                                       ELKV0049
      A(2,3)= XNZP*(-X+2.*Y-ZN)/8.                                      ELKV0050
      A(3,3)= XNYP*(-X-YN+2.*Z)/8.                                      ELKV0051
      A(1,4)= -YN*YPZP/4.                                               ELKV0052
      A(2,4)= -Y*XNZP/2.                                                ELKV0053
      A(3,4)= YN*XNYP/4.                                                ELKV0054
      A(1,5)= YNZP*(2.*X+Y+ZN)/8.                                       ELKV0055
      A(2,5)= XNZP*(X+2.*Y+ZN)/8.                                       ELKV0056
      A(3,5)= XNYN*(-X-Y+2.*Z-1.)/8.                                    ELKV0057
      A(1,6)= -X*YNZP/2.                                                ELKV0058
      A(2,6)=-XN*XPZP/4.                                                ELKV0059
      A(3,6)= XN*XPYN/4.                                                ELKV0060
      A(1,7)= YNZP*(2.*X-Y-ZN)/8.                                       ELKV0061
      A(2,7)= XPZP*(-X+2.*Y+ZN)/8.                                      ELKV0062
      A(3,7)= XPYN*(-XN-Y+2.*Z)/8.                                      ELKV0063
      A(1,8)= YN*YPZP/4.                                                ELKV0064
      A(2,8)= -Y*XPZP/2.                                                ELKV0065
      A(3,8)= YN*XPYP/4.                                                ELKV0066
      A(1,9)= ZN*YPZP/4.                                                ELKV0067
      A(2,9)= ZN*XPZP/4.                                                ELKV0068
      A(3,9)= -Z*XPYP/2.                                                ELKV0069
      A(1,10)= -ZN*YPZP/4.                                              ELKV0070
      A(2,10)=ZN*XNZP/4.                                                ELKV0071
      A(3,10)= -Z*XNYP/2.                                               ELKV0072
```

```
      A(1,11) = -ZN*YNZP/4.                                             ELKV0073
      A(2,11) = -ZN*XNZP/4.                                             ELKV0074
      A(3,11) = -Z*XNYN/2.                                              ELKV0075
      A(1,12) = ZN*YNZP/4.                                              ELKV0076
      A(2,12) = -ZN*XPZP/4.                                             ELKV0077
      A(3,12) = -Z*XPYN/2.                                              ELKV0078
      A(1,13) = YPZN*(2.*X-YN-Z)/8.                                     ELKV0079
      A(2,13) = XPZN*(-XN+2.*Y-Z)/8.                                    ELKV0080
      A(3,13) = XPYP*(XN-Y+2.*Z)/8.                                     ELKV0081
      A(1,14) = -X*YPZN/2.                                              ELKV0082
      A(2,14) = XN*YPZN/4.                                              ELKV0083
      A(3,14) = -XN*XPYP/4.                                             ELKV0084
      A(1,15) = YPZN*(2.*X+YN+Z)/8.                                     ELKV0085
      A(2,15) = XNZN*(-X+2.*Y-Z-1.)/8.                                  ELKV0086
      A(3,15) = XNYP*(X+YN+2.*Z)/8.                                     ELKV0087
      A(1,16) = -YN*YPZN/4.                                             ELKV0088
      A(2,16) = -Y*XNZN/2.                                              ELKV0089
      A(3,16) = -YN*XNYP/4.                                             ELKV0090
      A(1,17) = YNZN*(2.*X+Y+Z+1.)/8.                                   ELKV0091
      A(2,17) = XNZN*(X+2.*Y+Z+1.)/8.                                   ELKV0092
      A(3,17) = XNYN*(X+Y+2.*Z+1.)/8.                                   ELKV0093
      A(1,18) = -X*YNZN/2.                                              ELKV0094
      A(2,18) =-XP*XNZN/4.                                              ELKV0095
      A(3,18) =-XP*XNYN/4.                                              ELKV0096
      A(1,19) =YNZN*(2.*X-Y-Z-1.)/8.                                    ELKV0097
      A(2,19) =XPZN*(XN+2.*Y+Z)/8.                                      ELKV0098
      A(3,19) =XPYN*(XN+Y+2.*Z)/8.                                      ELKV0099
      A(1,20) = YP*YNZN/4.                                              ELKV0100
      A(2,20) =-Y*XPZN/2.                                               ELKV0101
      A(3,20) =-YN*XPYP/4.                                              ELKV0102
C                                                                       ELKV0103
C     AJ IS THE JACOBIAN MATRIX                                         ELKV0104
      CALL ERASE(AJ,9,B,60)                                             ELKV0105
      DO 20 M=1,3                                                       ELKV0106
      DO 20 N=1,3                                                       ELKV0107
      DO 20 K=1,20                                                      ELKV0108
```

```
   20 AJ(M,N)=AJ(M,N)+A(M,K)*E(K,N)
C
C     BJ IS THE INVERSE OF AJ
      BJ(1,1)=  (AJ(2,2)*AJ(3,3)-AJ(2,3)*AJ(3,2))
      BJ(1,2)=-(AJ(1,2)*AJ(3,3)-AJ(1,3)*AJ(3,2))
      BJ(1,3)=  (AJ(1,2)*AJ(2,3)-AJ(1,3)*AJ(2,2))
      BJ(2,1)=-(AJ(2,1)*AJ(3,3)-AJ(2,3)*AJ(3,1))
      BJ(2,2)=  (AJ(1,1)*AJ(3,3)-AJ(1,3)*AJ(3,1))
      BJ(2,3)=-(AJ(1,1)*AJ(2,3)-AJ(1,3)*AJ(2,1))
      BJ(3,1)=  (AJ(2,1)*AJ(3,2)-AJ(2,2)*AJ(3,1))
      BJ(3,2)=-(AJ(1,1)*AJ(3,2)-AJ(1,2)*AJ(3,1))
      BJ(3,3)=  (AJ(1,1)*AJ(2,2)-AJ(1,2)*AJ(2,1))
C
C     DJ IS THE DETERMINANT OF AJ
      DJ=AJ(1,1)*BJ(1,1)+AJ(1,2)*BJ(2,1)+AJ(1,3)*BJ(3,1)
C
C     B IS THE MATRIX OF DERIVATIVES OF THE INTERPOLATION FUNCTIONS
C     W.R.T. GLOBAL X,Y,Z COORDINATES
      DO 30 K=1,20
      DO 30 J=1,3
      DO 30 M=1,3
   30 B(J,K)= B(J,K)  + BJ(J,M)*A(M,K)
C
C     ASSEMBLE ELEMENT MATRIX ELK
      DO 40 J=1,20
      DO 40 K=J,20
      ELK(J,K)=ELK(J,K)+(B(1,J)*B(1,K)+B(2,J)*B(2,K)+B(3,J)*B(3,K))*
     1          WV(I)/ABS(DJ)
   40 CONTINUE
   50 CONTINUE
      RETURN
      END
```

```
      SUBROUTINE FMAP2( S,T,P,Q,DQ,XX,YY,ZZ,CJ,INDX )
C
C     THIS SUBROUTINE PERFORMS ISOPARAMETRIC MAPPING FROM A FACE OF THE
C     DAUGHTER ELEMENT ONTO THE FREE SURFACE OR CYLINDRICAL BOUNDARY
C     INDX=1 RETURNS JACOBIAN DETERMINANT & GLOBAL COORDINATES
C     INDX=2 RETURNS JACOBIAN DETERMINANT ONLY
C     INDX=3 RETURNS GLOBLE ANGLE OF POINT ON CYLINDRICAL BOUNDARY ONLY
C
      DIMENSION P(8,3),Q(8),DQ(2,8),XQ(2,3)
      IF(INDX.EQ.3) T=1.
C
C     Q ARE THE INTERPOLATION FUNCTIONS IN 2-D
      Q(1) = (1.+S)*(1.+T)*(S+T-1.)/4.
      Q(2) = (1.-S*S)*(1.+T)/2.
      Q(3) = (1.-S)*(1.+T)*(-S+T-1.)/4.
      IF(INDX.NE.3) GO TO 8
      XX=Q(1)*P(1,1)+Q(2)*P(2,1)+Q(3)*P(3,1)
      YY=Q(1)*P(1,2)+Q(2)*P(2,2)+Q(3)*P(3,2)
      CJ=0.
      IF(XX.NE.0..OR.YY.NE.0.) CJ=ATAN2(YY,XX)
      GO TO 99
    8 Q(4) = (1.-S)*(1.-T*T)/2.
      Q(5) = (1.-S)*(1.-T)*(-S-T-1.)/4.
      Q(6) = (1.-S*S)*(1.-T)/2.
      Q(7) = (1.+S)*(1.-T)*(S-T-1.)/4.
      Q(8) = (1.+S)*(1.-T*T)/2.
C
C     DQ ARE DERIVATIVES OF THE INTERPOLATIONS W.R.T. LOCAL COORDINATES
      DQ(1,1) = (1.+T)*(2.*S+T)/4.
      DQ(2,1) = (1.+S)*(S+2.*T)/4.
      DQ(1,2) = -S*(1.+T)
      DQ(2,2) = (1.-S*S)/2.
      DQ(1,3) = (1.+T)*(2.*S-T)/4.
      DQ(2,3) = (1.-S)*(-S+2.*T)/4.
      DQ(1,4) = -(1.-T*T)/2.
      DQ(2,4) = -(1.-S)*T
```

```
      DQ(1,5) = (1.-T)*(2.*S+T)/4.                                      FMAP0037
      DQ(2,5) = (1.-S)*(S+2.*T)/4.                                      FMAP0038
      DQ(1,6) = -S*(1.-T)                                               FMAP0039
      DQ(2,6) = -(1.-S*S)/2.                                            FMAP0040
      DQ(1,7) = (1.-T)*(2.*S-T)/4.                                      FMAP0041
      DQ(2,7) = (1.+S)*(-S+2.*T)/4.                                     FMAP0042
      DQ(1,8) = (1.-T*T)/2.                                             FMAP0043
      DQ(2,8) = -T*(1.+S)                                               FMAP0044
      IF( INDX .EQ. 2 ) GO TO 12                                        FMAP0045
C                                                                       FMAP0046
C     XX,YY,ZZ ARE GLOBAL COORDINATE VALUES                             FMAP0047
      XX=0.0                                                            FMAP0048
      YY=0.0                                                            FMAP0049
      ZZ=0.0                                                            FMAP0050
      DO 10 K=1,8                                                       FMAP0051
      XX=XX+Q(K)*P(K,1)                                                 FMAP0052
      YY=YY+Q(K)*P(K,2)                                                 FMAP0053
   10 ZZ=ZZ+Q(K)*P(K,3)                                                 FMAP0054
   12 CONTINUE                                                          FMAP0055
      CALL ERASE(XQ,6)                                                  FMAP0056
      DO 14 I=1,2                                                       FMAP0057
      DO 14 J=1,3                                                       FMAP0058
      DO 14 K=1,8                                                       FMAP0059
   14 XQ(I,J)=XQ(I,J)+DQ(I,K)*P(K,J)                                    FMAP0060
      E = XQ(1,1)*XQ(1,1)+XQ(1,2)*XQ(1,2)+XQ(1,3)*XQ(1,3)               FMAP0061
      F = XQ(1,1)*XQ(2,1)+XQ(1,2)*XQ(2,2)+XQ(1,3)*XQ(2,3)               FMAP0062
      G = XQ(2,1)*XQ(2,1)+XQ(2,2)*XQ(2,2)+XQ(2,3)*XQ(2,3)               FMAP0063
      CJ = SQRT(E*G-F*F)                                                FMAP0064
   99 RETURN                                                            FMAP0065
      END                                                               FMAP0066
```

```
      SUBROUTINE FORCE(SYSQ,NELEFX,NELEFZ,XYZ,NCON)
C
C     THIS SUBROUTINE CALCULATES HORIZONTAL & VERTICAL FORCE COEFFS.
C     FOR A SEMI- OR TOTALLY IMMERSED CYLINDER
C
      COMMON NELE,NNOD,NS,NB,NODR,NEQT,NBAND,NMAX,NTOTL,NTOTL2,NWK,
     *       THETAI,WAVET,R,H,NMAX2,NFX,NFZ,HH
      COMMON /IO/IREAD,IWRITE
      COMPLEX*8 SYSQ(NEQT),F
      REAL*4 PS(3),WS(3)
      INTEGER*4 NELEFX(1),NELEFZ(1),NCON(20,NELE),NR(8),INOD(8)
      REAL*4 XYZ(3,NNOD),P(8,3),Q(8),DQ(2,8)
C
C     QUADRATURE DATA
      DATA PS/.7745966 ,0.,-.7745966 /
      DATA WS/.5555556 ,.8888889 ,.5555556 /
      DATA INOD/5,4,3,10,15,16,17,11/
C
C     HH IS THE DEPTH OF IMMERSION
      CONST=1./(3.1415927*HH)
      F=0.
C
C     NFX,NFZ=0 IMPLY NO ELEMENTS ON THE CORRESPONDING SURFACES
      IF(NFX.EQ.0) GO TO 10
C
C     CALCULATION FOR HORIZONTAL FORCE
C
C     LOOP OVER ALL ELEMENTS ON CYLINDER CIRCUMFERENCE
      DO 100 L=1,NFX
      DO 200 I=1,8
      NR(I)=NCON(INOD(I),NELEFX(L))
      DO 200 J=1,3
  200 P(I,J)=XYZ(J,NR(I))
C
C     NUMERICAL INTEGRATION LOOPS
      DO 300 IS=1,3
```

```
      DO 300 IT=1,3                                                     FORC0037
      S=PS(IS)                                                          FORC0038
      T=PS(IT)                                                          FORC0039
      CALL FMAP2(S,T,P,Q,DQ,XX,YY,ZZ,CJ,1)                              FORC0040
      C=XX*CJ*WS(IS)*WS(IT)                                             FORC0041
      DO 400 I=1,8                                                      FORC0042
  400 F=F+Q(I)*SYSQ(NR(I))*C                                            FORC0043
  300 CONTINUE                                                          FORC0044
  100 CONTINUE                                                          FORC0045
      F=-CONST*F                                                        FORC0046
   10 WRITE(IWRITE,900)                                                 FORC0047
  900 FORMAT(//1X,14('*')/' *** FORCES ***'/1X,14('*')//' X-COMPONENT :'  FORC0048
     *)                                                                 FORC0049
      CALL OUTPUT(F,1)                                                  FORC0050
      F=0.                                                              FORC0051
      IF(NFZ.EQ.0) GO TO 20                                             FORC0052
C                                                                       FORC0053
C     CALCULATION FOR VERTICAL FORCE                                    FORC0054
C                                                                       FORC0055
C     LOOP OVER ALL ELEMENTS ON CYLINDER BASE                           FORC0056
      DO 500 L=1,NFZ                                                    FORC0057
      DO 600 I=1,8                                                      FORC0058
      NR(I)=NCON(I,NELEFZ(L))                                           FORC0059
      DO 600 J=1,3                                                      FORC0060
  600 P(I,J)=XYZ(J,NR(I))                                               FORC0061
C                                                                       FORC0062
C     QUADRATURE LOOPS                                                  FORC0063
      DO 700 IS=1,3                                                     FORC0064
      DO 700 IT=1,3                                                     FORC0065
      S=PS(IS)                                                          FORC0066
      T=PS(IT)                                                          FORC0067
      CALL FMAP2(S,T,P,Q,DQ,XX,YY,ZZ,CJ,2)                              FORC0068
      C=CJ*WS(IS)*WS(IT)                                                FORC0069
      DO 800 I=1,8                                                      FORC0070
  800 F=F+Q(I)*SYSQ(NR(I))*C                                            FORC0071
  700 CONTINUE                                                          FORC0072
```

```
500 CONTINUE                                                            FORC0073
    F=CONST*F                                                           FORC0074
 20 WRITE(IWRITE,901)                                                   FORC0075
901 FORMAT(//' Z-COMPONENT :')                                          FORC0076
    CALL OUTPUT(F,1)                                                    FORC0077
    RETURN                                                              FORC0078
    END                                                                 FORC0079
```

```
      SUBROUTINE HANKEL(NCOF,W,BJ,H1MN,DH1MN,NMAX ,NWK,BY,FNORM)
C
C     THIS SUBROUTINE CALCULATES & NORMALIZES REQUIRED HANKEL & RELATED
C     FUNCTIONS
C
      COMPLEX H1MN,DH1MN,CI
      REAL*4 FNORM(NWK,NMAX)
      INTEGER*4 NCOF
      DIMENSION H1MN(NWK,NMAX ),DH1MN(NWK,NMAX ),BJ(NMAX ),BY(NMAX ),
     *          W(NWK),NCOF(NWK)
      CI=(0.,1.)
      NM=NMAX
      NN=NM-1
      ARG=W(1)
C
C     BESSEL BJ & HANKEL H1MN (FIRST KIND) FUNCTIONS
C
C     LOOP TO SET UP PART OF NORMALIZATION FACTOR MATRIX FNORM
      DO 20 I=1,NM
      P=I-1
      V=ARG*ARG-P*P
      IF(ABS(V).GT.SQRT(ARG)) GO TO 18
      FNORM(1,I)=ARG**(-.3333)
      GO TO 20
   18 IF(V.LT.0.) GO TO 22
      FNORM(1,I)=V**(-.25)
      GO TO 20
   22 U=SQRT(-V)
      FNORM(1,I)=EXP(P*ALOG((P+U)/ARG)-U)/SQRT(U)
   20 CONTINUE
C
C     BJS,BYS,BKS ARE IBM SL-MATH SUPPLIED ROUTINES TO CALCULATE
C     J,Y AND K BESSEL FUNCTIONS RESPECTIVELY
      CALL  BJS (ARG,NN,BJ,IER)
      CALL  BYS (ARG,NN,BY,IER)
      H1MN(1,1)=(BJ(1)+CI*BY(1))/FNORM(1,1)
```

```
      DH1MN(1,1)=(-BJ(2)-CI*BY(2))/FNORM(1,1)                           HANK0037
      IF(NM.LT.2) GO TO 10                                              HANK0038
      DO  100  I=2,NM                                                   HANK0039
      H1MN(1,I)=(BJ(I)+CI*BY(I))/FNORM(1,I)                             HANK0040
      XC=(I-1)/ARG                                                      HANK0041
      DH1MN(1,I)=(FNORM(1,I-1)/FNORM(1,I))*H1MN(1,I-1)-XC*H1MN(1,I)     HANK0042
  100 CONTINUE                                                          HANK0043
   10 IF(NWK.LT.2) GO TO 600                                            HANK0044
C                                                                       HANK0045
C     MODIFIED BESSEL FUNCTIONS (SECOND KIND)                           HANK0046
C                                                                       HANK0047
      DO  200  M=2,NWK                                                  HANK0048
      ARG=W(M)                                                          HANK0049
      NM=NCOF(M)                                                        HANK0050
      NN=NM-1                                                           HANK0051
      DO 30 I=1,NM                                                      HANK0052
      P=I-1                                                             HANK0053
      U=SQRT(P*P+ARG*ARG)                                               HANK0054
   30 FNORM(M,I)=EXP(P*ALOG((P+U)/ARG)-U)/SQRT(U)                       HANK0055
      IF(NN.EQ.0) NN=1                                                  HANK0056
      CALL BKS(ARG,NN,BY,IER)                                           HANK0057
      DO 400 I=1,NM                                                     HANK0058
  400 H1MN(M,I)=BY(I)/FNORM(M,I)                                        HANK0059
      DH1MN(M,1)=-BY(2)/FNORM(M,1)                                      HANK0060
      IF(NM.LT.2) GO TO 200                                             HANK0061
      DO  300  N=2,NM                                                   HANK0062
      XC=(N-1)/ARG                                                      HANK0063
      DH1MN(M,N)=-(FNORM(M,N-1)/FNORM(M,N))*H1MN(M,N-1)-XC*H1MN(M,N)    HANK0064
  300 CONTINUE                                                          HANK0065
  200 CONTINUE                                                          HANK0066
  600 RETURN                                                            HANK0067
      END                                                               HANK0068
```

```
      SUBROUTINE INPUT( XYZ,NCON,NELES,NELEB,NELEFX,NELEFZ)
C
C     THIS SUBROUTINE SETS UP AND PRINTS ALL GEOMETRICAL & GRID DATA FOR
C     SEMI-IMMERSED CIRCULAR CYLINDRICAL DOCK
C     NO INPUT CARDS ARE USED
C
      INTEGER*4 NCON,NELES,NELEB,NOD
      COMMON NELE,NNOD,NS,NB,NODR,NEQT,NBAND,NMAX,NTOTL,NTOTL2,NWK,
     *       THETAI,WAVET,RB,H,NMAX2,NFX,NFZ,HH
      DIMENSION NCON(20,1),NELES(1),NELEB(1),XYZ(3,1)
      DIMENSION K(3),Z(5),A(32),R(3) ,NELEFX(1),NELEFZ(1)
      COMMON /IO/IREAD,IWRITE
C
C     ASSIGN CALLING PARAMETERS TO MESH0
      Z(1)=-.5
      Z(2)=-.625
      Z(3)=-.75
      RI=.25
      DO 200 I=1,32
  200 A(I)=(I-1)*3.1415927/16.
      NA=8
      NZ=1
      NNOD=1
      NELE=0
      NQ=0
      NB=0
      NFZ=0
      NFX=0
      NX=1
C
C     MESH0 SETS UP THE CORE OF ELEMENTS IN THE CENTER
      CALL MESH0(NA,NZ,NNOD,NELE,XYZ,NCON,RI,A,Z,NQ,NE,NFZ,NELEB,
     *           NELEFZ)
C
C     ASSIGN CALLING PARAMETERS TO MESH1
      R(1)=.5
```

```
      R(2)=.8                                                           INPT0037
      R(3)=1.                                                           INPT0038
      NR=1                                                              INPT0039
      NA=16                                                             INPT0040
      NQ=1                                                              INPT0041
      NB=0                                                              INPT0042
      NFX=0                                                             INPT0043
      MR=0                                                              INPT0044
C                                                                       INPT0045
C     MESH1 SETS UP CYLINDRICAL RINGS OF ELEMENTS                       INPT0046
      CALL MESH1(NR,NA,NZ,NNOD,NELE,XYZ,NCON,R,A,Z,NQ,                  INPT0047
     *NB,NFZ,NELEB,NELEFZ,NFX,NELEFX,NX,MR)                              INPT0048
C                                                                       INPT0049
C     SECOND CALL TO MESH1                                              INPT0050
      R(1)=1.                                                           INPT0051
      R(2)=1.15                                                         INPT0052
      R(3)=1.3                                                          INPT0053
      Z(1)=0.                                                           INPT0054
      Z(2)=-.3                                                          INPT0055
      Z(3)=-.5                                                          INPT0056
      Z(4)=-.625                                                        INPT0057
      Z(5)=-.75                                                         INPT0058
      NZ=2                                                              INPT0059
      NQ=0                                                              INPT0060
      NB=0                                                              INPT0061
      NS=0                                                              INPT0062
      NFX=0                                                             INPT0063
      MR=1                                                              INPT0064
      CALL MESH1(NR,NA,NZ,NNOD,NELE,XYZ,NCON,R,A,Z,NQ,NB,NS,NELEB,NELES, INPT0065
     *NFX,NELEFX,NX,MR)                                                 INPT0066
C                                                                       INPT0067
C     COMPLETE & PRINT A SUMMARY OF GEOMETRICAL & GRID DATA             INPT0068
C                                                                       INPT0069
      RR=R(2*NR+1)                                                      INPT0070
      H=ABS(Z(2*NZ+1))                                                  INPT0071
      HH=ABS(Z(2*NX+1))                                                 INPT0072
```

```
      NODR=(3*NZ+2)*NA
      NEQT=NNOD
      WRITE(IWRITE,901)
  901 FORMAT('1')
      WRITE(IWRITE,902)
  902 FORMAT(1X,32('*')/' *** GEOMETRY & PHYSICAL DATA ***'/
     *1X,32('*')//)
      WRITE(IWRITE,920)
  920 FORMAT(' ALL LENGTHS ARE NORMALIZED BY THE RADIUS OF THE ',
     *       'CYLINDER, A')
      WRITE(IWRITE,903) H,RR,HH
  903 FORMAT(/' ASYMPTOTIC DEPTH=',F10.4/' RADIUS OF SUPER-ELEMENT=',
     *F10.4/' SUBMERGED DEPTH OF UNIT CYLINDER=',F10.4/)
      WRITE(IWRITE,904) NNOD,NELS
  904 FORMAT(/' NO. OF NODAL POINTS=',I5/' NO. OF ELEMENTS=',I5/)
      WRITE(IWRITE,911) NB,(NELEB(I),I=1,NB)
  911 FORMAT(//I5,' ELEMENTS ON SUPERELEMENT BOUNDARY :',(/20I6))
      WRITE(IWRITE,912) NS,(NELES(I),I=1,NS)
  912 FORMAT(//I5,' ELEMENTS ON THE FREE SURFACE :',(/20I6))
      WRITE(IWRITE,913) NFX,(NELEFX(I),I=1,NFX)
  913 FORMAT(//I5,' ELEMENTS ON THE CYLINDER CIRCUMFERENCE :',(/20I6))
      IF(NFZ.LT.1) GO TO 20
      WRITE(IWRITE,914) NFZ,(NELEFZ(I),I=1,NFZ)
  914 FORMAT(//I5,' ELEMENTS ON THE CYLINDER BASE :',(/20I6))
C
C     NODE COORDINATE TABLE
   20 WRITE(IWRITE,905)
  905 FORMAT('1',24('*')/' *** NODE COORDINATES ***'/1X,24('*')//)
      WRITE(IWRITE,906)
  906 FORMAT(3(' NODE',6X,'X',9X,'Y',9X,'Z',9X)//1X,40('-*-')/)
      DO 950 I=1,NNOD,3
      N=MINO(3,NNOD-I+1)
      K(1)=I
      K(2)=I+1
      K(3)=I+2
  950 WRITE(IWRITE,907)(K(L),(XYZ(J,K(L)),J=1,3),L=1,N)
```

```
  907 FORMAT(3(I5,2X,F8.5,2X,F8.5,2X,F8.5,5X))
C
C     ELEMENT CONNECTIVITY TABLE
      WRITE(IWRITE,908)
  908 FORMAT('1',30('*')/' *** ELEMENT CONNECTIVITIES ***'/1X,30('*')//)
      WRITE(IWRITE,909)
  909 FORMAT(1X,'ELEM.  NODES...'//10X,'1      2      3      4      5      ',
     *       '6      7      8      9      10     11     12     13     14     15',
     *       '     16     17     18     19     20'/1X,42('-*-')/)
      WRITE(IWRITE,910) (J,(NCON(I,J),I=1,20),J=1,NELE)
  910 FORMAT(I5,20I6)
C
C     CALCULATE SEMI-BANDWIDTH FROM ELEMENT CONNECTIVITIES
      IBAND=0.
      DO 23 L=1,NELE
      MIN=100000
      MAX=-1
      DO 22 J=1,20
      MIN=MIN0(MIN,NCON(J,L))
   22 MAX=MAX0(MAX,NCON(J,L))
   23 IBAND=MAX0(IBAND,MAX-MIN)
      IBAND=IBAND+1
      NBAND=MAX0(IBAND,NODR)
      WRITE(IWRITE,917) NBAND,IBAND,NODR
  917 FORMAT(//' SEMI-BANDWIDTH OF GLOBAL MATRIX=',I5/
     *' SEMI-BANDWIDTH W.R.T. ELEMENT CONNECTIVITY=',I5/
     *' SEMI-BANDWIDTH W.R.T. BOUNDARY NODAL POINTS=',I5//)
C
      RETURN
      END
```

```
      SUBROUTINE MESHO(NA,NZ,IP,IE,XYZ,NCON,RI,A,Z,NQ,IB,IS,NBE,NSE)
C
C     THIS SUBROUTINE CONSTRUCTS A CYLINDRICAL CORE OF ELEMENTS
C     NODE COORDINATES, ELEMENT CONNECTIVITIES & OTHER GRID DATA ARE
C     GENERATED
C     NODE NUMBERING ASSURES MINIMIZATION OF BANDWIDTH
C
C     NA=# OF ELEMENTS IN THE ANGULAR DIRECTION TO BE GENERATED
C     NZ=# OF ELEMENTS TO BE GENERATED VERTICALLY
C     IP=BEGINNING NO. FOR NODE NUMBERING
C     IP CONTAINS ON RETURN BEGINNING # FOR SUBSEQUENT NODE NUMBERING
C     IE=BEGINNING # FOR ELEMENT NUMBERING
C     IE CONTAINS ON RETURN BEGINNING # FOR SUBSEQUENT ELEMENT
C     NUMBERING
C     XYZ: MATRIX FOR STORING GENERATED NODE COORDINATES
C     NCON: MATRIX FOR STORING GENERATED ELEMENT CONNECTIVITIES
C     RI: RADIAL COORDINATE VALUE FOR NODES
C     A(2*NA): VECTOR CONTAINING ANGULAR COORDINATE VALUES FOR NODES
C     Z(2*NZ+1): VECTOR CONTAINING VERTICAL COODINATE VALUES FOR NODES
C     NQ=# OF LAYERS OF ELEMENTS ABOVE NZ OUTSIDE OF CURRENT RING(S)
C     IB=BEGINNING # FOR NUMBERING ELEMENTS ON OUTERMOST CIRCUMFERENCE
C     IS=BEGINNING # FOR NUMBERING ELEMENTS ON THE TOP SURFACE
C     NBE: VECTOR FOR STORING NOS. OF ELEMENTS ON THE OUTERMOST
C     CIRCUMFERENCE
C     NSE: VECTOR FOR STORING NOS. OF ELEMENTS ON THE TOP SURFACE
C
      REAL*4 Z(1),A(1),XYZ(3,1)
      INTEGER*4 NCON(20,1),NBE(1),NSE(1),NTE(1)
C
C     GENERATE NODE COORDINATES
      JP=IP+1
      M2=2*NZ+1
      N4=NA*4
      DO 100 IZ=1,M2
      IP=IP+1
      XYZ(1,IP)=0.
```

```
      XYZ(2,IP)=0.                                                      MSH00037
      XYZ(3,IP)=Z(IZ)                                                   MSH00038
  100 CONTINUE                                                          MSH00039
      DO 300 IA=1,N4,4                                                  MSH00040
C                                                                       MSH00041
C     FOR ELEMENTS OF OTHER SHAPES, A ROUTINE TO RETURN X,Y,Z GIVEN     MSH00042
C     IZ,IA OR IP SHOULD REPLACE ASSIGNMENT STATEMENTS                  MSH00043
      X=RI*COS(A(IA))                                                   MSH00044
      Y=RI*SIN(A(IA))                                                   MSH00045
      DO 400 IZ=1,M2,2                                                  MSH00046
      IP=IP+1                                                           MSH00047
      XYZ(1,IP)=X                                                       MSH00048
      XYZ(2,IP)=Y                                                       MSH00049
      XYZ(3,IP)=Z(IZ)                                                   MSH00050
  400 CONTINUE                                                          MSH00051
  300 CONTINUE                                                          MSH00052
C                                                                       MSH00053
C     GENERATE ELEMENT CONNECTIVITIES ETC.                              MSH00054
      LQ=6*NQ                                                           MSH00055
      LQ2=2*NQ                                                          MSH00056
      LQ3=3*NQ                                                          MSH00057
      LR1=(2*NZ+1)*NA                                                   MSH00058
      LR2=NA*(NZ+1)                                                     MSH00059
      LR=LR1+LR2                                                        MSH00060
      LA1=2*NZ+1                                                        MSH00061
      LA2=NZ+1                                                          MSH00062
      LA=LA1+LA2                                                        MSH00063
      DO 600 IA=1,NA                                                    MSH00064
      DO 700 IZ=1,NZ                                                    MSH00065
      IE=IE+1                                                           MSH00066
      NCON(1,IE)=JP+LA1+LR2+(2*IA-1)*LA+(IZ-1)*2                        MSH00067
      NCON(2,IE)=NCON(1,IE)+LA1+1-IZ                                    MSH00068
      NCON(8,IE)=NCON(1,IE)-LA2+1-IZ                                    MSH00069
      NCON(3,IE)=NCON(1,IE)+LA-(IA/NA)*LR*2                             MSH00070
      NCON(7,IE)=NCON(1,IE)-LA                                          MSH00071
      NCON(5,IE)=JP+(IZ-1)*2                                            MSH00072
```

```
      NCON(11,IE)=NCON(5,IE)+1                                          MSH00073
      NCON(17,IE)=NCON(5,IE)+2                                          MSH00074
      NCON(4,IE)=JP+LA1+IA*LA2+(IZ-1)-(IA/NA)*NA*LA2                    MSH00075
      NCON(16,IE)=NCON(4,IE)+1                                          MSH00076
      NCON(6,IE)=NCON(4,IE)-LA2+(IA/NA)*NA*LA2                          MSH00077
      NCON(18,IE)=NCON(6,IE)+1                                          MSH00078
      IB=IB+1                                                           MSH00079
      NBE(IB)=IE                                                        MSH00080
      IF(NQ.EQ.0) GO TO 10                                              MSH00081
      NCON(1,IE)=NCON(1,IE)+LQ*IA-NQ                                    MSH00082
      NCON(2,IE)=NCON(2,IE)+LQ*IA                                       MSH00083
      NCON(8,IE)=NCON(8,IE)+LQ*(IA-1)+LQ3                               MSH00084
      NCON(3,IE)=NCON(3,IE)+LQ*IA+LQ2-(IA/NA)*LQ*NA                     MSH00085
      NCON(7,IE)=NCON(7,IE)+LQ*(IA-1)+LQ2                               MSH00086
   10 IF(IZ.NE.1) GO TO 20                                              MSH00087
      IS=IS+1                                                           MSH00088
      NSE(IS)=IE                                                        MSH00089
   20 NCON(9,IE)=NCON(1,IE)+1                                           MSH00090
      NCON(13,IE)=NCON(1,IE)+2                                          MSH00091
      NCON(14,IE)=NCON(2,IE)+1                                          MSH00092
      NCON(20,IE)=NCON(8,IE)+1                                          MSH00093
      NCON(10,IE)=NCON(3,IE)+1                                          MSH00094
      NCON(15,IE)=NCON(3,IE)+2                                          MSH00095
      NCON(12,IE)=NCON(7,IE)+1                                          MSH00096
      NCON(19,IE)=NCON(7,IE)+2                                          MSH00097
  700 CONTINUE                                                          MSH00098
  600 CONTINUE                                                          MSH00099
      RETURN                                                            MSH00100
      END                                                               MSH00101
```

```
      SUBROUTINE MESH1(NR,NA,NZ,IP,IE,XYZ,NCON,R,A,Z,NQ,IB,IS,NBE,NSE,
     *                 IT,NTE,NTN,MR)
C
C     THIS SUBROUTINE CONSTRUCTS CYLINDRICAL RINGS OF ELEMENTS
C     NODE COORDINATES, ELEMENT CONNECTIVITIES & OTHER GRID DATA ARE
C     GENERATED
C     NODE NUMBERING ASSURES MINIMIZATION OF BANDWIDTH
C
C     NR=# OF ELEMENT RINGS TO BE GENERATED RADIALLY
C     NA=# OF ELEMENTS IN THE ANGULAR DIRECTION TO BE GENERATED
C     NZ=# OF LAYERS OF ELEMENTS TO BE GENERATED VERTICALLY
C     IP=BEGINNING NO. FOR NODE NUMBERING
C     IP CONTAINS ON RETURN BEGINNING # FOR SUBSEQUENT NODE NUMBERING
C     IE=BEGINNING # FOR ELEMENT NUMBERING
C     IE CONTAINS ON RETURN BEGINNING # FOR SUBSEQUENT ELEMENT
C     NUMBERING
C     XYZ: MATRIX FOR STORING GENERATED NODE COORDINATES
C     NCON: MATRIX FOR STORING GENERATED ELEMENT CONNECTIVITIES
C     R(2*NR+1): VECTOR CONTAINING RADIAL COORDINATES FOR NODES
C     A(2*NA): VECTOR CONTAINING ANGULAR COORDINATE VALUES FOR NODES
C     Z(2*NZ+1): VECTOR CONTAINING VERTICAL COODINATE VALUES FOR NODES
C     NQ=# OF LAYERS OF ELEMENTS ABOVE NZ OUTSIDE OF CURRENT RING(S)
C     IB=BEGINNING # FOR NUMBERING ELEMENTS ON OUTERMOST CIRCUMFERENCE
C     IS=BEGINNING # FOR NUMBERING ELEMENTS ON THE TOP SURFACE
C     NBE: VECTOR FOR STORING NOS. OF ELEMENTS ON THE OUTERMOST
C     CIRCUMFERENCE
C     NSE: VECTOR FOR STORING NOS. OF ELEMENTS ON THE TOP SURFACE
C     IT=BEGINNING NO. FOR NUMBERING ELEMENTS ON THE INNERMOST
C     CIRCUMFERENCE UP TO NTN LAYERS DEEP
C     NTE: VECTOR FOR STORING NOS. OF ELEMENTS ON THE INNERMOST
C     CIRCUMFERENCE UP TO NTN DEEP
C     NTN=# OF LAYERS OF ELEMENTS TO BE CONSIDERED IN IT & NTE
C     MR SPECIFIES THE ANGULAR POSITION TO START NODE NUMBERING TO BE
C     COMPATIBLE TO PREVIOUS INNER ELEMENTS FOR MINIMUM BANDWIDTH
C
      REAL*4 Z(1),A(1),R(1),XYZ(3,1)
```

```
      INTEGER*4 NCON(20,1),NBE(1),NSE(1),NTE(1)                         MSH10037
C                                                                       MSH10038
C     GENERATE NODE COORDINATES                                         MSH10039
      JP=IP+1                                                           MSH10040
      N2=NA*2                                                           MSH10041
      M2=2*NZ+1                                                         MSH10042
      NN=NR*2+1                                                         MSH10043
      IF(NQ.NE.0)  NN=NN-1                                              MSH10044
      DO 200 IR=1,NN                                                    MSH10045
      RI=R(IR)                                                          MSH10046
      N=2-MOD(IR,2)                                                     MSH10047
      DO 300 JA=1,N2,N                                                  MSH10048
      IA=JA                                                             MSH10049
      IF(MOD(IR,2).NE.0)  IA=MOD(N2-2*(IR/2+MR)+JA-1,N2)+1              MSH10050
C                                                                       MSH10051
C     FOR ELEMENTS OF OTHER SHAPES, A ROUTINE TO RETURN X,Y,Z GIVEN     MSH10052
C     IR,JA,IZ OR IP SHOULD REPLACE ASSIGNMENT STATEMENTS               MSH10053
      X=RI*COS(A(IA))                                                   MSH10054
      Y=RI*SIN(A(IA))                                                   MSH10055
      M=N-MOD(JA,2)+1                                                   MSH10056
      DO 400 IZ=1,M2,M                                                  MSH10057
      IP=IP+1                                                           MSH10058
      XYZ(1,IP)=X                                                       MSH10059
      XYZ(2,IP)=Y                                                       MSH10060
      XYZ(3,IP)=Z(IZ)                                                   MSH10061
  400 CONTINUE                                                          MSH10062
  300 CONTINUE                                                          MSH10063
  200 CONTINUE                                                          MSH10064
C                                                                       MSH10065
C     GENERATE ELEMENT CONNECTIVITIES ETC.                              MSH10066
      LQ2=2*NQ                                                          MSH10067
      LQ3=3*NQ                                                          MSH10068
      LA1=2*NZ+1                                                        MSH10069
      LA2=NZ+1                                                          MSH10070
      LA=3*NZ+2                                                         MSH10071
      LR1=NA*(3*NZ+2)                                                   MSH10072
```

```
      LR2=NA*(NZ+1)                                                     MSH10073
      LR=NA*(4*NZ+3)                                                    MSH10074
      DO 500 IR=1,NR                                                    MSH10075
      JR=IR+MR                                                          MSH10076
      DO 600 IA=1,NA                                                    MSH10077
      II=0                                                              MSH10078
      IF(IA.EQ.NA-JR+1) II=1                                            MSH10079
      IJ=0                                                              MSH10080
      IF(IA.EQ.NA-JR) IJ=1                                              MSH10081
      DO 700 IZ=1,NZ                                                    MSH10082
      IE=IE+1                                                           MSH10083
      NCON(1,IE)=JP+IR*LR+LA*MCD(IA+JR,NA)+(IZ-1)*2                     MSH10084
      NCON(3,IE)=NCON(1,IE)-LR-LA+IJ*LR1                                MSH10085
      NCON(10,IE)=NCON(3,IE)+1                                          MSH10086
      NCON(15,IE)=NCON(3,IE)+2                                          MSH10087
      NCON(7,IE)=NCON(1,IE)-LA+IJ*LR1                                   MSH10088
      NCON(5,IE)=NCON(7,IE)-LR-LA+II*LR1                                MSH10089
      NCON(11,IE)=NCON(5,IE)+1                                          MSH10090
      NCON(17,IE)=NCON(5,IE)+2                                          MSH10091
      NCON(8,IE)=NCON(7,IE)+LA1-IZ+1                                    MSH10092
      NCON(4,IE)=NCON(8,IE)-LR-LA+II*LR1                                MSH10093
      NCON(16,IE)=NCON(4,IE)+1                                          MSH10094
      NCON(2,IE)=JP+IR*LR-LR2+LA2*IA+(IZ-1)-(IA/NA)*LR2                 MSH10095
      NCON(14,IE)=NCON(2,IE)+1                                          MSH10096
      NCON(6,IE)=NCON(2,IE)-LA2+(IA/NA)*LR2                             MSH10097
      NCON(18,IE)=NCON(6,IE)+1                                          MSH10098
      IF(IR.NE.NR) GO TO 10                                             MSH10099
      IB=IB+1                                                           MSH10100
      NEE(IB)=IE                                                        MSH10101
      IF(NQ.EQ.0) GO TO 10                                              MSH10102
      NCON(1,IE)=NCON(1,IE)+LQ3*(IA+1-NA*(IJ+II))+LQ2                   MSH10103
      NCON(7,IE)=NCON(7,IE)+LQ3*(IA-NA*II)+LQ2                          MSH10104
      NCON(8,IE)=NCON(8,IE)+LQ3*(IA+1-NA*II)                            MSH10105
   10 IF(IZ.NE.1) GO TO 20                                              MSH10106
      IS=IS+1                                                           MSH10107
      NSE(IS)=IE                                                        MSH10108
```

```
 20 NCON(9,IE)=NCON(1,IE)+1                                          MSH10109
    NCON(13,IE)=NCON(1,IE)+2                                         MSH10110
    NCON(12,IE)=NCON(7,IE)+1                                         MSH10111
    NCON(19,IE)=NCON(7,IE)+2                                         MSH10112
    NCON(20,IE)=NCON(8,IE)+1                                         MSH10113
    IF(IR.NE.1.OR.IZ.GT.NTN) GO TO 700                               MSH10114
    IT=IT+1                                                          MSH10115
    NTE(IT)=IE                                                       MSH10116
700 CONTINUE                                                         MSH10117
600 CONTINUE                                                         MSH10118
500 CONTINUE                                                         MSH10119
    RETURN                                                           MSH10120
    END                                                              MSH10121
```

```
      SUBROUTINE OUTPUT(A,N)                                            OUPT0001
C                                                                       OUPT0002
C     THIS SUBROUTINE OUTPUTS THE REAL & IMAGINERY PARTS, MAGNITUDE &   OUPT0003
C     PHASE OF EACH ELEMENT OF A COMPLEX VECTOR A, N LONG               OUPT0004
C                                                                       OUPT0005
      COMPLEX A(N)                                                      OUPT0006
      COMMON /IC/IREAD,IWRITE                                           OUPT0007
      WRITE(IWRITE,26)                                                  OUPT0008
   26 FORMAT('+',22X,'REAL PART',5X,'IMAG. PART',9X,'ABS. VALUE',       OUPT0009
     *           9X,'PHASE VALUE'/)                                     OUPT0010
      DO 22 I=1,N                                                       OUPT0011
      AR=REAL(A(I))                                                     OUPT0012
      AI= AIMAG(A(I))                                                   OUPT0013
      AT=0.                                                             OUPT0014
      IF(AR.NE.0..OR.AI.NE.0.) AT=ATAN2(AI,AR)                          OUPT0015
      AS= SQRT(AR*AR+AI*AI)                                             OUPT0016
      WRITE(IWRITE,24) I,A(I),AS,AT                                     OUPT0017
   22 CONTINUE                                                          OUPT0018
   24 FORMAT(I8,10X,2E15.6,4X,E15.6,5X,F13.6)                           OUPT0019
      RETURN                                                            OUPT0020
      END                                                               OUPT0021
```

```
      SUBROUTINE PLOAD( NELEB,NCON,XYZ,SYSQ,WK,WKH )
C
C     THIS SUBROUTINE ASSEMBLES THE LOAD VECTOR SYSQ
C     NOTE: ONLY THE LAST NODR ENTRIES IN SYSQ ARE NON-ZERO
C
      INTEGER*4 NELEB,NCON,NR
      REAL*4 PS(3),WS(3)
      COMPLEX EKR,TM,SYSQ,CI
      COMMON NELE,NNOD,NS,NB,NODR,NEQT,NBAND,NMAX,NTOTL,NTOTL2,NWK,
     *       THETAI,WAVET,R,H,NMAX2
      DIMENSION NELEB(NB),NCON(20,NELE),XYZ(3,NNOD),SYSQ(NEQT),WK(NWK),
     *          WKH(NWK)
      DIMENSION NR(8),P(8,3),Q(8),DQ(2,8),INOD(8)
C
C     QUADRATURE DATA
      DATA INOD/1,8,7,12,19,20,13,9/
      DATA PS/.7745967 ,0.,-.7745967 /
      DATA WS/.5555556 ,.8888889 ,.5555556 /
C
      CI=(0.,1.)
      CALL ERASE(SYSQ,2*NEQT)
C
C     LOOP OVER ALL ELEMENTS ON THE ARTIFICIAL BOUNDARY
      DO 40 L=1,NB
      K= NELEB(L)
      DO  8 I=1,8
      NR(I)=NCON(INOD(I),K)
      DO 8 J=1,3
    8 P(I,J)=XYZ(J,NR(I))
C
C     LOOPS OVER INTEGRATION POINTS
      DO 20 IS=1,3
      DO 20 IT=1,3
      S=PS(IS)
      T=PS(IT)
      CALL FMAP2( S,T,P,Q,DQ,XX,YY,ZZ,CJ,1 )
```

```
      VKR = WK(1)*(XX*COS(THETAI)+YY*SIN(THETAI))                       PLOD0037
      EKR = COS(VKR) +CI*SIN(VKR)                                       PLOD0038
      TM=CI*VKR/R*EKR*(COSH(WK(1)*(ZZ+H))/COSH(WKH(1)))*CJ*WS(IS)*WS(IT) PLOD0039
      DO 14 K=1,8                                                       PLOD0040
   14 SYSQ(NR(K)) = SYSQ(NR(K)) + TM*Q(K)                               PLOD0041
   20 CONTINUE                                                          PLOD0042
   40 CONTINUE                                                          PLOD0043
      RETURN                                                            PLOD0044
      END                                                               PLOD0045
```

```
      SUBROUTINE SOLV (A,B,NEQT,NBAND)                                  SOLV0001
C                                                                       SOLV0002
C     THIS SUBROUTINE PERFORMS GAUSS REDUCTION                          SOLV0003
C     A IS AN UPPER SYMMETRIC BAND STORED COMPLEX ARRAY OF COEFF. MATRIX SOLV0004
C     B IS THE COMPLEX LOAD VECTOR                                      SOLV0005
C     NEQT IS THE NO. OF EQUATIONS A REPRESENTS                         SOLV0006
C     NBAND IS THE SEMI-BANDWIDTH OF THE COEFF. MATRIX                  SOLV0007
C                                                                       SOLV0008
      COMPLEX A(1),B(1),Q,R                                             SOLV0009
      NSOLVE=NEQT-1                                                     SOLV0010
      NB=NBAND-1                                                        SOLV0011
      JF=NEQT-NB                                                        SOLV0012
C                                                                       SOLV0013
C     I FOR ROW PIVOTING                                                SOLV0014
      DO 100 I=1,NSOLVE                                                 SOLV0015
      Q=1.0/A(I)                                                        SOLV0016
      IF(I.GT.JF) NB=NEQT-I                                             SOLV0017
      NB1=NB+1                                                          SOLV0018
C                                                                       SOLV0019
C     NB=NO. OF ROWS TO ELIMINATE                                       SOLV0020
C     JI=ROW NO. ELIMINATION IS PERFORMED                               SOLV0021
      DO 200 II=1,NB                                                    SOLV0022
      JI=I+II                                                           SOLV0023
      R=A(I+II*NEQT)*Q                                                  SOLV0024
      B(JI)=B(JI)-R*B(I)                                                SOLV0025
C                                                                       SOLV0026
C     JJ=NO. OF COLS. TO CHANGE, IJ=COL. NO. UNDER OPERATION            SOLV0027
      JJ=NB1-II                                                         SOLV0028
      DO 300 IJ=1,JJ                                                    SOLV0029
      INDEX1=JI+(IJ-1)*NEQT                                             SOLV0030
      INDEX2=I+(II+IJ-1)*NEQT                                           SOLV0031
      A(INDEX1)=A(INDEX1)-R*A(INDEX2)                                   SOLV0032
  300 CONTINUE                                                          SOLV0033
  200 CONTINUE                                                          SOLV0034
  100 CONTINUE                                                          SOLV0035
      RETURN                                                            SOLV0036
```

SOLVOO37

END

```
      SUBROUTINE SURFAS( NELES,NCON,XYZ,SYSK )                          SFAS0001
C                                                                       SFAS0002
C     THIS SUBROUTINE ASSEMBLES 'FREE SURFACE' CONTRIBUTIONS INTO GLOBAL SFAS0003
C     MATRIX SYSK                                                       SFAS0004
C                                                                       SFAS0005
      COMPLEX SYSK                                                      SFAS0006
      INTEGER*4 NELES,NCON,NR                                           SFAS0007
      REAL*4 PS(3),WS(3)                                                SFAS0008
      COMMON NELE,NNOD,NS,NB,NODR,NEQT,NBAND,NMAX,NTOTL,NTOTL2,NWK,     SFAS0009
     *       THETAI,WAVET,R,H,NMAX2                                     SFAS0010
      DIMENSION NELES(NS),NCON(20,NELE),XYZ(3,NNOD),SYSK(NEQT,NBAND)    SFAS0011
      DIMENSION NR(8),P(8,3),EKS(8,8),Q(8),DQ(2,8)                      SFAS0012
C                                                                       SFAS0013
C     QUADRATURE DATA                                                   SFAS0014
      DATA PS/.7745967 ,0.,-.7745967 /                                  SFAS0015
      DATA WS/.5555556 ,.8888889 ,.5555556 /                            SFAS0016
C                                                                       SFAS0017
      PAI=3.1415926                                                     SFAS0018
      CONST=-(2.*PAI/WAVET)**2                                          SFAS0019
C                                                                       SFAS0020
C     LOOP OVER ALL ELEMENTS ON THE FREE SURFACE                        SFAS0021
      DO 40 L=1,NS                                                      SFAS0022
      CALL ERASE(EKS,64)                                                SFAS0023
      DO 10 I=1,8                                                       SFAS0024
      NR(I) = NCON(I,NELES(L))                                          SFAS0025
      DO 10 J=1,3                                                       SFAS0026
   10 P(I,J)=XYZ(J,NR(I))                                               SFAS0027
C                                                                       SFAS0028
C     NUMERICAL INTEGRATION LOOPS                                       SFAS0029
      DO 20 IS=1,3                                                      SFAS0030
      DO 20 IT=1,3                                                      SFAS0031
      S=PS(IS)                                                          SFAS0032
      T=PS(IT)                                                          SFAS0033
      CALL FMAP2( S,T,P,Q,DQ,XX,YY,ZZ,CJ,2 )                            SFAS0034
      DO 18 J=1,8                                                       SFAS0035
      DO 18 K=J,8                                                       SFAS0036
```

```
      EKS(J,K) = EKS(J,K)+Q(J)*Q(K)*CJ*CONST*WS(IS)*WS(IT)
   18 CONTINUE
   20 CONTINUE
C
C     ASSEMBLAGE
      DO 30 I=1,8
      DO 30 J=I,8
      IF( NR(J)-NR(I) .GE. 0 ) GO TO 26
      LR = NR(I)-NR(J)+1
      SYSK(NR(J),LR) = SYSK(NR(J),LR) + EKS(I,J)
      GO TO 30
   26 LS = NR(J)-NR(I)+1
      SYSK(NR(I),LS) = SYSK(NR(I),LS) + EKS(I,J)
   30 CONTINUE
   40 CONTINUE
      RETURN
      END
```

5.2.4.4 Sample output

```
*********************************
*** GEOMETRY & PHYSICAL DATA ***
*********************************

ALL LENGTHS ARE NORMALIZED BY THE RADIUS OF THE CYLINDER, A

ASYMPTOTIC DEPTH=     0.7500
RADIUS OF SUPER-ELEMENT=     1.3000
SUBMERGED DEPTH OF UNIT CYLINDER=     0.5000

NO. OF NODAL POINTS=  435
NO. OF ELEMENTS=   56

32 ELEMENTS ON SUPERELEMENT BOUNDARY :
 25    26    27    28    29    30    31    32    33    34    35    36    37    38    39    40    41    42    43    44
 45    46    47    48    49    50    51    52    53    54    55    56

16 ELEMENTS ON THE FREE SURFACE :
 25    27    29    31    33    35    37    39    41    43    45    47    49    51    53    55

16 ELEMENTS ON THE CYLINDER CIRCUMFERENCE :
 25    27    29    31    33    35    37    39    41    43    45    47    49    51    53    55

24 ELEMENTS ON THE CYLINDER BASE :
  1     2     3     4     5     6     7     8     9    10    11    12    13    14    15    16    17    18    19    20
 21    22    23    24
```

****
*** NODE COORDINATES ***
****

NODE	X	Y	Z	NODE	X	Y	Z	NODE	X	Y	Z
1	0.0	0.0	-0.50000	2	0.0	0.0	-0.62500	3	0.0	0.0	-0.75000
4	0.25000	0.0	-0.50000	5	0.25000	0.0	-0.75000	6	0.17678	0.17678	-0.50000
7	0.17678	0.17678	-0.75000	8	0.00000	0.25000	-0.50000	9	0.00000	0.25000	-0.75000
10	-0.17678	0.17678	-0.50000	11	-0.17678	0.17678	-0.75000	12	-0.25000	-0.00000	-0.50000
13	-0.25000	-0.00000	-0.75000	14	-0.17678	-0.17678	-0.50000	15	-0.17678	-0.17678	-0.75000
16	0.00000	-0.25000	-0.50000	17	0.00000	-0.25000	-0.75000	18	0.17678	-0.17678	-0.50000
19	0.17678	-0.17678	-0.75000	20	0.50000	0.0	-0.50000	21	0.50000	0.0	-0.62500
22	0.50000	0.0	-0.75000	23	0.49039	0.09755	-0.50000	24	0.49039	0.09755	-0.75000
25	0.46194	0.19134	-0.50000	26	0.46194	0.19134	-0.62500	27	0.46194	0.19134	-0.75000
28	0.41573	0.27779	-0.50000	29	0.41573	0.27779	-0.75000	30	0.35355	0.35355	-0.50000
31	0.35355	0.35355	-0.62500	32	0.35355	0.35355	-0.75000	33	0.27779	0.41573	-0.50000
34	0.27779	0.41573	-0.75000	35	0.19134	0.46194	-0.50000	36	0.19134	0.46194	-0.62500
37	0.19134	0.46194	-0.75000	38	0.09755	0.49039	-0.50000	39	0.09755	0.49039	-0.75000
40	0.00000	0.50000	-0.50000	41	0.00000	0.50000	-0.62500	42	0.00000	0.50000	-0.75000
43	-0.09754	0.49039	-0.50000	44	-0.09754	0.49039	-0.75000	45	-0.19134	0.46194	-0.50000
46	-0.19134	0.46194	-0.62500	47	-0.19134	0.46194	-0.75000	48	-0.27778	0.41573	-0.50000
49	-0.27778	0.41573	-0.75000	50	-0.35355	0.35355	-0.50000	51	-0.35355	0.35355	-0.62500
52	-0.35355	0.35355	-0.75000	53	-0.41573	0.27779	-0.50000	54	-0.41573	0.27779	-0.75000
55	-0.46194	0.19134	-0.50000	56	-0.46194	0.19134	-0.62500	57	-0.46194	0.19134	-0.75000
58	-0.49039	0.09755	-0.50000	59	-0.49039	0.09755	-0.75000	60	-0.50000	-0.00000	-0.50000
61	-0.50000	-0.00000	-0.62500	62	-0.50000	-0.00000	-0.75000	63	-0.49039	-0.09755	-0.50000
64	-0.49039	-0.09755	-0.75000	65	-0.46194	-0.19134	-0.50000	66	-0.46194	-0.19134	-0.62500
67	-0.46194	-0.19134	-0.75000	68	-0.41573	-0.27779	-0.50000	69	-0.41573	-0.27779	-0.75000
70	-0.35355	-0.35355	-0.50000	71	-0.35355	-0.35355	-0.62500	72	-0.35355	-0.35355	-0.75000
73	-0.27778	-0.41573	-0.50000	74	-0.27778	-0.41573	-0.75000	75	-0.19134	-0.46194	-0.50000
76	-0.19134	-0.46194	-0.62500	77	-0.19134	-0.46194	-0.75000	78	-0.09754	-0.49039	-0.50000
79	-0.09754	-0.49039	-0.75000	80	0.00000	-0.50000	-0.50000	81	0.00000	-0.50000	-0.62500
82	0.00000	-0.50000	-0.75000	83	0.09754	-0.49039	-0.50000	84	0.09754	-0.49039	-0.75000
85	0.19134	-0.46194	-0.50000	86	0.19134	-0.46194	-0.62500	87	0.19134	-0.46194	-0.75000
88	0.27779	-0.41573	-0.50000	89	0.27779	-0.41573	-0.75000	90	0.35355	-0.35355	-0.50000
91	0.35355	-0.35355	-0.62500	92	0.35355	-0.35355	-0.75000	93	0.41573	-0.27779	-0.50000
94	0.41573	-0.27779	-0.75000	95	0.46194	-0.19134	-0.50000	96	0.46194	-0.19134	-0.62500
97	0.46194	-0.19134	-0.75000	98	0.49039	-0.09755	-0.50000	99	0.49039	-0.09755	-0.75000
100	0.80000	0.0	-0.50000	101	0.80000	0.0	-0.75000	102	0.73910	0.30615	-0.50000
103	0.73910	0.30615	-0.75000	104	0.56569	0.56569	-0.50000	105	0.56569	0.56569	-0.75000
106	0.30615	0.73910	-0.50000	107	0.30615	0.73910	-0.75000	108	0.00000	0.80000	-0.50000
109	0.00000	0.80000	-0.75000	110	-0.30615	0.73910	-0.50000	111	-0.30615	0.73910	-0.75000
112	-0.56569	0.56569	-0.50000	113	-0.56569	0.56569	-0.75000	114	-0.73910	0.30615	-0.50000
115	-0.73910	0.30615	-0.75000	116	-0.80000	-0.00000	-0.50000	117	-0.80000	-0.00000	-0.75000
118	-0.73910	-0.30615	-0.50000	119	-0.73910	-0.30615	-0.75000	120	-0.56569	-0.56569	-0.50000
121	-0.56569	-0.56569	-0.75000	122	-0.30615	-0.73910	-0.50000	123	-0.30615	-0.73910	-0.75000
124	0.00000	-0.80000	-0.50000	125	0.00000	-0.80000	-0.75000	126	0.30615	-0.73910	-0.50000
127	0.30615	-0.73910	-0.75000	128	0.56569	-0.56569	-0.50000	129	0.56569	-0.56569	-0.75000
130	0.73910	-0.30615	-0.50000	131	0.73910	-0.30615	-0.75000	132	0.92388	-0.38268	0.0
133	0.92388	-0.38268	-0.50000	134	0.92388	-0.38268	-0.50000	135	0.92388	-0.38268	-0.62500
136	0.92388	-0.38268	-0.75000	137	0.98079	-0.19509	0.0	138	0.98079	-0.19509	-0.50000
139	0.98079	-0.19509	-0.75000	140	1.00000	0.0	0.0	141	1.00000	0.0	-0.50000
142	1.00000	0.0	-0.50000	143	1.00000	0.0	-0.62500	144	1.00000	0.0	-0.75000
145	0.98079	0.19509	0.0	146	0.98079	0.19509	-0.50000	147	0.98079	0.19509	-0.75000
148	0.92388	0.38268	0.0	149	0.92388	0.38268	-0.50000	150	0.92388	0.38268	-0.50000
151	0.92388	0.38268	-0.62500	152	0.92388	0.38268	-0.75000	153	0.83147	0.55557	0.0
154	0.83147	0.55557	-0.50000	155	0.83147	0.55557	-0.75000	156	0.70711	0.70711	0.0
157	0.70711	0.70711	-0.50000	158	0.70711	0.70711	-0.50000	159	0.70711	0.70711	-0.62500

160	0.70711	0.70711	-0.75000
163	0.55557	0.83147	-0.75000
166	0.38268	0.92388	-0.50000
169	0.19509	0.98079	0.0
172	0.00000	1.00000	0.0
175	0.00000	1.00000	-0.62500
178	-0.19509	0.98079	-0.50000
181	-0.38268	0.92388	-0.30000
184	-0.38268	0.92388	-0.75000
187	-0.55557	0.83147	-0.75000
190	-0.70711	0.70711	-0.50000
193	-0.83147	0.55557	0.0
196	-0.92388	0.38268	0.0
199	-0.92388	0.38268	-0.62500
202	-0.98079	0.19509	-0.50000
205	-1.00000	-0.00000	-0.30000
208	-1.00000	-0.00000	-0.75000
211	-0.98079	-0.19509	-0.75000
214	-0.92388	-0.38268	-0.50000
217	-0.83147	-0.55557	0.0
220	-0.70711	-0.70711	0.0
223	-0.70711	-0.70711	-0.62500
226	-0.55557	-0.83147	-0.50000
229	-0.38268	-0.92388	-0.30000
232	-0.38268	-0.92388	-0.75000
235	-0.19509	-0.98079	-0.75000
238	0.00000	-1.00000	-0.50000
241	0.19509	-0.98079	0.0
244	0.38268	-0.92388	0.0
247	0.38268	-0.92388	-0.62500
250	0.55557	-0.83147	-0.50000
253	0.70711	-0.70711	-0.30000
256	0.70711	-0.70711	-0.75000
259	0.83147	-0.55557	-0.75000
262	1.15000	0.0	-0.75000
265	1.06246	0.44009	-0.75000
268	0.81317	0.81317	-0.75000
271	0.44009	1.06246	-0.75000
274	0.00000	1.15000	-0.75000
277	-0.44009	1.06246	-0.75000
280	-0.81317	0.81317	-0.75000
283	-1.06246	0.44009	-0.75000
286	-1.15000	-0.00000	-0.75000
289	-1.06246	-0.44009	-0.75000
292	-0.81317	-0.81317	-0.75000
295	-0.44009	-1.06246	-0.75000
298	0.00000	-1.15000	-0.75000
301	0.44009	-1.06246	-0.75000
304	0.81317	-0.81317	-0.75000
307	1.06246	-0.44009	-0.75000
310	0.91924	-0.91924	-0.50000
313	1.08091	-0.72224	0.0
316	1.20104	-0.49749	0.0
319	1.20104	-0.49749	-0.62500
322	1.27502	-0.25362	-0.50000
325	1.30000	0.0	-0.30000
328	1.30000	0.0	-0.75000
331	1.27502	0.25362	-0.75000
334	1.20104	0.49749	-0.50000
337	1.08091	0.72224	0.0
340	0.91924	0.91924	0.0
343	0.91924	0.91924	-0.62500
346	0.72224	1.08091	-0.50000
349	0.49749	1.20104	-0.30000
352	0.49749	1.20104	-0.75000
355	0.25362	1.27502	-0.75000

161	0.55557	0.83147	0.0
164	0.38268	0.92388	0.0
167	0.38268	0.92388	-0.62500
170	0.19509	0.98079	-0.50000
173	0.00000	1.00000	-0.30000
176	0.00000	1.00000	-0.75000
179	-0.19509	0.98079	-0.75000
182	-0.38268	0.92388	-0.50000
185	-0.55557	0.83147	0.0
188	-0.70711	0.70711	0.0
191	-0.70711	0.70711	-0.62500
194	-0.83147	0.55557	-0.50000
197	-0.92388	0.38268	-0.30000
200	-0.92388	0.38268	-0.75000
203	-0.98079	0.19509	-0.75000
206	-1.00000	-0.00000	-0.50000
209	-0.98079	-0.19509	0.0
212	-0.92388	-0.38268	0.0
215	-0.92388	-0.38268	-0.62500
218	-0.83147	-0.55557	-0.50000
221	-0.70711	-0.70711	-0.30000
224	-0.70711	-0.70711	-0.75000
227	-0.55557	-0.83147	-0.75000
230	-0.38268	-0.92388	-0.50000
233	-0.19509	-0.98079	0.0
236	0.00000	-1.00000	0.0
239	0.00000	-1.00000	-0.62500
242	0.19509	-0.98079	-0.50000
245	0.38268	-0.92388	-0.30000
248	0.38268	-0.92388	-0.75000
251	0.55557	-0.83147	-0.75000
254	0.70711	-0.70711	-0.50000
257	0.83147	-0.55557	0.0
260	1.15000	0.0	0.0
263	1.06246	0.44009	0.0
266	0.81317	0.81317	0.0
269	0.44009	1.06246	0.0
272	0.00000	1.15000	0.0
275	-0.44009	1.06246	0.0
278	-0.81317	0.81317	0.0
281	-1.06246	0.44009	0.0
284	-1.15000	-0.00000	0.0
287	-1.06246	-0.44009	0.0
290	-0.81317	-0.81317	0.0
293	-0.44009	-1.06246	0.0
296	0.00000	-1.15000	0.0
299	0.44009	-1.06246	0.0
302	0.81317	-0.81317	0.0
305	1.06246	-0.44009	0.0
308	0.91924	-0.91924	0.0
311	0.91924	-0.91924	-0.62500
314	1.08091	-0.72224	-0.50000
317	1.20104	-0.49749	-0.30000
320	1.20104	-0.49749	-0.75000
323	1.27502	-0.25362	-0.75000
326	1.30000	0.0	-0.50000
329	1.27502	0.25362	0.0
332	1.20104	0.49749	0.0
335	1.20104	0.49749	-0.62500
338	1.08091	0.72224	-0.50000
341	0.91924	0.91924	-0.30000
344	0.91924	0.91924	-0.75000
347	0.72224	1.08091	-0.75000
350	0.49749	1.20104	-0.50000
353	0.25362	1.27502	0.0
356	0.00000	1.30000	0.0

162	0.55557	0.83147	-0.50000
165	0.38268	0.92388	-0.30000
168	0.38268	0.92388	-0.75000
171	0.19509	0.98079	-0.75000
174	0.00000	1.00000	-0.50000
177	-0.19509	0.98079	0.0
180	-0.38268	0.92388	0.0
183	-0.38268	0.92388	-0.62500
186	-0.55557	0.83147	-0.50000
189	-0.70711	0.70711	-0.30000
192	-0.70711	0.70711	-0.75000
195	-0.83147	0.55557	-0.75000
198	-0.92388	0.38268	-0.50000
201	-0.98079	0.19509	0.0
204	-1.00000	-0.00000	0.0
207	-1.00000	-0.00000	-0.62500
210	-0.98079	-0.19509	-0.50000
213	-0.92388	-0.38268	-0.30000
216	-0.92388	-0.38268	-0.75000
219	-0.83147	-0.55557	-0.75000
222	-0.70711	-0.70711	-0.50000
225	-0.55557	-0.83147	0.0
228	-0.38268	-0.92388	0.0
231	-0.38268	-0.92388	-0.62500
234	-0.19509	-0.98079	-0.50000
237	0.00000	-1.00000	-0.30000
240	0.00000	-1.00000	-0.75000
243	0.19509	-0.98079	-0.75000
246	0.38268	-0.92388	-0.50000
249	0.55557	-0.83147	0.0
252	0.70711	-0.70711	0.0
255	0.70711	-0.70711	-0.62500
258	0.83147	-0.55557	-0.50000
261	1.15000	0.0	-0.50000
264	1.06246	0.44009	-0.50000
267	0.81317	0.81317	-0.50000
270	0.44009	1.06246	-0.50000
273	0.00000	1.15000	-0.50000
276	-0.44009	1.06246	-0.50000
279	-0.81317	0.81317	-0.50000
282	-1.06246	0.44009	-0.50000
285	-1.15000	-0.00000	-0.50000
288	-1.06246	-0.44009	-0.50000
291	-0.81317	-0.81317	-0.50000
294	-0.44009	-1.06246	-0.50000
297	0.00000	-1.15000	-0.50000
300	0.44009	-1.06246	-0.50000
303	0.81317	-0.81317	-0.50000
306	1.06246	-0.44009	-0.50000
309	0.91924	-0.91924	-0.30000
312	0.91924	-0.91924	-0.75000
315	1.08091	-0.72224	-0.75000
318	1.20104	-0.49749	-0.50000
321	1.27502	-0.25362	0.0
324	1.30000	0.0	0.0
327	1.30000	0.0	-0.62500
330	1.27502	0.25362	-0.50000
333	1.20104	0.49749	-0.30000
336	1.20104	0.49749	-0.75000
339	1.08091	0.72224	-0.75000
342	0.91924	0.91924	-0.50000
345	0.72224	1.08091	0.0
348	0.49749	1.20104	0.0
351	0.49749	1.20104	-0.62500
354	0.25362	1.27502	-0.50000
357	0.00000	1.30000	-0.30000

358	0.00000	1.30000	-0.50000	359	0.00000	1.30000	-0.62500	360	0.00000	1.30000	-0.75000
361	-0.25362	1.27502	0.0	362	-0.25362	1.27502	-0.50000	363	-0.25362	1.27502	-0.75000
364	-0.49749	1.20104	0.0	365	-0.49749	1.20104	-0.30000	366	-0.49749	1.20104	-0.50000
367	-0.49749	1.20104	-0.62500	368	-0.49749	1.20104	-0.75000	369	-0.72224	1.08091	0.0
370	-0.72224	1.08091	-0.50000	371	-0.72224	1.08091	-0.75000	372	-0.91924	0.91924	0.0
373	-0.91924	0.91924	-0.30000	374	-0.91924	0.91924	-0.50000	375	-0.91924	0.91924	-0.62500
376	-0.91924	0.91924	-0.75000	377	-1.08091	0.72224	0.0	378	-1.08091	0.72224	-0.50000
379	-1.08091	0.72224	-0.75000	380	-1.20104	0.49749	0.0	381	-1.20104	0.49749	-0.30000
382	-1.20104	0.49749	-0.50000	383	-1.20104	0.49749	-0.62500	384	-1.20104	0.49749	-0.75000
385	-1.27502	0.25362	0.0	386	-1.27502	0.25362	-0.50000	387	-1.27502	0.25362	-0.75000
388	-1.30000	-0.00000	0.0	389	-1.30000	-0.00000	-0.30000	390	-1.30000	-0.00000	-0.50000
391	-1.30000	-0.00000	-0.62500	392	-1.30000	-0.00000	-0.75000	393	-1.27502	-0.25362	0.0
394	-1.27502	-0.25362	-0.50000	395	-1.27502	-0.25362	-0.75000	396	-1.20104	-0.49749	0.0
397	-1.20104	-0.49749	-0.30000	398	-1.20104	-0.49749	-0.50000	399	-1.20104	-0.49749	-0.62500
400	-1.20104	-0.49749	-0.75000	401	-1.08091	-0.72224	0.0	402	-1.08091	-0.72224	-0.50000
403	-1.08091	-0.72224	-0.75000	404	-0.91924	-0.91924	0.0	405	-0.91924	-0.91924	-0.30000
406	-0.91924	-0.91924	-0.50000	407	-0.91924	-0.91924	-0.62500	408	-0.91924	-0.91924	-0.75000
409	-0.72224	-1.08091	0.0	410	-0.72224	-1.08091	-0.50000	411	-0.72224	-1.08091	-0.75000
412	-0.49749	-1.20104	0.0	413	-0.49749	-1.20104	-0.30000	414	-0.49749	-1.20104	-0.50000
415	-0.49749	-1.20104	-0.62500	416	-0.49749	-1.20104	-0.75000	417	-0.25362	-1.27502	0.0
418	-0.25362	-1.27502	-0.50000	419	-0.25362	-1.27502	-0.75000	420	0.00000	-1.30000	0.0
421	0.00000	-1.30000	-0.30000	422	0.00000	-1.30000	-0.50000	423	0.00000	-1.30000	-0.62500
424	0.00000	-1.30000	-0.75000	425	0.25362	-1.27502	0.0	426	0.25362	-1.27502	-0.50000
427	0.25362	-1.27502	-0.75000	428	0.49749	-1.20104	0.0	429	0.49749	-1.20104	-0.30000
430	0.49749	-1.20104	-0.50000	431	0.49749	-1.20104	-0.62500	432	0.49749	-1.20104	-0.75000
433	0.72224	-1.08091	0.0	434	0.72224	-1.08091	-0.50000	435	0.72224	-1.08091	-0.75000

****
*** ELEMENT CONNECTIVITIES ***
****

ELEM. NODES...

	1	2	3	4	5	6	7	8	9	10	11	12	13	14	15	16	17	18	19	20
1	25	28	30	6	1	4	23	23	26	31	2	21	27	29	32	7	3	5	22	24
2	35	38	40	8	1	6	30	33	36	41	2	31	37	39	42	9	3	7	32	34
3	45	48	50	10	1	8	40	43	46	51	2	41	47	49	52	11	3	9	42	44
4	55	58	60	12	1	10	50	53	56	61	2	51	57	59	62	13	3	11	52	54
5	65	68	70	14	1	12	60	63	66	71	2	61	67	69	72	15	3	13	62	64
6	75	78	80	16	1	14	70	73	76	81	2	71	77	79	82	17	3	15	72	74
7	85	88	90	18	1	16	80	83	86	91	2	81	87	89	92	19	3	17	82	84
8	95	98	20	4	1	18	90	93	96	21	2	91	97	99	22	5	3	19	92	94
9	150	102	25	23	20	100	142	146	151	26	21	143	152	103	27	24	22	101	144	147
10	158	104	30	28	25	102	150	154	159	31	26	151	160	105	32	29	27	103	152	155
11	166	106	35	33	30	104	158	162	167	36	31	159	168	107	37	34	32	105	160	163
12	174	108	40	38	35	106	166	170	175	41	36	167	176	109	42	39	37	107	166	171
13	182	110	45	43	40	108	174	178	183	46	41	175	184	111	47	44	42	109	176	179
14	190	112	50	48	45	110	182	186	191	51	46	183	192	113	52	49	47	111	184	187
15	198	114	55	53	50	112	190	194	199	56	51	191	200	115	57	54	52	113	192	195
16	206	116	60	58	55	114	198	202	207	61	56	199	208	117	62	59	57	115	200	203
17	214	118	65	63	60	116	206	210	215	66	61	207	216	119	67	64	62	117	208	211
18	222	120	70	68	65	118	214	218	223	71	66	215	224	121	72	69	67	119	216	219
19	230	122	75	73	70	120	222	226	231	76	71	223	232	123	77	74	72	121	224	227
20	238	124	80	78	75	122	230	234	239	81	76	231	240	125	82	79	77	123	232	235
21	246	126	85	83	80	124	238	242	247	86	81	239	248	127	87	84	82	125	240	243
22	254	128	90	88	85	126	246	250	255	91	86	247	256	129	92	89	87	127	248	251
23	134	130	95	93	90	128	254	258	135	96	91	255	136	131	97	94	92	127	256	259
24	142	100	20	98	95	130	136	138	143	21	96	135	144	101	22	99	97	131	136	139
25	332	263	148	145	140	260	324	329	333	149	141	325	334	264	150	146	142	261	326	330
26	334	264	150	146	142	261	326	330	335	151	143	327	336	265	152	147	144	262	328	331
27	340	266	156	153	148	263	332	337	341	157	149	333	342	267	158	154	150	264	334	338
28	342	267	158	154	150	264	334	338	343	159	151	335	344	268	160	155	152	265	336	339
29	348	269	164	161	156	266	340	345	349	165	157	341	350	270	165	162	159	267	342	346
30	350	270	166	162	158	267	342	346	351	167	159	343	352	271	168	163	160	268	344	347
31	356	272	172	169	164	269	348	353	357	173	165	349	358	273	174	170	166	270	350	354
32	358	273	174	170	166	270	350	354	359	175	167	351	360	274	176	171	168	271	352	355
33	364	275	180	177	172	272	356	361	365	181	173	357	366	276	182	178	174	273	358	362
34	366	276	182	178	174	273	358	362	367	183	175	359	368	277	184	179	176	274	360	363
35	372	278	188	185	180	275	364	369	373	189	181	365	374	279	190	186	182	276	366	370
36	374	279	190	186	182	276	366	370	375	191	183	367	376	280	192	187	184	277	368	371
37	380	281	196	193	188	278	372	377	381	197	189	373	382	282	198	194	190	279	374	378
38	382	282	198	194	190	279	374	378	383	199	191	375	384	283	200	195	192	280	376	379
39	388	284	204	201	196	281	380	385	389	205	197	381	390	285	206	202	198	282	382	385
40	390	285	206	202	198	282	382	386	391	207	199	383	392	286	208	203	200	283	384	387
41	396	287	212	209	204	284	388	393	397	213	205	389	398	288	214	210	206	285	390	394
42	398	288	214	210	206	285	390	394	399	215	207	391	400	289	216	211	208	286	392	395
43	404	290	220	217	212	287	396	401	405	221	213	397	406	291	222	218	214	288	398	402
44	406	291	222	218	214	288	398	402	407	223	215	399	408	292	224	219	216	289	400	403
45	412	293	228	225	220	290	404	409	413	229	221	405	414	294	230	226	222	291	406	410
46	414	294	230	226	222	291	406	410	415	231	223	407	416	295	232	227	224	292	408	411
47	420	296	236	233	228	293	412	417	421	237	229	413	422	297	238	234	230	294	414	418
48	422	297	238	234	230	294	414	418	423	239	231	415	424	298	240	235	232	295	416	419
49	428	299	244	241	236	296	420	425	429	245	237	421	430	300	246	242	238	297	422	426
50	430	300	246	242	238	297	422	426	431	247	239	423	432	301	248	243	240	298	424	427
51	308	302	252	249	244	299	428	433	309	253	245	429	310	303	254	250	246	300	430	434
52	310	303	254	250	246	300	430	434	311	255	247	431	312	304	256	251	248	301	432	435

53	316	305	132	257	252	302	308	313	317	133	253	309	318	306	134	258	254	303	310	314
54	318	306	134	258	254	303	310	314	319	135	255	311	320	307	136	259	256	304	312	315
55	324	260	140	137	132	305	316	321	325	141	133	317	326	261	142	138	134	306	318	322
56	326	261	142	138	134	306	318	322	327	143	135	319	328	262	144	139	136	307	320	323

SEMI-BANDWIDTH OF GLOBAL MATRIX= 195
SEMI-BANDWIDTH W.R.T. ELEMENT CONNECTIVITY= 195
SEMI-BANDWIDTH W.R.T. BOUNDARY NODAL POINTS= 128

```
***************
*** CASE  1 ***
***************
```

DIMENSIONLESS WAVE PERIOD, T/SQRT(A/G)= 7.8839178
INCIDENCE ANGLE= 1.1495930 RADIANS

EIGENVALUE NO.	NO. OF COEFFS.	K	K*H	K*B
1	12	0.100000E+01	0.750000E+00	0.130000E+01
2	12	0.397767E+01	0.298325E+01	0.517097E+01
3	12	0.825545E+01	0.620658E+01	0.107543E+02
4	12	0.124987E+02	0.937401E+01	0.162483E+02
5	12	0.167045E+02	0.125284E+02	0.217159E+02

ARG. M	ORDER N	J(KR)	ENORM	NORMALIZED H(KR) REAL PT.	NORMALIZED H(KR) IMAG. PT.	NORMALIZED H'(KR) REAL PT.	NORMALIZED H'(KR) IMAG. PT.
0	0	0.620283E+00	0.877056E+00	0.707005E+00	0.126734E+00	-0.595209E+00	0.625401E+00
0	1	0.522024E+00	0.916267E+00	0.569729E+00	-0.598642E+00	0.238498E+00	0.773215E+00
1	2	0.181224E+00	0.130704E+01	0.140711E+00	-0.469049E+00	0.184852E+00	0.915296E+00
1	3	0.911627E-01	0.349317E+01	0.119611E-01	-0.351846E+00	0.256162E-01	0.147726E+01
0	4	0.683105E-02	0.150312E+02	0.454459E-03	-0.824352E+00	0.133440E-02	0.234155E+01
0	5	0.900877E-03	0.899356E+02	0.100167E-04	-0.835274E+00	0.374233E-04	0.239798E+01
0	6	0.985323E-04	0.480088E+03	0.149729E-06	-0.911335E+00	0.655934E-06	0.163278E+01
0	7	0.922507E-05	0.620568E+04	0.148651E-08	-0.304683E+00	0.788276E-08	0.426554E+01
0	8	0.751842E-06	0.662847E+05	0.113749E-10	-0.437714E+00	0.691740E-10	0.493263E+01
0	9	0.547125E-07	0.410778E+06	0.674814E-13	-0.405356E+00	0.462773E-12	0.591105E+01
0	10	0.357033E-08	0.111762E+07	0.319553E-15	-0.804964E+00	0.243914E-14	0.613102E+01
0	11	0.210434E-09	0.171416E+08	0.123639E-17	-0.374258E+00	0.103921E-16	0.175270E+01
1	0		0.249742E-02	0.122579E+01	0.0	-0.131945E+01	0.0
1	1		0.272502E-02	0.122758E+01	0.0	-0.136081E+01	0.0
1	2		0.353447E-02	0.123219E+01	0.0	-0.142302E+01	0.0
1	3		0.542134E-02	0.123800E+01	0.0	-0.152128E+01	0.0
1	4		0.976690E-02	0.124356E+01	0.0	-0.164939E+01	0.0
1	5		0.204346E-01	0.124812E+01	0.0	-0.180122E+01	0.0
1	6		0.491149E-01	0.125152E+01	0.0	-0.197146E+01	0.0
1	7		0.134058E+02	0.125394E+01	0.0	-0.215586E+01	0.0
1	8		0.431547E+02	0.125557E+01	0.0	-0.235177E+01	0.0
1	9		0.146614E+03	0.125663E+01	0.0	-0.255463E+01	0.0
2	0		0.648571E-05	0.123945E+01	0.0	-0.124582E+01	0.0
2	1		0.677943E-05	0.123968E+01	0.0	-0.130298E+01	0.0
2	2		0.774064E-05	0.124035E+01	0.0	-0.131633E+01	0.0
2	3		0.964579E-05	0.124139E+01	0.0	-0.134154E+01	0.0
2	4		0.131001E-04	0.124269E+01	0.0	-0.137609E+01	0.0
2	5		0.193544E-04	0.124413E+01	0.0	-0.141933E+01	0.0
2	6		0.310350E-04	0.124561E+01	0.0	-0.147050E+01	0.0
2	7		0.539919E-04	0.124704E+01	0.0	-0.152883E+01	0.0

2	8	0.101027E-01	0.124938E+01	0.0	-0.159356E+01	0.0
2	9	0.203889E-03	0.124959E+01	0.0	-0.166396E+01	0.0
3	0	0.217801E-07	0.124399E+01	0.0	-0.129171E+01	0.0
3	1	0.224393E-07	0.124406E+01	0.0	-0.128431E+01	0.0
3	2	0.245373E-07	0.124424E+01	0.0	-0.129564E+01	0.0
3	3	0.284683E-07	0.124460E+01	0.0	-0.130223E+01	0.0
3	4	0.350302E-07	0.124504E+01	0.0	-0.131797E+01	0.0
3	5	0.456659E-07	0.124558E+01	0.0	-0.133795E+01	0.0
3	6	0.631014E-07	0.124619E+01	0.0	-0.136199E+01	0.0
3	7	0.922188E-07	0.124684E+01	0.0	-0.138987E+01	0.0
3	8	0.142451E-06	0.124750E+01	0.0	-0.142139E+01	0.0
3	9	0.232322E-06	0.124916E+01	0.0	-0.145629E+01	0.0
4	0	0.795336E-10	0.124628E+01	0.0	-0.127466E+01	0.0
4	1	0.813431E-10	0.124630E+01	0.0	-0.127504E+01	0.0
4	2	0.870175E-10	0.124639E+01	0.0	-0.127942E+01	0.0
4	3	0.973549E-10	0.124653E+01	0.0	-0.128625E+01	0.0
4	4	0.113689E-09	0.124672E+01	0.0	-0.129522E+01	0.0
4	5	0.139266E-09	0.124699E+01	0.0	-0.130667E+01	0.0
4	6	0.177956E-09	0.124727E+01	0.0	-0.132049E+01	0.0
4	7	0.237510E-09	0.124759E+01	0.0	-0.133668E+01	0.0
4	8	0.330937E-09	0.124794E+01	0.0	-0.135512E+01	0.0
4	9	0.481137E-09	0.124810E+01	0.0	-0.137572E+01	0.0

```
**********************
*** SYSTEM SOLUTION ***
**********************
```

NODAL POINT	REAL PART	IMAG. PART	ABS. VALUE	PHASE VALUE
1	0.477302E+00	-0.275234E+00	0.550799E+00	-0.523252
2	0.476876E+00	-0.275123E+00	0.550548E+00	-0.523231
3	0.477039E+00	-0.275198E+00	0.550727E+00	-0.523252
4	0.590410E+00	-0.475195E+00	0.680067E+00	-0.759558
5	0.590416E+00	-0.474956E+00	0.680337E+00	-0.759102
6	0.590760E+00	-0.416925E+00	0.654679E+00	-0.690180
7	0.590685E+00	-0.416711E+00	0.654404E+00	-0.690212
8	0.492925E+00	-0.274587E+00	0.564246E+00	-0.508245
9	0.492767E+00	-0.274558E+00	0.564053E+00	-0.508336
10	0.449834E+00	-0.133742E+00	0.469294E+00	-0.288991
11	0.449819E+00	-0.133895E+00	0.469324E+00	-0.289333
12	0.422760E+00	-0.768399E-01	0.429666E+00	-0.179793
13	0.422848E+00	-0.770188E-01	0.429815E+00	-0.180168
14	0.449389E+00	-0.133566E+00	0.468818E+00	-0.289902
15	0.449368E+00	-0.133718E+00	0.468843E+00	-0.289226
16	0.492217E+00	-0.274237E+00	0.563457E+00	-0.508314
17	0.492054E+00	-0.274204E+00	0.563299E+00	-0.508404
18	0.504254E+00	-0.416640E+00	0.654111E+00	-0.690544
19	0.504167E+00	-0.416422E+00	0.653905E+00	-0.690372
20	0.496133E+00	-0.675321E+00	0.837978E+00	-0.937183
21	0.495325E+00	-0.675373E+00	0.837541E+00	-0.937998
22	0.496353E+00	-0.668894E+00	0.833741E+00	-0.933117
23	0.498256E+00	-0.667099E+00	0.832635E+00	-0.929242
24	0.498146E+00	-0.662620E+00	0.828984E+00	-0.926156
25	0.506664E+00	-0.645318E+00	0.820453E+00	-0.905183
26	0.505970E+00	-0.640160E+00	0.822263E+00	-0.877981
27	0.506266E+00	-0.641337E+00	0.817070E+00	-0.872557
28	0.518955E+00	-0.610220E+00	0.801051E+00	-0.866047
29	0.518357E+00	-0.606361E+00	0.797557E+00	-0.863675
30	0.532745E+00	-0.562614E+00	0.774824E+00	-0.812659

31	0.532549E+00	-0.562871E+00	0.774875E+00	-0.813072
32	0.531202E+00	-0.558412E+00	0.779269E+00	-0.810290
33	0.543935E+00	-0.501046E+00	0.739536E+00	-0.744378
34	0.542366E+00	-0.499332E+00	0.736543E+00	-0.743112
35	0.549956E+00	-0.430174E+00	0.698212E+00	-0.663791
36	0.551635E+00	-0.431942E+00	0.700625E+00	-0.664302
37	0.548226E+00	-0.428411E+00	0.695764E+00	-0.663126
38	0.548607E+00	-0.352969E+00	0.652347E+00	-0.571715
39	0.546542E+00	-0.351922E+00	0.650044E+00	-0.572081
40	0.537829E+00	-0.272677E+00	0.603003E+00	-0.469229
41	0.538352E+00	-0.272548E+00	0.603407E+00	-0.468643
42	0.535047E+00	-0.272343E+00	0.603370E+00	-0.470823
43	0.518321E+00	-0.192522E+00	0.552920E+00	-0.355660
44	0.516464E+00	-0.193041E+00	0.551362E+00	-0.357695
45	0.490442E+00	-0.116495E+00	0.524068E+00	-0.233214
46	0.491657E+00	-0.114782E+00	0.524878E+00	-0.229352
47	0.489180E+00	-0.117754E+00	0.503153E+00	-0.236223
48	0.457374E+00	-0.476166E-01	0.459845E+00	-0.103722
49	0.456637E+00	-0.497038E-01	0.459334E+00	-0.108421
50	0.422350E+00	0.119271E-01	0.422504E+00	0.027249
51	0.422345E+00	0.119371E-01	0.422264E+00	0.028273
52	0.422261E+00	0.811337E-02	0.422359E+00	0.119213
53	0.389401E+00	0.569027E-01	0.393615E+00	0.145172
54	0.390025E+00	0.538862E-01	0.393705E+00	0.137297
55	0.362877E+00	0.901696E-01	0.373912E+00	0.243551
56	0.361227E+00	0.929580E-01	0.372946E+00	0.251874
57	0.363925E+00	0.870757E-01	0.374197E+00	0.234853
58	0.345481E+00	0.110678E+00	0.362726E+00	0.310535
59	0.347027E+00	0.107181E+00	0.363202E+00	0.299560
60	0.340015E+00	0.114475E+00	0.360248E+00	0.335152
61	0.339155E+00	0.118725E+00	0.359335E+00	0.316729
62	0.342239E+00	0.114129E+00	0.360767E+00	0.321881
63	0.345252E+00	0.110736E+00	0.362567E+00	0.312294
64	0.346814E+00	0.107211E+00	0.363057E+00	0.299812
65	0.362443E+00	0.972351E-01	0.373457E+00	0.244333
66	0.360448E+00	0.930353E-01	0.372646E+00	0.252328
67	0.363515E+00	0.871496E-01	0.373815E+00	0.235294
68	0.388443E+00	0.573378E-01	0.393003E+00	0.145630
69	0.394237E+00	0.542265E-01	0.393153E+00	0.137855
70	0.421564E+00	0.116943E-01	0.423705E+00	0.337640
71	0.423326E+00	0.121651E-01	0.423503E+00	0.328365
72	0.421962E+00	0.834703E-02	0.421545E+00	0.213827
73	0.456235E+00	-0.472431E-01	0.456732E+00	-0.137176
74	0.455955E+00	-0.433433E-01	0.458221E+00	-0.137834
75	0.494098E+00	-0.116032E+00	0.502657E+00	-0.232877
76	0.490520E+00	-0.114350E+00	0.503672E+00	-0.225337
77	0.487684E+00	-0.117279E+00	0.501781E+00	-0.235857
78	0.516842E+00	-0.191897E+00	0.553301E+00	-0.355522
79	0.515033E+00	-0.192431E+00	0.549826E+00	-0.357564
80	0.536317E+00	-0.271909E+00	0.601307E+00	-0.462226
81	0.536947E+00	-0.271832E+00	0.603824E+00	-0.463639
82	0.533561E+00	-0.271573E+00	0.598698E+00	-0.470359
83	0.546870E+00	-0.351417E+00	0.650317E+00	-0.573[illegible]
84	0.544845E+00	-0.350995E+00	0.648632E+00	-0.572170
85	0.548156E+00	-0.429003E+00	0.636073E+00	-0.664559
86	0.550200E+00	-0.431065E+00	0.698954E+00	-0.664580
87	0.546468E+00	-0.427293E+00	0.631706E+00	-0.663607
88	0.542337E+00	-0.499992E+00	0.737646E+00	-0.744795
89	0.540840E+00	-0.497347E+00	0.734750E+00	-0.743529
90	0.531697E+00	-0.561970E+00	0.773635E+00	-0.812271
91	0.531596E+00	-0.562306E+00	0.771811E+00	-0.813469
92	0.530295E+00	-0.557831E+00	0.769668E+00	-0.812699
93	0.558272E+00	-0.609810E+00	0.800296E+00	-0.866365
94	0.517577E+00	-0.606073E+00	0.797701E+00	-0.864993
95	0.536202E+00	-0.645079E+00	0.820017E+00	-0.905349
96	0.535623E+00	-0.647990E+00	0.821915E+00	-0.908197

97	0.535976E+00	-0.641237E+00	0.816821E+00	-0.902760
98	0.498076E+00	-0.666992E+00	0.832441E+00	-0.929379
99	0.498044E+00	-0.662614E+00	0.828918E+00	-0.926248
100	0.444268E+00	-0.910065E+00	0.101272E+01	-1.116655
101	0.444806E+00	-0.906781E+00	0.101000E+01	-1.113750
102	0.480362E+00	-0.870549E+00	0.994265E+00	-1.066578
103	0.480568E+00	-0.867405E+00	0.991604E+00	-1.064917
104	0.566025E+00	-0.748474E+00	0.938462E+00	-0.923314
105	0.565186E+00	-0.745554E+00	0.935567E+00	-0.922746
106	0.641926E+00	-0.537579E+00	0.837291E+00	-0.697161
107	0.640064E+00	-0.535754E+00	0.834694E+00	-0.696917
108	0.643979E+00	-0.268738E+00	0.697791E+00	-0.395298
109	0.641699E+00	-0.268518E+00	0.695614E+00	-0.396309
110	0.546114E+00	-0.421837E-02	0.546121E+00	-0.207724
111	0.544736E+00	-0.563361E-02	0.544765E+00	-0.213342
112	0.388869E+00	0.195861E+00	0.435409E+00	0.466577
113	0.388946E+00	0.193477E+00	0.434412E+00	0.461595
114	0.249287E+00	0.307313E+00	0.395704E+00	0.889273
115	0.250585E+00	0.304783E+00	0.394570E+00	0.882679
116	0.193946E+00	0.342360E+00	0.393479E+00	1.055376
117	0.195761E+00	0.339754E+00	0.392116E+00	1.048771
118	0.249045E+00	0.307336E+00	0.395543E+00	0.889784
119	0.250339E+00	0.304804E+00	0.394430E+00	0.883196
120	0.388476E+00	0.195934E+00	0.435037E+00	0.467106
121	0.388488E+00	0.193553E+00	0.434034E+00	0.462233
122	0.545430E+00	-0.400182E-02	0.545445E+00	-0.007434
123	0.544048E+00	-0.545487E-02	0.544035E+00	-0.010026
124	0.643266E+00	-0.268443E+00	0.696978E+00	-0.395374
125	0.640926E+00	-0.268246E+00	0.694759E+00	-0.396374
126	0.641127E+00	-0.537219E+00	0.836450E+00	-0.697445
127	0.639256E+00	-0.535144E+00	0.833837E+00	-0.697199
128	0.565478E+00	-0.748236E+00	0.937892E+00	-0.923626
129	0.564629E+00	-0.745113E+00	0.935031E+00	-0.922459
130	0.480081E+00	-0.870408E+00	0.994026E+00	-1.066756
131	0.480226E+00	-0.867263E+00	0.991341E+00	-1.065095
132	0.526037E+00	-0.146922E+01	0.156755E+01	-1.226978
133	0.456677E+00	-0.122099E+01	0.130350E+01	-1.212655
134	0.444298E+00	-0.105079E+01	0.114086E+01	-1.177770
135	0.448637E+00	-0.100768E+01	0.110301E+01	-1.151313
136	0.448371E+00	-0.985711E+00	0.108290E+01	-1.143893
137	0.454105E+00	-0.150982E+01	0.157663E+01	-1.278634
138	0.198470E+00	-0.108292E+01	0.115407E+01	-1.217875
139	0.408979E+00	-0.101626E+01	0.109546E+01	-1.198190
140	0.426915E+00	-0.152321E+01	0.158191E+01	-1.297533
141	0.377075E+00	-0.126646E+01	0.132140E+01	-1.281433
142	0.383173E+00	-0.109221E+01	0.115747E+01	-1.233396
143	0.193165E+00	-0.108548E+01	0.111986E+01	-1.212068
144	0.195468E+00	-0.102628E+01	0.109984E+01	-1.232991
145	0.454196E+00	-0.150932E+01	0.157666E+01	-1.278586
146	0.399077E+00	-0.108297E+01	0.115416E+01	-1.217734
147	0.439092E+00	-0.101632E+01	0.109556E+01	-1.188115
148	0.526189E+00	-0.146922E+01	0.156061E+01	-1.226887
149	0.456827E+00	-0.122043E+01	0.130357E+01	-1.212752
150	0.444514E+00	-0.105091E+01	0.114155E+01	-1.177637
151	0.448854E+00	-0.100776E+01	0.110322E+01	-1.151775
152	0.448582E+00	-0.985822E+00	0.108308E+01	-1.143764
153	0.438815E+00	-0.149125E+01	0.153090E+01	-1.193346
154	0.513488E+00	-0.998297E+00	0.111956E+01	-1.044788
155	0.507755E+00	-0.930965E+00	0.106043E+01	-1.071486
156	0.771232E+00	-0.127131E+01	0.148696E+01	-1.025507
157	0.653377E+00	-0.105596E+01	0.124175E+01	-1.016721
158	0.594761E+00	-0.907155E+00	0.108474E+01	-0.993471
159	0.584467E+00	-0.868693E+00	0.104701E+01	-0.978551
160	0.577741E+00	-0.849256E+00	0.102714E+01	-0.973421
161	0.993146E+00	-0.109804E+01	0.142178E+01	-0.882497
162	0.675268E+00	-0.786794E+00	0.103677E+01	-0.861074

163	0.645972E+00	-0.737097E+00	0.982098E+00	-0.851189
164	0.101013E+01	-0.877933E+00	0.133833E+01	-0.715495
165	0.944314E+00	-0.739733E+00	0.111727E+01	-0.714086
166	0.738636E+00	-0.634992E+00	0.974062E+00	-0.710088
167	0.712913E+00	-0.610562E+00	0.938594E+00	-0.708168
168	0.699365E+00	-0.597918E+00	0.920133E+00	-0.707343
169	0.106443E+01	-0.615450E+00	0.122955E+01	-0.524233
170	0.770234E+00	-0.457170E+00	0.895652E+00	-0.535662
171	0.724796E+00	-0.435921E+00	0.845787E+00	-0.541477
172	0.105610E+01	-0.333098E+00	0.110739E+01	-0.335527
173	0.879580E+00	-0.285043E+00	0.924603E+00	-0.313367
174	0.761018E+00	-0.266662E+00	0.806385E+00	-0.337032
175	0.730602E+00	-0.264934E+00	0.777155E+00	-0.347827
176	0.715056E+00	-0.263080E+00	0.761916E+00	-0.352545
177	0.974096E+00	-0.541385E-01	0.973602E+00	-0.055635
178	0.706442E+00	-0.780548E-01	0.710742E+00	-0.110049
179	0.666082E+00	-0.917419E-01	0.672370E+00	-0.136872
180	0.828865E+00	0.199936E+00	0.852634E+00	0.236695
181	0.694997E+00	0.152160E+00	0.711459E+00	0.215535
182	0.613566E+00	0.942683E-01	0.620786E+00	0.152043
183	0.594502E+00	0.739021E-01	0.599078E+00	0.123675
184	0.584209E+00	0.653451E-01	0.587852E+00	0.111399
185	0.640361E+00	0.406794E+00	0.758645E+00	0.565942
186	0.493723E+00	0.237837E+00	0.548023E+00	0.449918
187	0.478887E+00	0.197584E+00	0.519046E+00	0.331313
188	0.436563E+00	0.564833E+00	0.713879E+00	0.912795
189	0.377711E+00	0.453435E+00	0.597145E+00	0.876252
190	0.363859E+00	0.346619E+00	0.503913E+00	0.764011
191	0.365824E+00	0.315873E+00	0.483325E+00	0.712255
192	0.365062E+00	0.301254E+00	0.472808E+00	0.689846
193	0.245917E+00	0.669296E+00	0.713042E+00	1.218690
194	0.242309E+00	0.426174E+00	0.490095E+00	1.059140
195	0.257881E+00	0.374727E+00	0.454808E+00	0.968044
196	0.893360E-01	0.734228E+00	0.739643E+00	1.449718
197	0.369949E-01	0.595425E+00	0.603223E+00	1.409311
198	0.143065E+00	0.474578E+00	0.495673E+00	1.278002
199	0.163416E+00	0.438744E+00	0.468189E+00	1.214252
200	0.170936E+00	0.422304E+00	0.455587E+00	1.186165
201	-0.991832E-02	0.766156E+00	0.766208E+00	1.582438
202	0.790685E-01	0.561259E+00	0.507457E+00	1.414345
203	0.114534E+00	0.448273E+00	0.462673E+00	1.320647
204	-0.457093E-01	0.776392E+00	0.777736E+00	1.629603
205	-0.122198E-01	0.631478E+00	0.631557E+00	1.590146
206	0.570574E-01	0.508569E+00	0.511760E+00	1.453971
207	0.843276E-01	0.472914E+00	0.480374E+00	1.394136
208	0.950453E-01	0.456409E+00	0.466200E+00	1.365454
209	-0.897964E-02	0.766116E+00	0.766169E+00	1.582518
210	0.789965E-01	0.561245E+00	0.507452E+00	1.414680
211	0.114454E+00	0.448265E+00	0.462646E+00	1.320409
212	0.992189E-01	0.734194E+00	0.739551E+00	1.449862
213	0.968812E-01	0.595372E+00	0.603203E+00	1.409486
214	0.142927E+00	0.474554E+00	0.495611E+00	1.278255
215	0.163252E+00	0.438724E+00	0.468113E+00	1.214564
216	0.170774E+00	0.422289E+00	0.455512E+00	1.186501
217	0.245746E+00	0.669141E+00	0.712885E+00	1.218964
218	0.241804E+00	0.426144E+00	0.489967E+00	1.054674
219	0.257650E+00	0.374717E+00	0.454748E+00	0.968450
220	0.436351E+00	0.564691E+00	0.713637E+00	0.912909
221	0.377500E+00	0.453340E+00	0.589926E+00	0.876426
222	0.363596E+00	0.346534E+00	0.503659E+00	0.764322
223	0.365513E+00	0.315861E+00	0.483062E+00	0.712657
224	0.364763E+00	0.301199E+00	0.471047E+00	0.691239
225	0.640089E+00	0.406658E+00	0.758343E+00	0.565983
226	0.493409E+00	0.237866E+00	0.547726E+00	0.449116
227	0.478533E+00	0.197588E+00	0.517721E+00	0.331580
228	0.328566E+00	0.199772E+00	0.852311E+00	0.216590

229	0.694714E+00	0.152048E+00	0.711158E+00	0.215467
230	0.613220E+00	0.942385E-01	0.620419E+00	0.152485
231	0.594060E+00	0.739164E-01	0.598641E+00	0.123790
232	0.583798E+00	0.653655E-01	0.587846E+00	0.111592
233	0.971807E+00	-0.543051E-01	0.973323E+00	-0.255822
234	0.706042E+00	-0.786630E-01	0.710345E+00	-0.110124
235	0.665638E+00	-0.916991E-01	0.671925E+00	-0.136899
236	0.105583E+01	-0.333270E+00	0.110718E+01	-0.335751
237	0.879267E+00	-0.285125E+00	0.924341E+00	-0.313577
238	0.760576E+00	-0.266659E+00	0.805967E+00	-0.337217
239	0.730094E+00	-0.264863E+00	0.776631E+00	-0.348014
240	0.714594E+00	-0.263027E+00	0.761465E+00	-0.352839
241	0.106416E+01	-0.615593E+00	0.122939E+01	-0.524443
242	0.769842E+00	-0.457165E+00	0.895353E+00	-0.535879
243	0.724343E+00	-0.435862E+00	0.845369E+00	-0.541693
244	0.100987E+01	-0.876062E+00	0.133822E+01	-0.715694
245	0.844638E+00	-0.731818E+00	0.111712E+01	-0.714306
246	0.738248E+00	-0.638952E+00	0.973742E+00	-0.713317
247	0.712400E+00	-0.610369E+00	0.938117E+00	-0.708417
248	0.698920E+00	-0.597815E+00	0.919713E+00	-0.707586
249	0.902917E+00	-0.109820E+01	0.142172E+01	-0.882675
250	0.674937E+00	-0.786678E+00	0.103653E+01	-0.851700
251	0.645596E+00	-0.737034E+00	0.979803E+00	-0.851435
252	0.771030E+00	-0.127136E+01	0.148689E+01	-1.025640
253	0.653136E+00	-0.105600E+01	0.124166E+01	-1.016883
254	0.598438E+00	-0.977197E+00	0.108453E+01	-0.930696
255	0.584084E+00	-0.868585E+00	0.104673E+01	-0.978797
256	0.577379E+00	-0.849172E+00	0.102687E+01	-0.973666
257	0.638624E+00	-0.139126E+01	0.153064E+01	-1.140463
258	0.513210E+00	-0.994193E+00	0.111894E+01	-1.094266
259	0.507452E+00	-0.930852E+00	0.106218E+01	-1.071685
260	0.410483E+00	-0.151627E+01	0.157065E+01	-1.336415
261	0.348529E+00	-0.114994E+01	0.121150E+01	-1.276486
262	0.384455E+00	-0.109862E+01	0.115199E+01	-1.263500
263	0.512053E+00	-0.146523E+01	0.155232E+01	-1.234592
264	0.421089E+00	-0.111014E+01	0.118732E+01	-1.208252
265	0.415801E+00	-0.105976E+01	0.113842E+01	-1.196899
266	0.764484E+00	-0.127280E+01	0.148875E+01	-1.028913
267	0.600914E+00	-0.963762E+00	0.113575E+01	-1.013277
268	0.592654E+00	-0.920031E+00	0.108901E+01	-1.036251
269	0.101353E+01	-0.840297E+00	0.134245E+01	-0.735163
270	0.777209E+00	-0.670939E+00	0.102675E+01	-0.712147
271	0.745973E+00	-0.642487E+00	0.984513E+00	-0.711032
272	0.106654E+01	-0.329331E+00	0.111432E+01	-0.300027
273	0.811023E+00	-0.263335E+00	0.852826E+00	-0.314398
274	0.776437E+00	-0.257733E+00	0.818596E+00	-0.323499
275	0.832086E+00	0.209471E+00	0.958047E+00	0.246618
276	0.641994E+00	0.134749E+00	0.655983E+00	0.236898
277	0.617843E+00	0.138892E+00	0.629178E+00	0.192106
278	0.429471E+00	0.572708E+00	0.715849E+00	0.927361
279	0.351318E+00	0.466541E+00	0.537305E+00	0.858147
280	0.346125E+00	0.376834E+00	0.511670E+00	0.827442
281	0.748063E-01	0.735830E+00	0.739592E+00	1.469478
282	0.952988E-01	0.531924E+00	0.540393E+00	1.393517
283	0.117072E+00	0.497009E+00	0.578412E+00	1.359625
284	-0.625596E-01	0.774681E+00	0.777203E+00	1.651378
285	-0.392268E-02	0.562944E+00	0.562958E+00	1.577765
286	0.144493E-01	0.527182E+00	0.527360E+00	1.543394
287	0.746900E-01	0.735727E+00	0.739508E+00	1.469624
288	0.951805E-01	0.531883E+00	0.540332E+00	1.393720
289	0.106946E+00	0.496973E+00	0.508350E+00	1.358834
290	0.429255E+00	0.572578E+00	0.715615E+00	0.927495
291	0.351098E+00	0.466472E+00	0.537107E+00	0.858373
292	0.345891E+00	0.376783E+00	0.511434E+00	0.828119
293	0.331802E+00	0.209312E+00	0.857733E+00	0.246518
294	0.641687E+00	0.134677E+00	0.655682E+00	0.236877

295	0.617525E+00	0.118843E+00	0.628857E+00	0.190127
296	0.196428E+01	-0.329507E+00	0.119843E+01	-0.300244
297	0.810687E+00	-0.263796E+00	0.852527E+00	-0.314592
298	0.776089E+00	-0.257774E+00	0.817778E+00	-0.320683
299	0.191332E+01	-0.880455E+00	0.134239E+01	-0.715356
300	0.776895E+00	-0.670980E+00	0.102654E+01	-0.712377
301	0.745647E+00	-0.642508E+00	0.984280E+00	-0.711235
302	0.764276E+00	+0.127295E+01	0.148476E+01	-1.030083
303	0.600658E+00	+0.963784E+00	0.113569E+01	-1.013473
304	0.582374E+00	-0.920005E+00	0.108864E+01	-1.036455
305	0.511898E+00	+0.146521E+01	0.155205E+01	-1.234683
306	0.420923E+00	-0.111009E+01	0.116721E+01	-1.209365
307	0.415616E+00	-0.105967E+01	0.113826E+01	-1.197020
308	0.746596E+00	+0.128830E+01	0.148900E+01	-1.245571
309	0.628978E+00	-0.107503E+01	0.124551E+01	-1.241918
310	0.549137E+00	-0.998215E+00	0.119910E+01	-1.037621
311	0.569630E+00	-0.958688E+00	0.111515E+01	-1.034669
312	0.577613E+00	-0.969059E+00	0.112815E+01	-1.033281
313	0.594741E+00	-0.139968E+01	0.152080E+01	-1.168399
314	0.475091E+00	-0.108457E+01	0.118407E+01	-1.137928
315	0.464301E+00	-0.105268E+01	0.115207E+01	-1.135280
316	0.469501E+00	-0.146693E+01	0.154023E+01	-1.251042
317	0.430743E+00	-0.122389E+01	0.128783E+01	-1.254365
318	0.379382E+00	-0.113589E+01	0.119757E+01	-1.248849
319	0.370188E+00	-0.119098E+01	0.115208E+01	-1.243670
320	0.376969E+00	-0.110287E+01	0.116552E+01	-1.241439
321	0.388156E+00	-0.150013E+01	0.154954E+01	-1.117621
322	0.319211E+00	-0.116227E+01	0.120530E+01	-1.332759
323	0.318776E+00	-0.112831E+01	0.117248E+01	-1.245447
324	0.360988E+00	-0.151011E+01	0.155245E+01	-1.336724
325	0.310660E+00	-0.126013E+01	0.129774E+01	-1.139763
326	0.296652E+00	-0.116935E+01	0.120639E+01	-1.322347
327	0.291550E+00	-0.112330E+01	0.116052E+01	-1.316953
328	0.297862E+00	-0.113566E+01	0.117407E+01	-1.314292
329	0.388228E+00	-0.150014E+01	0.154956E+01	-1.317559
330	0.319282E+00	-0.116229E+01	0.120534E+01	-1.322724
331	0.318852E+00	-0.112834E+01	0.117263E+01	-1.295333
332	0.369643E+00	-0.146692E+01	0.154027E+01	-1.257152
333	0.290878E+00	-0.122391E+01	0.128769E+01	-1.254264
334	0.379523E+00	-0.113592E+01	0.119765E+01	-1.248345
335	0.370343E+00	-0.109853E+01	0.115218E+01	-1.243557
336	0.377145E+00	-0.110295E+01	0.116565E+01	-1.241337
337	0.594915E+00	-0.139959E+01	0.152078E+01	-1.168372
338	0.435272E+00	-0.108455E+01	0.118411E+01	-1.157787
339	0.468308E+00	-0.105269E+01	0.115216E+01	-1.152219
340	0.746784E+00	-0.128811E+01	0.148992E+01	-1.245395
341	0.291980E+00	-0.107495E+01	0.124556E+01	-1.241236
342	0.589345E+00	-0.995121E+00	0.119913E+01	-1.037425
343	0.569859E+00	-0.958656E+00	0.111524E+01	-1.034478
344	0.577857E+00	-0.969050E+00	0.112826E+01	-1.033093
345	0.900671E+00	-0.111817E+01	0.143545E+01	-0.892719
346	0.736427E+00	-0.868158E+00	0.111926E+01	-0.887752
347	0.699736E+00	-0.843184E+00	0.108936E+01	-0.845167
348	0.102871E+01	-0.693462E+00	0.136254E+01	-0.715152
349	0.961572E+00	-0.747139E+00	0.114038E+01	-0.714165
350	0.902973E+00	-0.695065E+00	0.106202E+01	-0.713449
351	0.772956E+00	-0.698424E+00	0.102169E+01	-0.713213
352	0.782093E+00	-0.676030E+00	0.103375E+01	-0.712765
353	0.123856E+01	-0.617796E+00	0.126038E+01	-0.532241
354	0.856046E+00	-0.484075E+00	0.983435E+00	-0.534649
355	0.832849E+00	-0.472234E+00	0.957415E+00	-0.515809
356	0.103517E+01	-0.318210E+00	0.119046E+01	-0.282772
357	0.116002E+00	-0.269577E+00	0.954846E+00	-0.286217
358	0.952808E+00	-0.253720E+00	0.889750E+00	-0.249172
359	0.920037E+00	-0.246217E+00	0.856203E+00	-0.241697
360	0.829274E+00	-0.250068E+00	0.866155E+00	-0.242878

361	0.100471E+01	-0.216099E-01	0.100494E+01	-0.021505
362	0.783955E+00	-0.265338E-01	0.784354E+00	-0.033835
363	0.763119E+00	-0.306185E-01	0.763728E+00	-0.040102
364	0.844567E+00	0.243724E+00	0.879023E+00	0.289946
365	0.738541E+00	0.196956E+00	0.735406E+00	0.271133
366	0.661476E+00	0.177493E+00	0.684875E+00	0.262154
367	0.537458E+00	0.166344E+00	0.658804E+00	0.255256
368	0.645303E+00	0.166157E+00	0.666351E+00	0.252111
369	0.633564E+00	0.454246E+00	0.779579E+00	0.622024
370	0.521177E+00	0.338925E+00	0.645720E+00	0.594614
371	0.491331E+00	0.322463E+00	0.587698E+00	0.580794
372	0.406968E+00	0.626300E+00	0.730165E+00	0.973754
373	0.346783E+00	0.498347E+00	0.637131E+00	0.962849
374	0.328219E+00	0.456206E+00	0.562007E+00	0.947134
375	0.319805E+00	0.433397E+00	0.538617E+00	0.935083
376	0.325416E+00	0.435857E+00	0.543936E+00	0.929467
377	0.195687E+00	0.700971E+00	0.727773E+00	1.298560
378	0.168500E+00	0.529029E+00	0.555216E+00	1.262447
379	0.171767E+00	0.506751E+00	0.535070E+00	1.243992
380	0.360939E-01	0.753018E+00	0.753470E+00	1.536157
381	0.323532E-01	0.620814E+00	0.621656E+00	1.517428
382	0.187850E-01	0.569638E+00	0.570957E+00	1.502813
383	0.440485E-01	0.542577E+00	0.544362E+00	1.499789
384	0.977292E-01	0.546493E+00	0.548484E+00	1.483665
385	-0.422222E-01	0.776979E+00	0.781337E+00	1.676228
386	-0.422183E-01	0.588141E+00	0.589654E+00	1.642452
387	-0.305966E-01	0.564558E+00	0.565386E+00	1.624940
388	-0.119722E+00	0.782879E+00	0.791980E+00	1.722547
389	-0.879966E-01	0.645942E+00	0.651909E+00	1.706194
390	-0.719410E-01	0.592991E+00	0.597339E+00	1.631526
391	-0.614215E-01	0.565239E+00	0.568567E+00	1.679037
392	-0.594852E-01	0.569453E+00	0.572449E+00	1.673342
393	-0.422784E-01	0.776937E+00	0.781222E+00	1.676375
394	-0.422777E-01	0.588153E+00	0.589670E+00	1.642545
395	-0.306523E-01	0.564535E+00	0.565367E+00	1.625941
396	0.259860E-01	0.752940E+00	0.753389E+00	1.536297
397	0.132546E-01	0.620756E+00	0.621593E+00	1.518882
398	0.186819E-01	0.569563E+00	0.570995E+00	1.502987
399	0.439467E-01	0.542523E+00	0.544300E+00	1.499967
400	0.476192E-01	0.548351E+00	0.548422E+00	1.483856
401	0.195528E+00	0.700852E+00	0.727616E+00	1.298727
402	0.168349E+00	0.528952E+00	0.555056E+00	1.262663
403	0.171609E+00	0.506684E+00	0.534957E+00	1.244232
404	0.406665E+00	0.636158E+00	0.729934E+00	0.979876
405	0.346598E+00	0.498241E+00	0.626939E+00	0.963077
406	0.328024E+00	0.456111E+00	0.561816E+00	0.947316
407	0.319617E+00	0.433314E+00	0.538438E+00	0.935271
408	0.325215E+00	0.435776E+00	0.543752E+00	0.929675
409	0.633318E+00	0.450077E+00	0.779260E+00	0.622031
410	0.500943E+00	0.338618E+00	0.604765E+00	0.594683
411	0.491085E+00	0.322373E+00	0.587443E+00	0.580896
412	0.394302E+00	0.243598E+00	0.878727E+00	0.290837
413	0.708306E+00	0.196828E+00	0.735145E+00	0.271146
414	0.661220E+00	0.177385E+00	0.684601E+00	0.262104
415	0.537213E+00	0.166249E+00	0.658543E+00	0.255213
416	0.645338E+00	0.166071E+00	0.666073E+00	0.251986
417	0.100444E+01	-0.217975E-01	0.100468E+01	-0.021698
418	0.783619E+00	-0.266442E-01	0.784072E+00	-0.033988
419	0.762813E+00	-0.307086E-01	0.763431E+00	-0.040235
420	0.109496E+01	-0.319409E+00	0.114029E+01	-0.282996
421	0.915749E+00	-0.269720E+00	0.958644E+00	-0.246435
422	0.952533E+00	-0.253831E+00	0.889519E+00	-0.289380
423	0.819782E+00	-0.246322E+00	0.855969E+00	-0.293890
424	0.828989E+00	-0.250159E+00	0.865912E+00	-0.293075
425	0.109834E+01	-0.617979E+00	0.126020E+01	-0.512500
426	0.955765E+00	-0.484172E+00	0.983236E+00	-0.514873

427	0.832539E+00	-0.472304E+00	0.957179E+00	-0.516032
428	0.102853E+01	-0.893656E+00	0.136253E+01	-0.715348
429	0.861355E+00	-0.747251E+00	0.114031E+01	-0.714583
430	0.802732E+00	+0.695173E+00	0.106190E+01	-0.713715
431	0.772740E+00	-0.668543E+00	0.102180E+01	-0.713229
432	0.781851E+00	-0.676105E+00	0.103364E+01	-0.712994
433	0.900069E+00	-0.111837E+01	0.143583E+01	-0.892917
434	0.706201E+00	-0.868236E+00	0.111918E+01	-0.887953
435	0.689464E+00	-0.843210E+00	0.108920E+01	-0.885376

COEFF. IN THE EXPANSION FOR THE RAD-FIELD

EIGENVALUE 1	REAL PART	IMAG. PART	ABS. VALUE	PHASE VALUE
1	-0.192277E+00	-0.334099E+00	0.385477E+00	-2.333014
2	0.297521E+00	0.556937E-01	0.282865E+00	0.191323
3	0.555545E-04	0.171494E-03	0.180258E-03	1.257522
4	0.331931E-02	-0.717776E-01	0.719503E-01	-1.534584
5	0.867297E-05	0.221242E-05	0.895062E-05	0.249772
6	-0.332184E-02	-0.938731E-05	0.332165E-02	-1.138766
7	0.251286E-05	0.224114E-05	0.336707E-05	0.728335
8	-0.527781E-06	0.700512E-04	0.700532E-04	1.573331
9	0.736150E-06	0.523047E-06	0.902046E-06	0.617752
10	0.319373E-06	0.194128E-07	0.319612E-06	0.224176
11	0.321778E-07	0.249534E-07	0.958828E-07	0.234803
12	0.116774E-07	0.737857E-08	0.138132E-07	0.563513
13	0.599031E-08	-0.206420E-08	0.549292E-08	-0.338262
14	0.330615E-09	0.187850E-10	0.331148E-09	0.056757
15	0.119472E-09	-0.275341E-09	0.300143E-09	-1.161405
16	-0.219246E-10	-0.435442E-10	0.483063E-10	-2.143334
17	-0.423863E-11	-0.114357E-10	0.140943E-10	-2.135123
18	-0.377788E-11	-0.108960E-11	0.393167E-11	-2.867797
19	0.178623E-13	0.214492E-12	0.214716E-12	1.545821
20	0.123060E-12	0.219291E-12	0.251460E-12	1.059419
21	0.539480E-13	0.113546E-12	0.125710E-12	1.127249
22	-0.590211E-13	0.149195E-14	0.589603E-13	3.115984
23	-0.338605E-14	0.289855E-14	0.429263E-14	2.461817

EIGENVALUE 2	REAL PART	IMAG. PART	ABS. VALUE	PHASE VALUE
1	-0.512841E+00	0.289692E+00	0.589005E+00	2.627398
2	-0.162500E+01	0.843459E+01	0.858930E+01	1.761125
3	0.640407E-02	-0.529289E-02	0.830823E-02	-0.692685
4	0.337018E+01	0.156431E+00	0.337382E+01	0.046342
5	0.103106E-02	-0.164070E-02	0.193778E-02	-1.009736
6	0.960140E-03	-0.411359E+00	0.411360E+00	-1.564461
7	-0.104036E-03	-0.410649E-03	0.423623E-03	-1.818923
8	-0.263512E-01	0.638977E-04	0.263532E-01	3.133168
9	-0.355560E-04	-0.484366E-04	0.600877E-04	-2.274036
10	0.751373E-04	0.945269E-03	0.948251E-03	1.491475
11	0.402233E-04	0.710083E-04	0.816092E-04	1.055407
12	0.270891E-04	-0.156742E-04	0.312969E-04	-0.524548
13	0.255557E-06	0.238150E-04	0.298161E-04	1.562224
14	-0.421453E-05	0.785953E-05	0.891821E-05	2.060038
15	-0.321785E-05	0.304699E-05	0.443156E-05	2.333460
16	-0.244589E-05	0.361564E-05	0.436523E-05	2.165560
17	-0.110465E-06	-0.195438E-05	0.195750E-05	-1.627259
18	-0.182950E-06	0.985642E-06	0.100248E-05	1.754324
19	0.503112E-07	+0.818791E-06	0.820245E-06	-1.5[illegible]9423

EIGENVALUE 3	REAL PART	IMAG. PART	ABS. VALUE	PHASE VALUE
1	0.270513E+03	-0.155526E+03	0.312035E+03	-0.523782

2	0.822393E+02	-0.424283E+03	0.432179E+03	-1.379338
3	-0.245172E+00	0.214253E+00	0.325558E+00	2.423391
4	-0.102903E+03	-0.485590E+01	0.103018E+03	-3.094439
5	-0.146931E+00	0.127341E+00	0.194434E+00	2.427502
6	-0.317155E-01	0.658733E+01	0.658741E+01	1.575612
7	0.133901E+00	0.443313E-01	0.141049E+00	0.319716
8	-0.113733E+01	0.531362E-02	0.113734E+01	3.136921
9	0.909692E-01	-0.452721E-01	0.101612E+00	-0.461777
10	-0.282548E-01	0.284290E+00	0.285690E+00	1.669865
11	-0.110059E-01	-0.312963E-01	0.150681E-01	-1.890036
12	0.404511E-01	-0.115575E-01	0.420697E-01	-0.278300
13	-0.393623E-02	-0.256024E-01	0.209751E-01	-1.759579
14	0.119562E-01	-0.263685E-01	0.289525E-01	-1.185996
15	0.950008E-02	-0.602444E-02	0.112492E-01	-0.565149
16	0.293751E-02	-0.896191E-02	0.119716E-01	-0.845941
17	0.692276E-03	0.377984E-03	0.667566E-03	0.479520
18	0.201041E-02	-0.316724E-02	0.375142E-02	-1.005215
19	-0.606443E-03	-0.898518E-04	0.613112E-03	-2.994514

EIGENVALUE 4	REAL PART	IMAG. PART	ABS. VALUE	PHASE VALUE
1	0.157935E+06	-0.910427E+05	0.182207E+06	-0.522928
2	0.515128E+05	-0.267041E+06	0.271964E+06	-1.383234
3	0.106297E+03	-0.855966E+02	0.136976E+03	-0.677933
4	-0.409537E+05	-0.423498E+04	0.411522E+05	-3.045964
5	0.769781E+02	-0.822211E+02	0.112632E+03	-0.819329
6	-0.291767E+01	0.169475E+05	0.169475E+05	1.572970
7	0.254236E+02	-0.656180E+02	0.703710E+02	-1.201156
8	0.252575E+04	-0.666649E+02	0.252663E+04	-0.026388
9	-0.778847E+01	-0.915099E+03	0.120162E+02	-2.275981
10	0.210817E+02	-0.315927E+03	0.316610E+03	-1.504165
11	-0.542784E+01	0.186273E+02	0.194020E+02	1.859337
12	-0.226542E+02	-0.479237E+01	0.230209E+02	-2.962874
13	-0.739550E+01	0.197895E+02	0.211263E+02	1.928434
14	-0.466250E+01	0.110098E+02	0.119563E+02	1.971386
15	-0.470168E+01	0.495190E+01	0.110066E+02	2.012156
16	-0.479022E+01	0.531326E+01	0.693389E+01	2.333447
17	0.467610E-01	0.210705E+00	0.227869E+00	1.141189
18	-0.127517E+01	0.262448E+01	0.291786E+01	2.023082
19	0.147534E+01	-0.257999E+01	0.297203E+01	-1.051340

EIGENVALUE 5	REAL PART	IMAG. PART	ABS. VALUE	PHASE VALUE
1	-0.140714E+09	0.810308E+08	0.162377E+09	2.619115
2	-0.539287E+08	0.279198E+09	0.284398E+09	1.761603
3	-0.317784E+05	-0.199631E+05	0.375285E+05	-2.583697
4	0.191606E+09	0.471684E+07	0.191715E+09	0.046390
5	-0.129635E+04	0.264321E+04	0.294359E+04	2.026772
6	0.440902E+05	-0.186108E+08	0.186108E+08	-1.568426
7	-0.286698E+04	0.427708E+04	0.514908E+04	2.161319
8	-0.254596E+07	-0.116937E+04	0.254596E+07	-3.141133
9	-0.249963E+04	0.299992E+04	0.389830E+04	2.263865
10	-0.174687E+04	0.275659E+06	0.275665E+06	1.577134
11	-0.319251E+03	0.618503E+03	0.713868E+03	2.034445
12	0.210971E+05	0.148101E+04	0.211491E+05	0.070179
13	0.104399E+04	-0.291520E+03	0.108353E+04	-0.272300
14	0.401206E+03	-0.285565E+04	0.288369E+04	-1.431213
15	0.625041E+03	-0.460237E+03	0.776187E+03	-0.634664
16	0.911453E+03	-0.879977E+03	0.119700E+04	-0.825888
17	0.112742E+03	-0.100215E+03	0.150844E+03	-0.726642
18	0.223435E+03	-0.610911E+03	0.650489E+03	-1.220167
19	0.127273E+02	-0.512628E+01	0.137204E+02	-0.382899

****

```
*** OPTICAL THEOREM ***          L.H.S.=  0.1940644E+00
************************          R.H.S.=  0.1940985E+00

**************
*** FORCES ***
**************
X-COMPONENT :        REAL PART     IMAG. PART        ABS. VALUE        PHASE VALUE
     1             -0.201278E+00   0.104171E+01      0.106398E+01        1.761663

Z-COMPONENT :        REAL PART     IMAG. PART        ABS. VALUE        PHASE VALUE
     1              0.957784E+00  -0.552250E+00      0.110559E+01       -0.523029
```

6. CONCLUDING REMARKS

6.1 Suggested Improvements

In general, especially when larger or more complex geometries, or incident waves of higher frequency are to be studied, the following modifications and extensions to our present program are recommended (and may be necessary):

A. Secondary storage: The large core requirements we experienced strongly suggest the use of additional storage on secondary devices, which enables many core-saving alternatives:

1) Data storage: When many different wavelengths or modes are to be analyzed using the same grid structure, a large portion of the data (such as geometrical information, the global matrix $[K_V]$ due to the volume integral) can be saved in secondary storage and need be initiated only once.

2) Program overlay: The present flow of control among the programs require only a few programs to be in core at one time while all the other subroutines may be stored externally. Such a scheme results in only a small primary storage saving, however, as the total object code is only $\sim$ 80K long.

3) Partitioning: This is the most useful and often necessary extention to a program using Gauss elimination for solution. While partitioning a Gauss elimination solver is straightforward, efficient assembling of the equation matrices in partitioned form require special manipulations. Experience with similar procedures in other problems (such as finite element methods in structural

mechanics), however, can be adapted quite directly.

B. Conversion to double precision: In this type of problem, a sizeable number of complex unknowns together with a large bandwidth are involved. The great number of operations required to solve such a system necessitates a careful consideration of possible round-off accumulation. Our experience in this and other problems indicates that in some of the examples presented (~ 500 unknowns, ~ 200 bandwidth, ~ 10^7 complex operations), we are already close to a regime where the accuracy of single precision becomes inadequate. By converting to double-precision, round-off accumulation error is essentially eliminated. While in principle, the conversion is trivial in our present program, the increased storage need makes other modifications involving use of secondary storage (such as partitioning) necessary. The increase in computational time associated with double precision is, however, not significant.

C. Substructuring: By treating the overall finite element domain as an assembly of several smaller regions, the overall problem can be analyzed separately in terms of each of these substructures. Such a modification is particularly effective when the geometry or expected physical behavior suggests ready subdivisions of the element domain. In an attempt to extend the original Atlantic Generating Station two-dimensional finite-element problem (Chen and Mei, 1974) to higher frequencies, a new program using secondary storage capabilities which involved sub-structuring (see Fig. 6.1) (but not partitioning) was

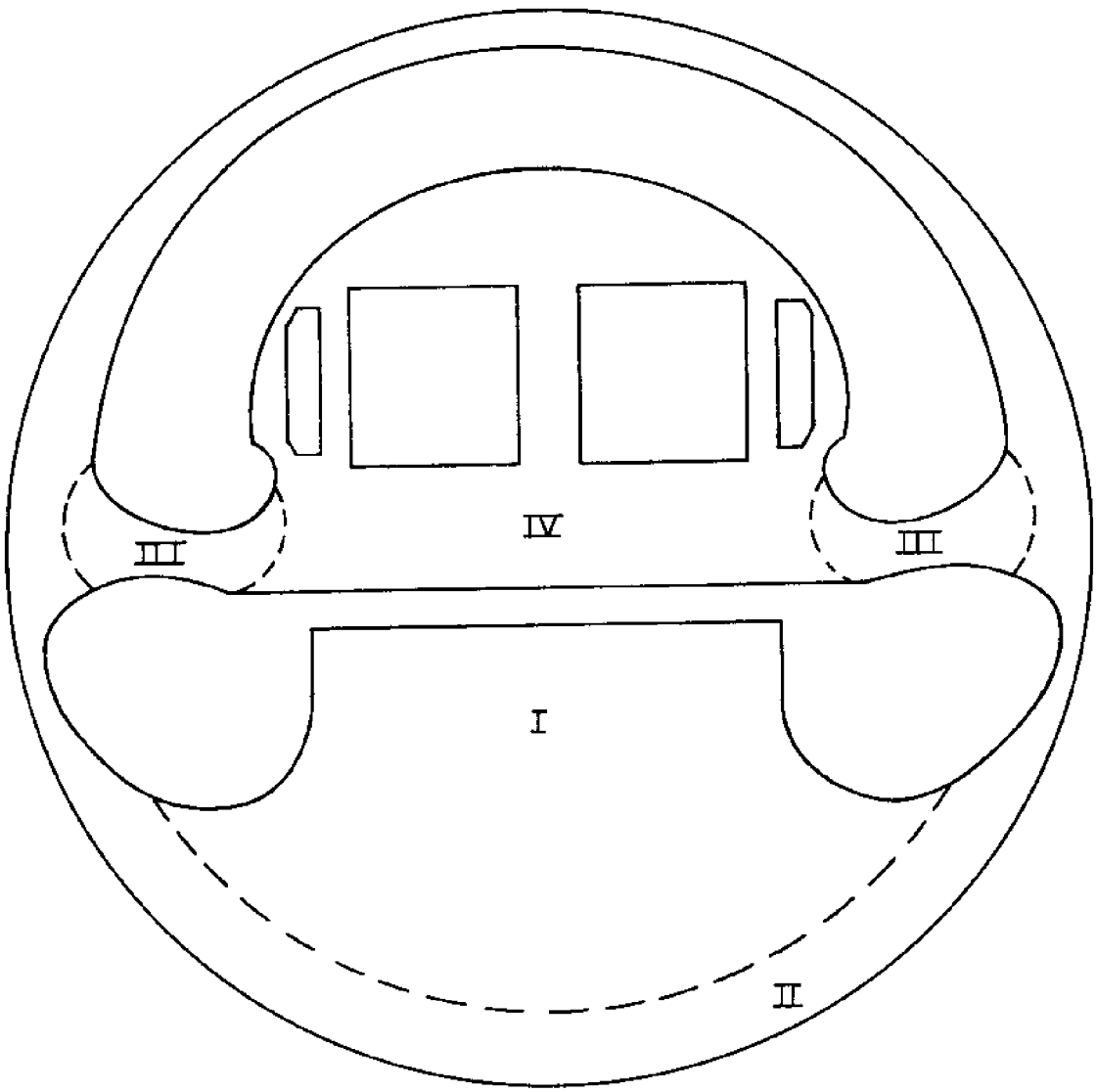

Figure 6.1 Substructuring the AGS into four regions

previously developed by the authors but was not completed for lack of time. Our experience indicates that it is always important to include all the elements on the artificial boundary in one substructure to avoid unnecessary increase in bandwidth.

D. Use of symmetry: When the geometry under consideration possesses one or more vertical planes of symmetry, the program can be modified so that only one symmetric segment need be studied. The procedure is illustrated schematically in Fig. 6.2 for the case with a single plane of symmetry. While two separate (one symmetric, one antisymmetric) problems must now be solved, each of them only involves half the original number of nodal unknowns and bandwidth. The new computational time required would only be one-fourth and the storage one half of the non-symmetric problem. Again, a two-dimensional finite element program using symmetry was previously developed and tested. The treatment of the symmetric (half) problem with a semi-circular outer boundary and Neumann boundary conditions on the plane of symmetry is similar to Chen and Mei for their rectangular and semi-circular harbors. For the antisymmetric (half) problem, the Dirichlet boundary conditions on the symmetry plane are imposed as essential boundary conditions (loadings) after the global matrix is assembled.

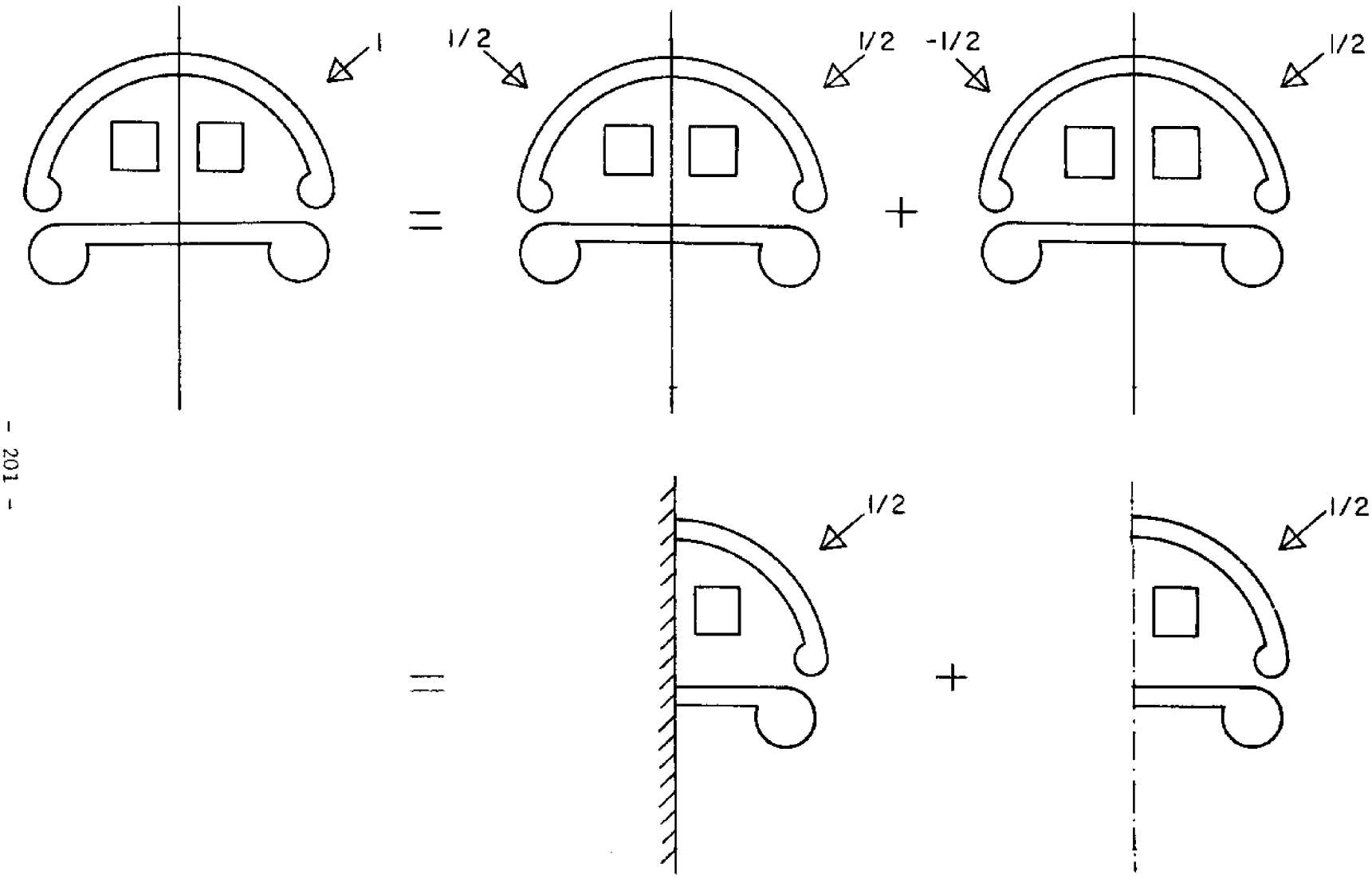

Figure 6.2 Splitting a problem with one (vertical) plane of symmetry into two half problems

6.2 Recommendations and Cost Estimates for the Atlantic Generating Station Problem

For the specific case of the offshore harbor problem for the Atlantic Generating Station the following extensions to the present program are recommended:

1) Change all storage variables from single- to double-precision accuracy;
2) full partitioning in assemblage and Gauss elimination solution by using secondary storage; and
3) if an assumption of symmetry is reasonably valid (i.e., if the ocean bottom contours run approximately parallel to the length of the generating station), modifications be made to utilize symmetry to solve only a (symmetric) half of the problem.

Assuming a mean radius, a, of the circular breakwater of about 900 feet and a mean storm far-field depth of $\sim$ 70 feet, we estimate, using our earlier criterion (Section 4.2), that a total of $\sim$ 6500 nodes with a bandwidth of $\sim$ 550 is required for a $\sim$ 8.5 second or higher ($ka \lesssim 17$) incident wave. About 6 hours of computational time would be required for each wavelength (or mode), and if symmetry is present, about 1.8 hours per point. The above estimate is arrived at by a direct extrapolation of the timing of the present examples which use no secondary storage. Clearly, an appreciable cost associated with the necessary input/output operations between primary and secondary devices, which is very much machine dependent, must also be added.

Finally, the problem of radiation of waves due to forced oscillations of one or two platforms in the AGS harbor can be treated by the wave force

program with very little modification required. This is due to the mathematical similarities in the two problems. Since there are six degrees of freedom for each platform, the number of added mass and damping coefficients involved is of course large and the total computer time needed depends on the thoroughness of the investigation intended.

6.3 Conclusions

The hybrid element method presented in this work is found to be a powerful one for three-dimensional water wave scattering problems. While only relatively simple geometries have been studied, it is clear that by using secondary storage and increasing precision of machine representation to reduce round-off accumulation error, the extension to treating more complicated structures including depth variations is straightforward. The method is hence a practical one for engineering applications.

In our numerical experiments using simple geometries, the hybrid element method is already quite competitive with known Green function schemes. Experience indicates that our computing cost is essentially governed by the number of finite element nodes. For finite element method, the number of nodes increases with the fluid volume, while for Green function method the number of area elements required increases with the total wetted solid surface. Thus as the number and complexity of solid components increase in a given fluid region, we expect the hybrid element method to be less costly while the opposite is true for Green function method. In light of this, and of the virtual lack of any tedious analytic preparation required, the hybrid element method, is, in our opinion a

powerful alternative to the Green function method for three-dimensional water wave problems.

We emphasize once more that the problem of radiation by an oscillating body is mathematically very similar to the scattering problem we have treated. The linearized boundary value problem for a radiation problem is obtained by setting the incident potential ϕ_I to be zero and replacing ϕ_s by $\phi = \phi_r$ (radiated potential) in Eqs. (1.2.1) - (1.2.4), and requiring further that

$$\frac{\partial\phi}{\partial n} = V_n$$

on the oscillating body S_B where V_n is prescribed for a given oscillating mode. The proper functional is now (Bai and Yeung, 1974):

$$J(\phi) = \int_V \frac{1}{2} (\nabla\phi)^2 dV - \int_F \frac{\omega^2}{2g} \phi^2 \, dF - \int_{S_B} V_n \phi dS$$

$$+ \int_S \left(\frac{\phi'}{2} - \phi\right) \frac{\partial\phi'}{\partial r} \, dS$$

The modification of the present program to solve the radiation problem can be trivially achieved; the forcing comes now from the integral over S_B and not S. The total coefficient (stiffness) matrix is completely unchanged, while the forcing integrals I_5, I_6 (see Eq. (2.0)) are no longer present and all the forcing terms come from the integral

$$\int_{S_B} V_n \phi dS$$

which can be directly evaluated by quadrature after V_n is given or computed.

LIST OF REFERENCES

1. Abramowitz, M. and Stegun, I. A. (ed), Handbook of Mathematical Functions with Formulas, Graphs, and Mathematical Tables, Applied Math. series 55, National Bureau of Standards, U. S. Dept. of Commerce. June 1964, p. 895.

2. Bai, K. J. and Yeung, R., "Numerical Solution of Free-Surface Flow Problems", Proceedings of the Tenth Symposium on Naval Hydrodynamics, June 1974 (in press).

3. Black, J. L., "Wave Forces on Vertical Axisymmetric Bodies", Journal of Fluid Mechanics, Vol. 67, Part 2, 1975, pp. 369-376.

4. Black, J. L., Mei, C. C. and Bray, M. C. G., "Radiation and Scattering of Water Waves by Rigid Bodies", Journal of Fluid Mechanics, Vol. 46, Part 1, 1971, pp. 151-164.

5. Chen, H. S. and Mei, C. C., "Oscillations and Wave Forces in a Man-Made Harbor in the Open Sea", Proceedings of the Tenth Symposium on Naval Hydrodynamics, June 1974 (in press).

   also

   Chen, H. S. and Mei, C. C., "Oscillations and Wave Forces in an Offshore Harbor", Technical Report No. 190, Ralph M. Parsons Laboratory for Water Resources and Hydrodynamics, Dept. of Civil Engineering, M.I.T., Cambridge, Mass. August 1974.

6. Garrett, C. J. R., "Wave Forces on a Circular Dock", Journal of Fluid Mechanics, Vol. 46, Part 1, 1971, pp. 129-139.

7. Garrison, C. J., "Hydrodynamics of Large Objects in the Sea; Part I - Hydrodynamic Analysis", Journal of Hydronautics, Vol. 8, No. 1, January 1974, pp. 5-12.

8. Gottfried, K., Quantum Mechanics, Volume I: Fundamentals, W. A. Benjamin, Inc., New York, March 1966, pp. 106-109.

9. Haskind, M.D., "The Exciting Forces and Wetting of Ships in Waves", (in Russian) Izv. Akad. Nauk SSSR, Otd. Tekh. Nauk, 1957, Vol. 7, pp. 65-79. English translation: David Taylor Model Basin Translation, No. 307.

10. Jonsson, I. G., Skovgaard, O. and Brink-Kjaer, O., "Diffraction and Refraction Calculations for Waves Attacking an Island", submitted to Journal of Marine Research, Manuscript--November 1975.

11. Kopal, Z., Numerical Analysis, Second Edition, John Wiley & Sons, Inc., New York, 1961, p. 562.

12. Lautenbacher, C. C., "Gravity Wave Refraction by Islands", Journal of Fluid Mechanics, Vol. 41, Part 3, 1970, pp. 655-672.

13. Longuet-Higgins, M. S., "On the Trapping of Wave Energy Round Islands", Journal of Fluid Mechanics, Vol. 29, Part 4, 1967, pp. 781-821.

14. MacCamy, R. C. and Fuchs, R. A., "Wave Forces on Piles: a Diffraction Theory", Institute of Engineering Research, Waves Investigation Lab., Series 3, Issue 334, Berkeley, California, February 1952.

15. Newman, J. N., "The Interaction of Stationary Vessels with Regular Waves", Proceedings of the Eleventh Symposium on Naval Hydrodynamics, April 1976 (in press).

16. Smith, R. and Sprinks, T., "Scattering of Surface Waves by a Conical Island", Journal of Fluid Mechanics, Vol. 72, Part 2, 1975, pp. 373-384.

17. Vastano, A. C. and Reid, R. O., "A Numerical Study of the Tsunami Response at an Island", Dept. of Oceanography, Texas A & M University, A & M Project 471, Ref. 66-26T, 1966.

18. Vastano, A. C. and Reid, R. O., "Tsunami Response for Islands: Verification of a Numerical Procedure", Journal of Marine Research, Vol. 25, Part 2, 1967, pp. 129-139.

19. Wehausen, J. V., "The Motion of Floating Bodies", Annual Review of Fluid Mechanics, Vol. 3, 1971, pp. 237-268.

20. Zienkiewicz, O. C., et al., "Iso-Parameter and Associated Element Families for Two- and Three-Dimensional Analysis", Finite Elements Methods in Stress Analysis, Holand, I., and Bellg K. (ed), Tapir Press, Trondheim, Norway, 1969, pp. 383-432.

LIST OF FIGURES

Figure		Page
1.1	The Boundary Value Problem	13
1.2	Introduction of the Artificial Circular Cylindrical Boundary, S	13
2.1	The 20-node Hexahedral Element with Exterior Nodes Only (in Local Coordinates)	23
2.2	The Daughter Arbitrarily Oriented, Quadratic-sided Hexahedral Element in Global Coordinates After Isoparametric Mapping	23
3.1	Wave Incident on a Bottom-seated Circular Cylinder of Radius a ($\theta_I = \pi$; h = a)	40
3.2	Finite Element Structure for a Uniform Cylinder: 36 Elements, 342 Nodal Points.	42
3.3	Wave incident on a Floating Cylindrical Dock of Radius a ($\theta_I = \pi$; h = .75a)	47
3.4	Finite Element Structure for a Floating Dock: 56 Elements, 435 Nodal Points	47
3.5	(a) Horizontal Force Coefficient for a Semi-immersed Cylinder ($\frac{h}{a} = .75$; $\frac{H}{a} = .5$; $\theta_I = \pi$). +, amplitude; x, phase: finite element solution ——, amplitude;-----, phase: Garrett, 1971 results	50
	(b) Vertical Force Coefficient for a Semi-immersed Cylinder (See Description in Figure 3.5 (a))	51
3.6	Forces on a square dock: ——— + ———, magnitude; -- x --, phase. Normal incidence: $\theta_I = \pi$.	
	(a) Horizontal Force Coefficient	54
	(b) Vertical Force Coefficient	55
	(c) Moment Coefficient About y-axis	56

Figure		Page
3.7	Forces on a Square Dock: ——— + ———, magnitude -- x --, phase. Oblique Incidence: $\theta_I = 5\pi/4$.	
	(a) Horizontal Force Coefficient	57
	(b) Vertical Force Coefficient	58
	(c) Moment Coefficient About Horizontal Axis	59
3.8	Run-up, η/a_o, on the Sides of a Square Barge: (+) ———: (nodal) magnitude; (x) ----: (nodal) phase. Normal incidence: $\theta_I = \pi$.	
	(a) $k_o a = 1$	60
	(b) $k_o a = 2$	61
	(c) $k_o a = 3$	62
	(d) $k_o a = 4$	63
3.9	Run-up, η/a_o, on the Sides of a Square Barge: (+) ——— : (nodal) magnitude; (x) ----: (nodal) phase. Oblique Incidence: $\theta_I = 5\pi/4$.	
	(a) $k_o a = 1$	64
	(b) $k_o a = 2$	65
	(c) $k_o a = 3$	66
	(d) $k_o a = 4$	67
3.10	Differential Scattering Cross-section, $\lvert A(\theta)\rvert^2$, for a Square Barge. Normal Incidence: $\theta_I = \pi$.	
	(a) $k_o a = 1$	68
	(b) $k_o a = 2$	69
	(c) $k_o a = 3$	70
	(d) $k_o a = 4$	71

Figure | Page

3.11 Differential Scattering Cross-section, $|A(\theta)|^2$, for a Square Barge. Oblique Incidence: $\theta_I = 5\pi/4$.

(a) $k_o a = 1$ 72

(b) $k_o a = 2$ 73

(c) $k_o a = 3$ 74

(d) $k_o a = 4$ 75

3.12 Polar Plot of Differential Scattering Cross-section, $|A(\theta)^2|$, for a Square Barge. Normal Incidence: $\theta_I = \pi$.

(a) $k_o a = 1$ 76

(b) $k_o a = 2$ 77

(c) $k_o a = 3$ 78

(d).(i) $k_o a = 4$ 79

(d).(ii) $k_o a = 4$. Details for $\frac{\pi}{4} < \theta < \frac{3\pi}{4}$ and $\frac{5\pi}{4} < \theta < \frac{7\pi}{4}$. 80

3.13 Polar Plot of Differential Scattering Cross-section, $|A(\theta)|^2$, for a Square Barge. Oblique Incidence: $\theta_I = 5\pi/4$.

(a) $k_o a = 1$ 81

(b) $k_o a = 2$ 82

(c) $k_o a = 3$ 83

(d) $k_o a = 4$ 84

3.14 Geometry and Finite-element Structure for an Elliptical Island with a Circular Base. (Major and Minor axes: $A = a$, $B = .5a$; "draft" of elliptic cylinder: $H = .5a$, radius of circular toe: $R = 1.5a$; water depth: $h = a$ 87

3.15 Run-up, η/a_o, on an Elliptic Island with a Circular Base: (+) ——— : (nodal) magnitude; (x) ---- : (nodal) phase. Wave Incident from $x \sim +\infty$. ($\theta_I = \pi$).

(a) $k_o a = 1$ 88

(b) $k_o a = 2$ 89

(c) $k_o a = 3$ 90

Figure		Page
3.16	Run-up, η/a_o, on an Elliptic Island with a Circular Base: (+) ———: (nodal) magnitude; (x) ----: (nodal) phase. Wave Incident from y $\sim +\infty$. ($\theta_I = 3\pi/2$).	
	(a) $k_o a = 1$	91
	(b) $k_o a = 2$	92
	(c) $k_o a = 3$	93
3.17	Differential Scattering Cross-section, $\lvert A(\theta)\rvert^2$, for an Elliptic Island with a Circular Base. Wave Incident from x $\sim +\infty$. ($\theta_I = \pi$).	
	(a) $k_o a = 1$	94
	(b) $k_o a = 2$	95
	(c) $k_o a = 3$	96
3.18	Differential Scattering Cross-section, $\lvert A(\theta)\rvert^2$, for an Elliptic Island with a Circular Base. Wave Incident from y $\sim +\infty$. ($\theta_I = 3\pi/2$).	
	(a) $k_o a = 1$	97
	(b) $k_o a = 2$	98
	(c) $k_o a = 3$	99
3.19	Polar Plot of Differential Scattering Cross-section, $\lvert A(\theta)\rvert^2$, for an Elliptic Island with a Circular Base. Wave Incident from x $\sim +\infty$. ($\theta_I = \pi$).	
	(a) $k_o a = 1$	100
	(b) $k_o a = 2$	101
	(c) $k_o a = 3$	102
3.20	Polar Plot of Differential Scattering Cross-section, $\lvert A(\theta)\rvert^2$, for an Elliptic Island with a Circular Base. Wave Incident from y $\sim +\infty$. ($\theta_I = 3\pi/2$).	
	(a) $k_o a = 1$	103
	(b) $k_o a = 2$	104
	(c) $k_o a = 3$	105

Figure		Page
4.1	Relative Error in Optical Theorem for the Square Dock under Obliquely Incident Waves ($\theta_I = 5\pi/4$).	108
4.2	Relative Error in the Magnitude of the Horizontal Force on a Uniform Cylinder.	110
4.3	Relative Error in the Magnitude of the Run-up on a Uniform Cylinder at: + : $\theta = 0$; X: $\theta = \pi/2$; o: $\theta = \pi$. ($\theta_I = \pi$).	111
5.1	Flow Chart for the Program	120 - 122
5.2	An Example Using Both Automatic Generation (in Region $\tilde{V}$) and Direct Input (in Region $\hat{V}$) to set up Finite Element Grids.	125
6.1	Substructuring the AGS into Four Regions	199
6.2	Splitting a problem with one (vertical) Plane of Symmetry into Two Half Problems.	201

LIST OF TABLES

TABLE		Page
3.1	Comparison Between Analytic and Finite Element Results for Scattering Off a Uniform Cylinder ($\theta_I = \pi$): Horizontal Force Coefficient C_F and Free Surface Elevation η/a_o at $r = a$.	44
3.2	Comparison Between Analytic and Finite Element Results for Scattering off a Uniform Cylinder ($\theta_I = \pi$): Coefficients α_{mn}, β_{mn} of the Exterior Solution. $k_o a = 1$.	45
3.3	Computed Horizontal and Vertical Force Coefficients for a Semi-immersed Circular Cylinder ($\frac{h}{a} = .75$, $\frac{H}{a} = .5$)	49
4.1	Comparison of Results for Diffraction by a Uniform Cylinder, $k_o a = 1$, $\theta_I = \pi$, Using a Variety of Finite Element Grid Structures: pxq —— p Rings Stacked Vertically of q Finite Elements Each.	113
4.2	Comparison of Results for Diffraction by a Square Barge, $k_o a = 1$, $\theta_I = \pi$, Using a Range of Numbers of Coefficient Terms.	115
5.1	Summary of Computational Requirements.	118

LIST OF SYMBOLS

a	Typical horizontal dimension of a body (radius for a cylinder, half-length for a square)
a_o	Incident wave amplitude
$A(\theta)$	Angular variation of the far-field scattered potential
B	All solid surfaces including bottom
C.C.	Complex conjugale of preceding term
$C_{F_x}, C_{F_y}, C_{F_z}, C_{M_x}, C_{M_y}, C_{M_z}$	Force and moment coefficients respectively in x, y, z directions
$E_{\lvert F \rvert}$	Relative error in the total horizontal force on a uniform cylinder
E_{OPT}	Relative error defined by the Optical Theorem
E_S	Relative error in the total scattering cross-section
$E_{\lvert \eta \rvert_\theta}$	Relative error in the run-up on the body at θ
F	Total free surface Finite element region free surface inside S
$\vec{F}$	Total force vector
F_i	Component of total force in i-direction
g	Acceleration due to gravity
h	Constant (far-field) water depth
H	Typical vertical dimension of a body (water depth for a uniform cylinder, draft for floating docks)
$H_n^{(1)}(x)$	Hankel function of the first kind, order n argument x
i	Imaginary unit; $= \sqrt{-1}$

$I_1, I_2, \ldots I_6$	Integrals in $J(\phi)$
$J(\phi)$	The stationary functional
$J_n(x)$	Bessel function, order n argument x
k_o	(real) wave-number associated with the incident wave
k_m	$m = 1, 2, 3 \ldots$ imaginary part of the imaginary roots of the dispersion relation
$K_n(x)$	Modified Bessel function of the second kind, order n argument x
L_e	Average dimension of finite elements in a given grid
M	Number of vertical eigenfunctions in the exterior analytic representation minus one
$\vec{M}$	Total moment vector
M_i	Component of total moment about i-axis
M_V	Number of finite elements in V
M^e	Number of nodes in a finite element
$\vec{n}$	Unit normal vector pointing out of fluid region under consideration
$N_o, N_1, N_2 \ldots, N_m$	Number of radial eigenfunction for each vertical mode in the exterior analytic representation
N_i^e	Interpolation functions for an element
N_S	Number of nodes on S
N_T	Total number of unknown coefficients in exterior analytic representation
N_V	Number of finite element nodes in V
r	Radial coordinate; $= \sqrt{x^2 + y^2}$

r_S	Radius of the artificial cylinder S
R	(Complex) reflection coefficient in two-dimensional scattering
S	Vertical circular cylindrical artificial surface separating finite element and analytic regions
S_∞	Control surface at infinity
t	Time
T	(Complex) transmission coefficient in two-dimensional scattering
V	Total fluid volume Finite element fluid volume inside S
$\tilde{V}$	Finite element region with grids generated automatically
$\hat{V}$	Finite element region with grids generated by (hand) input
W_i	Weighting function for quadrature point i
x, y, z	Rectilinear coordinates
x_i, y_i, z_i	(Global) nodal coordinate values of a finite element
α_{mn}, β_{mn}	Coefficients of the exterior eigenfunction expression
$\delta(\ )$	Absolute error in
$\Delta(\ )$	Relative error in
ε	A small number ; Belongs to
ε_n	Jacobi symbol; = 1 for n = 0; = 2 for n = 1, 2, 3 ...
κ_m	Imaginary roots of the dispersion relation
ξ, η, ζ	Local coordinates of an element
ξ_i, η_i	Quadrature points in local coordinates

η	Free surface elevation
θ	Polar angle (azimuth); $= \tan^{-1}(\frac{y}{x})$
θ_I	Incidence angle
ρ	Density of fluid
ω	Radian frequency of the incident wave
ϕ	Total velocity potential
ϕ_s	Scattered velocity potential
ϕ_I	Incident velocity potential
Φ	$= \mathrm{Re}[\phi e^{-i\omega t}]$
Im( )	Imaginary part of
Re( )	Real part of
∇	Gradient operator; $= (\frac{\partial}{\partial x}, \frac{\partial}{\partial y}, \frac{\partial}{\partial z})$
$\frac{\partial}{\partial n}$	$= \vec{n} \cdot \nabla$
$\lvert\ \rvert$	Absolute value of (a real number) Magnitude of (a complex number) Determinant of a matrix
$\subset$	A subset of
$\cup$	Union of
$\{\ \}$	A vector
$(\ )^*$	Complex conjugate of
$(\ )'$	Of the analytic region exterior to S Derivative with respect to argument
$(\ )^e$	Of an element
$(\ )^T$	Transpose of
$[\ ]^{-1}$	Inverse of (a matrix)

$\hat{(\ )}$	of S
$\overline{(\ )}$	Of the free surface
$[J]$, $[J_F]$, $[J_S]$	Jacobian matrix of coordinate transformation for volume, free surface and S
$[K]$	Total (global) equation matrix
$[K']$	Total (global) matrix after (static) condensation
$[K_C^e]$, $[K_C]$	(Full) matrix due to an integral in $J(\phi)$
$[K_D]$	(Diagonal) matrix due to an integral in $J(\phi)$
$[K_F{}^e]$, $[K_F]$	Matrix due to integral over free surface
$[K_V{}^e]$, $[K_V]$	Matrix due to the volume integral
$\{N^e\}$	Vector of interpolation functions
$\{Q\}$	Total load (right-hand-side) vector after (static) condensation
$\{Q_C\}$, $\{Q_p{}^e\}$, $\{Q_p\}$	Vectors due to integrals in $J(\phi)$
$[X^e]$	Matrix of node coordinate values for an element
$\{\mu\}$	Vector of coefficient unknowns
$\{\psi\}$	Vector containing both FEM and coefficient unknowns

APPENDIX A

A PROOF OF THE OPTICAL THEOREM

The Optical Theorem for three-dimensional scattering of water waves (Eq. 4.1.2) can be proved by applying Green's Theorem and using the method of stationary phase.*

Consider an incident wave given as in Eq. (2.1.a):

$$\phi_I = -\frac{iga_o}{\omega}\frac{\cosh k_o(z+h)}{\cosh k_o h} e^{ik_o r\cos(\theta-\theta_I)}$$

$$= b\, f_o(z)\, e^{ik_o r\cos(\theta-\theta_I)} \qquad \text{(A.1.a)}$$

where we have defined

$$f_o(z) \equiv \frac{\sqrt{2}\cosh k_o(z+h)}{\sqrt{h+\frac{g}{\omega^2}\sinh^2 k_o h}} \qquad \text{(A.1.b)}$$

and

$$b \equiv \left(-\frac{iga_o}{\omega}\right)\frac{\sqrt{h+\frac{g}{\omega^2}\sinh^2 k_o h}}{\sqrt{2}\cosh k_o h}\ , \text{ a constant} \qquad \text{(A.1.c)}$$

and h is the far-field constant depth.

At infinity, the scattered wave (Eq. (1.3.4)) can be written as

$$\phi_s \sim c\, A(\bar{\phi})\, f_o(z)\, \frac{e^{ik_o r}}{\sqrt{k_o r}} \qquad (k_o r \to \infty) \qquad \text{(A.2.a)}$$

---

*The proof here is quite well-known in classical physics and is not different in essence from that given in Gottfried, 1966.

where we define

$$A(\theta) \equiv -\left(\frac{iga_o}{\omega}\right)^{-1} \sum_{n=0}^{\infty} (-i)^n (\alpha_{on} \cos n\theta + \beta_{on} \sin n\theta) \tag{A.2.b}$$

and

$$c \equiv b \sqrt{\frac{2}{\pi}}\ e^{-i\pi/4} \cosh k_o h \tag{A.2.c}$$

Applying Green's Theorem to $\phi = \phi_I + \phi_s$ and ϕ^* over the entire fluid region, V, we have

$$0 = \int_V (\phi\nabla^2\phi^* - \phi^*\nabla^2\phi)\,dV = \int_{S_\infty} \left(\phi \frac{\partial\phi^*}{\partial r} - \phi^* \frac{\partial\phi}{\partial r}\right) dS_\infty \tag{A.3}$$

by virtue of Eq. (1.2.1) in V, and Eq. (1.2.2), (1.2.3) on F and B respectively.

It follows that

$$\int_{S_\infty} \mathrm{Im}\left[\phi \frac{\partial\phi^*}{\partial r}\right] dS = 0 \tag{A.4}$$

and upon substituting in Eqs. (A.1), (A.2), expanding and performing depth integration, we have

$$0 = \lim_{k_o r \to \infty} \int_0^{2\pi} d\theta r \quad \mathrm{Im}\ [-ik_o\ |b|^2 \cos(\theta - \theta_I)\ ]$$

$$+ \lim_{k_o r \to \infty} \int_0^{2\pi} d\theta r \quad \mathrm{Im}\ [-ik_o bc^*\ A^*(\theta)\ \frac{e^{-ik_o r[1-\cos(\theta - \theta_I)]}}{\sqrt{k_o r}}$$

$$- ik_o\ b^* c\ A(\theta)\ \frac{e^{ik_o r[1-\cos(\theta - \theta_I)]}}{\sqrt{k_o r}} \cos(\theta - \theta_I)]$$

$$- |c|^2 \int_0^{2\pi} d\theta \quad |A(\theta)|^2 \tag{A.5}$$

where order $(k_o r)^{-1/2}$ terms vanish in the limit.

Now, the first integrand is periodic in θ and the integral vanishes identically. The second integral, I (say), can be evaluated using a stationary phase argument since $k_o r >> 1$. In this limit, contribution to the integral is neglegible except near stationary phase points $\theta - \theta_I = 0$ and π, in fact, only for

$$(\theta - \theta_I)^2 \sim O(k_o r)^{-1} = \varepsilon \quad \text{(say)} \qquad (\varepsilon << 1)$$

and

$$(\theta - \theta_I - \pi)^2 \sim O(k_o r)^{-1}$$

Expanding $\cos(\theta - \theta_I)$ in Taylor series in turn about zero and π, keeping only leading contribution in both exponent and coefficient, and evaluating A at the stationary points, we have

$$I \sim \mathrm{Im}\left[-i \sqrt{k_o r}\, bc^* A^*(\theta_I) \int_{-\varepsilon}^{\varepsilon} e^{-ik_o r(\theta - \theta_I)^2/2}\, d(\theta - \theta_I) - \mathrm{C.C.}\right]$$

$$+ \mathrm{Im}\left[-i \sqrt{k_o r}\, bc^* A^*(\theta_I + \pi) \int_{-\varepsilon}^{\varepsilon} e^{-2ik_o r}\, d(\theta - \theta_I - \pi) + \mathrm{C.C.}\right]$$

$$(k_o r \to \infty\ , \varepsilon \ll 1)$$

where C.C. denotes the complex conjugate of the preceding term. Now the second term vanishes identically upon taking the imaginary part, and the first term can be rewritten so that

$$I \sim 2\ \mathrm{Im}\left[-i \sqrt{k_o r}\, bc^* A^*(\theta_I) \int_{-\varepsilon}^{\varepsilon} e^{-ik_o r(\theta - \theta_I)^2/2}\, d(\theta - \theta_I)\right]$$

$$(k_o r \to \infty,\ \varepsilon \ll 1)$$

Set

$$s^2 = ik_o r\ (\theta - \theta_I)^2/2, \text{ i.e. } \theta - \theta_I = \sqrt{\frac{2}{ik_o r}}\, s,$$

then on taking the limit

$$I = 2 \text{ Im } [-i \sqrt{\frac{2}{i}} \, bc^* \, A^*(\theta_I) \int_{-\sqrt{i}\,\infty}^{\sqrt{i}\infty} e^{-s^2} \, ds]$$

The Fresnel integral is simply $\sqrt{\pi}$, and substituting in Eq. (A.2.c) for b, we finally have

$$I = - \frac{2\pi \, |c|^2}{\cosh k_o h} \text{ Re}[A(\theta_I)]$$

Whence, Eq. (A.5) becomes

$$0 = - \frac{2\pi \, |c|^2}{\cosh k_o h} \text{ Re}[A(\theta_I)] - |c|^2 \int_0^{2\pi} |A(\theta)|^2 \, d\theta$$

or

$$\frac{1}{2\pi} \int_0^{2\pi} |A(\theta)|^2 \, d\theta = - \frac{\text{Re}[A(\theta_I)]}{\cosh k_o h}$$

as stated in Eq. (4.1.2).